LBL-12655
c.2

Lawrence Berkeley Laboratory
UNIVERSITY OF CALIFORNIA

CHEMICAL BIODYNAMICS DIVISION

STRUCTURAL EFFECTS ON THE CIRCULAR DICHROISM
OF ETHIDIUM-NUCLEIC ACID COMPLEXES

Kenneth Steven Dahl
(Ph.D. thesis)

April 1981

TWO-WEEK LOAN COPY

This is a Library Circulating Copy
which may be borrowed for two weeks.
For a personal retention copy, call
Tech. Info. Division, Ext. 6782

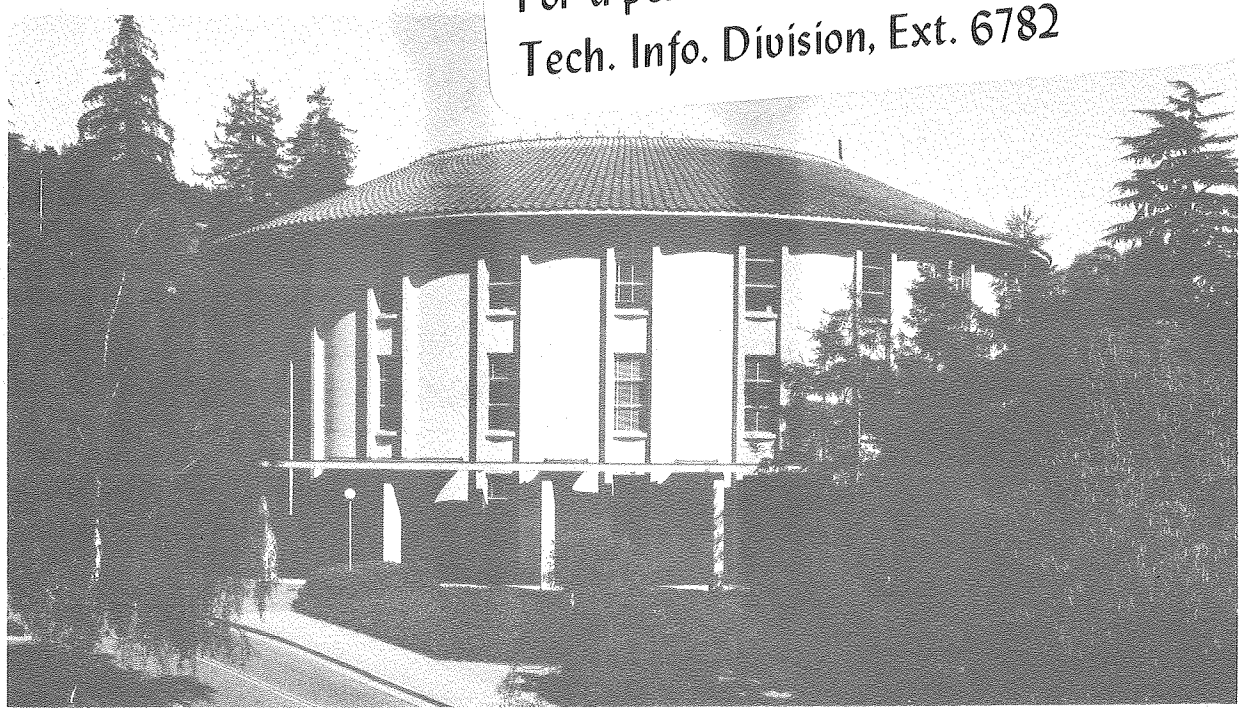

Prepared for the U.S. Department of Energy under Contract W-7405-ENG-48

DISCLAIMER

This document was prepared as an account of work sponsored by the United States Government. While this document is believed to contain correct information, neither the United States Government nor any agency thereof, nor the Regents of the University of California, nor any of their employees, makes any warranty, express or implied, or assumes any legal responsibility for the accuracy, completeness, or usefulness of any information, apparatus, product, or process disclosed, or represents that its use would not infringe privately owned rights. Reference herein to any specific commercial product, process, or service by its trade name, trademark, manufacturer, or otherwise, does not necessarily constitute or imply its endorsement, recommendation, or favoring by the United States Government or any agency thereof, or the Regents of the University of California. The views and opinions of authors expressed herein do not necessarily state or reflect those of the United States Government or any agency thereof or the Regents of the University of California.

LBL-12655

STRUCTURAL EFFECTS ON THE CIRCULAR DICHROISM OF ETHIDIUM-NUCLEIC ACID COMPLEXES

Kenneth Steven Dahl

Ph.D. Thesis

Lawrence Berkeley Laboratory
University of California
Berkeley, CA 94720

This work was supported in part by the National Institutes of Health Grant No. GM-10840 and by the Division of Biomedical and Environmental Research of the U.S. Department of Energy under Contract No. W-7405-ENG-48.

STRUCTURAL EFFECTS ON THE CIRCULAR DICHROISM OF ETHIDIUM-NUCLEIC ACID COMPLEXES

by

Kenneth Steven Dahl

ABSTRACT

Binding of the frameshift mutagen ethidium bromide to dinucleoside phosphates (dimers) of different base sequences was studied by optical methods, notably UV-visible spectroscopy, circular dichroism (CD), and fluorescence detected circular dichroism (FDCD). The ethidium ion intercalated between the base pairs of the minihelix formed by the complementary dimers; the stoichiometry of the complex was 2:1 dimer:dye. Equilibrium constants for complex formation showed a general preference for dye binding to complementary sequences in the order:

$$Py(3'\text{-}5')Pu > Pu(3'\text{-}5')Pu \equiv Py(3'\text{-}5')Py > Pu(3'\text{-}5')Py$$

where Py = a pyrimidine base and Pu = a purine base. Complexes with ribodinucleoside phosphates had larger formation constants than their deoxyribo- analogues. Above 300 nm, where only the dye absorbs, the induced CD spectra of the complexes had bands at 375 nm, 330 nm, and near 307 nm. The magnitude of the 307 nm band per bound dye depended upon the base sequence in the dimers. The CD spectra of these complexes down to 220 nm were obtained by FDCD measurements; between 220 and 300 nm both positions and magnitudes of the CD bands were sequence dependent. A study of ethidium ion binding to dCA_5G + dCT_5G tested for any site preference of dye binding and for any correspondence be-

---

This manuscript was printed from originals provided by the author.

tween the dimer:dye FDCD spectra and oligomer:dye FDCD spectra.

Ethidium ion binding and optical activity in complexes with calf thymus DNA were studied as a function of NaCl concentration. The binding constant was dependent upon salt concentration, increasing as the ionic strength decreased. The magnitude of the induced CD band at 307 nm also increased as the ionic strength decreased. Possible mechanisms for this behavior and the previously observed (Houssier et al. (1974) *Biopolymers 13*, 1141-1160) induced CD dependence upon the dye binding ratio were presented. The available evidence favored a mechanism which considered the effects of the complete nucleic acid/bound dye/counterion system on the optical properties of the dye.

Tenco

"Dr. Hoenikker used to say that any scientist who couldn't explain to an eight-year-old what he was doing was a charlatan."

"Then I'm dumber than an eight-year-old...I don't even know what a charlatan is."

Kurt Vonnegut, Jr.

Cat's Cradle

DEDICATION

To my grandparents

Vivian and Ernest Madson

Alma and Carl Dahl

who have enriched life in many ways

To my parents

Mari and Fredrick Dahl

whose love, support, and confidence in my ability has been of inestimable aid

ACKNOWLEDGEMENTS

In setting out to acknowledge those people who have in some way helped me during the course of this work, I find that I could cite many more than I am prepared to and so add extra pages to this already long manuscript. Failure of a name to appear here does not imply an oversight of your welcome company and assistance, but rather a desire to wrap this thing up on my part.

Foremost among the people deserving special thanks during my time in Berkeley is my research director, Nacho Tinoco, who often must have wondered just what I was doing (as did I), but was there to provide guidance and encouragement during the roughest parts. His approach to research direction encourages self-direction and the ability to learn from mistakes; this was a most satisfactory arrangement for me.

Barbara Dengler and David Koh were the font of all practical knowledge in the lab and superb organizers of the group parties which never seemed to let up. David and his wife Nora also deserve special thanks for the many holiday dinners I attended at their home.

Ken Adamson, Dean Luehrs, and Leslie Leifer, three excellent instructors, first sparked my interest in chemistry. Their classes were always a delightful place to learn in. Mark Malnor was a collaborator, if that is the proper term, in many zany and madcap adventures in those early labs.

Marc Maestre and Charlie Reich provided assistance and advice during the design and construction of the FDCD. The oft-maligned Charlie was always a firm advocate of the technique's true worth, a

position best left in the memories of those who heard him expound upon it.

Two postdocs, Frank Martin and Bruce Johnson, were a stabilizing influence in the lab. Frank, with his myriad projects, willingly collaborated in the work with dCA_5G and dCT_5G and was always ready to discuss matters. Bruce furnished many moments of unintended mirth with his knowledge of practically everything. His soliliquies on slugs and "gorgeous" days are classics and his exuberant personality is sorely missed.

Steve Winkle never ceased to amaze with his fertile imagination, which often carried over to his interpretation of data. It never took more than one suggestion to pull him away from his work to hit the bars.

The friendship of two comrades from the first days, Carlos Bustamante and Arthur Pardi, is most treasured. Carlos, with his candor and otherworldly viewpoint, provided an unusual view of events. He is also largely responsible for my (still scanty) knowledge of polyelectrolyte theory. Art is the silent partner in this work, much of which was initiated by him. He was always ready to discuss our progress, or lack of it, and goals in sessions often punctuated with the comment "Why are we doing this, again?". He also wins the award for being the toughest critic of this dissertation by eliminating many a Cosellian turn of phrase and demanding clearer explanations.

Jeff Nelson was the source of needed assistance during my many struggles with perfidious computers and programming; often, if he didn't know the answer, just explaining my problem to him served to

aid in its solution. He and Kathy Morden, a constant source of good cheer, were also the most frequent recipients of my barbed comments, which were often made without thought at the spur of the moment. That I could still count on their friendship after these incidents is a tribute to their patience.

Joe Kao, one of the leading practitioners of the graveyard shift school of research, made many a tedious evening more tolerable by serving as someone to talk to. He also was willing to talk about everything, particularly subjects outside of chemistry, which was a refreshing change. David Keller, despite his innocent looks, always seemed to win at poker, depriving me of bus fare.

With thanks to all these people and more, I can look back upon four-and-a-half enjoyable years here.

This work was supported in part by National Institutes of Health Grant GM 10840 and by the Division of Biomedical and Environmental Research of the U.S. Department of Energy under Contract No. W-7405-ENG-48.

TABLE OF CONTENTS

DEDICATION i

ACKNOWLEDGEMENTS ii

TABLE OF CONTENTS v

Chapter I INTRODUCTION

1. Background 1
2. Purpose and Scope of This Study 16

Chapter II DINUCLEOSIDE PHOSPHATE - ETHIDIUM ION INTERACTIONS

1. Introduction 23
2. Experimental 24
   A) Materials 24
   B) Methods 25
3. Results 27
   A) Optical Titrations 27
   B) Optical Melts 31
   C) Thermodynamics of the Binding Reaction 47
   D) Induced CD of Dimer:Dye Complexes 47
4. Discussion 55
   A) Stoichiometry of the Complexes 55
   B) Sequence Preferences in the Complexes 56
   C) Induced CD of the Complexes 60

Chapter III FLUORESCENCE DETECTED CIRCULAR DICHROISM OF DIMER-ETHIDIUM ION COMPLEXES

1. Introduction 64
2. Experimental 65

A) Materials 65

B) Methods 66

i) Modification of a Cary 60 for FDCD 66

ii) Manipulation of FDCD Data 69

iii) Calibration of the Instrument 70

iv) Measurement of FDCD Spectra 71

v) Fluorescence Measurements 74

3. Results 76

A) Sequence Dependence of FDCD Spectra 76

B) Assignment of Spectral Bands 85

C) CD Spectrum of Complexes from FDCD 88

4. Discussion 95

A) Sequence Dependence of Complexes' CD 95

B) The "Exciton" Band 103

C) Is There Energy Transfer in the Complexes? 103

Chapter IV ETHIDIUM ION BINDING WITH dCA_5G + dCT_5G

1. Introduction 106

2. Experimental 106

A) Materials 106

B) Methods 107

3. Results and Discussion 108

A) Melting of dCA_5G:dCT_5G:EI 108

B) Circular Dichroism Studies 113

C) FDCD Spectra of dCA_5G:dCT_5G:EI 120

Chapter V COUNTERION EFFECTS ON DNA:ETHIDIUM ION COMPLEXES

1. Introduction 130

2. Experimental 132

A) Materials 132

B) Methods 132

i) Dialyses 132

ii) Spectral Studies 136

iii) Theory 137

3. Results 139

A) Stability of DNA 139

B) Binding of Ethidium Ion to DNA 142

C) Induced CD of DNA/Ethidium Ion Complexes 150

D) Counterion Changes with Dye Binding 156

4. Discussion 163

Chapter VI CONCLUSIONS

1. The Problem Revisited 167

2. New Evidence Bearing on the Problem 167

3. The Model 170

4. Further Experiments 172

BIBLIOGRAPHY 175

Appendix A COMPUTER PROGRAMS FOR ERROR ANALYSIS AND DATA FITTING IN BENESI-HILDEBRAND PLOTS AND $\Delta\varepsilon_{bound}$ 180

Appendix B SUPER SPECTRUM DATA SYSTEM 201

Appendix C COMPUTER PROGRAMS AT LBL 202

Appendix D DNA/ETHIDIUM ION COMPLEX CHARGE DENSITY 238

Chapter I

INTRODUCTION

1. Background

One of the more fascinating areas of scientific inquiry over the past thirty-five years has been focused on the structure and function of the nucleic acids: deoxyribonucleic acid (DNA) and ribonucleic acid (RNA). After the publication of the right-handed double helix structure for DNA by Watson and Crick (1953), studies in succeeding years gradually revealed the processes by which the genetic message is preserved from generation to generation through replication of DNA and how the message is transcribed and translated via RNA intermediates into proteins (for reviews, see Watson, 1976; Kornberg, 1980).

In light of the known mutagenic and carcinogenic properties of certain molecules, among them, polycyclic and heterocyclic aromatics, studies aimed at uncovering their means of producing changes in the genetic message were undertaken. Models specifying how these molecules interacted with nucleic acids were proposed, among them, the intercalation model of Lerman (1961). As shown schematically in Figure 1.1, the aromatic dye molecules, which are similar in thickness to the base pairs of the double-stranded nucleic acid, slip into the helix between adjacent base pairs, both lengthening the helix and distorting the regularity of the backbone by unwinding the helix (Waring, 1970). Many of these same intercalators were found to be frameshifters, that is, they somehow caused either an insertion or a deletion of bases in the genome during replication. One model for this process (Streisinger et al., 1966) proposed that the intercalat-

Figure 1.1. Schematic representation of the double helix of DNA. Left: DNA in the B form with the base pairs perpendicular to the helix axis. Right: B form DNA bound with intercalating dye molecules.

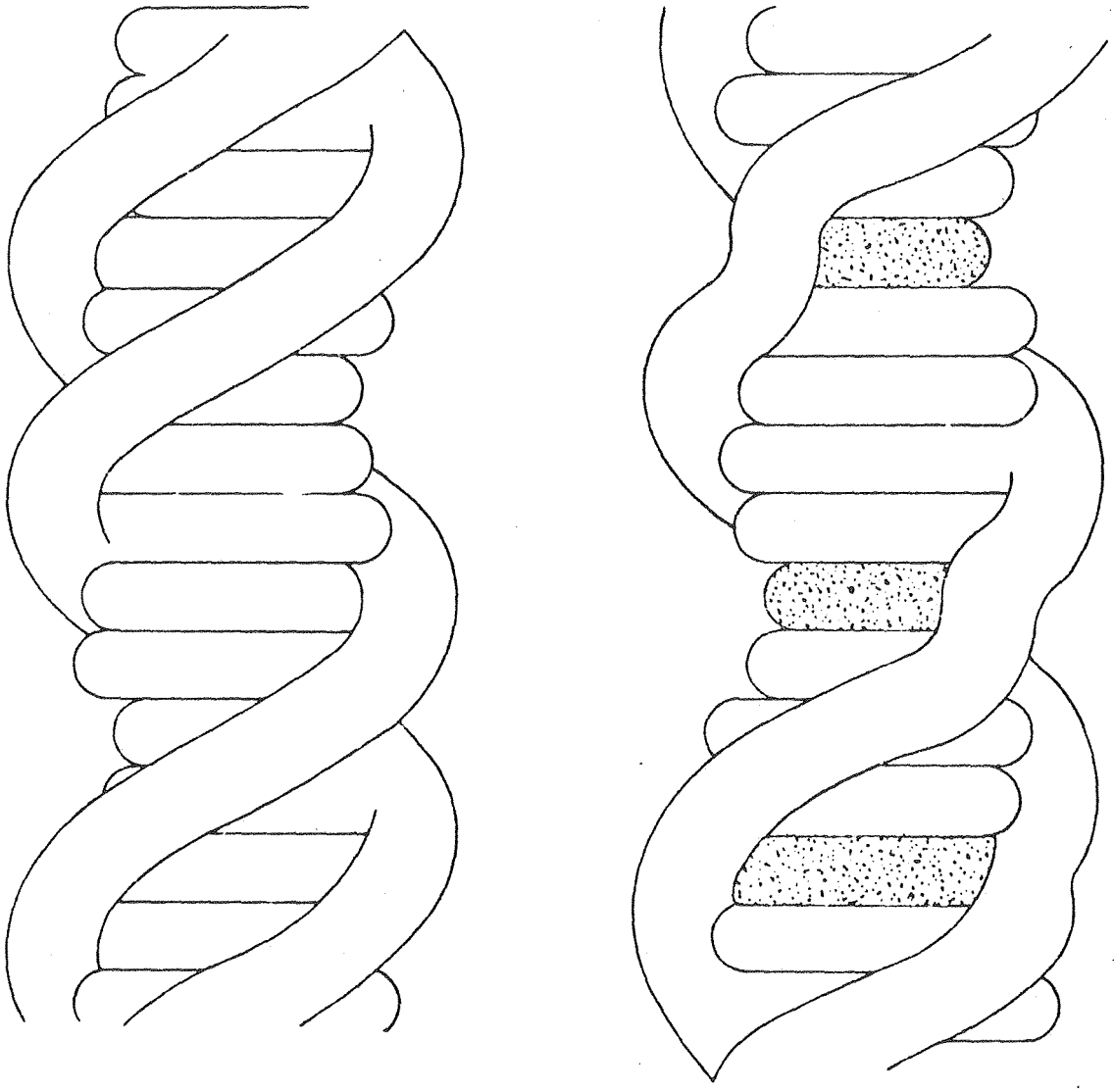

ing drugs stabilized intermediate looped structures (Figure 1.2) that may form during DNA replication, resulting in a new strand with bases inserted or deleted. One widely studied frameshift mutagen is ethidium bromide (Figure 1.3). It shows frameshifting activity in the Ames test (McCann et al., 1975) and intercalates into both DNA (LePecq & Paoletti, 1967) and double-stranded RNA (Douthart et al., 1973). Among the features which make ethidium bromide popular for intercalation studies are solubility in water, a low tendency to self-aggregate (Reinhardt & Krugh, 1978), an absorption shift in the visible spectrum upon binding to nucleic acids (Waring, 1965), a marked fluorescence intensity increase upon binding (LePecq & Paoletti, 1967), and acquisition of an induced optical activity when bound in nucleic acids (Aktipis & Martz, 1970). These spectroscopic features of the dye were not only seen upon binding to polymers, but were also present when it bound to complementary nucleic acid fragments as small as two base pairs long (Krugh & Reinhardt, 1975; Krugh et al., 1975; Reinhardt & Krugh, 1978). Sobell and co-workers (Tsai et al., 1977; Jain et al., 1977) were even able to obtain refined crystal structures at atomic resolution of ethidium ion complexes with 5-iodoUpA and 5-iodoCpG.

The induced CD spectrum with the dinucleoside mono- and diphosphates, together with nuclear magnetic resonance chemical shifts of the dye protons, led to the conclusion that an ethidium ion was intercalated between the two base pairs of the minihelix in the complexes (Krugh & Reinhardt, 1975; Krugh et al., 1975). The structures obtained from the X-ray data confirmed that the phenanthridinium ring

Figure 1.2. The Streisinger model of frameshift mutagenesis.

FRAMESHIFT MUTATIONS

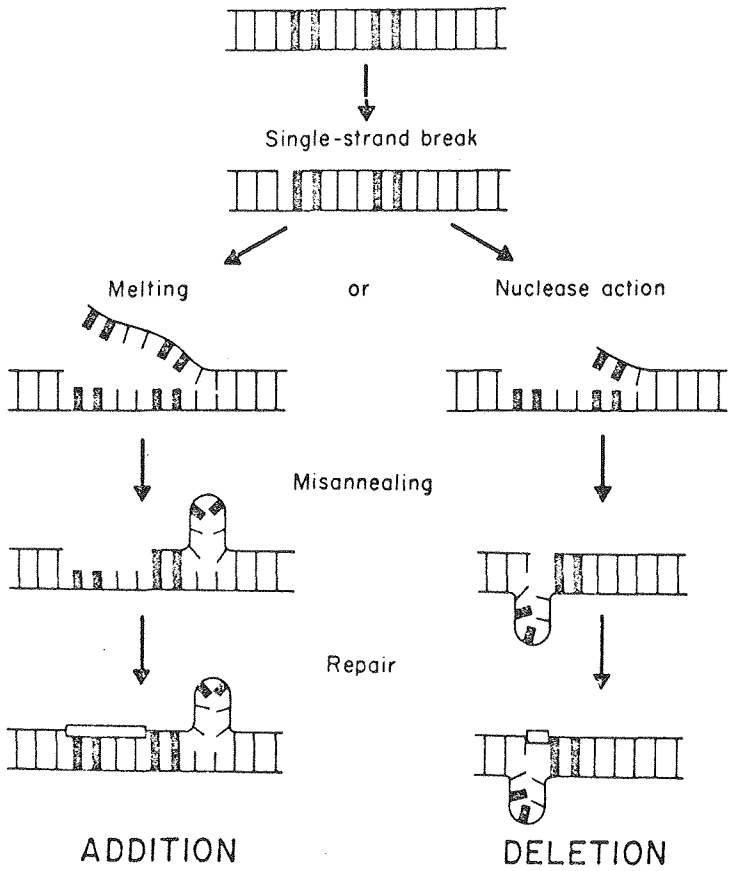

XBL 782-7420A

Figure 1.3. Structure of ethidium bromide, a frameshift mutagen.

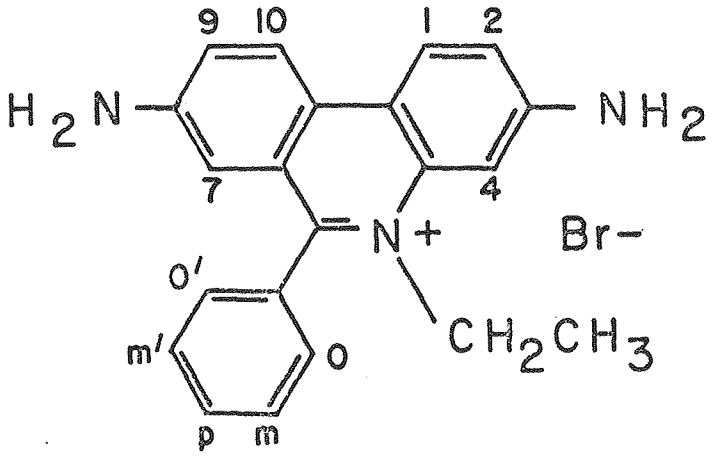

Ethidium Bromide

XBL 782-7422

of a dye molecule was stacked between the base pairs in each minihelix; in addition, a second dye was stacked outside of one base pair. In the solid state the dimer:dye stoichiometry thus was 2:2. On the other hand, all evidence pointed to a 2:1 dinucleoside phosphate:dye complex in solution as long as an excess amount of dinucleoside phosphate relative to ethidium ion was maintained (Krugh & Reinhardt, 1975).

From an optical spectroscopist's point of view, perhaps the most interesting of the above observations is the induced optical activity above 300 nm acquired by the ethidium ion (EI) when bound in nucleic acids. In Figure 1.4, characteristic circular dichroism (CD) bands at 307, 330, and 375 nm are shown for the calf thymus DNA:EI complex; an additional negative band corresponding to the visible absorption band of the dye is found at 510 nm. The magnitude of $\Delta\varepsilon$ per bound ethidium ion in DNA at 307 and 330 nm strongly depends upon the ratio of bound dye to phosphate and increases as dye bound/phosphate (r) increases. This is charted for the 307 nm band in Figure 1.5 with data taken from several studies of the phenomenon (Dalgleish et al., 1971; Aktipis & Kindelis, 1973). This curve was reproducible, within error, for binding to nucleic acids of different base contents (Dalgleish et al., 1971; Aktipis & Martz, 1974; Williams & Seligy, 1974) and for dye binding through a wide range of added monovalent counterion concentrations (Aktipis & Kindelis, 1973; Houssier et al., 1974). Increases in $\Delta\varepsilon_{bound}^{\lambda\ max}$ with increasing dye binding were also seen for ethidium ion binding to calf thymus DNA that had been denatured by heating and recooling (Aktipis et al., 1975) and for the binding of ethidium ion analogues to DNA (Kindelis & Aktipis, 1978). The behavior of the

Figure 1.4. Induced circular dichroism spectra for ethidium bound to CpG (X) and calf thymus DNA at binding ratios of 0.20 dye/phosphate (□) and 0.10 dye/phosphate (◇). The molar CD ($\Delta\varepsilon$) is calculated *per bound dye*. The salt content of the DNA solutions is ~80 mM NaCl.

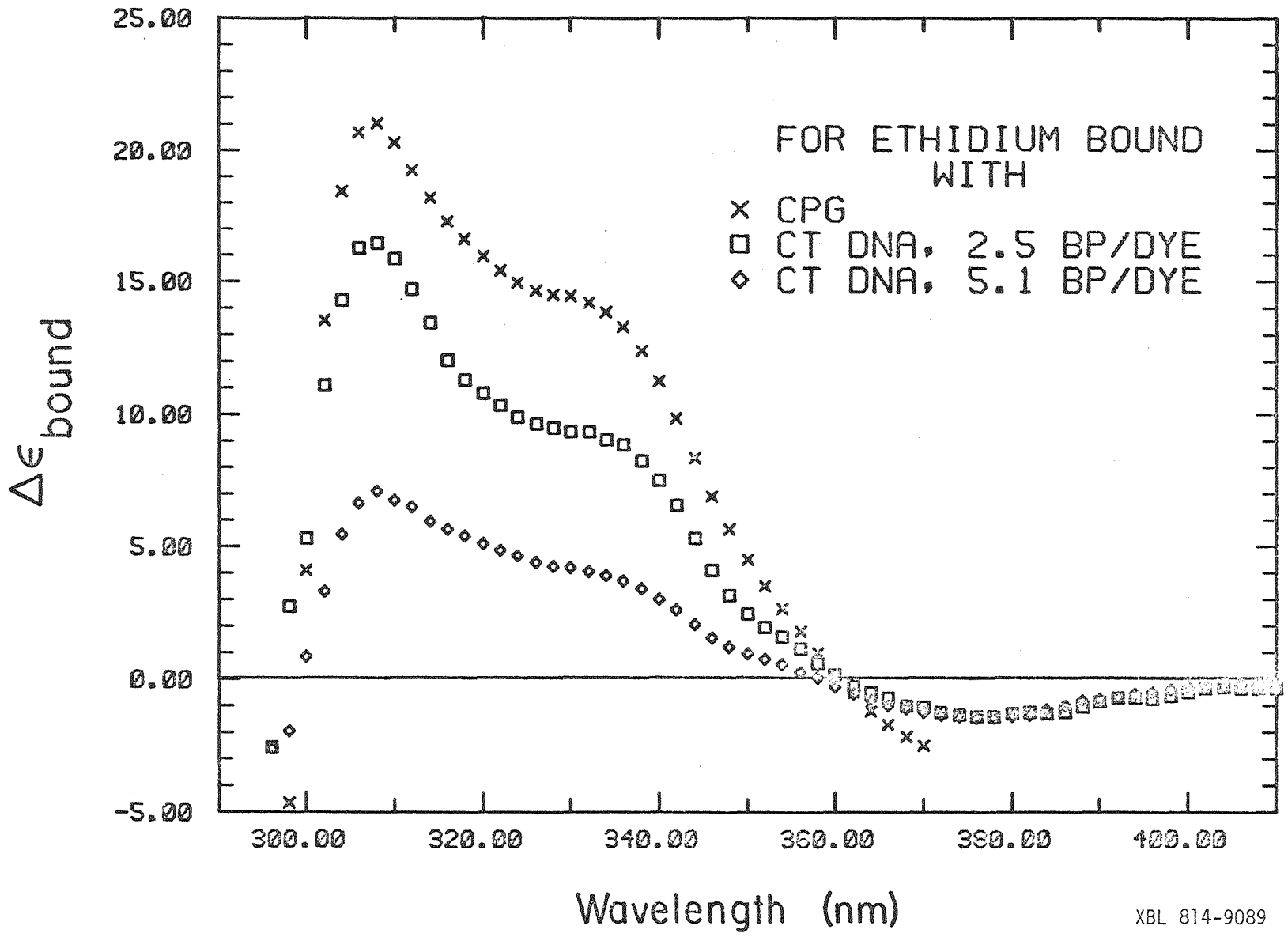
FOR ETHIDIUM BOUND
WITH
× CPG
□ CT DNA, 2.5 BP/DYE
◇ CT DNA, 5.1 BP/DYE
25.00
20.00
15.00
10.00
5.00
0.00
-5.00
300.00
320.00
340.00
360.00
380.00
400.00
Δε bound
Wavelength (nm)

XBL 814-9089

Figure 1.5. Variation of the magnitude of the induced CD per bound dye at 307 nm with the extent of ethidium binding. The molar induced CD, $\Delta\varepsilon_{bound}$, is calculated on the basis of bound dye. The extent of binding, r, is defined as the moles of bound dye per mole of DNA residues (phosphate). Data were taken from Dalgleish et al. (1971) and Aktipis and co-workers (1973, 1974), and represent a synthesis of results in different salt concentrations and nucleic acid sequences.

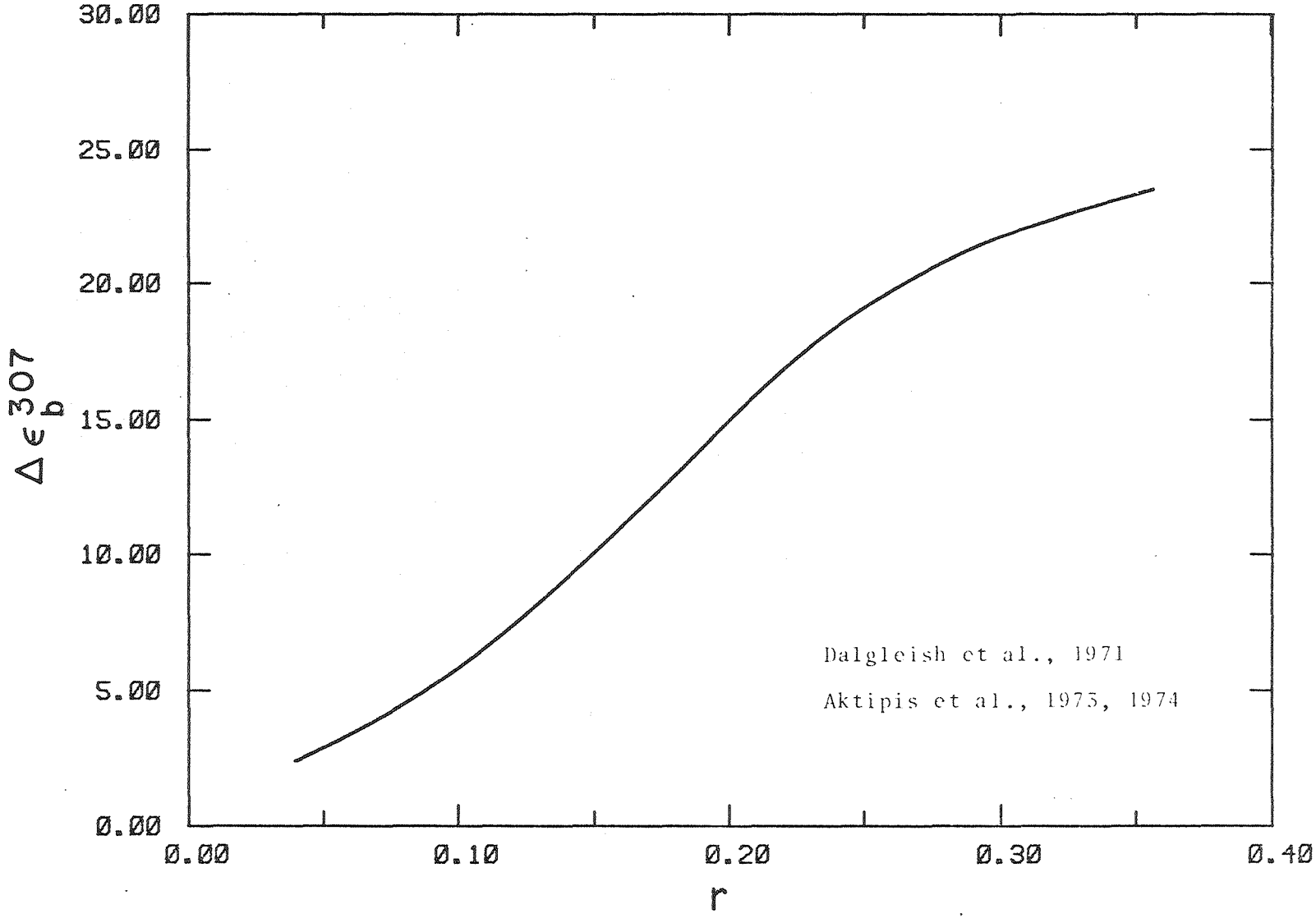

XBL 8011-12113

longest wavelength CD band at 510 nm was different: it remained relatively constant with increasing binding ratios (Houssier et al., 1974).

Dalgleish and co-workers (1969), in a study of the induced optical activity for aminoacridine dyes bound to DNA, proposed qualitative explanations for the variations of $\Delta\varepsilon^{\lambda}_{bound}$ with binding ratio:

> Two possible explanations can be advanced. (1) The variation is the result of interaction between bound ligands, which naturally increases as the number of molecules in a given interacting group increases...
>
> (2) The progressive binding of ligand molecules alters continuously the shape of the macromolecule, so that the environment of any bound ligand is determined by the number of bound ligands in its vicinity...

Mechanisms (five in all) in terms of the electronic properties of the dye and helix for the induced CD of the aminoacridines in DNA were presented by Jackson and Mason (1971). These mechanisms, together with the general picture presented by Dalgleish et al. (1969), were applied to the problem of the induced CD of ethidium ion bound in DNA. For the band at 510 nm, the asymmetry of the intercalation site in the macromolecule alone was advanced as the reason for the induced optical activity; such an interaction would remain unchanged as the extent of dye binding increased (Aktipis & Kindelis, 1973; Houssier et al., 1974). The behavior of the near UV band at 307 nm was attributed to two distinct mechanisms based on the general presentation of Dalgleish et al. (1969). The first held that at low binding ratios the induced CD per bound dye was due to the asymmetry of the binding site and thus was low. As more dye molecules intercalated in the DNA, direct interaction between transitions on two or more adjacently bound

(assuming neighbor exclusion) dye molecules gave rise to increasing magnitudes of the CD band. These interactions could either be between different transitions on the ligands (non-degenerate excitons) or the same transitions on the ligands (degenerate excitons); the latter were given greater credence because a second, roughly equal, negative CD band at 290 nm was seen under certain conditions (Aktipis & Kindelis, 1973; Houssier et al., 1974; Williams & Seligy, 1974). A second mechanism for the 307 nm band behavior was based upon symmetry arguments and attributed the induced CD in the dye to the static asymmetric perturbing field of the rest of the complex (Lee et al., 1973). In this mechanism, increased ethidium ion intercalation would alter this perturbing field and, in this case, the change in this field would increase the induced CD magnitude per bound dye.

The leveling off of the $\Delta\varepsilon^{307}_{bound}$ vs. r curve at higher r values ($r > 0.25$) was attributed to saturation of the available intercalation sites under the neighbor exclusion model (Armstrong et al., 1970; Bresloff & Crothers, 1975). In this model, intercalation of a dye molecule between two base pairs rendered the immediately adjacent sites unavailable for dye binding. Thus, the limit of dye intercalation was at $r = 0.25$; any binding beyond this was "outside" binding due to electrostatic attractions between the charged dye and the DNA phosphates (Waring, 1965). Since only intercalated dye molecules exhibited an induced CD, the magnitude of these bands (307 and 330 nm) leveled off near this limit and then decreased since outside binding increased the amount of bound dye, but not the amount of intercalated dye (Houssier et al., 1974; Williams & Seligy, 1974).

In a series of experiments designed to more fully characterize

the interaction between the dinucleoside phosphates and the ethidium ion, Pardi (1980) obtained equilibrium constants and thermodynamic parameters which established the formation of the 2:1 complex in an excess of the self-complementary dimers CpG and dCpG. As had been done previously, measurements of the induced CD per bound dye were made for these complexes (see Figure 1.4 for CpG complex). The striking feature of these spectra were the bands at 307 nm, which were comparable in magnitude to those for DNA that was saturated with ethidium ion ($r \approx 0.25$). This observation called into question the exciton mechanism proposed to explain the behavior of this band: if the greater magnitudes were simply due to a greater likelihood of dye-dye interactions at higher binding ratios in DNA, why should there be equally large magnitudes when no second dye molecule to interact with the intercalated drug was present in the dimer complex? Further work by Pardi uncovered a possible effect of salt concentration on this band: by lowering the salt concentration at a fixed binding ratio in DNA:EI complexes, $\Delta\varepsilon^{307}_{bound}$ increased. Quite possibly the second mechanism, which invoked the effects of the static field of the helix on the dye transitions, was responsible for the induced CD's binding dependence instead.

2. Purpose and Scope of This Study

We intend to examine more fully the possible mechanisms for the induced CD spectrum of ethidium ion bound in nucleic acids and also to account for variations in the spectrum as the extent of binding changes. We employ both old and new methods for studying this binding.

We begin by looking at the interaction of ethidium ion with di-

nucleoside phosphates (loosely referred to here as dimers) of RNA and DNA (Figure 1.6), using sequences which are both self-complementary and non-self-complementary (see Figure 1.7 for the complementary Watson-Crick base pairs). We obtain equilibrium constants and thermodynamic parameters for the formation of 2:1 complexes, and also examine their induced CD spectra. We find evidence for some sequence dependence in the binding as well as sequence variations in both the thermodynamic parameters and induced CD. These are all discussed in Chapter II.

In Chapter III we use a technique which relies on both the enhanced fluorescence and induced optical activity of ethidium ion in the dimer:dye complexes to obtain their CD spectra down to 220 nm. This technique is fluorescence detected circular dichroism (FDCD), and the construction and operation of this instrument are also outlined in this chapter. One of the discoveries of Chapter III, the apparent sequence dependence of the FDCD spectra for the dimer:dye complexes, is used in Chapter IV to attempt to discern any binding site preference for ethidium ion in a longer sequence formed by the complementary heptamers dCA_5G and dCT_5G.

The dependence of DNA:EI complexes' induced CD spectra upon counterion concentration is further investigated in Chapter V. Here we find an effect similar to that seen by Pardi (1980): $\Delta\varepsilon^{307}_{bound}$ increases as the counterion concentration decreases, all other things being equal. We use polyelectrolyte theory (Manning, 1978) to propose an explanation for this effect. Finally, in Chapter VI, we consider mechanisms for the induced CD of ethidium ion and its dependence upon binding ratios. We propose a possible mechanism for this behav-

ior in light of our new evidence and suggest further experiments to test its validity.

Figure 1.6. Structure of a ribo- dinucleoside phosphate, CpG. Replacement of each 2' OH group by H results in the deoxy-ribo- dinucleoside phosphate, dCpG.

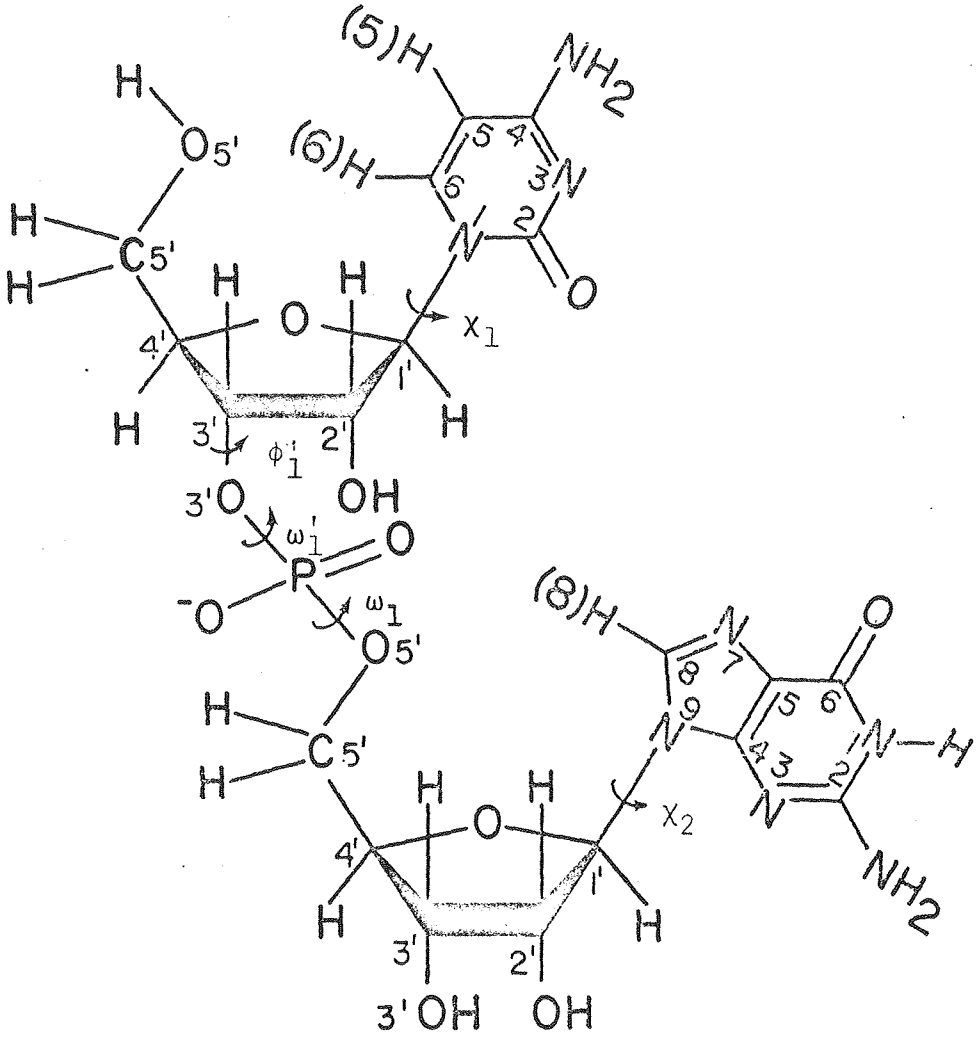

CpG

XBL 8011-12115

Figure 1.7. Watson-Crick complementary base pairs for DNA. Replacement of the CH_3 group of thymine by H results in uracil, its RNA analogue.

WATSON - CRICK BASE PAIRS

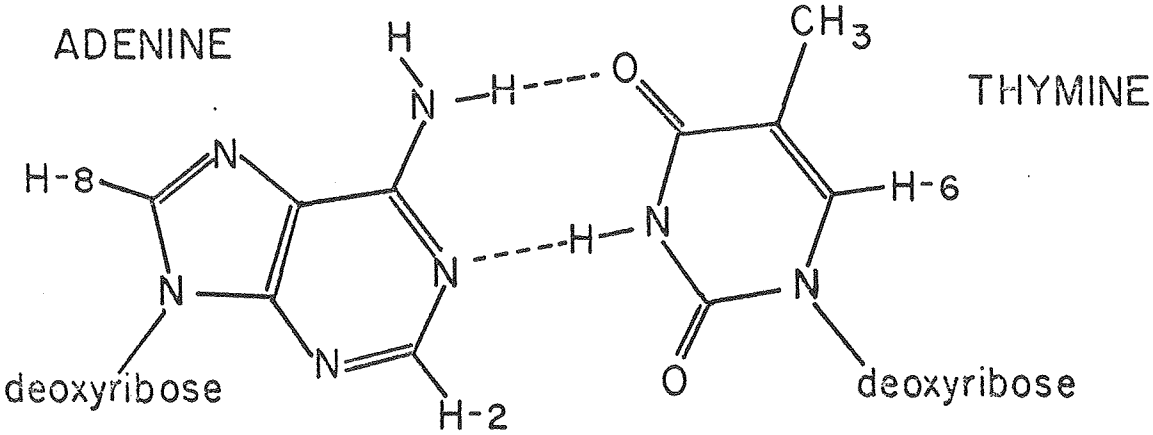

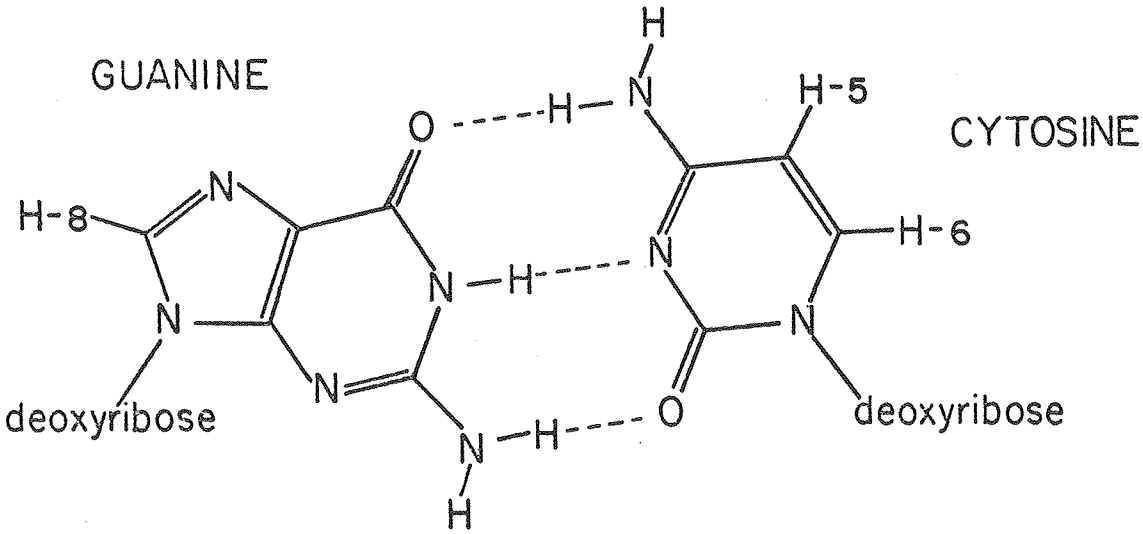

XBL 801-7722

Chapter II

DINUCLEOSIDE PHOSPHATE - ETHIDIUM ION INTERACTIONS

1. Introduction

Several optical studies of the binding of ethidium ion (EI) to the dinucleoside mono- and di- phosphates have previously been done. In these studies, the sequences of the dimers were both self-complementary and non-self-complementary (Krugh & Reinhardt, 1975) and both deoxyribo- and ribo- nucleosides were utilized (Krugh et al., 1975; Reinhardt & Krugh, 1978). Until the study of Pardi (1980), no quantitative conclusions had been reached on the strength of the binding, although pyrimidine (3'-5') purine sequences were known to bind the dye more readily than purine (3'-5') pyrimidine sequences. Furthermore, the complexes' stoichiometry was 2:1 dimer:dye when an excess of the dimer(s) was present (Krugh & Reinhardt, 1975; Reinhardt & Krugh, 1978).

Pardi (1980) established the 2:1 stoichiometry of the dinucleoside phosphate:ethidium ion complex when the dye was present in an excess of the self-complementary dimer CpG and showed that aggregates of this complex did not form under his experimental conditions. Equilibrium constants for the complexes of ethidium ion with CpG, dCpG, and UpA were obtained, as well as enthalpies and entropies of formation for the first two dimers' complexes. In addition to these results, he also examined the induced circular dichroism of CpG:CpG:EI and found the magnitude of the CD band at 307 nm *per bound dye* ($\Delta\varepsilon^{307}_{bound}$) was as large (~22 L/mol-cm) as it was for DNA saturated

with ethidium ion (Aktipis & Kindelis, 1973).

In this chapter we extend the quantitative binding study of ethidium ion with dimers to include five new base sequences, among them, non-self-complementary dimers. Our results are consistent with Pardi's conclusions and further bolster his contention that dye-dye interactions are not necessarily responsible for the increase in the 307 nm CD band as the extent of binding increases.

2. Experimental

A) Materials

Ethidium bromide was purchased from Sigma Chemical. The ribodinucleoside (3'-5') phosphates: CpG, UpA, CpA, UpG, ApA, UpU, ApG, CpU, ApU, and GpC, were purchased from Sigma. The deoxyribo- dinucleoside (3'-5') phosphates dCpG and dTpA were purchased from Collaborative Research. All dimers except UpA and dTpA were used without further purification. UpA and dTpA displayed several bands under UV viewing of thin layer chromatograms developed in 70:30 v/v ethanol: 1 M ammonium acetate. Each dimer was spotted on Whatmann $3\frac{M}{M}$ chromatography paper (previously developed in ethanol to remove any impurities) and developed in 80:20 v/v ethanol:water. The dimer bands were cut out, moistened with doubly distilled water, and eluted from the paper by analytical centrifugation. The fractions were pooled, filtered through a 0.45 μ Millipore filter, frozen, and lyophilized. This procedure was repeated with the substitution of a 50:50 v/v ethanol:water solvent for the second development. Upon completion of the process, each dimer displayed only one band on a thin layer chromatogram.

The buffer used in all cases was composed of 0.18 M NaCl, 8 mM

Na_2HPO_4, 20 mM NaH_2PO_4, and 0.1 mM Na_2EDTA and had a measured pH of 7.0.

B) Methods

Ethidium bromide was dissolved in doubly distilled water, followed by freezing and lyophilization. This procedure was repeated twice. Stock solutions of this material were prepared with doubly distilled water and were kept cool and in the dark. Stock solutions of the dimers were prepared by dissolving each in doubly distilled water and were kept in the refrigerator.

Concentrations were monitored optically using a Cary 118 spectrophotometer. The molar extinction coefficient of ethidium ion was taken as ε_{480} 5600 (Waring, 1965). The extinction coefficients for the ribo- dimers at pH 7 and 25^{0}C were taken from Warshaw (1966); the extinction coefficients for the deoxyribo- dimers at pH 7 were taken from P-L Biochemicals Reference Guide and Price List 105 (p. 27, 1977). The molar extinction coefficients on a *per dimer* basis were ε_{255} 19,800 for CpG, ε_{259} 24,600 for UpA, $\varepsilon_{261.5}$ 21,000 for CpA, ε_{255} 20,000 for UpG, $\varepsilon_{257.5}$ 27,400 for ApA, ε_{261} 19,600 for UpU, ε_{255} 25,000 for ApG, ε_{265} 16,200 for CpU, ε_{260} 24,000 for ApU, $\varepsilon_{255.5}$ 18,000 for GpC, ε_{254} 19,700 for dCpG, and ε_{260} 20,800 for dTpA.

Solutions containing variable amounts of the dimers and a constant dye concentration were diluted to a fixed volume with buffer. Ethidium ion concentrations were typically around 0.04 mM, while the total dimer concentration was in excess of this by 8-fold up to 250-fold, depending upon the ease of complex formation. For complexes with the non-self-complementary dimers, roughly equal amounts (within 10%) of the two dimers were added to each solution. Complex for-

mation was monitored by measuring the shift of the band in the visible spectrum (Waring, 1965) and spectra were measured either on the Cary 118 or a Gilford 250 spectrophotometer with scanning option. Spectra were digitized and stored for later use via interfaced Pet minicomputers and software partially provided by Mr. Jeff Nelson. Temperatures of the sample cells were maintained to ± 0.4 ^{0}C by an external bath (Neslab Instruments) on the Cary 118 and to ± 0.1 ^{0}C by a Gilford 2527 thermoelectric temperature programmer on the Gilford 250. All spectra were run in 1 cm path length quartz micro cells (Precision Cells).

Binding studies were carried out at 0 ^{0}C in all cases. Binding was also studied at 5 and 10 ^{0}C for some dimers. The equilibrium constants at different temperatures were used to determine ΔH^0 and ΔS^0 for complex formation by van't Hoff plots of ln K vs. T^{-1}. Additional points were provided for some plots by performing optical melts on solutions with known dimer:dye ratios. The melting temperature of the complex, T_m, was defined as the midpoint of the transition and, at this point, half the available dye was bound in the complex and half was free in solution.

Circular dichroism (CD) spectra of the complexes were run on a Cary 60 spectropolarimeter equipped with a Cary 6001 accessory. Cell temperature was maintained at 0 ^{0}C (± 0.2 ^{0}C) with a thermoelectrically cooled temperature jacket (Allen et al., 1972) connected to a Hallikainen Thermotrol. Quartz micro cells of 1.0 and 0.5 cm were used. Solutions prepared for the binding studies were also used in the circular dichroism study. A baseline spectrum on an equal amount of total dimer was deducted from each spectrum. Spectra were digitized and

stored using a PDP 8/E minicomputer and the revised Super Spectrum software (Appendix B).

Mixing and instrumental errors in the determinations of the equilibrium constants and $\Delta\varepsilon_{bound}$ were calculated with the propagation formulae in Bevington (1969). The estimated errors in pipetting and mixing were ~10%. Errors in the absorbance and CD spectra arose from baseline shifts and noise during measurement. The estimated errors for the spectra were ~2% of the chart's full scale value during a run. All analyses are discussed further in Appendix A.

3. Results

A) Optical Titrations

The shift of the 480 nm absorption band of a fixed amount of ethidium ion mixed with successively larger amounts of dTpA is shown in Figure 2.1. This shift is analogous to that seen when the dye binds to nucleic acids and can be used to determine the binding constant for the reaction if a stoichiometry is known or assumed. The greatest difference in absorbance between the dye with no dimer present and the same amount of dye in an excess of dimer occurs at 465 nm, and data at this wavelength are used in all these calculations.

Writing the general reaction for two dimer molecules combining with one dye:

$$NpN_a + NpN_b + EI \rightleftarrows \text{Complex} \qquad (1)$$

the equilibrium expression is

$$K = \frac{[C_{Cplx}]}{[C^0_{NpN_a} - kC_{Cplx}][C^0_{NpN_b} - kC_{Cplx}][C^0_{EI} - C_{Cplx}]} \qquad (2)$$

Figure 2.1. Titration of 0.043 mM ethidium ion with increasing amounts of dTpA. Cell length is 1 cm and the temperature is $0^{o}C$.

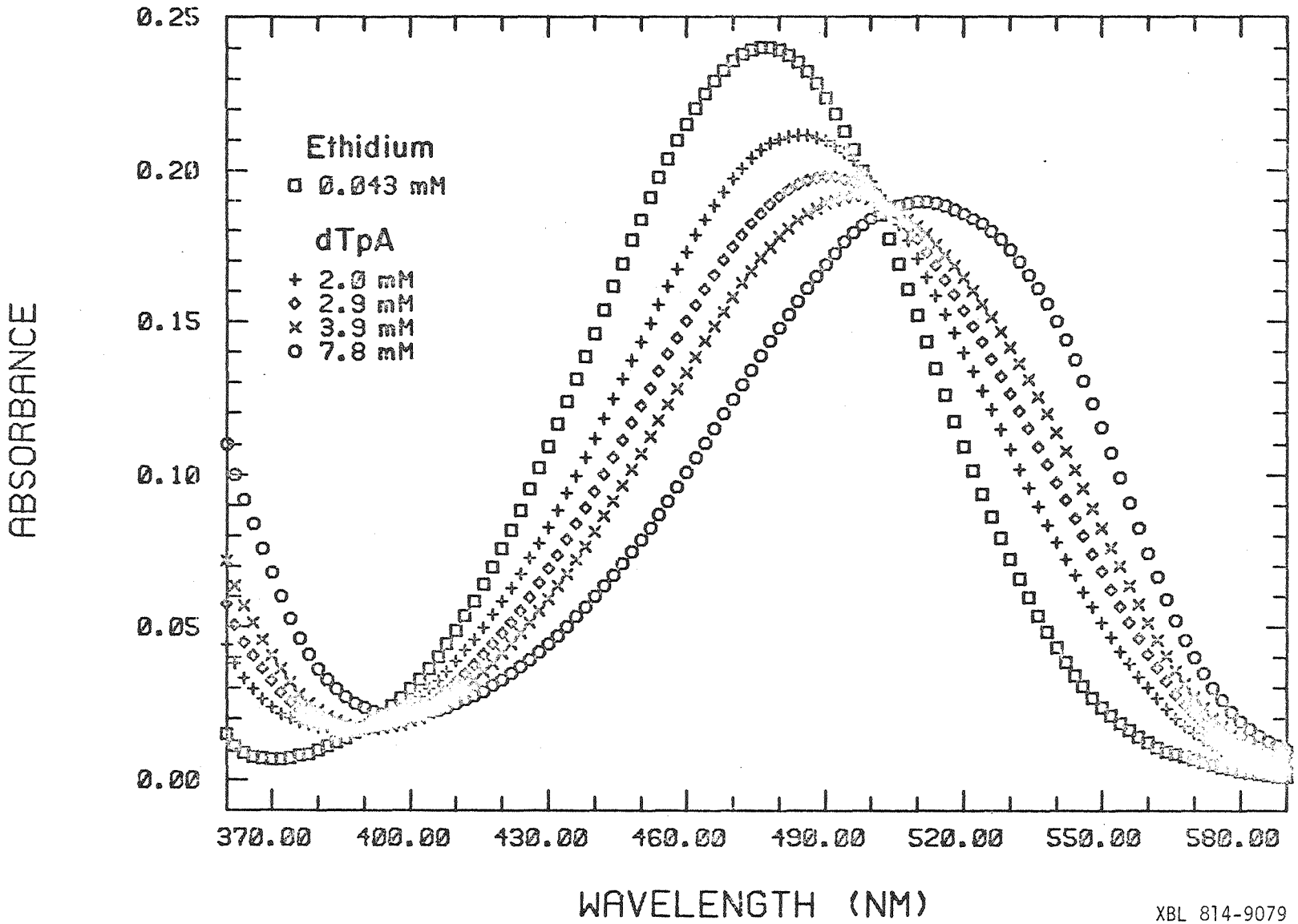
Ethidium
0.043 mM
dTpA
2.0 mM
2.9 mM
3.9 mM
7.8 mM
ABSORBANCE
0.25
0.20
0.15
0.10
0.05
0.00
370.00
400.00
430.00
460.00
490.00
520.00
550.00
580.00
WAVELENGTH (NM)

XBL 814-9079

where k = 1 if the dimers are non-self-complementary ($NpN_a \neq NpN_b$) and k = 2 if the dimers are self-complementary ($NpN_a = NpN_b$). $C^0_{NpN_a}$, $C^0_{NpN_b}$, and C^0_{EI} are the total concentrations of dimer a, dimer b, and ethidium ion, respectively. C_{Cplx} is the equilibrium concentration of the complex. Analysis of the data was performed using the method of Benesi and Hildebrand (1949). For cell lengths of 1 cm we can write

$$C_{Cplx} = \frac{A - \varepsilon_f C^0_{EI}}{\varepsilon_b - \varepsilon_f} \tag{3}$$

where A is the measured absorbance of the solution of dimer(s) plus dye, $\varepsilon_f C^0_{EI}$ is the measured absorbance of the dye solution alone, and ε_f and ε_b are the molar extinction coefficients of the free and complexed dye, respectively. Substituting (3) into (2) and rearranging, we obtain the form

$$\frac{C^0_{EI}}{A - \varepsilon_f C^0_{EI}} = \frac{1}{[C^0_{NpN_a} - kC_{Cplx}][C^0_{NpN_b} - kC_{Cplx}][\varepsilon_b - \varepsilon_f]\,K} + \frac{1}{[\varepsilon_b - \varepsilon_f]} \tag{4}$$

which, by plotting the left-hand quantity vs. $\{[C^0_{NpN_a} - kC_{Cplx}][C^0_{NpN_b} - kC_{Cplx}]\}^{-1}$ will yield both $[\varepsilon_b - \varepsilon_f]$ and K from the slope and intercept if the data are linear. The equilibrium concentrations of the dimers were initially unknown, but as a first approximation we set C_{Cplx} at zero and used only the initial concentrations of each (which were larger than any amount of complex which may have formed). Arriving at K via (4), we then obtained C_{Cplx} via (2). Restarting the process with this value in (4), we iterated to convergence of the e-

quilibrium constant to within 1%. Convergence typically occurred within four iterations (see Appendix A for the computer program used to perform this calculation).

Benesi-Hildebrand plots for the formation of 2:1 dimer:dye complexes with ethidium ion and the dimers UpA; dTpA; CpA and UpG; ApA and UpU; ApG and CpU; and ApU are shown in Figures 2.2a - 2.2f. All plots exhibit good linear fits to the data, indicating the assumption of a 2:1 stoichiometry was valid. Table I lists the equilibrium constants and $[\varepsilon_b - \varepsilon_f]$ for each case, along with the results for the dimers CpG and dCpG from Pardi (1980). The data are grouped in related general sequences, i.e., all ribo- dinucleoside sequences of the pyrimidine (3'-5') purine type and so forth, to facilitate comparison of sequence similarities and differences. No equilibrium constant for GpC plus ethidium ion could be measured owing to the formation of a precipitate in the mixture, even at room temperature.

B) Optical Melts

Additional values for the equilibrium constants of complex formation were obtained by performing optical melts on solutions of known dimer:dye concentrations. Monitoring of the absorbance at 465 nm throughout the melt measured the amount of ethidium ion bound in the complex at any temperature. A typical melt is displayed in Figure 2.3. The same lower baseline was applied to all melts for a particular dimer:dye system. Melts were successfully run only with the CpA/UpG/EI system; dimer:dye ratios here ranged from 10:1 up to 90:1. For the ApA/UpU/EI and ApG/CpU/EI systems we were unable to obtain a lower baseline at similar dimer:dye ratios. The lower stability of these complexes left much of the dye unbound, even at low temperatures.

Figure 2.2a. Benesi-Hildebrand plot of UpA:UpA:EI complex. Line represents least squares fit to the data. Concentrations are 0.031 - 0.049 mM for ethidium ion and 0.59 - 4.0 mM for UpA. Temperature is 0^0C.

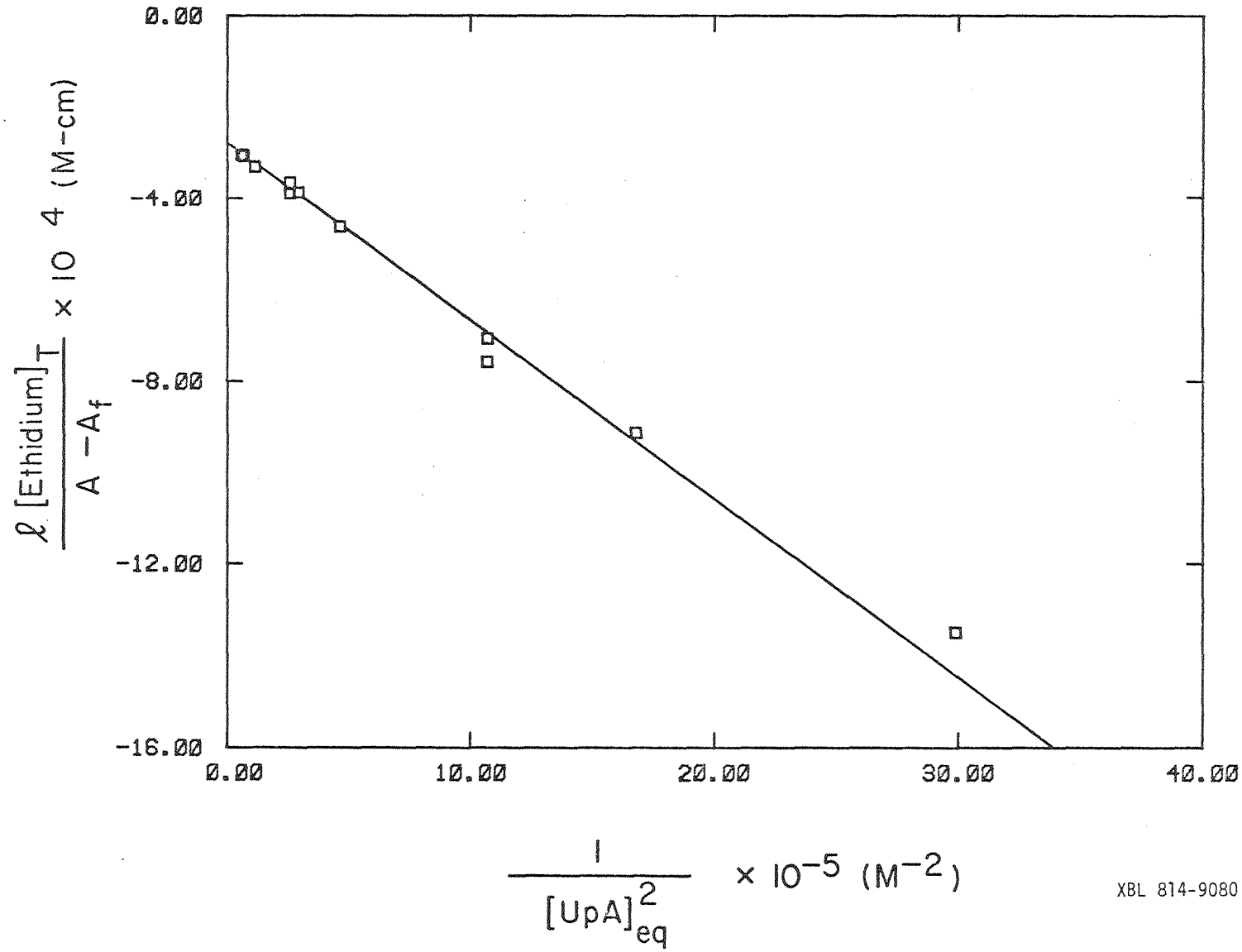
0.00
-4.00
-8.00
-12.00
-16.00
0.00
10.00
20.00
30.00
40.00
$\frac{\ell\,[\text{Ethidium}]_T}{A - A_f} \times 10^4$ (M-cm)
$\frac{1}{[\text{UpA}]^2_{eq}} \times 10^{-5}$ (M^{-2})

XBL 814-9080

Figure 2.2b. Benesi-Hildebrand plot of dTpA:dTpA:EI complex. Line represents least squares fit to the data. Concentrations are 0.043 mM for ethidium ion and 1.5 - 7.8 mM for dTpA. Temperature is 0^0C.

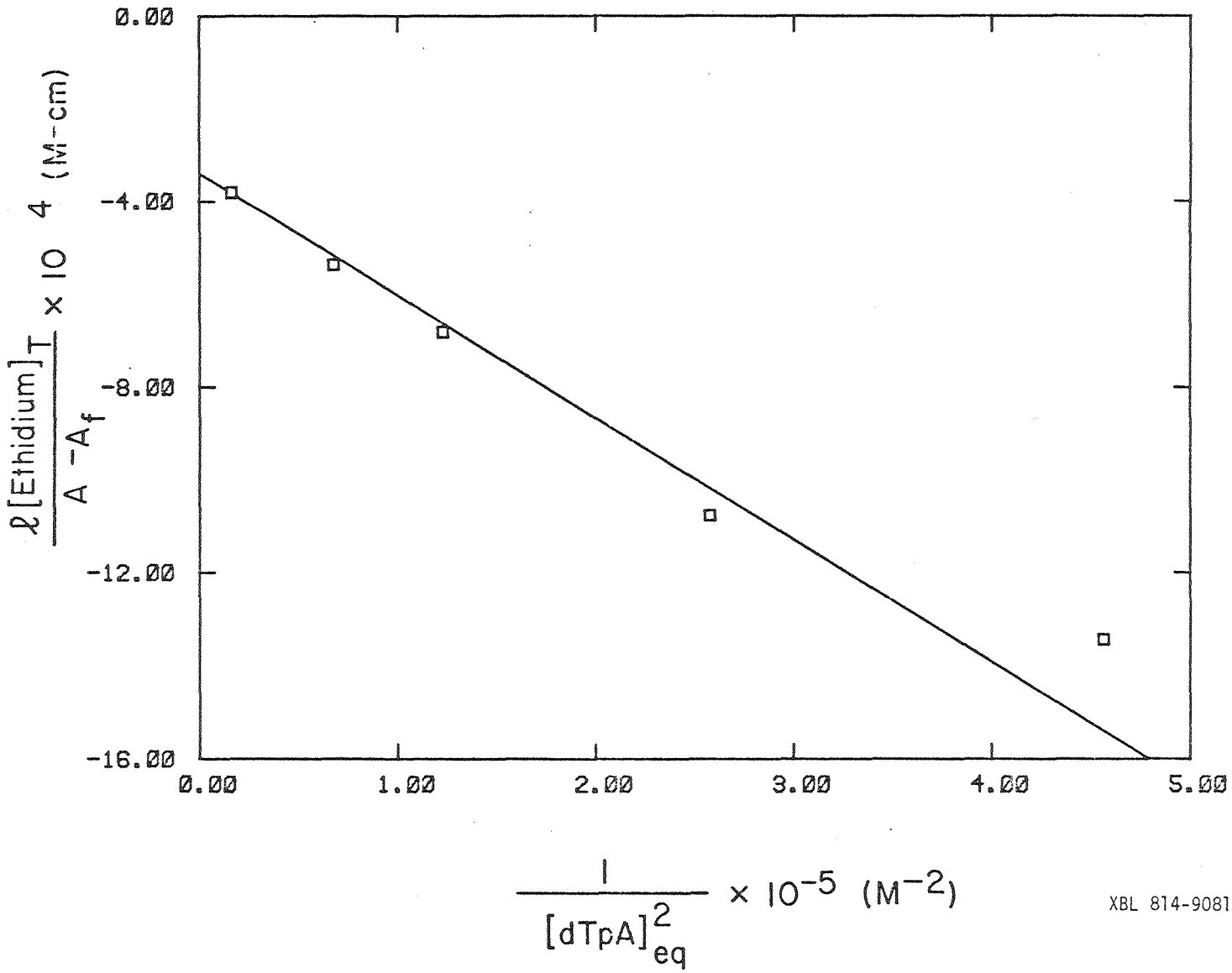
0.00
-4.00
-8.00
-12.00
-16.00
0.00
1.00
2.00
3.00
4.00
5.00
$\frac{\ell[\text{Ethidium}]_T}{A - A_f} \times 10^4$ (M-cm)
$\frac{1}{[\text{dTpA}]^2_{eq}} \times 10^{-5}$ (M^{-2})

XBL 814-9081

Figure 2.2c. Benesi-Hildebrand plot of CpA:UpG:EI complex. Lines represent least squares fit to the data. Concentrations are 0.039 mM for ethidium ion, 0.16 - 1.8 mM for CpA, and 0.15 - 1.8 mM for UpG.

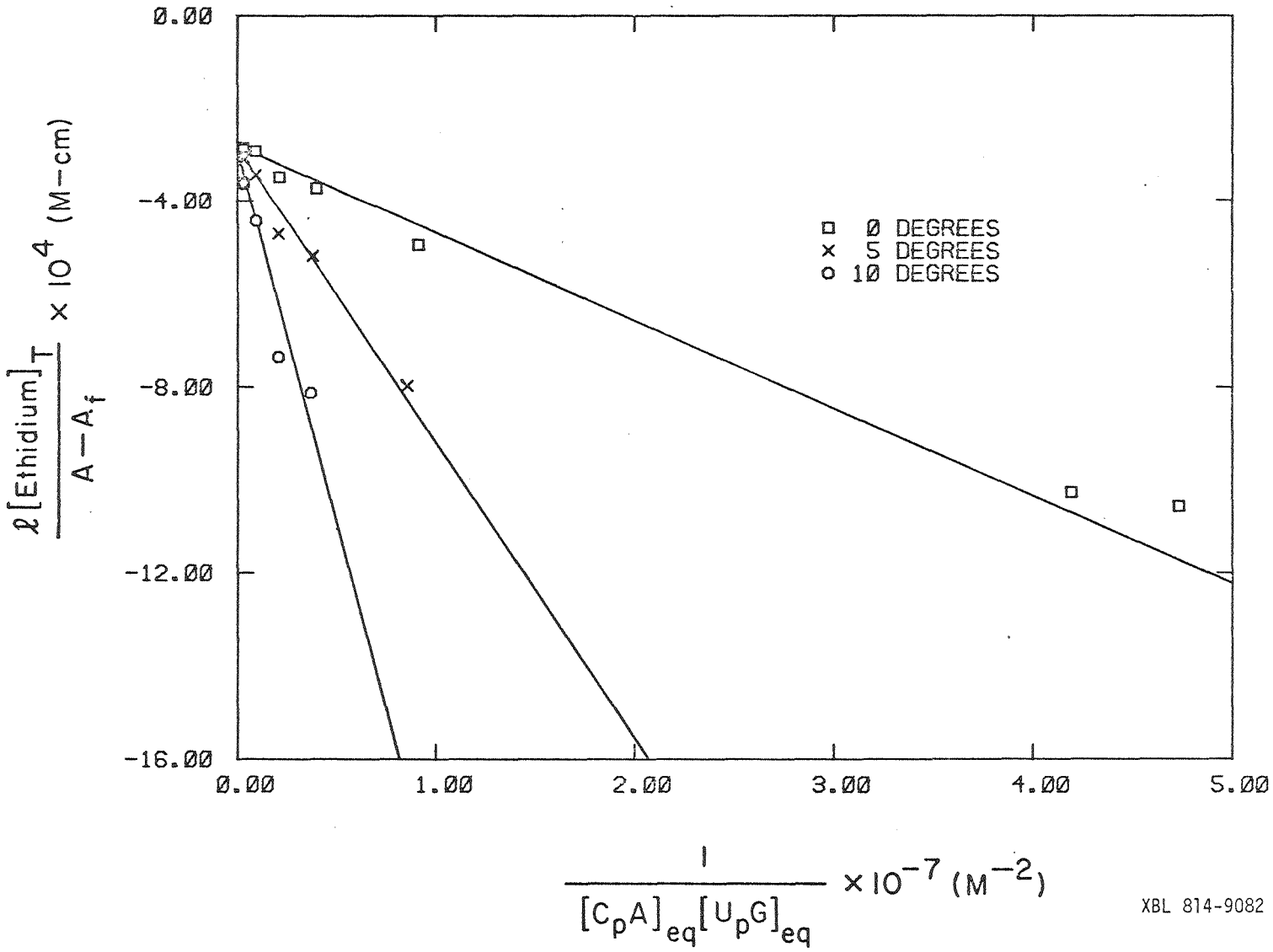
0.00
-4.00
-8.00
-12.00
-16.00
0.00
1.00
2.00
3.00
4.00
5.00
□ 0 DEGREES
× 5 DEGREES
○ 10 DEGREES
$\frac{\ell[\text{Ethidium}]_T}{A - A_f} \times 10^4$ (M-cm)
$\frac{1}{[C_pA]_{eq}[U_pG]_{eq}} \times 10^{-7}$ (M^{-2})

XBL 814-9082

Figure 2.2d. Benesi-Hildebrand plot of ApA:UpU:EI complex. Lines represent least squares fit to the data. Concentrations are 0.039 mM for ethidium ion, 1.5 - 4.9 mM for ApA, and 1.5 - 5.0 mM for UpU.

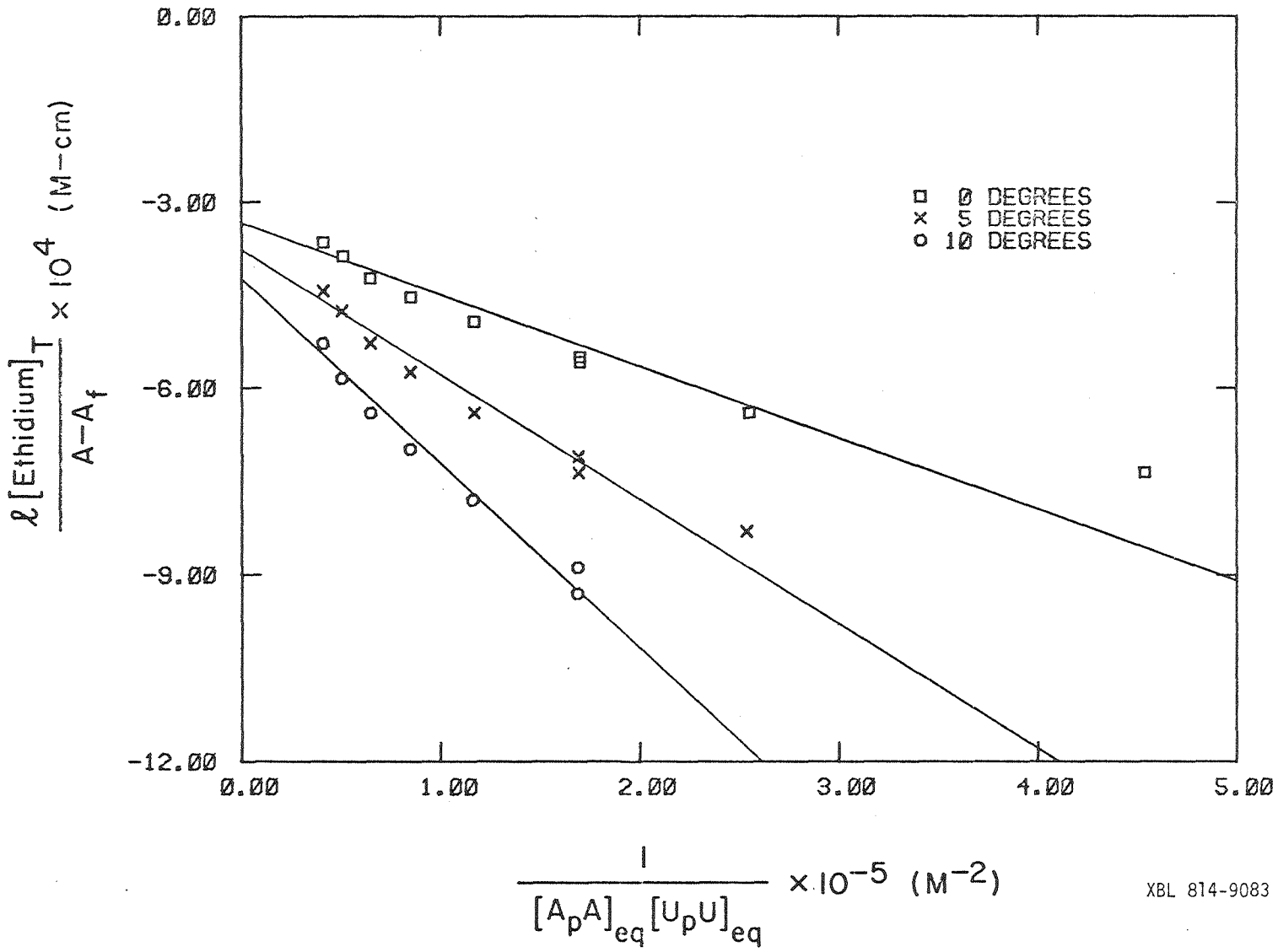
0.00
-3.00
-6.00
-9.00
-12.00
0.00
1.00
2.00
3.00
4.00
5.00
0 DEGREES
5 DEGREES
10 DEGREES
$\frac{\ell\,[\text{Ethidium}]_T}{A-A_f} \times 10^4$ (M-cm)
$\frac{1}{[A_pA]_{eq}[U_pU]_{eq}} \times 10^{-5}$ (M^{-2})

XBL 814-9083

Figure 2.2e. Benesi-Hildebrand plot of ApG:CpU:EI complex. Lines represent least squares fit to the data. Concentrations are 0.042 mM for ethidium ion, 1.6 - 3.9 mM for ApG, and 1.6 - 4.0 mM for CpU.

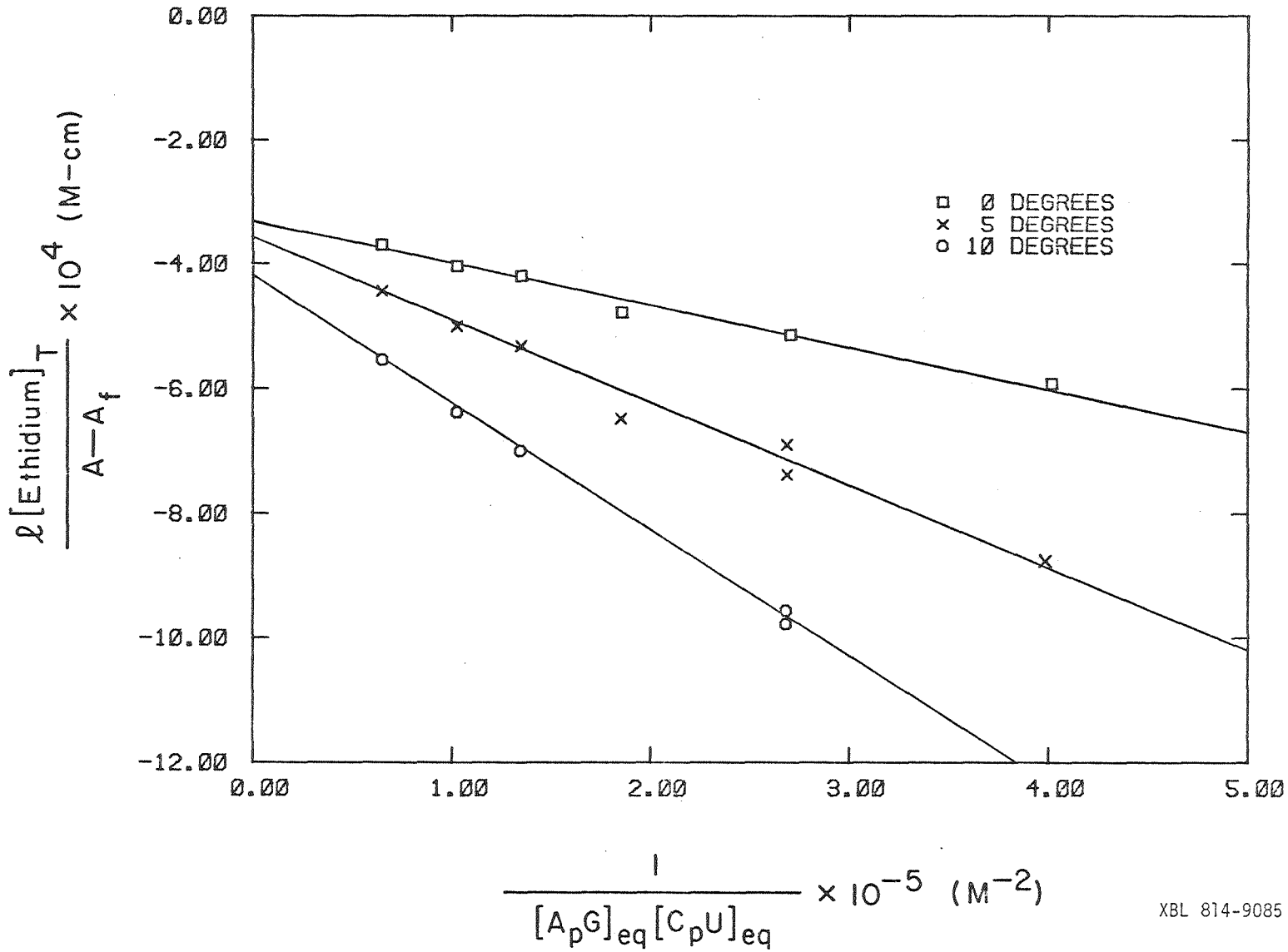
0.00
-2.00
-4.00
-6.00
-8.00
-10.00
-12.00
0.00
1.00
2.00
3.00
4.00
5.00
0 DEGREES
5 DEGREES
10 DEGREES
$\frac{\ell[\text{Ethidium}]_T}{A-A_f} \times 10^4$ (M-cm)
$\frac{1}{[A_pG]_{eq}[C_pU]_{eq}} \times 10^{-5}$ (M^{-2})

XBL 814-9085

Figure 2.2f. Benesi-Hildebrand plot of ApU:ApU:EI complex. Line represents least squares fit to the data. Concentrations are 0.040 mM for ethidium ion and 4.4 - 11 mM for ApU. Temperature is 0^0C.

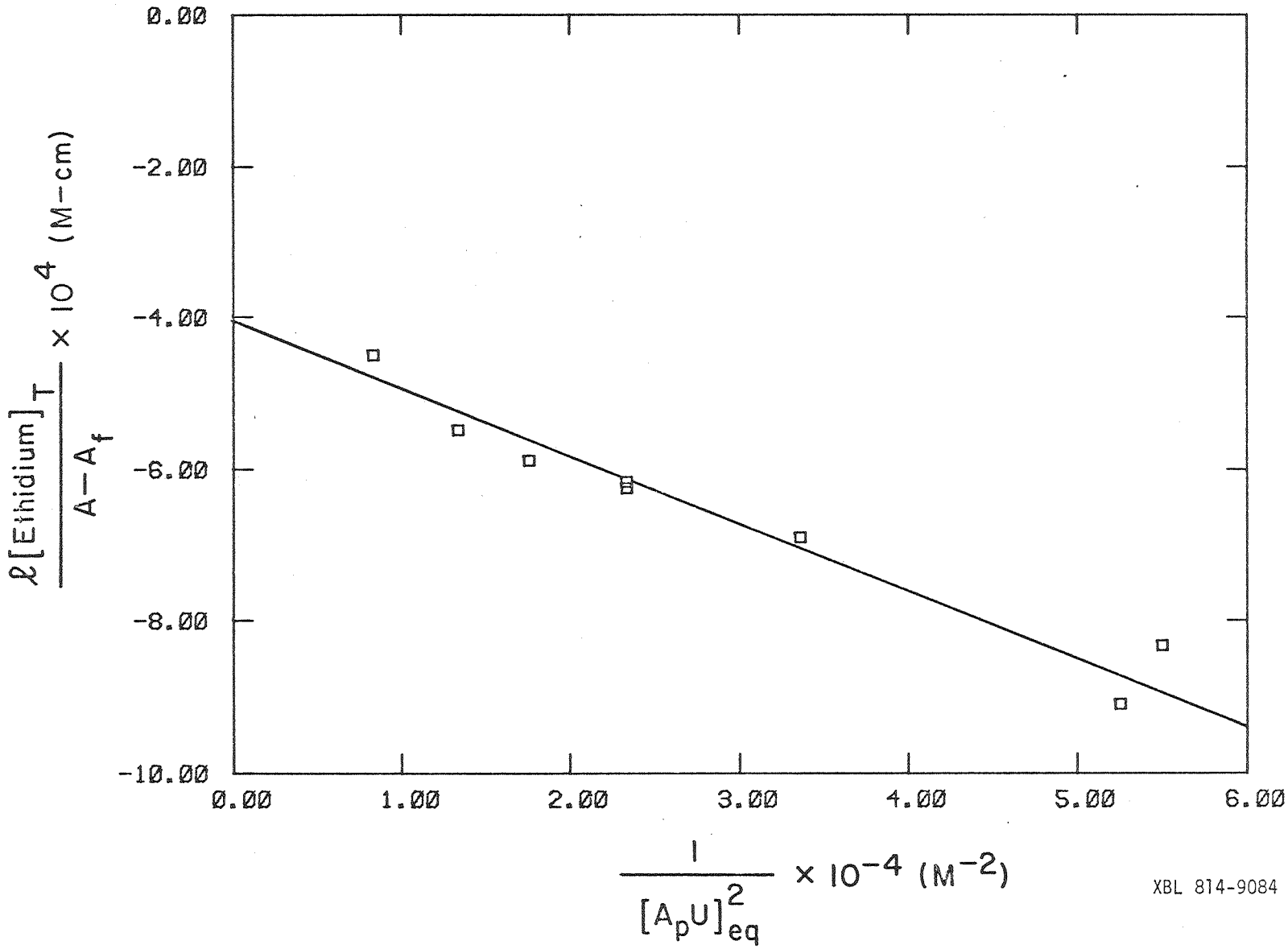
0.00
-2.00
-4.00
-6.00
-8.00
-10.00
0.00
1.00
2.00
3.00
4.00
5.00
6.00
$\frac{\ell[\text{Ethidium}]_T}{A-A_f} \times 10^4$ (M-cm)
$\frac{1}{[A_pU]^2_{eq}} \times 10^{-4}$ (M^{-2})

XBL 814-9084

TABLE I

BENESI-HILDEBRAND FITS OF ETHIDIUM ION BINDING TO MINIHELICAL SEQUENCES

Complex	Temperature (^0C)	$K \times 10^{-5}$ (M^{-2})	$\varepsilon_b - \varepsilon_f$ (L/mol-cm)
CpG:CpG:EI[a]	0	890 ± 200	-3400 ± 200
	5	420 ± 150	-3200 ± 300
UpA:UpA:EI	0	7.2 ± 1.0	-3600 ± 200
CpA:UpG:EI	0	150 ± 20	-3500 ± 100
	5	46 ± 7	-3500 ± 200
	10	19 ± 5	-3200 ± 400
dCpG:dCpG:EI[a]	0	65 ± 10	-3500 ± 200
	5	15 ± 2	-3300 ± 100
dTpA:dTpA:EI	0	1.3 ± 0.3	-2900 ± 400
ApA:UpU:EI	0	3.0 ± 0.4	-2900 ± 100
	5	1.9 ± 0.3	-2600 ± 200
	10	1.4 ± 0.3	-2300 ± 200
ApG:CpU:EI	0	4.9 ± 1.2	-3000 ± 300
	5	2.7 ± 0.6	-2800 ± 300
	10	2.1 ± 0.6	-2400 ± 400
ApU:ApU:EI	0	0.5 ± 0.1	-2500 ± 200

[a]Data from Pardi (1980).

Figure 2.3. Optical melt of CpA:UpG:EI complex monitored at 465 nm in 1 cm cell. Concentrations are 0.039 mM for ethidium ion, 3.5 mM for CpA, and 3.5 mM for UpG.

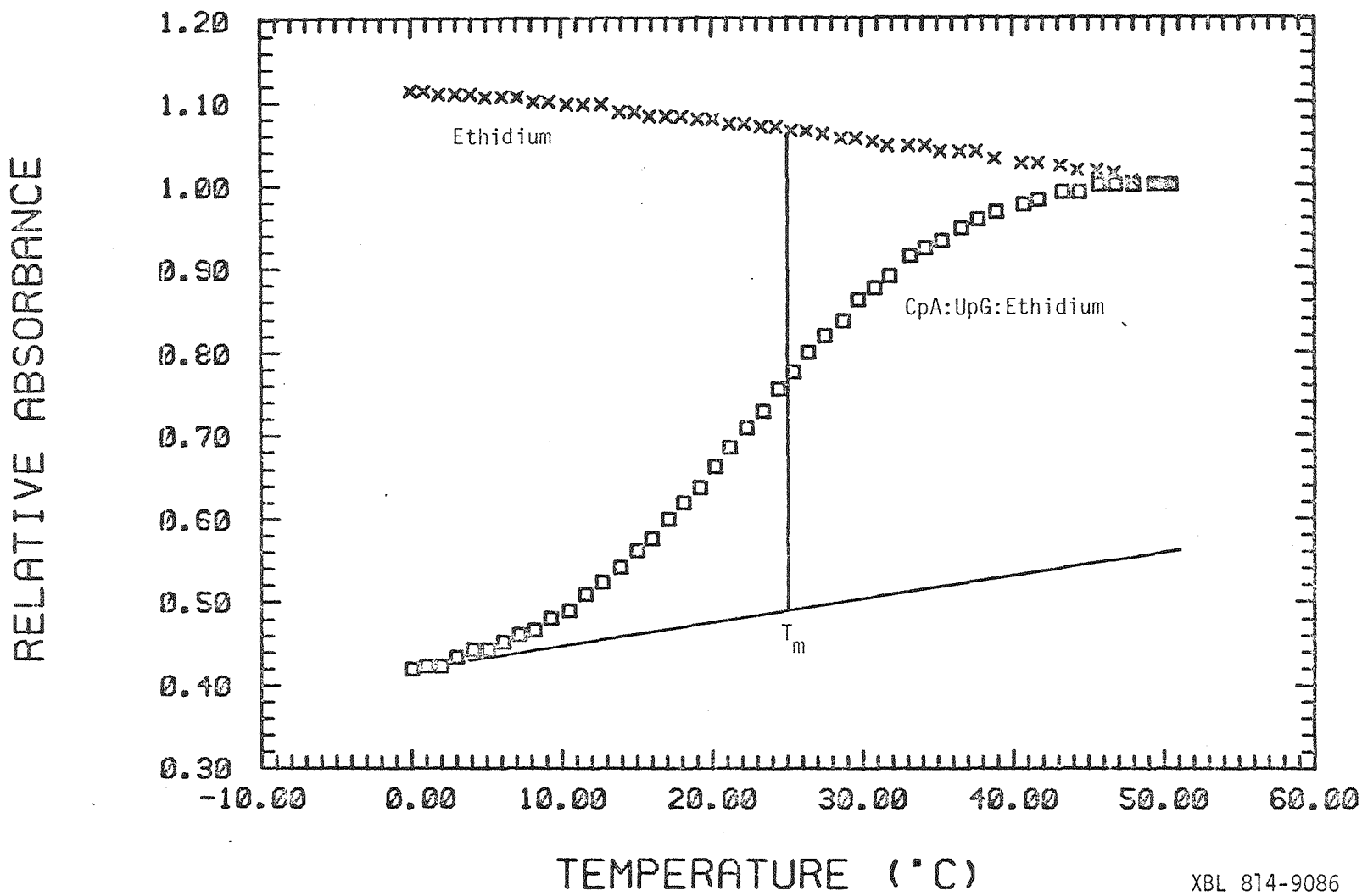
RELATIVE ABSORBANCE
1.20
1.10
1.00
0.90
0.80
0.70
0.60
0.50
0.40
0.30
-10.00
0.00
10.00
20.00
30.00
40.00
50.00
60.00
TEMPERATURE (°C)
Ethidium
CpA:UpG:Ethidium
T_m

XBL 814-9086

The melting temperature, T_m, is the temperature where one half of the total ethidium ion in solution remains complexed and the rest is free. This assumes two-state behavior for the dye during the melting process. The T_m is then the midpoint of the optical melt transition. Using equation (2), we can write an expression for K at this temperature:

$$K = \frac{1}{(a - k/2)(b - k/2)[C^0_{EI}]^2} \qquad (5)$$

where a is the concentration ratio of dimer NpN_a to total dye and b is the same number for NpN_b. Experimentally, for self-complementary dimers, a = b and k = 2, while for non-self-complementary dimers, a ≈ b, generally, and k = 1. Each pair of K and T_m values from these studies was used in the van't Hoff plots (below).

C) Thermodynamics of the Binding Reaction

Determinations of the enthalpy and entropy of the binding of ethidium ion to dimers were carried out using the equilibrium constants from both the binding studies and the optical melts. Van't Hoff plots of ln K vs. T^{-1} for CpA/UpG/EI, ApA/UpU/EI, and ApG/CpU/EI are presented in Figure 2.4. ΔH^0 and ΔS^0 for each are listed in Table II, together with those obtained by Pardi (1980) for CpG and dCpG plus ethidium ion. ΔH^0 for dCpG, -29 kcal, is comparable to that of dpCpG with ethidium ion, where ΔH^0 = -27 to -30.6 kcal, depending upon the method of measurement (Davanloo & Crothers, 1976).

D) Induced CD of Dimer:Dye Complexes

Measurements of the induced circular dichroism from 370 to 290 nm for ethidium ion in all the solutions from the binding studies were

Figure 2.4. Van't Hoff plots for ethidium complexes with CpA/UpG (□), ApA/UpU (◇), and ApG/CpU (X). Lines represent least squares fit to the data and estimated error associated with each point.

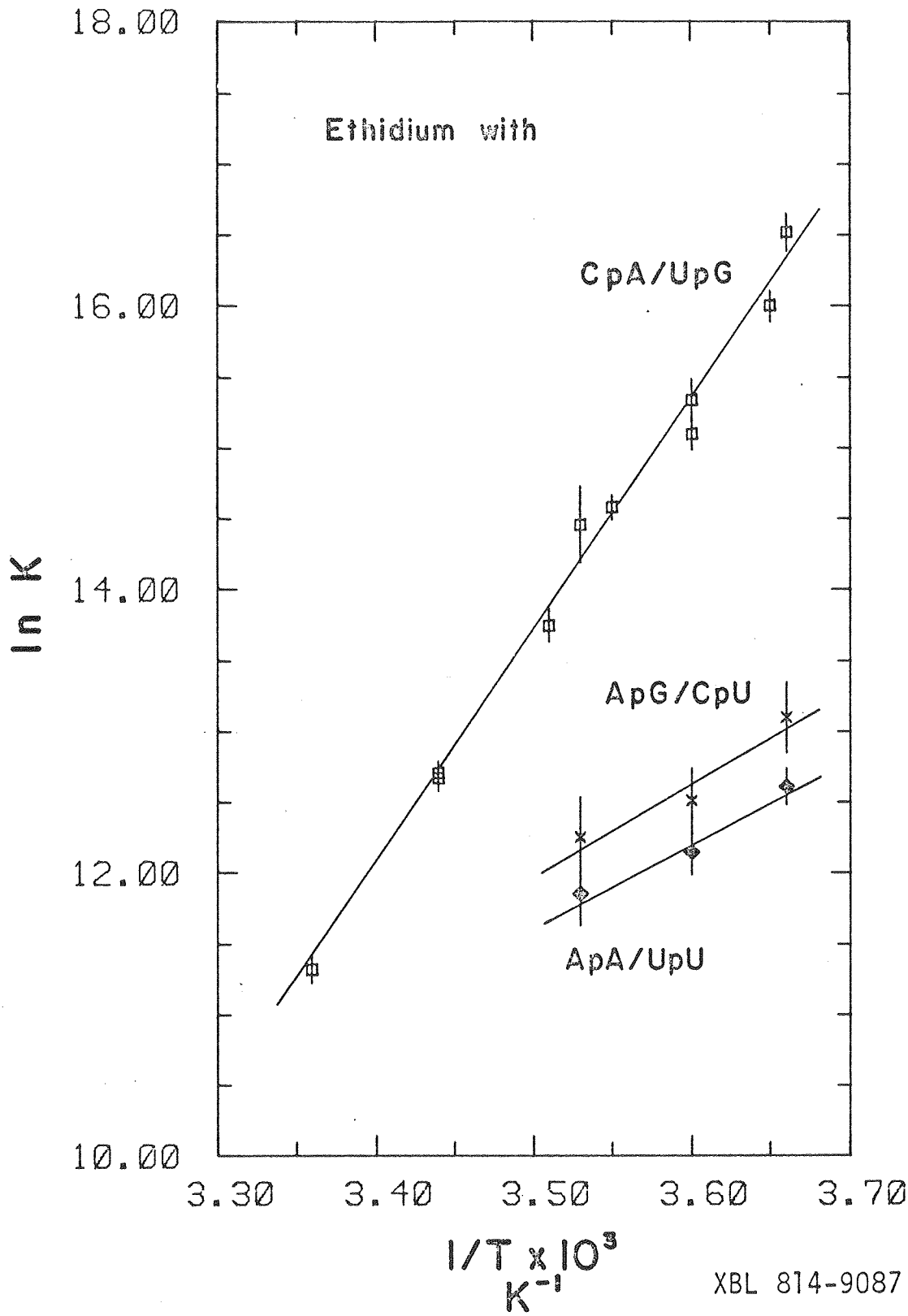
Ethidium with
CpA/UpG
ApG/CpU
ApA/UpU
ln K
18.00
16.00
14.00
12.00
10.00
3.30
3.40
3.50
3.60
3.70
1/T x 10³
K⁻¹

XBL 814-9087

TABLE II

THERMODYNAMICS OF ETHIDIUM ION BINDING

TO MINIHELICAL SEQUENCES

Complex	ΔH^0 (kcal/mol)	ΔS^0 (cal/mol)
CpG:CpG:EI[a]	-32	-84
CpA:UpG:EI	-32 ± 1	-86 ± 4
dCpG:dCpG:EI[a]	-29	-69
ApA:UpU:EI	-12 ± 2	-18 ± 7
ApG:CpU:EI	-13 ± 3	-22 ± 12

[a]Data from Pardi (1980).

attempted. An observable induced CD spectrum was obtained for all cases except for ApU plus dye, where no significant CD signal for the ApU/EI mixture above the ApU baseline was seen, even at the highest dimer:dye ratio (11 mM:0.040 mM). The molar CD per bound dye may be very low for this complex. For GpC plus ethidium ion we obtained the same spectrum as Krugh et al. (1975), but a precipitate was suspended in the cell. We believe the spectrum is largely due to scattering by this precipitate.

The induced CD spectra for UpA; dTpA; CpA plus UpG; ApA plus UpU; and ApG plus CpU plus ethidium ion are presented in Figure 2.5. The quantity $\Delta\varepsilon_{bound}$ is the molar CD *per bound dye*, i.e., per mole of complex. Values of $\Delta\varepsilon_{bound}$ were calculated using

$$\Delta\varepsilon_{bound} = \theta^0/(32.98[C_{Cplx}]\ell) \qquad (6)$$

where θ^0 is the measured ellipticity of the solution in degrees, C_{Cplx} is the equilibrium concentration of the complex, and ℓ is the path length in cm.

The largest induced CD band is between 300 and 310 nm and the maximum position varies with the base sequence. The wavelength maxima and $\Delta\varepsilon_{bound}^{\lambda\ max}$ are listed with those from ethidium ion with CpG and dCpG (Pardi, 1980) in Table III. The maximum values of $\Delta\varepsilon_{bound}$ remain quite constant throughout the range of dimer:dye ratios studied for each sequence of bases. Krugh & Reinhardt (1975), using solutions in which all ethidium ion present was bound in the complex (as judged by the shift in the visible absorption band), also obtained $\Delta\varepsilon_{bound}$ values for some of the same sequences. Their results compare favorably with ours in most cases (Table III).

Figure 2.5. Induced CD spectra per bound ethidium ion at 0^0C for 2:1 dimer:dye complexes.

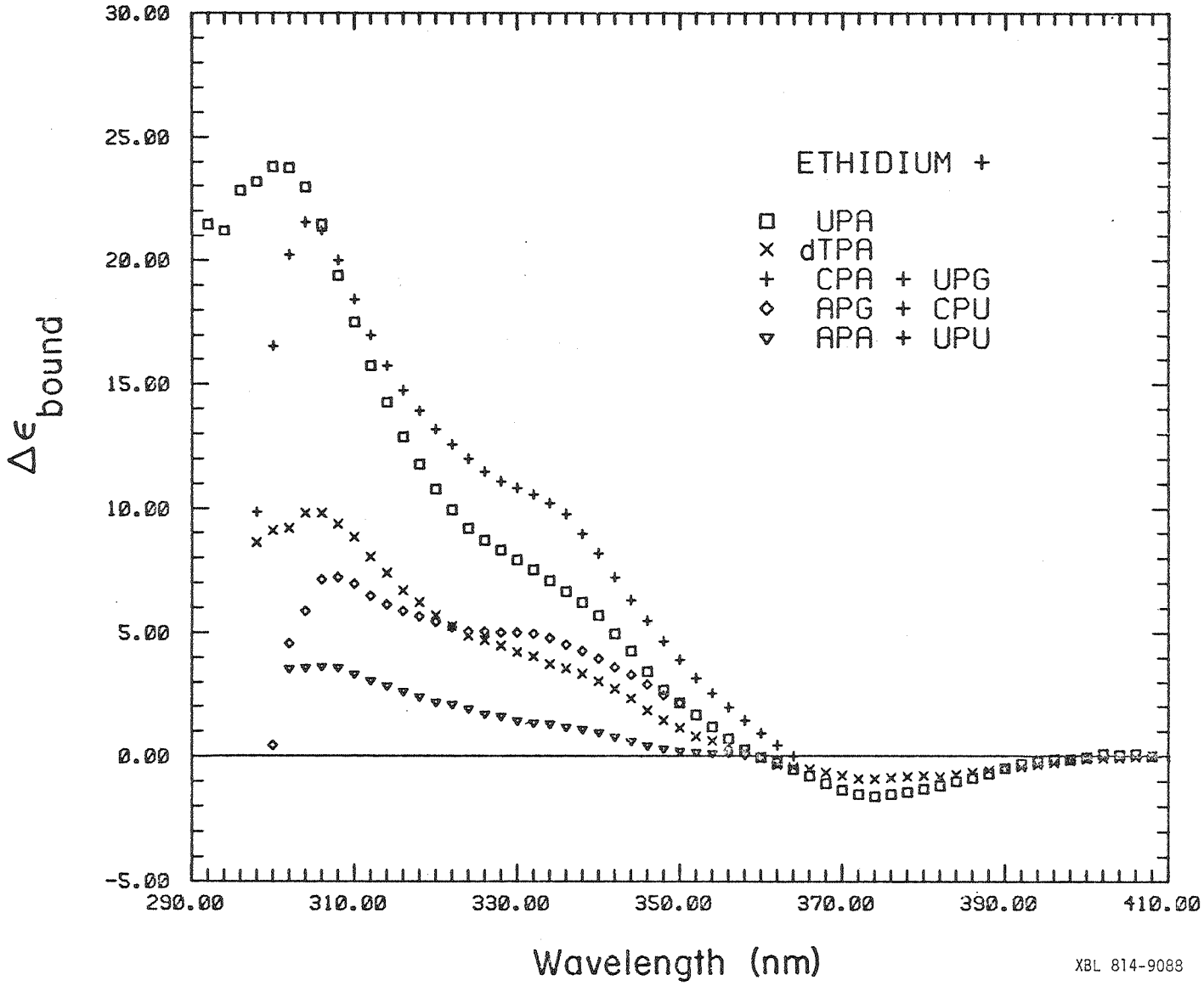
ETHIDIUM +
UPA
dTPA
CPA + UPG
APG + CPU
APA + UPU
30.00
25.00
20.00
15.00
10.00
5.00
0.00
-5.00
290.00
310.00
330.00
350.00
370.00
390.00
410.00
Δε bound
Wavelength (nm)

XBL 814-9088

TABLE III

INDUCED CD PER BOUND ETHIDIUM ION

IN MINIHELICAL COMPLEXES

Complex at 0^0C	Wavelength (nm)	$\Delta\varepsilon_{bound}$ (L/mol-cm)
CpG:CpG:EI	307	22 ± 3 [a]
	307	20 [b]
UpA:UpA:EI	301	23 ± 4
CpA:UpG:EI	305	22 ± 4
	305	21.4 [b]
dCpG:dCpG:EI	307	15 ± 3 [a]
dTpA:dTpA:EI	305	10 ± 5
ApA:UpU:EI	306	3.7 ± 0.8
	303	9.0 [b]
ApG:CpU:EI	308	7.4 ± 0.7

[a]Data from Pardi (1980).

[b]Data from Krugh & Reinhardt (1975).

4. Discussion

A) Stoichiometry of the Complexes

Krugh and co-workers (Krugh & Reinhardt, 1975; Krugh et al., 1975) stated that with excess dimer to ethidium ion, any minihelical complex formed in solution was likely 2:1 dimer:dye. However, the crystalline complexes of ethidium ion with 5-iodoUpA and 5-iodoCpG were composed of two dimers and two dyes (Tsai et al., 1977; Jain et al., 1977), even though the mother liquor originally contained an excess of the dimer in each case (Krugh & Reinhardt, 1975). More recently, fluorescence lifetime measurements of ethidium ions (Reinhardt & Krugh, 1978) established the existence of only one bound species in solution with excess CpG and roughly equal bound populations in crystals with CpG, confirming the 2:1 and 2:2 stoichiometries, respectively. Pardi (1980) obtained optical and equilibrium sedimentation evidence which also established the solution stoichiometry as CpG:CpG:EI.

We assumed the 2:1 dimer:dye stoichiometry in all our analyses, primarily because we always worked with an excess of dimer in each solution. That this was indeed the stoichiometry can be substantiated with two experimental observations: 1) the linearity of the data in the Benesi-Hildebrand plots, and 2) the constancy of $\Delta\varepsilon_{bound}$ for each complex through a wide range of dimer to dye concentration ratios.

Attempts to fit our data to either 1:1 or 2:2 complex stoichiometries (see Pardi, 1980, for methods) all failed to produce a better fit than for a 2:1 complex, even at lower dimer:dye concentration ratios where these other complexes would more likely form. Either of these two competing stoichiometries would also have caused significant

deviations from linearity in our Benesi-Hildebrand plots (Figures 2.2a - 2.2f), especially as the dimer concentration decreased. No such deviations occurred in our data.

The occurence of either alternate stoichiometry (1:1 or 2:2) would also have caused decreases in $\Delta\varepsilon_{bound}$ at lower dimer to dye concentration ratios. A qualitative reason for this can be advanced. First, any bound ethidium ion, no matter what the stoichiometry, would have displayed a red-shifted visible absorbance band. Such shifts were seen by Pardi (1980) in binding studies with single non-self-complementary dimers where no double-stranded minihelices formed. LePecq and Paoletti (1967) also saw this shift when ethidium ion bound via electrostatic attraction to the polyanion polyvinyl sulfate. Second, any dye bound, but not intercalated, would not exhibit an induced CD spectrum. Pardi (1980) observed this for the 1:1 complexes, and any outside stacking of dye on a 2:1 complex would presumably contribute little to the CD also. In combination, both effects would cause $\Delta\varepsilon_{bound}$ to decrease at lower dimer to dye concentration ratios; the absence of such decreases in our data rules out these competing stoichiometries.

B) Sequence Preferences in the Complexes

Previous studies of ethidium ion binding to dimers (Krugh & Reinhardt, 1975; Krugh et al., 1975; Reinhardt & Krugh, 1978; Lee & Tinoco, 1978) emphasized its relative preference for binding to pyrimidine (3'-5') purine sequences. We can explore this observation on a quantitative basis with this work and Pardi's (1980).

The grouping of complexes in Table I reveals a general sequence dependence for ethidium ion binding with complementary dimers. At $0^{0}C$

this order is (Py = pyrimidine, Pu = purine):

$$Py(3'\text{-}5')Pu > Pu(3'\text{-}5')Pu \equiv Py(3'\text{-}5')Py > Pu(3'\text{-}5')Py.$$

This is consistent with previous results which showed the preference for Py(3'-5')Pu over Pu(3'-5')Py; we place the remaining general sequence (Pu(3'-5')Pu ≡ Py(3'-5')Py) in the picture also. A similar order of ethidium ion binding preference has been presented for G·C base pairs in deoxytetranucleotides (Kastrup et al., 1978). The equilibrium constants for the strongest (CpG) and weakest (ApU) complexes differ considerably: by a full four orders of magnitude.

The equilibrium constants we have determined are for an overall equilibrium:

$$NpN_a + NpN_b + EI \rightleftarrows NpN_a{:}NpN_b{:}EI \ . \tag{7}$$

For the purposes of discussion, this overall reaction can be broken down into three reactions:

$$NpN_a + NpN_b \overset{K_1}{\rightleftarrows} NpN_a{:}NpN_b \text{ (wound)} \tag{8}$$

$$NpN_a{:}NpN_b \text{ (wound)} \overset{K_2}{\rightleftarrows} NpN_a{:}NpN_b \text{ (unwound)} \tag{9}$$

$$NpN_a{:}NpN_b \text{ (unwound)} + EI \overset{K_3}{\rightleftarrows} NpN_a{:}NpN_b{:}EI \tag{10}$$

where our overall equilibrium constant is the product $K_1K_2K_3$. The actual mechanism for complex formation depends upon sequence and is different from this scheme (Davanloo & Crothers, 1976), but individual contributions to the formation of the minihelix complexes can be considered within this framework.

Equation (8) represents the formation of minihelices in solution in the absence of the dye. Equation (9) represents the unwinding and separation of the two minihelix base pairs to accomodate a dye molecule, while equation (10) represents the intercalation of ethidium ion into the opened minihelix.

Krugh and co-workers (Young & Krugh, 1975; Krugh et al., 1976) measured the equilibrium constant K_1 for the formation of a double-stranded minihelix with the complementary dimers dpCpG, dpGpC, CpG, GpC, and GpU plus ApC between 0 and 5 ^{0}C. All the equilibrium constants were on the order of 10 M^{-1} or less. Since our overall constants range from 5000 on up, the contribution of minihelix formation to the overall free energy of dimer:dye complex formation is probably small.

The energetics of the remaining two reactions have been evaluated in calculations by Ornstein and Rein (1979a, 1979b). Their calculations showed that minihelix unwinding (9) was energetically unfavorable ($\Delta H > 0$), but very specific for the general base sequence. The loss of stronger base-base stacking interactions in Pu(3'-5')Py sequences vs. Py(3'-5')Pu sequences partially accounted for the observed preferences for dye binding. Base-phosphate interactions comprised the remainder of the preference and again favored the Py(3'-5') Pu sequences; this last contribution was lessened if the phosphates were electrically neutral (Ornstein & Rein, 1979a).

Other calculations showed that the dye:minihelix interactions in reaction (10) were enthalpicly favorable ($\Delta H < 0$), but the Pu(3'-5')Py sequences were preferred over their isomeric Py(3'-5')Pu sequences; this last factor was reversed by the greater contribution to the spec-

ificity from reaction (9) (Ornstein & Rein, 1979b). Thus, the sequence specificity is provided in (9) but the driving force for binding is from (10). Important contributions in reaction (10) were provided by the dye-base interactions (overlap) and the phosphate-dye interactions (hydrogen bonding between the DNA phosphates and the amino groups of the dye). In their X-ray studies, Sobell and co-workers (Tsai et al., 1977; Jain et al., 1977) also noted the importance of dye-base overlap, while Kindelis and Aktipis (1978) found that monoamino derivatives of the ethidium ion formed conformationally different complexes with DNA from the diamino derivatives, possibly because their hydrogen bonding properties were different.

Our equilibrium constants and other thermodynamic data are all consistent with these previous studies: Py(3'-5')Pu sequences form stronger complexes with the ethidium ion than Pu(3'-5')Py sequences. The likely reasons for this preference are those proposed in the previous studies. Complexes with complementary Pu(3'-5')Pu + Py(3'-5')Py sequences fall between these two cases. Removal of the small reaction (8) contribution to reaction (7)'s large total free energy shows that the contributions from (9) and (10) constitute the major driving force for the overall reaction in our results.

Comparisons of complex stabilities for analogous ribo- and deoxyribo- sequences are possible with these results. In each case (CpG vs. dCpG and UpA vs. dTpA), the ribo- sequence forms the stronger complex with ethidium ion. Krugh and co-workers (1975) observed the same effect with CpG and dpCpG but cautioned that direct comparison was restricted by the extra phosphate group on the deoxyribo- dimer. Both our deoxyribo- sequences have equilibrium constants smaller than their

ribo- analogues by a factor of ~10. Double-stranded RNA with G·C contents greater than 20% is more stable than DNA (Bloomfield et al., 1974); this might partially account for the greater stability of the CpG:CpG:EI complex compared to dCpG:dCpG:EI. However, the results for UpA:UpA:EI vs. dTpA:dTpA:EI run contrary to this: the deoxyribo-sequence should be more stable than the ribo- analogue. Whether all deoxyribo- dimer:dye complexes are less stable than their ribo- analogues requires further study.

The applicability of these results, especially the binding constants, to dye binding with longer oligomers and polymers is an interesting question. The binding of ethidium ion to longer sequences usually occurs with some sizable population of extant double strands. Since our results give overall constants for complex formation from two single strands plus dye, direct comparison with the equilibrium constants usually obtained with longer sequences is invalid. Still, the relative magnitudes of the constants, e.g. the ~1000-fold difference between a CpG and an ApU complex, may remain intact in longer sequences. Thus, a single macroscopic binding constant for dye binding to DNA or double-stranded RNA may mask contributions from many classes of binding sites, each with their own microscopic, but experimentally indistinguishable (at this time) binding constants.

C) Induced CD of the Complexes

The induced CD spectra of ethidium ion intercalated in complementary sequences of both deoxyribo- and ribo- dimers are all similar to those with polymers: bands are observed at 375, 330, and near 307 nm (Aktipis & Martz, 1970; Douthart et al.,1973). The similarity ends, however, when the magnitudes at 307 and 330 nm per bound dye are com-

pared for the dimer complexes and the polymers. In polymers, the magnitudes of these bands are low when few dyes are bound but they rise steadily as the extent of binding increases (Dalgleish et al., 1971; Aktipis & Kindelis, 1973; Aktipis & Martz, 1974; Houssier et al., 1974; Williams & Seligy, 1974). In the dimers, on the other hand, the magnitudes of the bands are large. In fact, the dimer $\Delta\varepsilon_{bound}^{\lambda\ max}$ values more closely resemble those of the polymers at higher r values where virtually every intercalation site is occupied, especially the dimers with Py(3'-5')Pu sequences (Table III).

One question that immediately comes to mind is whether the CD's of the dimer complexes serve as models for longer sequences. In the only reported CD study to date of ethidium ion binding with oligomers, Kastrup et al. (1978) examined dye binding with pdC-dG-dC-dG (2 dC-dG sites), pdC-dC-dG-dG (1 dC-dG site), pdG-dG-dC-dC, and pdG-dC-dG-dC (1 dC-dG site). For dye plus pdC-dG-dC-dG, both dC-dG sites were occupied at an added EI/strand ratio of 1, and the measured molar CD per bound dye at 305 nm was ~15 L/mol-cm, a value identical to ours for the dCpG:dCpG:EI complex where $\Delta\varepsilon_{bound}^{305} = 15 \pm 3$ L/mol-cm. Binding stoichiometries for the dye with the other three self-complementary tetramers were less well-defined; however, at added EI/strand ratios of 1, $\Delta\varepsilon_{bound}^{305}$ for each was ~11 L/mol-cm for pdC-dC-dG-dG, ~10 L/mol-cm for pdG-dG-dC-dC, and ~6 L/mol-cm for pdG-dC-dG-dC. The lower magnitudes for $\Delta\varepsilon_{bound}^{305}$ in the two sequences with one (presumably) preferred dC-dG binding site indicates that bases beyond the nearest neighbors may influence the magnitude of the CD band or that the dye molecules are bound in other sites.

A commonly accepted explanation for increasing polymer $\Delta\varepsilon_{bound}$ val-

ues near 307 nm with increasing dye binding maintains that contributions from the interaction between bound dye molecules can be added to the small CD contribution from the inherent asymmetry of the site (Houssier et al., 1974). The interaction is more likely to occur as more dye binds (and the dyes are closer to each other, on average), so the induced CD per bound dye increases. This exciton interaction between transitions on the dyes then might account for the negative lobe in the induced CD at 290 nm which is seen under certain circumstances (Aktipis & Kindelis, 1974; Aktipis & Martz, 1974; Williams & Seligy, 1974; Balcerski & Pysh, 1976).

The objections raised to this theory by Pardi (1980) centered on the fact that the magnitudes of the induced CD band around 307 nm for ethidium ion bound with CpG, dCpG, and UpA all were as large as in a DNA sample fully bound with the dye, yet only one dye molecule was present in the 2:1 complex. Furthermore, his equilibrium sedimentation study of CpG:CpG:EI showed that it was not forming aggregates, so dye-dye interactions between stacked complexes were not occurring. Clearly, if exciton interactions between intercalated dyes were not responsible for the large CD bands near 307 nm with dimers, maybe such interactions did not explain the changes in the induced CD with polymers.

For the sake of clarity, the question of the ethidium ion's induced CD in nucleic acids should be divided into two parts. First, what is the contribution to the CD from the inherent asymmetry of the binding site, and second, why does the induced CD per bound dye between 300 and 350 nm increase as more dye binds? With the dimer:dye results we can answer the first question: the apparent induced CD associated with the binding site asymmetry is large, and probably sequence depen-

dent. Naturally, there is the question of an exact correspondence between the dimer:dye complexes and complexes of the dye with longer sequences. The relative orientations of the base pairs and the dye may be less constrained in the dimer:dye complexes than in longer sequences, where bases beyond the nearest neighbors may restrict dye:base orientations in the binding site, but at present this does not seem significant because $\Delta\varepsilon_{bound}^{\lambda\ max}$ remains large in tetramer:dye complexes (Kastrup et al., 1978). More work with oligomers is needed to resolve this question. If the inherent asymmetry of the site contributes a large magnitude to the induced CD, previous approaches to the second question were misleading. Rather than ask what possible interactions contribute additional intensity to the low inherent CD of the near UV bands for ethidium ion in polymers as more dye binds, perhaps it is better to ask what interactions could reduce the intensity of the CD due to the site asymmetry as dye binding decreases. This is the point of view we will take into the succeeding chapters.

Chapter III

FLUORESCENCE DETECTED CIRCULAR DICHROISM OF DIMER-ETHIDIUM ION COMPLEXES

1. Introduction

In any solution containing more than one optically active species, the circular dichroism (CD) spectrum is sensitive to local structure around each chromophore, but it also a sum of contributions from all. Resolution of a particular chromophore's contribution from the entire spectrum may be difficult, or impossible. On the other hand, a single fluorophore mixed with other absorbing species can be readily isolated by measuring its fluorescence excitation profile. A single technique which unites the sensitivity of fluorescence with CD's conformational information is fluorescence detected circular dichroism (FDCD).

In FDCD, a sample is excited with circularly polarized light and the intensity of emission is measured as a function of the incident beam's circular polarization sense (Turner et al., 1974). Thus, FDCD is analogous to CD since both techniques provide information about the ground state of the molecule (Tinoco & Turner, 1976).

The use of fluorescence detected CD to study the complexes of ethidium ion with nucleic acids was first performed by Turner and coworkers (unpublished results) who looked at the complex formed with dCpG. The advantages of FDCD in these systems stem from the fact that the fluorescence quantum yield of the dye is enhanced up to 20-fold upon binding in the dimer:dye complex (Reinhardt & Krugh, 1978) and the dye is in a chiral environment. Thus, any FDCD signal in these

systems is almost solely from the dimer:dye complex. This is most convenient because the large excess of dimer relative to dye obscures the conventional CD spectrum of the complex below 300 nm in many cases.

The results of FDCD studies on the dimer:dye complexes studied in Chapter II are presented in this chapter. They show that the CD spectrum of the complexes below 300 nm is sensitive to the dimers' base sequence.

2. Experimental

A) Materials

The dinucleoside phosphates, ethidium bromide, and buffer were prepared as in Chapter II. In several cases, solutions used in the determination of binding constants were employed in the FDCD studies also. Rhodamine B was obtained from Eastman Kodak.

α-Naphthylamine was obtained from Sigma. The material was a deep red amorphous mass, so purification by steam distillation was necessary. The steam feeder line was passed through two traps to remove any particulate matter. The slightly translucent distillate was cooled and then filtered through a 0.2 μm polycarbonate filter (Bio-Rad). Baseline solutions for FDCD were prepared from this stock by dilutions with either doubly distilled water or buffer. The pH of these solutions was ~ 7 as measured with indicator strips (Merck). All solutions were kept in the dark and refrigerated when not in use. α-Naphthylamine is an OSHA-regulated carcinogen and restrictions on its use are in effect. Purification of the compound was performed in a restricted access area; all glassware was cleaned separately and the washings collected in a separate waste container. The fluores-

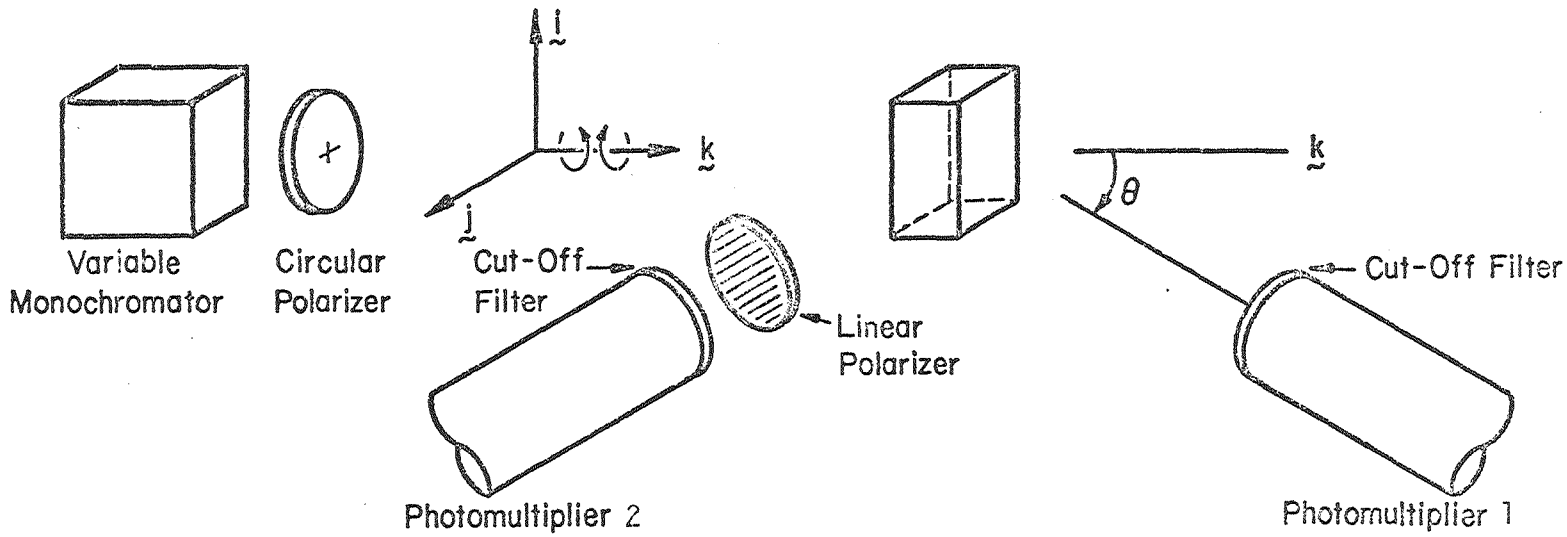

XBL 788-10398

of potassium dichromate in 10^{-2} M KOH (Dorman et al., 1973) and an adjustable mount kindly provided by Dr. Marc Maestre. Each tube exhibited an artifact of ±1 millidegree on the 40 millidegree scale in the regions of dichromate absorbance. All fluorescence cells were also tested in this fashion; none showed artifacts above the level present in the photomultipliers.

A preamplification circuit for the photomultipliers was constructed after Turner (1978). The operational amplifier was from Union Carbide Electronics (H7020A); this model is no longer available, see Turner (1978) for an alternate. Jacks from either photomultiplier tube could be connected to the preamp depending upon the type of measurement desired. Each phototube was shielded with mu metal.

ii) Manipulation of FDCD Data

Multiple FDCD scans (5 to 9) were necessary due to the large amount of noise. Acquisition, storage, averaging, smoothing, and other manipulations of the data were performed on the PDP 8/E computer (Digital) with the revised Super Spectrum software (Appendix B) and also on the CDC 6400/6600/7600 computer system at Lawrence Berkeley Laboratory (Appendix C). Signals at dynode voltages above 950 volts were judged unreliable and ignored in subsequent analyses.

The signal from an FDCD measurement at the chart recorder on the Cary 60 is given by

$$\theta_F^0 = -14.32(\Delta\varepsilon_F/\varepsilon_F - R) \qquad (1)$$

$$R = \Delta A\left(\frac{1}{A} - \frac{2.303}{10^A - 1}\right) \qquad (2)$$

where θ_F^0 is the ellipticity in degrees, $\Delta\varepsilon_F$ (= $\varepsilon_{FL} - \varepsilon_{FR}$) is the molar circular dichroism of the fluorophore in L/mol-cm, ε_F is the molar extinction coefficient of the fluorophore (also in L/mol-cm), ΔA (= $A_L - A_R$) is the circular dichroism of the sample, and A is its absorbance (Tinoco & Turner, 1976). The factor $\Delta\varepsilon_F/\varepsilon_F$ is referred to as the Kuhn anisotropy or the Kuhn dissymmetry factor of the fluorophore.

Equations (1) and (2) are for the general case. When only one fluorescent, optically active species is present $\Delta A/A = \Delta\varepsilon_F/\varepsilon_F$, and these reduce to the form

$$\theta_F^0 = -32.98\Delta A/(10^A - 1) \qquad (3)$$

(Tinoco & Turner, 1976). For calibration of the instrument, the CD spectrum of the standard, d-10-camphorsulfonic acid (Eastman Kodak), is calculated from the FDCD and absorbance spectra by rearranging (3) to obtain

$$\theta^0 = -\theta_F^0(10^A - 1) \qquad (4)$$

where the relation $\theta^0 = 32.98\Delta A$ has been used.

iii) Calibration of the Instrument

After calibration of the 6001 CD accessory according to the manufacturer's instructions, the new elevator was mounted in the Cary 60. Since the larger elevator was used for both CD and FDCD measurements, it was first calibrated in the CD mode. Prior to calibration, the Pockels cell on this elevator was aligned by minimizing the CD artifact for a solution of potassium dichromate in 10^{-2} M KOH.

Calibration of the new elevator for CD proceeded by connecting the leads for the CD photomultiplier tube to the preamplifier, follow-

ed by rotation of the mount into the path of the excitation beam. Using visible light (540 nm) and slits opened to 1 mm, the beam was centered on the phototube by placement of an opaque card with a small hole in the beam. When light passed by the hole reflected off the tube and was centered on the hole, the tube was properly aligned. After the mount was immobilized, calibration of the CD proceeded as for the Cary 6001 accessory. A 1 cm cell containing 4.3 mM (1 mg/ml) d-10-camphorsulfonic acid in doubly distilled water was set in the cell holder. Scans of the CD spectrum from 340 to 240 nm were made and the trimpot (R12 in Figure 5, Turner, 1978) was adjusted on the preamplifier until a maximum ellipticity of 312 millidegrees was measured (Cassim & Yang, 1969).

To calibrate the elevator for FDCD, the CD phototube leads were disconnected and the CD tube was rotated out of the excitation beam. The FDCD tube leads were connected and a Schott KV 380 interference filter was mounted in front of this phototube. To obtain a sufficiently strong signal, 21.5 mM (5 mg/ml) camphorsulfonic acid in a 1 cm fluorescence cell was used to take the FDCD spectrum. For this and all FDCD measurements, the slit multiplier was set at the maximum (10.0), as opposed to the usual setting for conventional CD (5.0) to increase the incident light intensity. The baseline solution was α-naphthylamine in buffer; this solution had an absorbance (1 cm) of 0.67 at 305 nm. To check calibration of the FDCD, the CD spectrum of the standard from FDCD and absorbance spectra via equation (4) is compared with the conventional CD spectrum in Figure 3.2; the agreement between the two curves is within 10%.

iv) Measurement of FDCD Spectra

Figure 3.2. Calibration curves of the FDCD instrument for d-10-camphorsulfonic acid (5 mg/ml) from CD measurements alone (□) and from FDCD and absorbance measurements via equation (4) (X).

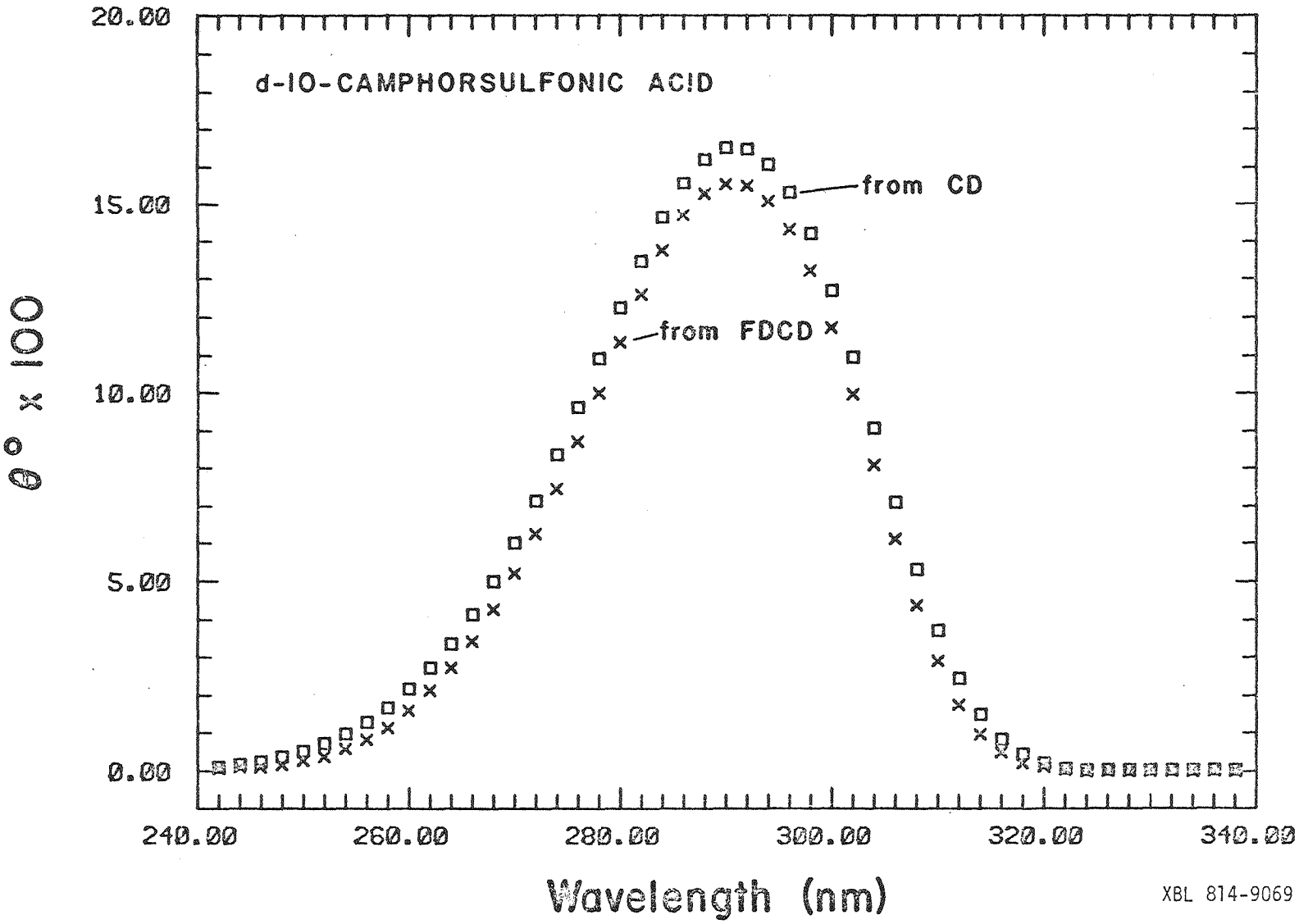
d-10-CAMPHORSULFONIC ACID
from CD
from FDCD
20.00
15.00
10.00
5.00
0.00
240.00
260.00
280.00
300.00
320.00
340.00
θ° x 100
Wavelength (nm)

XBL 814-9069

Quartz fluorescence cells (Precision Cells) of 2 mm and 3 mm path lengths were utilized for all FDCD measurements of the ethidium ion:dinucleoside phosphate complexes. A Schott KV 408 interference filter excluded all scattered or emitted light below 408 nm. In the tests for photoselection, a linear polarizer (Polaroid, HN32, 0.030") was mounted in front of the cutoff filter. No photoselection was observed for any of the complexes (see Chapter IV). Solutions of α-naphthylamine, either in water (15 OD units at 305 nm), or in buffer (1.5 OD units at 305 nm), were used for baselines depending upon the optical density of the dimer/dye solution.

Measurements of the CD and absorbance spectra at 0^0C were performed on the Cary 60 with Cary 6001 CD accessory, and either the Cary 118 or Gilford 250 spectrometers, respectively. The temperature was maintained as in Chapter II. Path lengths were selected to keep the absorbance below 2 at the maximum.

v) Fluorescence Measurements

Corrected excitation profiles of ethidium ion, both alone and in the presence of CpG, were run at 0^0C on a Perkin-Elmer MPF-44B fluorescence spectrophotometer. A Perkin-Elmer DCSU-2 unit was used to correct the profiles for lamp and photomultiplier characteristics. These instruments were kindly made available by Dr. Alex Glazer. The temperature was maintained with an external bath (Neslab) to within $\pm 0.2^0$C. Solutions in buffer of ethidium ion (0.046 mM) alone and with CpG (0.53 mM) were scanned in a 2 mm path fluorescence cell. Slit widths were 2.4 mm (8 nm bandwidth) at the emission monochrometer and 1.8 mm (6 nm bandwidth) at the excitation monochrometer. Emission was monitored at 590 nm and the excitation spectra scanned from 225 to 550 nm.

Constancy of the free dye quantum yield over the profile range was checked against Rhodamine B by calculating the ratio

$$(I_R/A_R)\cdot(A_E/I_E)$$

from 225 to 550 nm (LePecq & Paoletti, 1967). I_R and I_E are the fluorescence intensities for the Rhodamine B and ethidium ion, respectively, and A_R and A_E are the absorbances of the same.

The ratio of quantum yields for equal amounts of dye bound in the complex and free in solution is

$$Q = \frac{q_b}{q_f} = \frac{I_b}{I_f}\cdot\frac{A_f}{A_b} \qquad (5)$$

(LePecq & Paoletti, 1967), where I_b and I_f are the fluorescence intensities for bound and free ethidium ion and A_b and A_f are the absorbances of the same. The excitation profile (I_b) of the CpG/EI mixture was corrected for the small amount of fluorescence due to the free dye (~5% of total dye). Concentrations of free dimer, free dye, and complex were calculated from the equilibrium constant at 0^0C and the total dye and dimer concentrations. Errors in the final concentrations were estimated at 25% and were due primarily to the equilibrium constant's error.

The absorbance of the bound dye, A_b, was calculated by deducting contributions of free CpG and free dye from the mixture absorbance. This provided $A_{complex}$, from which an estimated contribution from the bases in the complex equal to $2C_{complex}\varepsilon_{CpG}$, where ε_{CpG} is the extinction coeffiecient of CpG, was subtracted to yield A_b. This assumed the CpG absorbance characteristics were not changed in the complex, an as-

sumption similar to that made with the DNA:EI complexes (LePecq & Paoletti, 1967). For wavelengths greater than 310 nm, the resulting absorbance profile showed little difference from that of the mixture alone as expected, owing to the small amount of free dye and the absence of dimer absorbance in this region.

3. Results

A) Sequence Dependence of FDCD Spectra

The Kuhn anisotropy as a function of wavelength is presented for different dimer:dye complexes in Figures 3.3a through 3.3d. Above 300 nm, all the complexes exhibit a positive anisotropy. This corresponds to the induced CD band seen in this region for all the complexes except ApU:ApU:EI. The fact we were able to measure a spectrum for this last complex underscores the usefulness of FDCD for obtaining a CD spectrum where conventional CD fails. It should be noted again that the FDCD signal is solely from ethidium ion bound in the dimer:dye complex.

A change from a ribonucleoside sequence to an analogous deoxyribonucleoside sequence has no effect on the complexes' band positions. In the CpG vs. dCpG complexes (Figure 3.3a) this is evident. For the UpA vs. dTpA complexes (Figure 3.3b), agreement is seen below 240 nm and above 290 nm (within error). The high optical density of the dTpA mixture may be responsible for the discrepancy between the two spectra between 240 and 290 nm, where the absorbance was greatest.

Below 300 nm, where the dimers themselves possess CD spectra, distinct differences in the Kuhn anisotropy exist from complex to complex. These spectral differences may reflect the individual optical properties of the surrounding bases in the complex, different relative ori-

Figure 3.3a. Kuhn anisotropy spectra for CpG:CpG:EI complex (top) and dCpG:dCpG:EI complex (bottom). Estimated errors are represented by lines. Maximum absorbances for FDCD measurements were 2.57 in a 3 mm cell at 254 nm for CpG complex and 2.96 in a 3 mm cell at 253 nm for dCpG complex.

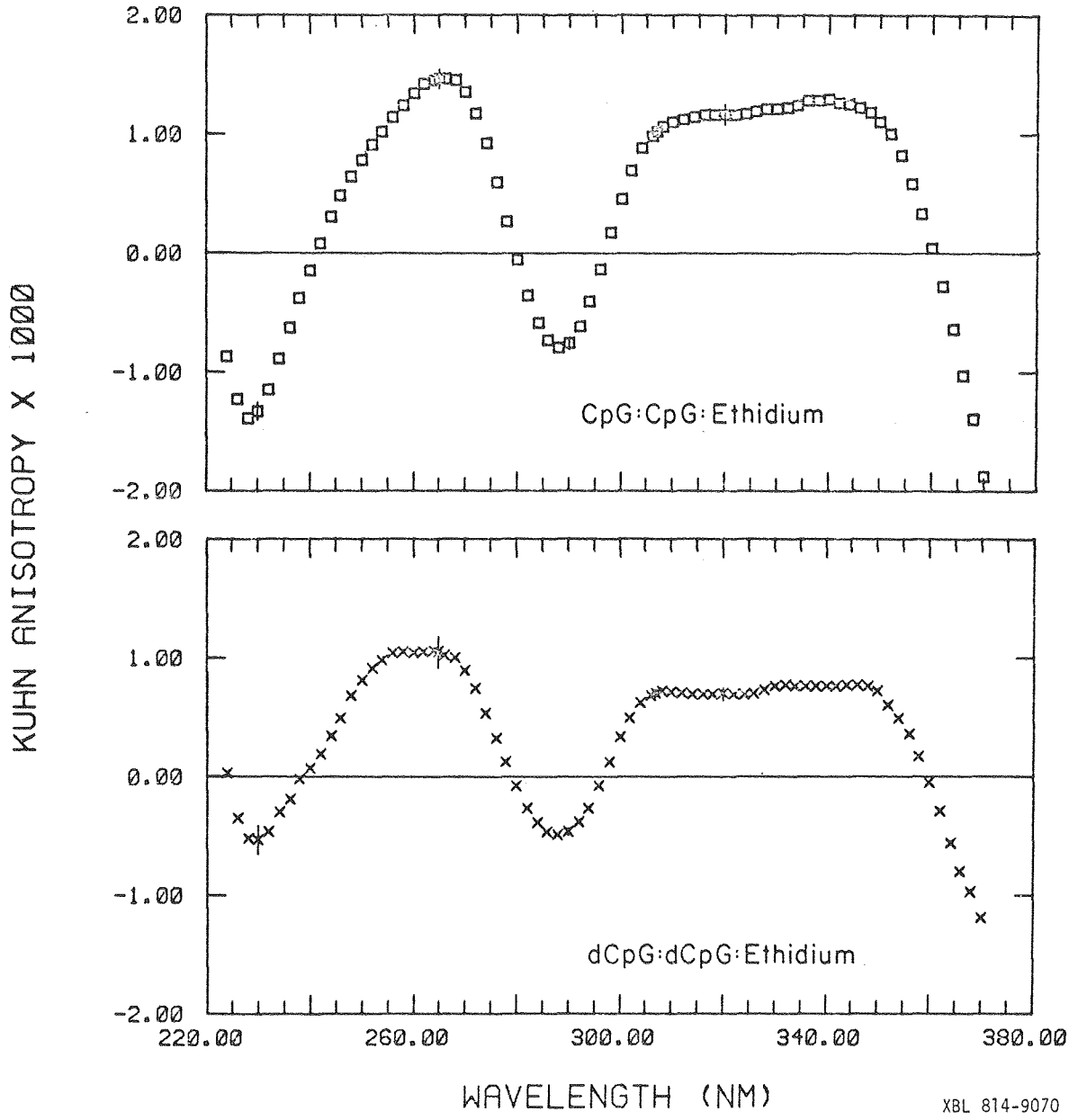
2.00
1.00
0.00
-1.00
-2.00
CpG:CpG:Ethidium
2.00
1.00
0.00
-1.00
-2.00
dCpG:dCpG:Ethidium
KUHN ANISOTROPY X 1000
220.00
260.00
300.00
340.00
380.00
WAVELENGTH (NM)
XBL 814-9070

Figure 3.3b. Kuhn anisotropy spectra for UpA:UpA:EI complex (top) and dTpA:dTpA:EI complex (bottom). Estimated errors are represented by lines. Maximum absorbances for FDCD measurements were 8.07 in a 3 mm cell at 259 nm for UpA complex and 31.1 in a 2 mm cell at 261 nm for dTpA complex.

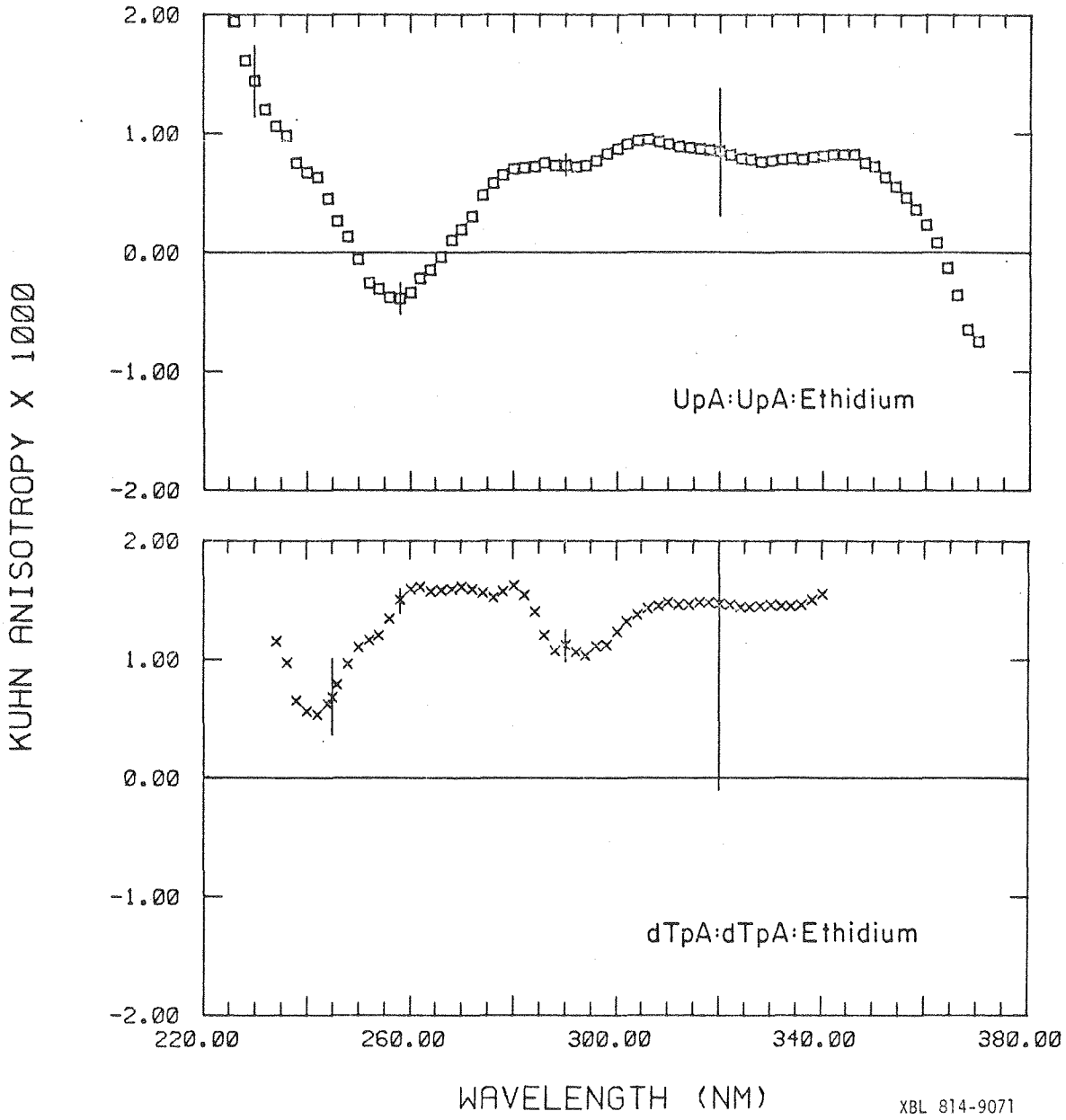
2.00
1.00
0.00
-1.00
-2.00
UpA:UpA:Ethidium
2.00
1.00
0.00
-1.00
-2.00
dTpA:dTpA:Ethidium
KUHN ANISOTROPY X 1000
220.00
260.00
300.00
340.00
380.00
WAVELENGTH (NM)
XBL 814-9071

Figure 3.3c. Kuhn anisotropy spectra for CpA:UpG:EI complex (top) and ApG:CpU:EI complex (bottom). Estimated errors are represented by lines. Maximum absorbances for FDCD measurements were 5.95 in a 3 mm cell at 259 nm for CpA/UpG complex and 21.3 in a 2 mm cell at 262 nm for ApG/CpU complex.

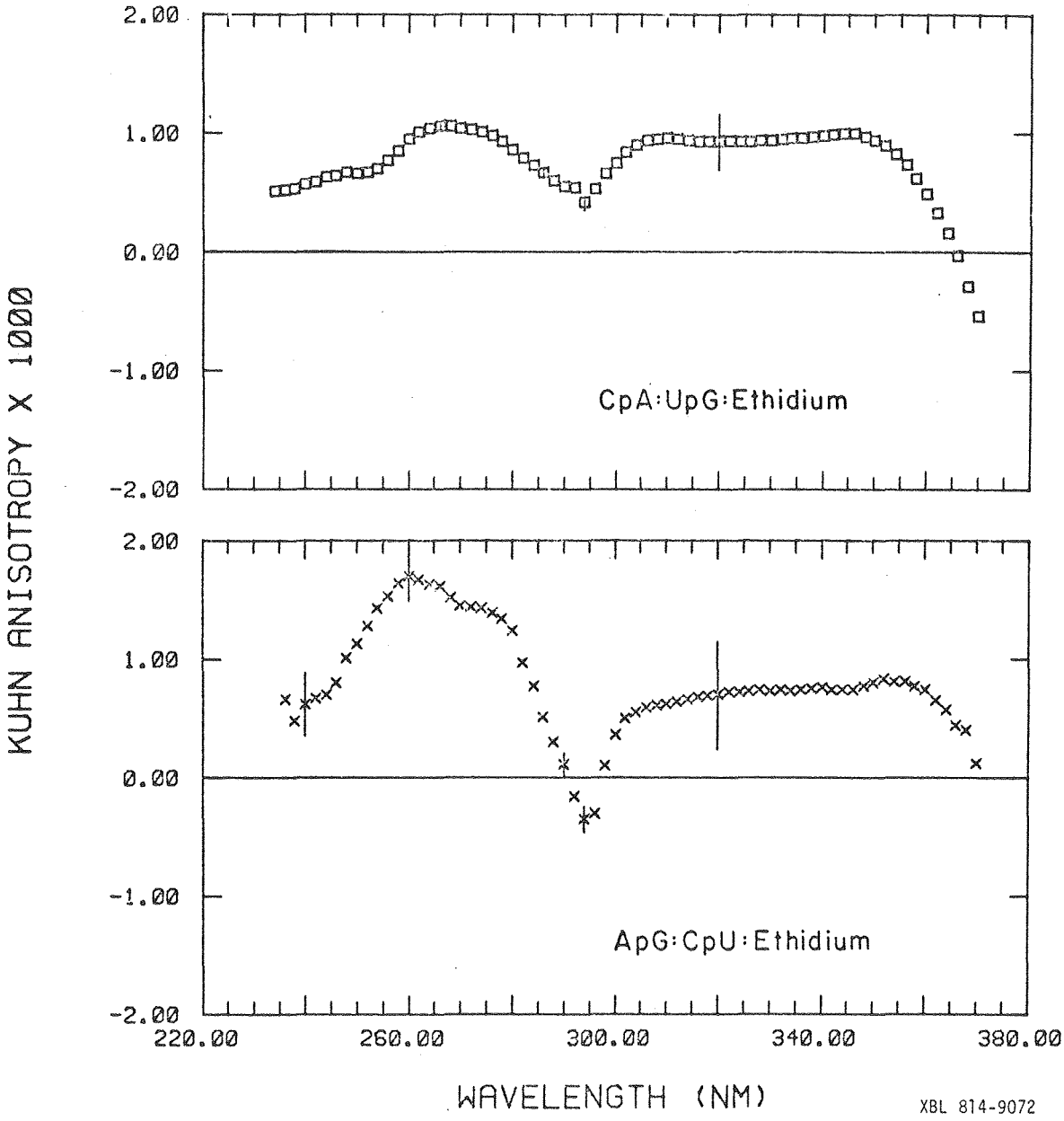
2.00
1.00
0.00
-1.00
-2.00
CpA:UpG:Ethidium
2.00
1.00
0.00
-1.00
-2.00
ApG:CpU:Ethidium
KUHN ANISOTROPY X 1000
220.00
260.00
300.00
340.00
380.00
WAVELENGTH (NM)

XBL 814-9072

Figure 3.3d. Kuhn anisotropy spectra for ApA:UpU:EI complex (top) and ApU:ApU:EI complex (bottom). Estimated errors are represented by lines. Maximum absorbances for FDCD measurements were 44 in a 2 mm cell at 259 nm for ApA/UpU complex and 48 in a 2 mm cell at 260 nm for ApU complex.

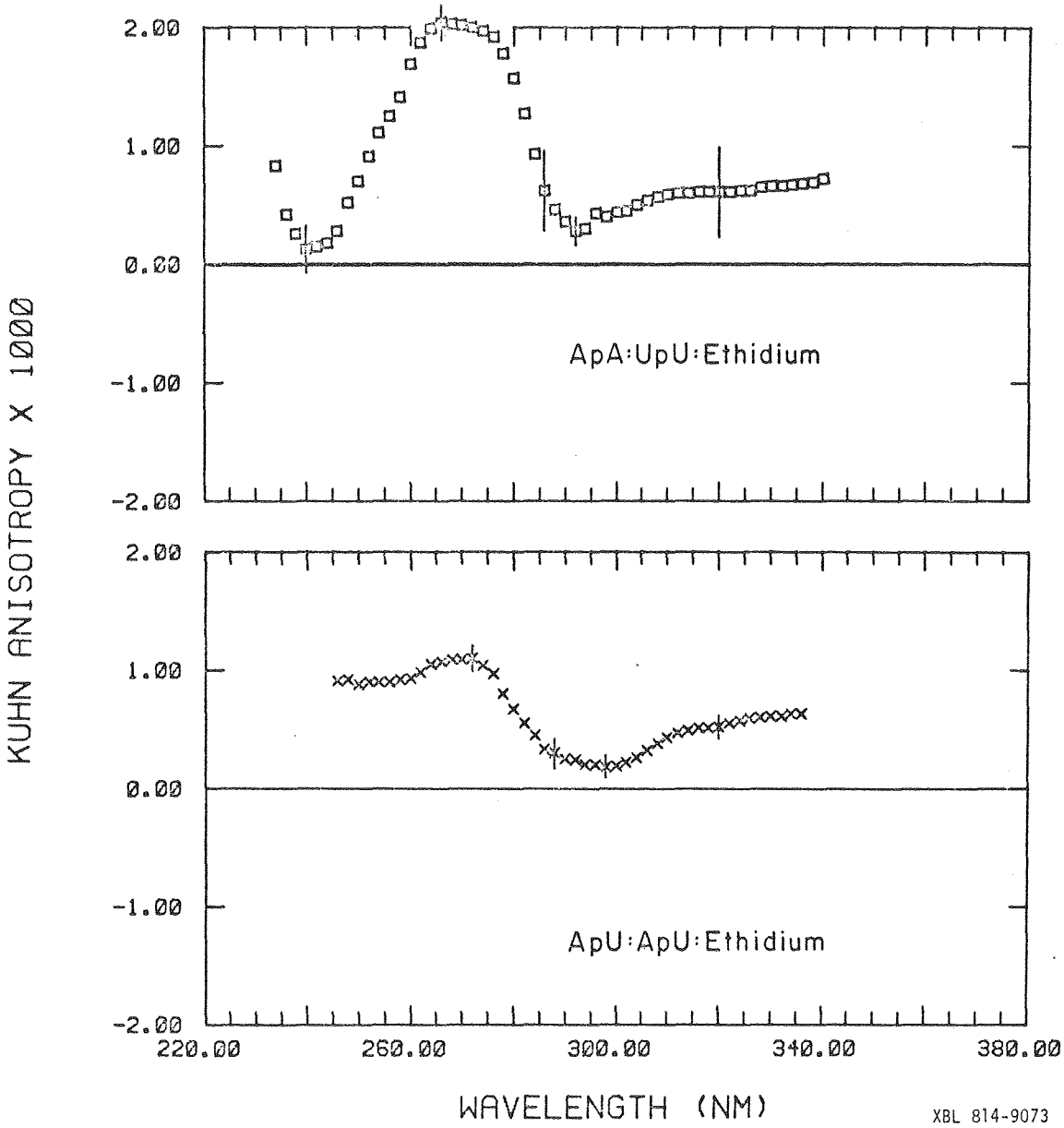
2.00
1.00
0.00
-1.00
-2.00
ApA:UpU:Ethidium
2.00
1.00
0.00
-1.00
-2.00
ApU:ApU:Ethidium
220.00
260.00
300.00
340.00
380.00
KUHN ANISOTROPY X 1000
WAVELENGTH (NM)
XBL 814-9073

entations of the dye in each complex, energy transfer from nearby bases to the dye, or combinations of these effects.

B) Assignment of Spectral Bands

The Kuhn anisotropy is related to the electronic and magnetic properties of the fluorophore through the equation

$$\frac{\Delta\varepsilon_F}{\varepsilon_F} = \frac{4R_{0A}}{D_{0A}} = \frac{4\,\mathrm{Im}\ \underset{\sim}{\mu}_{0A}\cdot\underset{\sim}{m}_{A0}}{\underset{\sim}{\mu}_{0A}\cdot\underset{\sim}{\mu}_{0A}}$$

where the transition proceeded from the ground state 0 to the excited state A, R_{0A} is the rotational strength of the transition, and D_{0A} is its dipole strength (Tinoco & Turner, 1976). Im denotes the imaginary part, and $\underset{\sim}{\mu}_{0A}$ and $\underset{\sim}{m}_{A0}$ are the electric and magnetic dipole moments. The anisotropy should approximately be flat for each transition, providing the transition is energetically removed from other transitions, because R_{0A} and D_{0A} are constant (Tinoco & Turner, 1976). Overlapping transitions in the dye or with other groups will make the spectrum more complicated. The FDCD spectrum thus provides a measure of the interaction of dye transitions with neighboring transitions.

In Figure 3.4, the Kuhn anisotropy of CpG:CpG:EI is centered between absorption profiles for the complex and for ethidium ion bound in DNA (Sutherland & Sutherland, 1970), and profiles for free dimer and dye. We have obtained a profile similar to Sutherland and Sutherland's for bound dye in the CpG:CpG:EI complex (Figure 3.6). Several approximately flat regions of the anisotropy can be assigned.

The positive lobe of the Kuhn anisotropy above 300 nm can be ascribed solely to dye transitions as mentioned earlier: only the dye absorbs light in this region. The transition responsible for the nega-

Figure 3.4. Top: Extinction profiles for CpG:CpG:EI (□) and ethidium ion bound in calf thymus DNA (X). Center: Kuhn anisotropy for CpG:CpG:EI from FDCD. Bottom: Extinction profiles for CpG (△) and ethidium ion (▽).

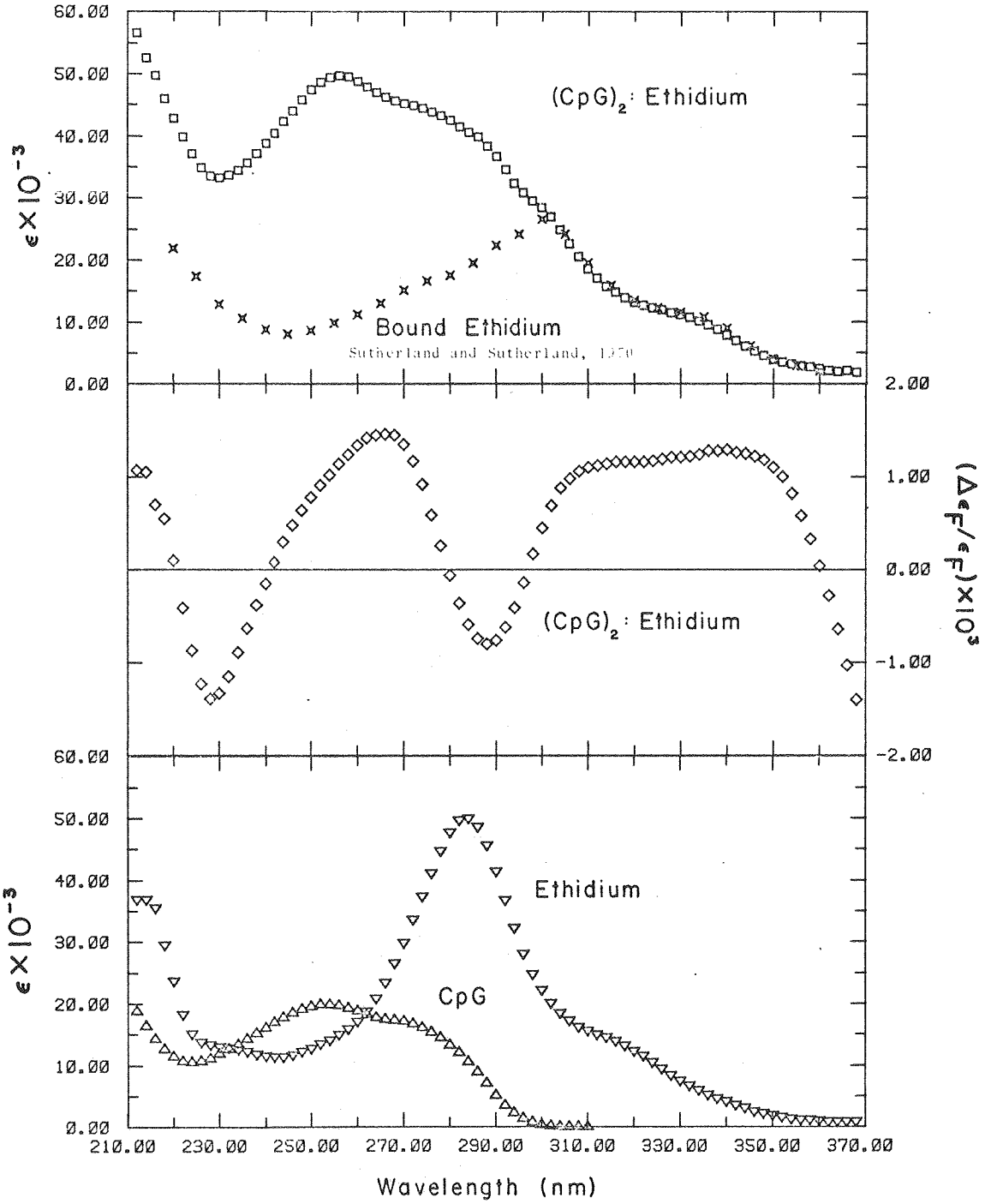

XBL 8011-12715

tive lobe of the anisotropy centered on 290 nm is the dye's strongest (Hudson & Jacobs, 1975), which is apparently reduced in intensity and red-shifted when the dye is bound (see the fluorescence excitation profiles, below).

The next anisotropy band between 240 and 280 nm is assigned to interactions between dye and base transitions. In this region of the complex absorption profile much of the energy is absorbed by the bases in the complex. Assignments of the remaining bands in the anisotropy (below 240 nm) are much more difficult to perform with the evidence at hand.

Comparisons of Kuhn anisotropies with absorption profiles cannot be done with other complexes because the high dimer/low dye concentrations and the small amounts of complex render attempts to deduce the complexes' absorption profiles statistically indefensible. However, insofar as the anisotropies of the other complexes resemble that of CpG:CpG:EI, we can make the same assignments for them. Above 300 nm the positive bands correspond to the previously obtained induced CD's and originate on the dye. Most of the spectra show at least a relative minimum near 290 nm in the anisotropy; this band also arises from a dye transition. Bands between 250 and 280 nm arise from dye-base interactions, presumably. The UpA:UpA:EI anisotropy presents a problem: it does not possess the same general features below 300 nm as the others. The applicability of the assignments to this complex is open to question.

C) CD Spectrum of Complexes from FDCD

Up to this point, analyses of the FDCD, CD, and absorbance spectra by equations (1) and (2) to obtain $\Delta\varepsilon_F/\varepsilon_F$ have been "clean": no assumptions of stoichiometries or amounts of species present have been needed.

Experimentally, either a FDCD spectrum could be measured or not.

One useful quantity to obtain from the Kuhn anisotropy, $\Delta\varepsilon_F/\varepsilon_F$, is the CD of the fluorophore in the complex, $\Delta\varepsilon_F$. To do this we need to derive ε_F for the complex in some way. Ideally, the best method for arriving at ε_F is to measure a corrected excitation profile of the bound dye, normalize this profile to the absorbance profile of the complex above 300 nm (where only the dye absorbs), and use the normalized profile extending down to 225 nm for ε_F.

The corrected excitation profiles for equal amounts of ethidium ion, alone and complexed with CpG, are shown in Figure 3.5. Two facts are evident: the efficiency of fluorescence is enhanced considerably upon dye binding to the dimer, and the profile for bound dye is merely red-shifted from the free dye version. The ratio of quantum yields for bound vs. free ethidium ion at different wavelengths from equation (5) are presented in Table IV. The enhancement of fluorescence upon ethidium ion intercalation into nucleic acids has been observed previously (LePecq & Paoletti, 1967; Krugh & Reinhardt, 1975; Reinhardt & Krugh, 1978; Kastrup et al., 1978). Particularly noteworthy is its relative independence of wavelength, even down in the ultraviolet where the bases absorb. This last feature was unexpected; energy transfer from the bases to the dye had been observed in DNA (LePecq & Paoletti, 1967; Sutherland & Sutherland, 1970).

In Figure 3.6, the excitation profile for CpG:CpG:EI has been normalized to the absorbance profile of the complex at 480 nm and divided by the complex concentration to obtain ε_F. Comparison with the profile derived from the corrected absorbance of the mixture shows each are similar. The main absorbance band at 285 nm in the free dye has shifted

Figure 3.5. Corrected excitation profiles for ethidium ion alone (X) and bound in a 2:1 complex with CpG (◇).

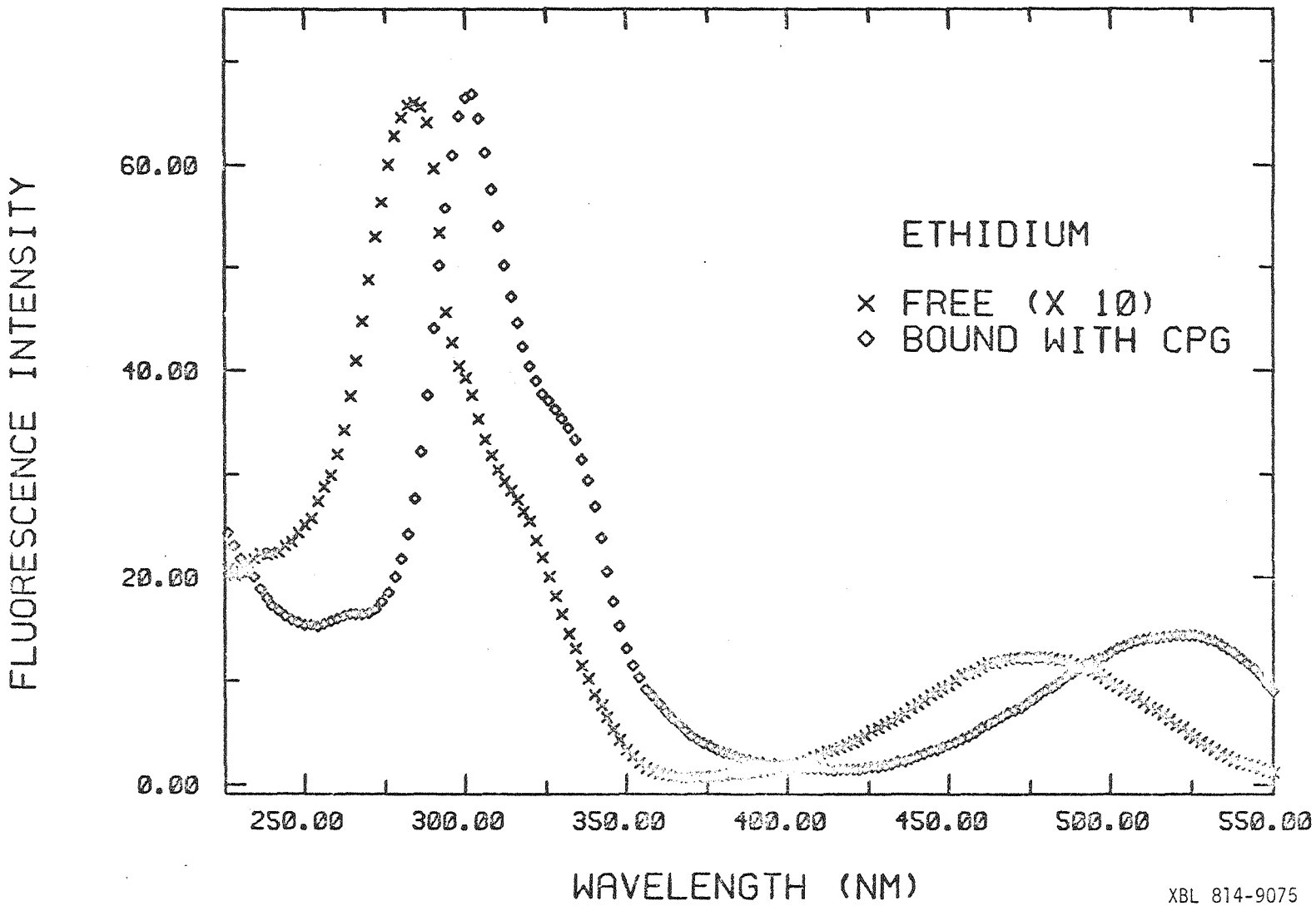
ETHIDIUM
× FREE (X 10)
◇ BOUND WITH CPG
FLUORESCENCE INTENSITY
0.00
20.00
40.00
60.00
250.00
300.00
350.00
400.00
450.00
500.00
550.00
WAVELENGTH (NM)

XBL 814-9075

TABLE IV

RELATIVE QUANTUM YIELDS

FOR BOUND VS. FREE ETHIDIUM ION

Wavelength (nm)	(q_b/q_f) [a] (0^0C)
546	21 [b]
500	17
450	15
400	16
350	17
300	15
280	17
260	16
240	28

[a] Estimated errors for values above 300 nm are ±20%; below 300 nm they are larger (±35%) due to the assumptions made for A_b derivation.

[b] Krugh & Reinhardt (1975) reported a value of ~ 18 at 25^0C.

Figure 3.6. Absorbance profiles for CpG:CpG:EI from corrected fluorescence excitation profile normalized at 480 nm (□) and from complex absorbance profile less the dimer's contribution (X).

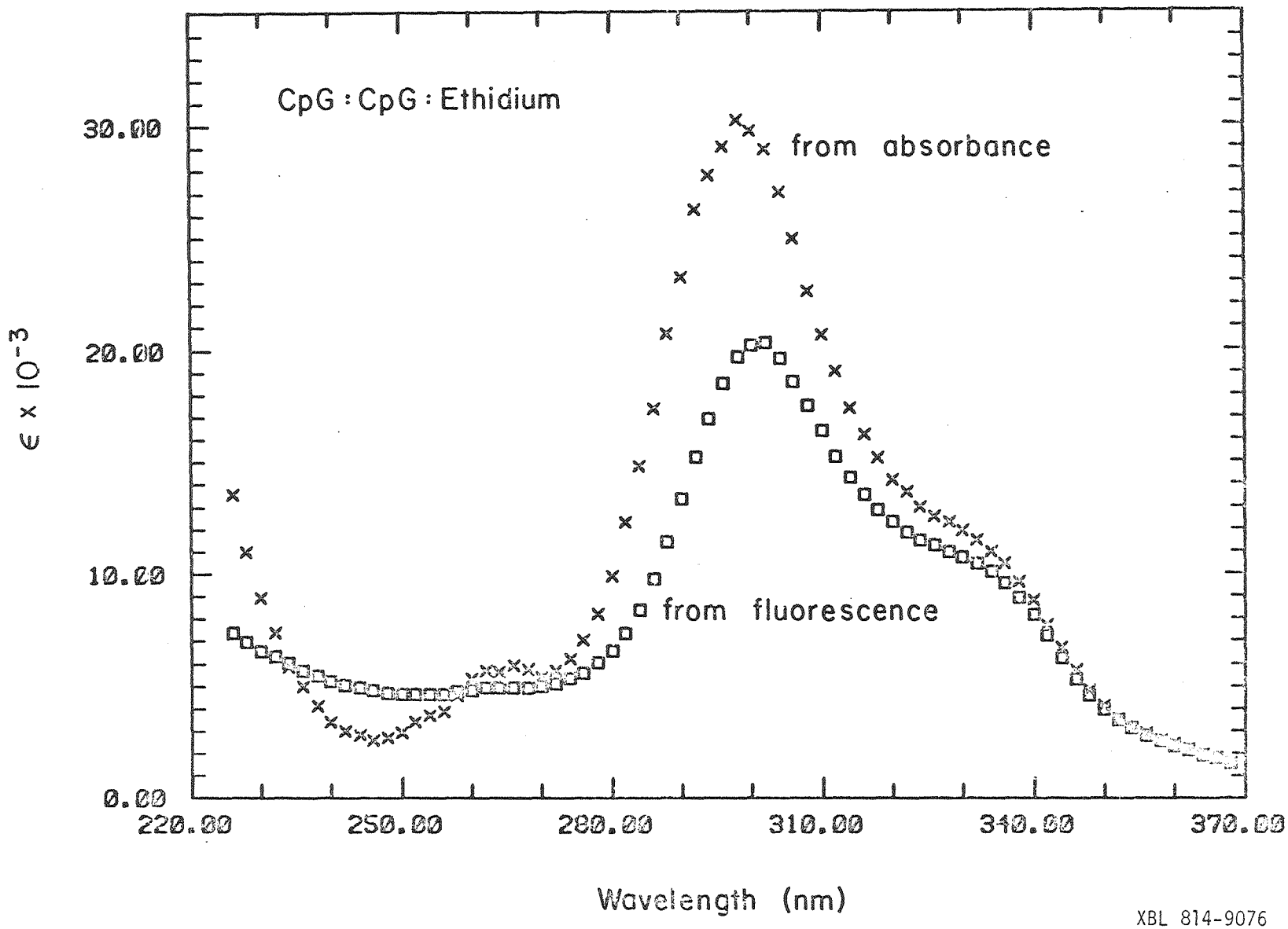
CpG : CpG : Ethidium
from absorbance
from fluorescence
30.00
20.00
10.00
0.00
220.00
250.00
280.00
310.00
340.00
370.00
ε x 10^-3
Wavelength (nm)

XBL 814-9076

out to ~300 nm in the complex and lost ~50% of its intensity. The lack of features below 270 nm is indicative of little or no energy transfer from the bases to the dye (compare with complex's absorbance profile in Figure 3.4).

In Figure 3.7, the CD spectrum of CpG:CpG:EI from the product of $\Delta\varepsilon_F/\varepsilon_F$ and ε_F is presented, along with the spectrum obtained by deducting the free CpG contribution from the CpG/EI mixture CD (these two curves are shown in Figure 3.8). Coincident bands occur throughout the two CD's of the complex, but they differ in magnitudes below 300 nm, particularly below 280 nm. By assuming that the excitation profile for the CpG complex is the same for the dCpG complex, a comparison of the CD spectra from FDCD and the mixture CD (less the free dimer contribution) can be made for dCpG:dCpG:EI. This is shown in Figure 3.9. Here again, relatively good agreement on band positions is attained, but band magnitudes differ. Above 300 nm, the magnitudes of $\Delta\varepsilon_{bound}$ from both methods: ~22 L/mol-cm at 307 nm for the CpG complex and ~14 L/mol-cm at 305 nm for the dCpG complex, agree well with previous results (Chapter II).

4. Discussion

A) Sequence Dependence of Complexes' CD

We have measured the Kuhn anisotropy in six of the possible ten different nearest neighbor sequences for ethidium ion binding in double-stranded RNA and also, in DNA, assuming the spectral similarities seen for the CpG and dCpG complexes are true for all analogous sequences. All the spectra are significantly different from one another, particularly below 300 nm. In the absence of complicating factors such as interactions of the dye with bases beyond the nearest neighbors, or different

Figure 3.7. CD spectrum for CpG:CpG:EI from product of $\Delta\varepsilon_F/\varepsilon_F$ and ε_F (normalized fluorescence excitation profile) (□) and from mixture CD less free dimer contribution (X). Errors in band magnitudes are 30%.

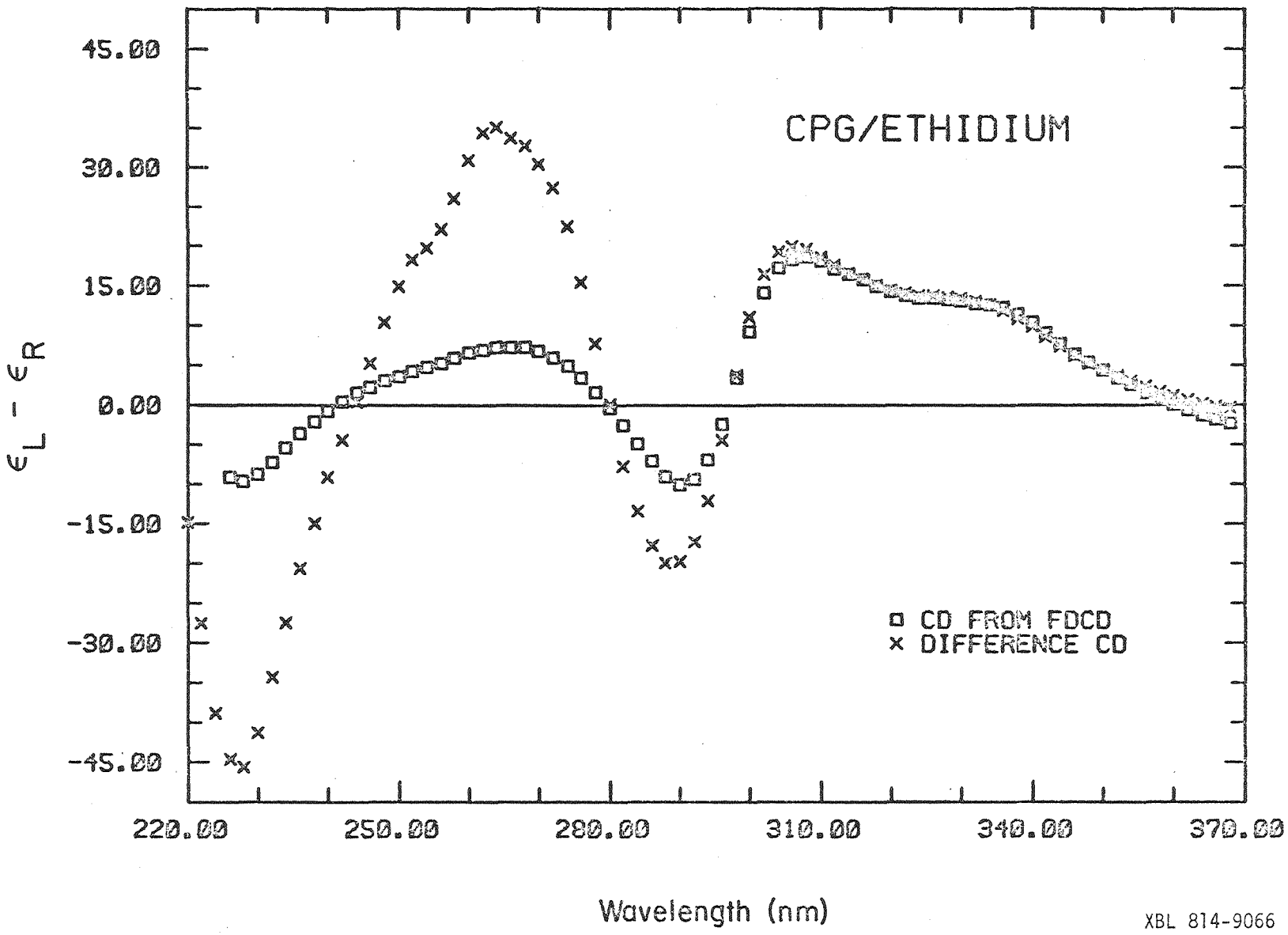
CPG/ETHIDIUM
45.00
30.00
15.00
0.00
-15.00
-30.00
-45.00
$\epsilon_L - \epsilon_R$
220.00
250.00
280.00
310.00
340.00
370.00
Wavelength (nm)
CD FROM FDCD
DIFFERENCE CD

XBL 814-9066

Figure 3.8. CD spectra of CpG (0.41 mM) plus ethidium ion (0.043 mM) mixture at $0^{0}C$ (□) and for free CpG (0.33 mM) in mixture (X). Free CpG contribution was calculated from a CD spectrum of CpG alone (0.41 mM) and concentrations derived from the equilibrium constant. Path length is 3 mm. The CD spectrum of the CpG:CpG:EI complex was obtained from these by subtraction of the free CpG component from the mixture CD and taking into account the complex concentration (0.039 mM).

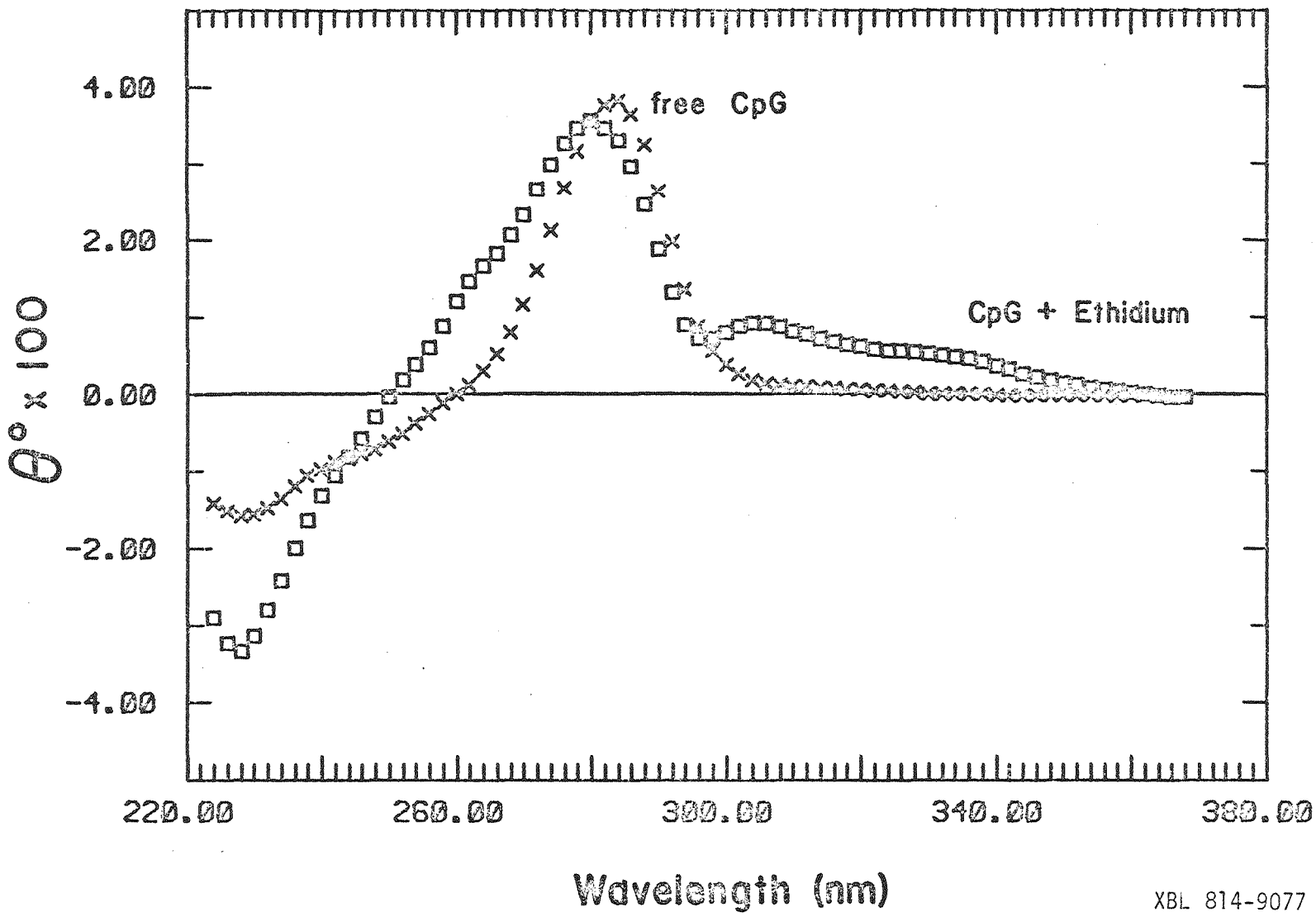
free CpG
CpG + Ethidium
4.00
2.00
0.00
-2.00
-4.00
θ° x 100
220.00
260.00
300.00
340.00
380.00
Wavelength (nm)

XBL 814-9077

Figure 3.9. CD spectrum for dCpG:dCpG:EI from product of $\Delta\varepsilon_F/\varepsilon_F$ and ε_F (normalized fluorescence excitation profile) (□) and from mixture CD less free dimer contribution (X). Errors in band magnitudes are 30%.

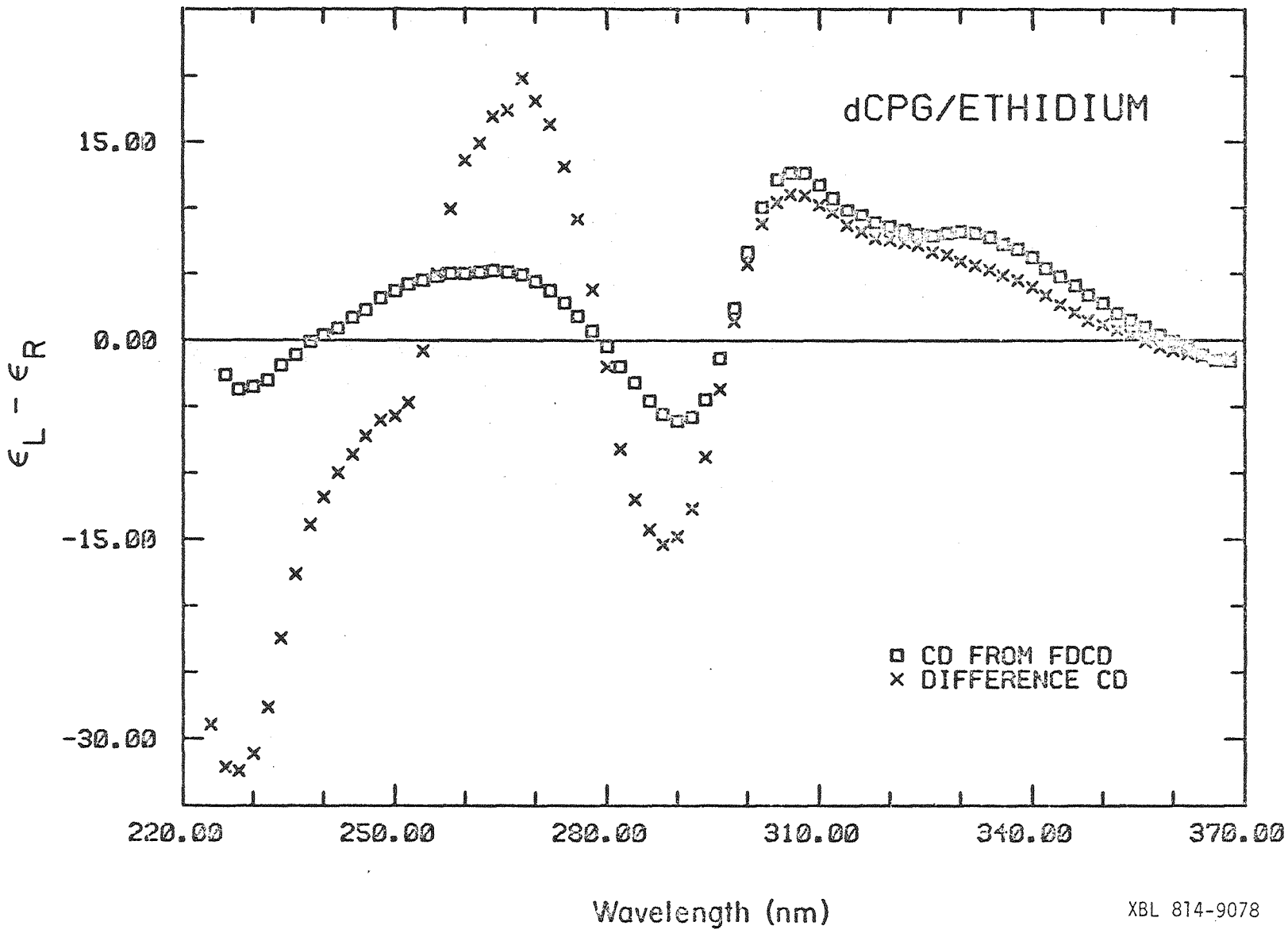
dCPG/ETHIDIUM
15.00
0.00
-15.00
-30.00
$\epsilon_L - \epsilon_R$
220.00
250.00
280.00
310.00
340.00
370.00
Wavelength (nm)
CD FROM FDCD
DIFFERENCE CD

XBL 814-9078

geometries, these spectra can be utilized in attempts to distinguish preferential binding of the ethidium ion in longer sequences.

Why each complex has a different spectrum is a difficult question to answer in the absence of further experiments. In the X-ray structures of ethidium ion complexed with 5-iodoUpA and 5-iodoCpG (Tsai et al., 1977; Jain et al., 1977), the intercalated dye molecules each overlap by roughly equal amounts with the base pairs, and the substituents on the phenanthridinium ring are in the minor groove of the minihelix. Thus, the differences in the anisotropies of the CpG and UpA complexes are more likely due to the different electronic properties of the bases, assuming the structures in the crystals apply in solution.

The effect of switching the orientation of one base pair in a sequence is observable in Figure 3.3c, where an A·U base pair is rotated about its dyad axis. The primary effect is an intensifying of bands below 300 nm for CpU:ApG:EI relative to CpA:UpG:EI; no effect is seen on the positions of the relative maxima and minima. If the dye molecules are oriented identically in each complex, then this difference is attributable to the change in the neighboring electronic environment of the dye. A second comparison can be made with UpA:UpA:EI (Figure 3.3b, top) and ApA:UpU:EI (Figure 3.3d, top), where again an A·U base pair has been rotated about its dyad axis. In this case, the changes are drastic. For self-complementary dimers, the symmetry of the minihelix leaves the environment of the dye unaltered after a rotation about its pseudo-C_2 axis through the phenanthridinium ring. On the other hand, with non-self-complementary dimers, this rotation does change the dye's environment. Thus, even if there is a similar extent of base-dye overlap in each complex, the orientation of the dye may be different and

contribute to differences in the CD spectra also. Calculations of the CD spectra for the complexes may aid in judging the relative importance of these different effects.

B) The "Exciton" Band

One of the pieces of evidence cited in support of the dye-dye exciton theory for the induced CD of ethidium ion:nucleic acid complexes was the negative CD band near 295 nm seen at high ionic strengths (Aktipis & Kindelis, 1973; Aktipis & Martz, 1974; Balcerski & Pysh, 1976). The absence of the band at lower salt concentrations was attributed to overlap of the large positive band in the nucleic acid's CD at 275 nm; this band's intensity decreased at higher ionic strengths (Aktipis & Kindelis, 1973; Balcerski & Pysh, 1976).

We observed a negative band at 290 nm in the Kuhn anisotropy of ethidium ion in complexes with CpG, dCpG, and CpU/ApG and a relative minimum in the complexes with CpA/UpG and ApA/UpU (Figures 3.3a-d). There is only one dye to two dimers in these complexes and stacks of the 2:1 complexes do not form, so the possibility of dye-dye excitons in these complexes does not exist: such interactions are not responsible for this band in the dimer complexes. We believe this band arises from transitions on the dye, most likely the transition at 285 nm in the free dye which is red-shifted in the complex. The appearance of this CD band in 2:1 complexes suggests it might be a manifestation of the asymmetry of the binding site, both in these complexes and in polymers. If this is so, overlap of the nucleic acid's CD band at lower ionic strengths could still mask this band; it would reappear at high ionic strengths where the 275 nm band loses intensity.

C) Is There Energy Transfer in the Complexes?

In our analysis of the CD spectrum for the CpG:CpG:EI complex we originally assumed energy transfer from the bases to the dye occurred. We believed such transfer might take place because LePecq and Paoletti (1967) observed it in DNA. They found that about half the energy absorbed by the DNA bases was transferred to the dye at phosphate/dye binding ratios near 14 and, furthermore, the transfer originated from bases not more than five base pairs away. This last result was nearly duplicated by Sutherland and Sutherland (1970), who found that transfer originated from bases 3.5 base pairs away.

The corrected fluorescence excitation profile of bound ethidium ion was enhanced above the bound dye difference spectrum in calf thymus DNA (Sutherland & Sutherland, 1970). This was an indication that energy transfer from the bases to the dye occurred. In our study of the CpG:CpG:EI complex we saw no significant difference between the corrected excitation profile and the absorbance profile for bound dye only (Figure 3.6) below 300 nm. Energy transfer in the ethidium ion complexes with dimers is seemingly nonexistent. However, in the calculation of the complex's CD spectrum by two theoretically equal methods (Figure 3.7), differences in the results above any calculated errors are evident below 300 nm. In this case, the excitation profile is missing intensity below 300 nm, suggesting that energy transfer might occur after all. This question is difficult to resolve one way or another at present.

LePecq and Paoletti (1967) measured the ratio of ethidium ion fluorescence enhancement at 260 nm to the enhancement in the visible as a function of phosphate/dye. They found the enhancement ratio was constant above P/D = 20, but that it rapidly dropped by almost a full factor of 3 near P/D = 5. Under their method of analysis, the percentage

of energy transfer from DNA to the dye would also drop an equal amount, down to 10-15% transferred. Our 2:1 dimer:dye complex is effectively at P/D = 4, so we estimate that the efficiency of energy transfer in our complexes is only ~10%, a figure that is apparently too low for us to measure in the fluorescence excitation profiles, if true.

Why the bases 3.5 to 5 base pairs away should be the most efficient in transferring energy to the bound ethidium ion while those closer to the dye are less efficient is an interesting question. The bases several base pairs away might be oriented in the optimum relative position to the dye for energy transfer, even though they are at greater distances than the nearer base pairs. The orientation factor may be more important than distance to the dye for the transfer. Calculations of energy transfer in DNA:EI complexes have been done (Paoletti & LePecq, 1971; Genest et al., 1974; LeBret et al., 1977), but more work in this area might prove illuminating, particularly on the question of energy transfer from the nearest and next-nearest neighbors to the dye.

Chapter IV

ETHIDIUM ION BINDING WITH dCA_5G + dCT_5G

1. Introduction

Since the ethidium ion (EI) exhibited sequence dependence in binding to complementary dinucleoside phosphates, the next logical step was to see if such specificity applied in longer sequences. Two separate investigations of binding to deoxytetranucleoside triphosphates (Patel & Canuel, 1976) and deoxytetranucleotides (Kastrup et al., 1978) have been reported. In each, the binding of dye in a Py(3'-5')Pu site (if present) predominated over binding to other site types. Ethidium ion binding in ribo- and deoxyribo- oligonucleosides with the general sequences CA_nG, CU_mG, and CT_mG where n and m are 5 or 6 is under study in this lab; a preliminary report of results can be found in Tinoco et al. (1981).

We report some CD and FDCD measurements on dCA_5G + dCT_5G + EI. In these experiments the ratio of dye to each single strand was ~1/3, so most of the minihelices contained no ethidium ion; those that did, bound only one dye. Three types of binding site exist in these minihelices: Py(3'-5')Pu (dC-dA:dT-dG, 1 site), Pu(3'-5')Pu (dA-dA:dT-dT, 4 sites), and another Pu(3'-5')Pu (dA-dG:dC-dT, 1 site). Evidence from the dimer studies indicates that dC-dA:dT-dG is the preferred binding site. We test this hypothesis in a comparison of the FDCD spectrum of the heptamer complex with the spectra obtained from dimer complexes (Chapter II).

2. Experimental

A) Materials

The deoxyribo-heptanucleoside hexaphosphates dCA_5G and dCT_5G were

prepared by the diester chemical method using triisopropylbenzenesulfonyl chloride as the condensing agent (Khorana, 1968); these compounds were provided by Dr. Frank Martin. The molar extinction coefficients were calculated from the dinucleoside phosphates' and mononucleotides' values using the nearest neighbor approximation (*Handbook of Biochemistry, Selected Data for Molecular Biology*, 3rd Edition, CRC Press, p. 586). Molar extinction coefficients per strand were ε_{260} 79,000 for dCA_5G and ε_{260} 58,000 for dCT_5G.

Ethidium ion solutions were prepared as in Chapter II. The buffer for these experiments was composed of 0.2 M NaCl, 10 mM phosphate, pH 7.0. Two solutions of dye: alone (0.026 mM) and mixed with dCA_5G and dCT_5G (0.070 mM in each strand), were prepared in buffer for all experiments.

B) Methods

Optical melts at 260 and 280 nm were run on the Gilford 250 with 2 mm cells as described in Chapter II. Absorbance spectra in the ultraviolet (2 mm cell) and the visible (1 cm cell) were also taken on this instrument. CD and FDCD spectra were run in a 2 mm cell on the Cary 60 as in Chapter III; the cutoff filter for FDCD was a Schott KV 408. Spectra were measured at 1, 5, 15, 25, 34, and 50^{0}C for the absorbance and CD, and at 1, 25, and 34^{0}C for the FDCD.

Photoselection in the FDCD was tested with a linear polarizer mounted in front of the cutoff filter (Tinoco et al., 1977) in one of two positions: polarization sense vertical ($\phi = 0^0$) and polarization sense horizontal ($\phi = 90^0$). In addition, the normal FDCD spectrum with no polarizer was taken. Each averaged spectrum was analyzed via equations (1) and (2) of Chapter II with the CD and absorbance

spectra to obtain $\Delta\varepsilon_F/\varepsilon_F$ (= g_F). The three Kuhn anisotropies were then run in the equations of Table V to evaluate any photoselection in the heptamer minihelix:EI complex. Photoselected behavior was assumed if $\Delta\varepsilon_{33,F}/\varepsilon_F$ did not randomly scatter around a value of zero across the spectrum. The average Kuhn anisotropy from Table V, equation (1) was plotted in each case.

3. Results and Discussion

A) Melting of dCA_5G:dCT_5G:EI

The optical melt of the dCA_5G/dCT_5G/EI mixture is shown in Figure 4.1. The absorbance at 280 nm, which is near an isosbestic point for minihelix absorbance, monitors the amount of dye bound at any temperature (Dr. Frank Martin, personal communication). On the other hand, at 260 nm, the dye absorbance is low and the melting of the helix can be followed. The melting temperature, T_m, for the helix alone is 25 ± 1^{0}C, while in the presence of approximately 1 ethidium ion for every 3 helices it is 27 ± 1^{0}C. The apparent melting temperature for the dye in the helix from the absorbance at 280 nm is 34 ± 1^{0}C. The difference in the helix melting temperatures in the mixture can be rationalized with a model in which the dye molecules bind to extant double-stranded regions rather than remain free in solution, i.e. there is migration of an ethidium ion from a complex that is melting to other remaining minihelices (Dr. Frank Martin, personal communication). This preference for dye binding to double-stranded sites was also observed in denatured DNA (Aktipis et al., 1975). Under this model, at 27^{0}C, 50% (ca. 0.035 mM) of the helices have reverted to single strands while ~80% (0.020 mM) of the dye molecules remain bound; at 34^{0}C, ~20% (0.014 mM) of the minihelices remain and 50% (ca. 0.013 mM) of the dye

TABLE V

EQUATIONS FOR PHOTOSELECTED FDCD

Measured Quantities[a]

Phototube, polarizer orientation	Kuhn anisotropy ($= g_F$)
$\theta = 90^0$, no polarizer	$\dfrac{6\Delta\varepsilon_F/\varepsilon_F + 2\Delta\varepsilon_{33,F}/\varepsilon_F}{7 - \varepsilon_{33,F}/\varepsilon_F}$
$\theta = 90^0$, $\phi = 0^0$	$\dfrac{4\Delta\varepsilon_F/\varepsilon_F - 2\Delta\varepsilon_{33,F}/\varepsilon_F}{3 + \varepsilon_{33,F}/\varepsilon_F}$
$\theta = 90^0$, $\phi = 90^0$	$\dfrac{\Delta\varepsilon_F/\varepsilon_F + 2\Delta\varepsilon_{33,F}/\varepsilon_F}{2 - \varepsilon_{33,F}/\varepsilon_F}$

where

$\Delta\varepsilon_F/\varepsilon_F = 4R/D$ = average Kuhn anisotropy

$\Delta\varepsilon_{33,F}/\varepsilon_F = 4R_{33}/3D$ α Kuhn anisotropy along emission transition moment

$\varepsilon_{33,F}/\varepsilon_F = D_{33}/3D$ α absorption along emission transition moment

[a]Tinoco et al. (1977).

TABLE V

EQUATIONS FOR PHOTOSELECTED FDCD

Solution for Unknowns

$$\Delta\varepsilon_F/\varepsilon_F = (2g_\perp g_N - g_{||}g_N - g_{||}g_\perp)/M \quad (1)$$

$$\Delta\varepsilon_{33,F}/\varepsilon_F = (3g_\perp g_{||} - 2g_N g_{||} - g_N g_\perp)/M \quad (2)$$

$$\varepsilon_{33,F}/\varepsilon_F = (-3g_\perp - 4g_{||} + 7g_N)/M \quad (3)$$

where $M = g_\perp - 2g_{||} + g_N$

$g_N = g_F$ at $\theta = 90^0$, no polarizer

$g_\perp = g_F$ at $\theta = 90^0$, $\phi = 0^0$

$g_{||} = g_F$ at $\theta = 90^0$, $\phi = 90^0$

Figure 4.1. Optical melt of dCA_5G (0.079 mM), dCT_5G (0.079 mM), and ethidium ion (0.026 mM) mixture. Measurements at 260 nm track the nucleic acid components during the melt; those at 280 nm track the dye only. Melting temperatures are 25 ± 1^{0}C for the helix in absence of the dye, 27 ± 1^{0}C for the helix in the presence of the dye, and 34 ± 1^{0}C for the dye in the presence of the helix.

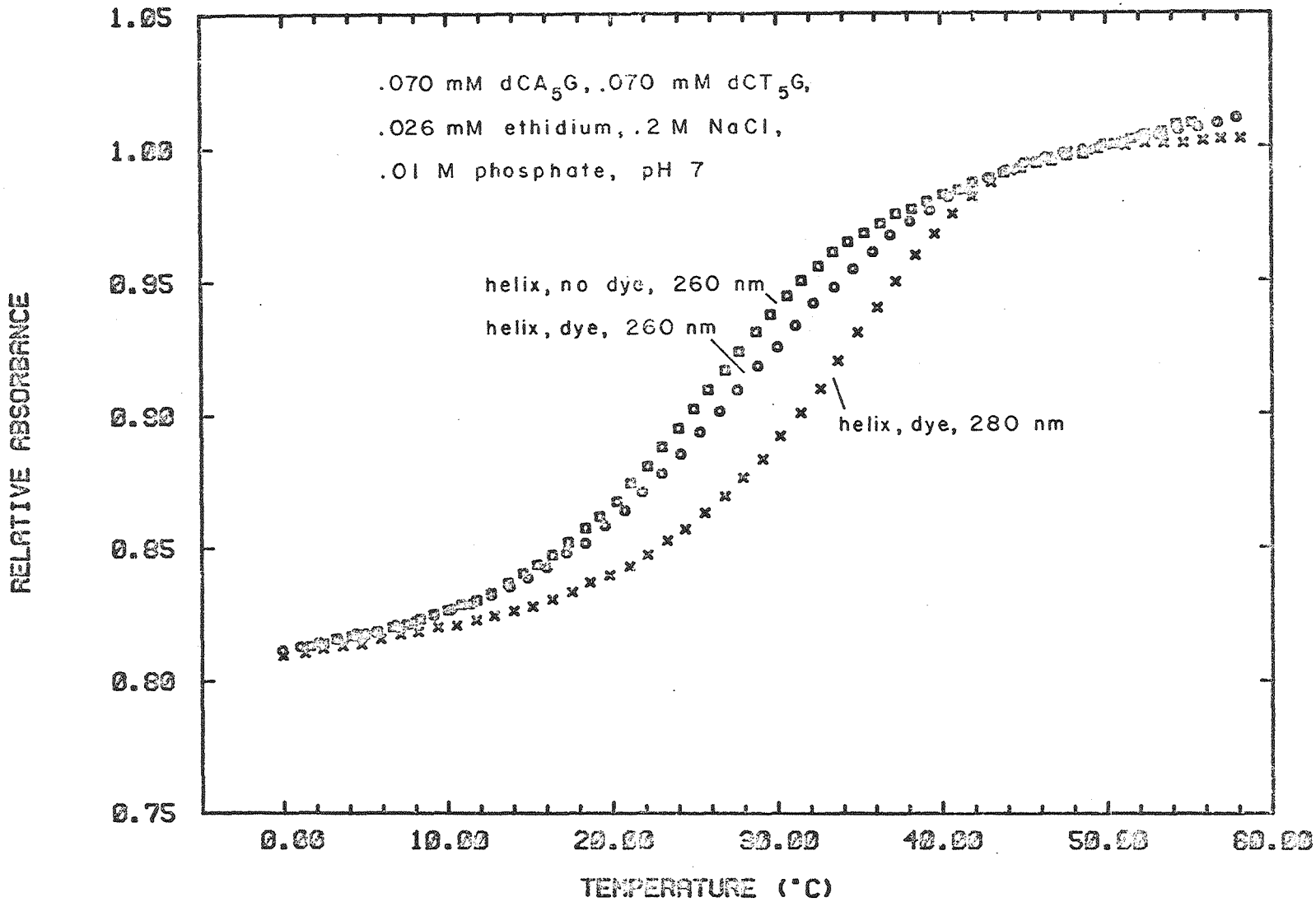

XBL 8011-12716

molecules are free in solution. Thus, up to ~34^{0}C, there is an average of one ethidium ion or less bound in the minihelices, a suitable situation to distinguish preferences for different intercalation sites.

Two binding curves are presented in Figure 4.2. In Figure 4.2a, the absorbance difference at 466 nm between ethidium ion alone and in the mixture is plotted vs. temperature; in Figure 4.2b, the absorbance λ_{max} for dye alone and in the dCA_5G/dCT_5G mixture is plotted vs. temperature. Each mixture curve approaches an asymptotic limit at low temperature, indicating almost all the dye is bound there. The maximum wavelength for fully bound dye, 518 nm, agrees with previous results of dye complexes with dimers (Krugh & Reinhardt, 1975; Krugh et al., 1975; Reinhardt & Krugh, 1978), tetramers (Kastrup et al., 1978), and DNA (Waring, 1965).

B) Circular Dichroism Studies

The CD spectrum of dCA_5G:dCT_5G as a function of temperature is displayed in Figure 4.3; in Figure 4.4, ethidium ion has been added to the solution. The appearance of the induced CD band above 300 nm at low temperatures is indicative of dye intercalation into the minihelix. The negative CD lobe between 290 and 300 nm increases by roughly a factor of two when the dye binds in the heptamer at 1^{0}C. The spectra before and after ethidium ion binding are relatively unchanged below 290 nm.

After subtraction of the minihelix baseline contribution to the CD, $\Delta\varepsilon$ per bound dye at 310 nm is 2.1 ± 0.5 L/mol-cm at 1^{0}C, assuming all dye is bound. This value is lower than in complexes with the dimers (Table III). Even with the apparent decrease in $\Delta\varepsilon_{bound}$ when ethidium ion binds in a deoxyribo- sequence (compared to its ribo- an-

Figure 4.2. Binding curves for 0.026 mM ethidium ion in the presence of dCA_5G + dCT_5G (0.070 mM in each strand). (a) Difference in absorbance at 466 nm vs. temperature for ethidium alone and in the presence of the helix. (b) Wavelength of maximum absorbance vs. temperature for ethidium alone and in the mixture.

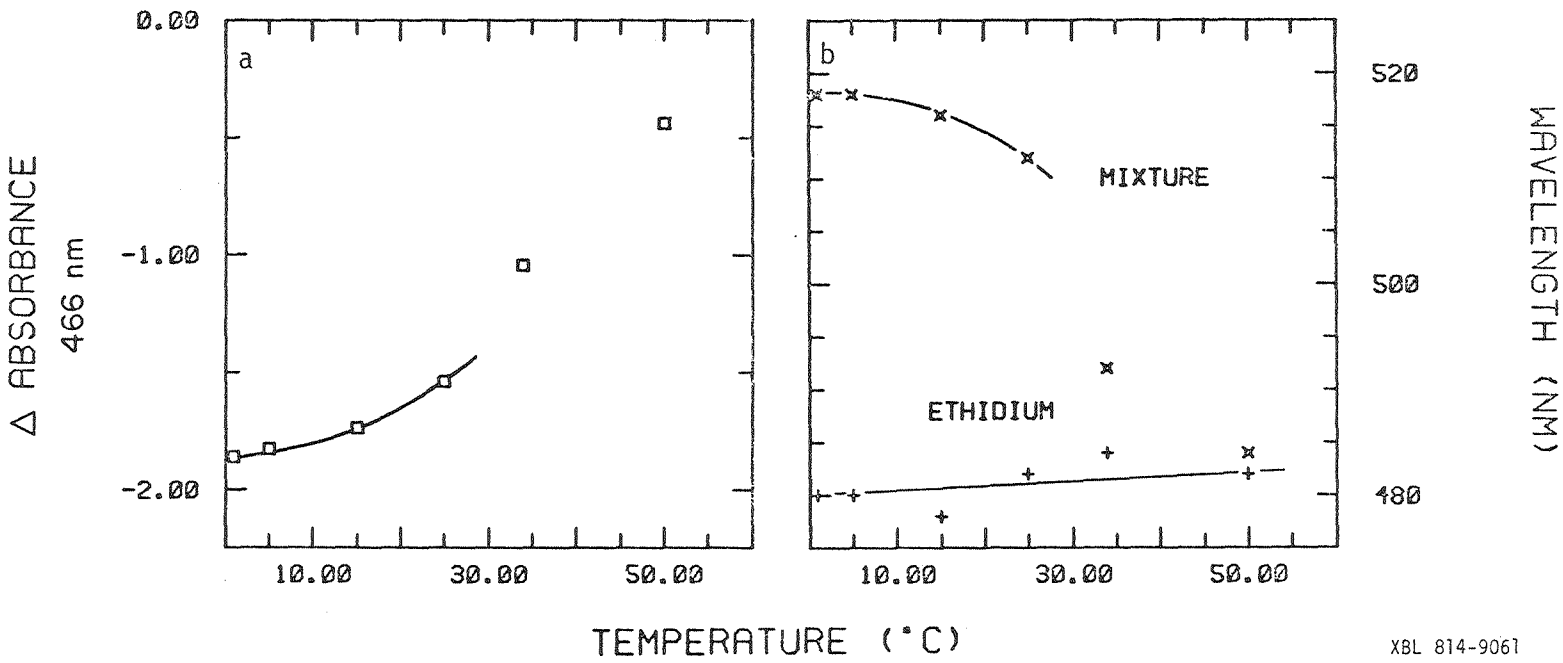
0.00
-1.00
-2.00
Δ ABSORBANCE
466 nm
a
b
MIXTURE
ETHIDIUM
520
500
480
WAVELENGTH (NM)
10.00
30.00
50.00
10.00
30.00
50.00
TEMPERATURE (°C)

XBL 814-9061

Figure 4.3. Circular dichroism spectra of dCA_5G + dCT_5G mixture (0.070 mM in each strand) vs. temperature. Cell length is 2 mm.

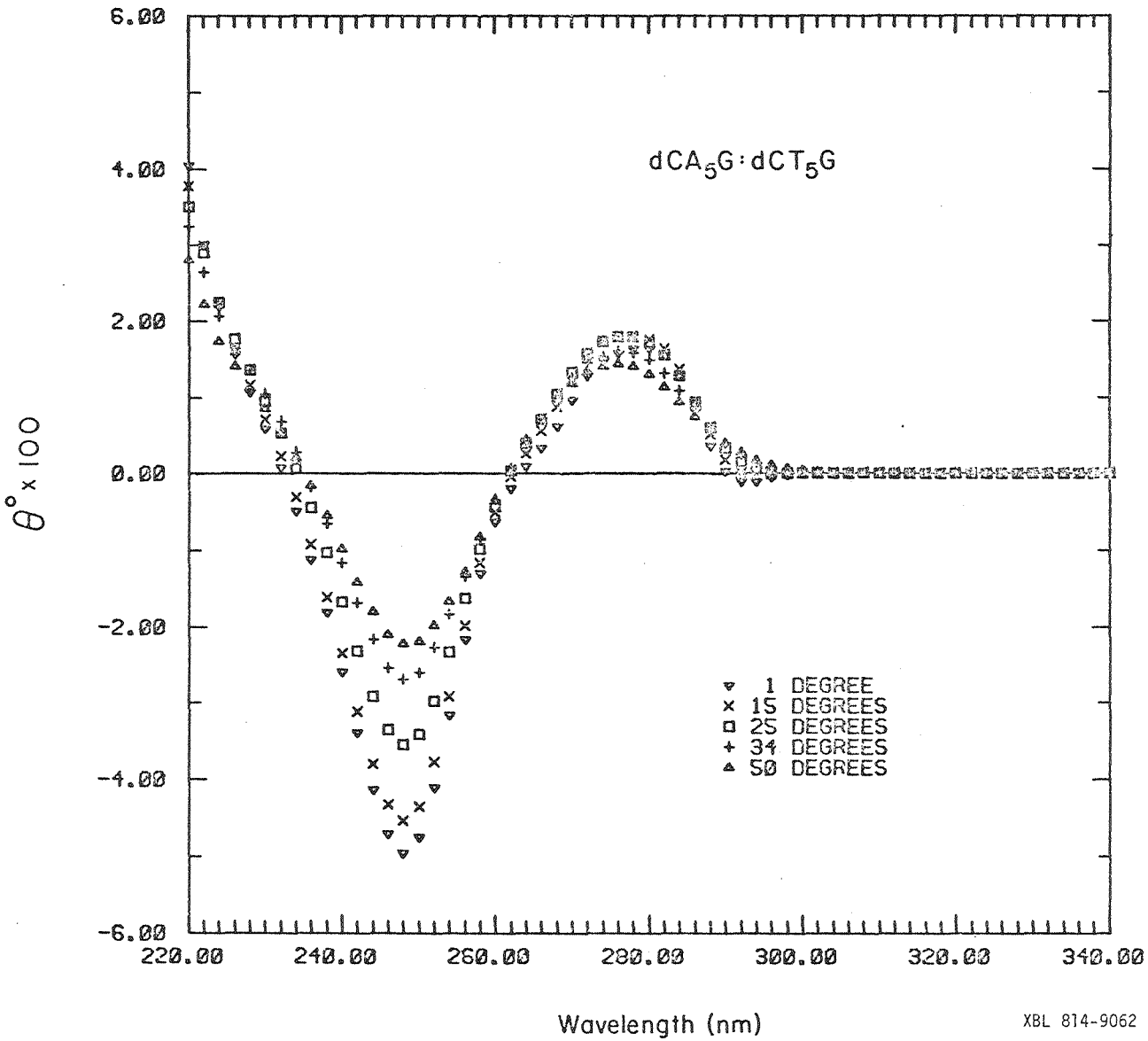
dCA5G:dCT5G
6.00
4.00
2.00
0.00
-2.00
-4.00
-6.00
θ° x 100
220.00
240.00
260.00
280.00
300.00
320.00
340.00
Wavelength (nm)
1 DEGREE
15 DEGREES
25 DEGREES
34 DEGREES
50 DEGREES

XBL 814-9062

Figure 4.4. Circular dichroism spectra for ethidium ion (0.026 mM) in the mixture of dCA_5G + dCT_5G (0.070 mM in each strand). Cell length is 2 mm. Spectra at 1 and 15^0C have been multiplied by 50 above 300 nm.

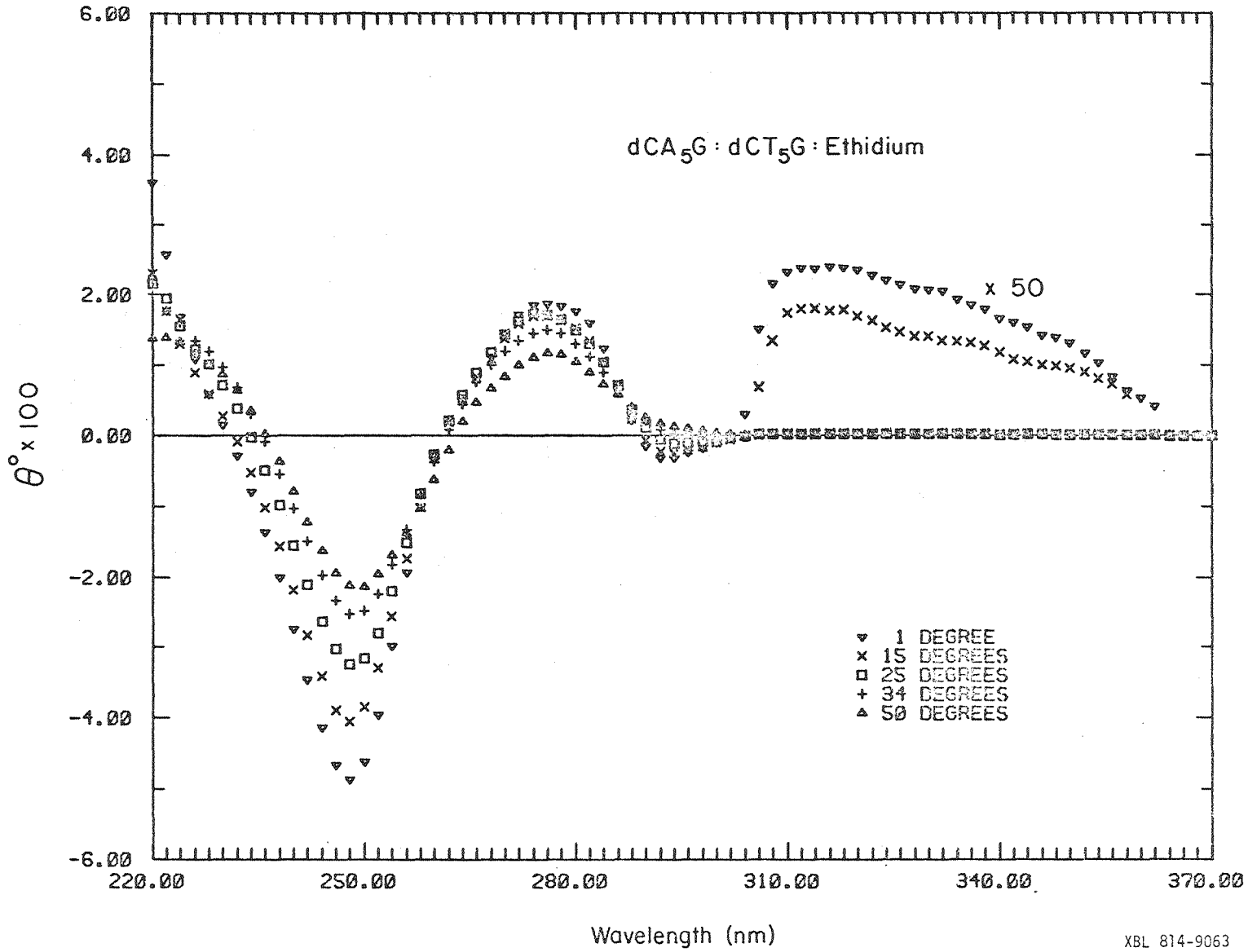
dCA5G : dCT5G : Ethidium
x 50
1 DEGREE
15 DEGREES
25 DEGREES
34 DEGREES
50 DEGREES
6.00
4.00
2.00
0.00
-2.00
-4.00
-6.00
θ° x 100
220.00
250.00
280.00
310.00
340.00
370.00
Wavelength (nm)

XBL 814-9063

alogue), it is difficult to make a case for preferential binding of dye in the dC-dA:dT-dG site with this result. Contributions to the dye's induced CD from bases beyond the immediate base pairs may also be significant in longer sequences so that the dimer complexes' CD's are not adequate models for comparison.

C) FDCD Spectra of dCA_5G:dCT_5G:EI

The averaged FDCD signals at two temperatures for dCA_5G:dCT_5G:EI with and without a linear polarizer are shown in Figure 4.5. The noise level at 34^{0}C is higher than at 1^{0}C; this is because half the dye present is free in solution at the higher temperature (see Figure 4.1).

In the FDCD measurements of dimer:ethidium complexes, the spectra taken with a polarizer were virtually coincident with the spectrum taken without it, or at least they were equally offset from it. We see similar behavior in the dCA_5G:dCT_5G:EI complex at 34^{0}C. This is a crude indication that photoselection is not occurring in the FDCD (Turner et al., unpublished results). The true test for photoselection comes in the analysis with the three anisotropies by equation (2) in Table V. The dimer:ethidium ion complexes showed no measurable anisotropy along the emission transition moment axis ($\Delta\varepsilon_{33,F}/\varepsilon_F$): all values were scattered randomly about an anisotropy of zero. The same result occurs for dCA_5G:dCT_5G:EI at 34^{0}C; we conclude that there is no photoselection in these cases. For the heptamer:dye complex at 1^{0}C, $\Delta\varepsilon_{33,F}/\varepsilon_F$ was skewed toward a nonzero anisotropy, indicating some degree of photoselection. Equilibrium sedimentation studies of dCA_5G + dCT_5G at low temperatures uncovered evidence of aggregation by the minihelices (Nelson et al., 1981). The longer rotational lifetimes of the aggregates are probably responsible for the photoselection at 1^{0}C.

Figure 4.5. Averaged FDCD signals for the ethidium ion (0.026 mM)/dCA_5G (0.070 mM)/dCT_5G (0.070 mM) mixture in 2 mm cell at 1^{0}C (top) and 34^{0}C (bottom). Vertical lines represent 95% confidence limits.

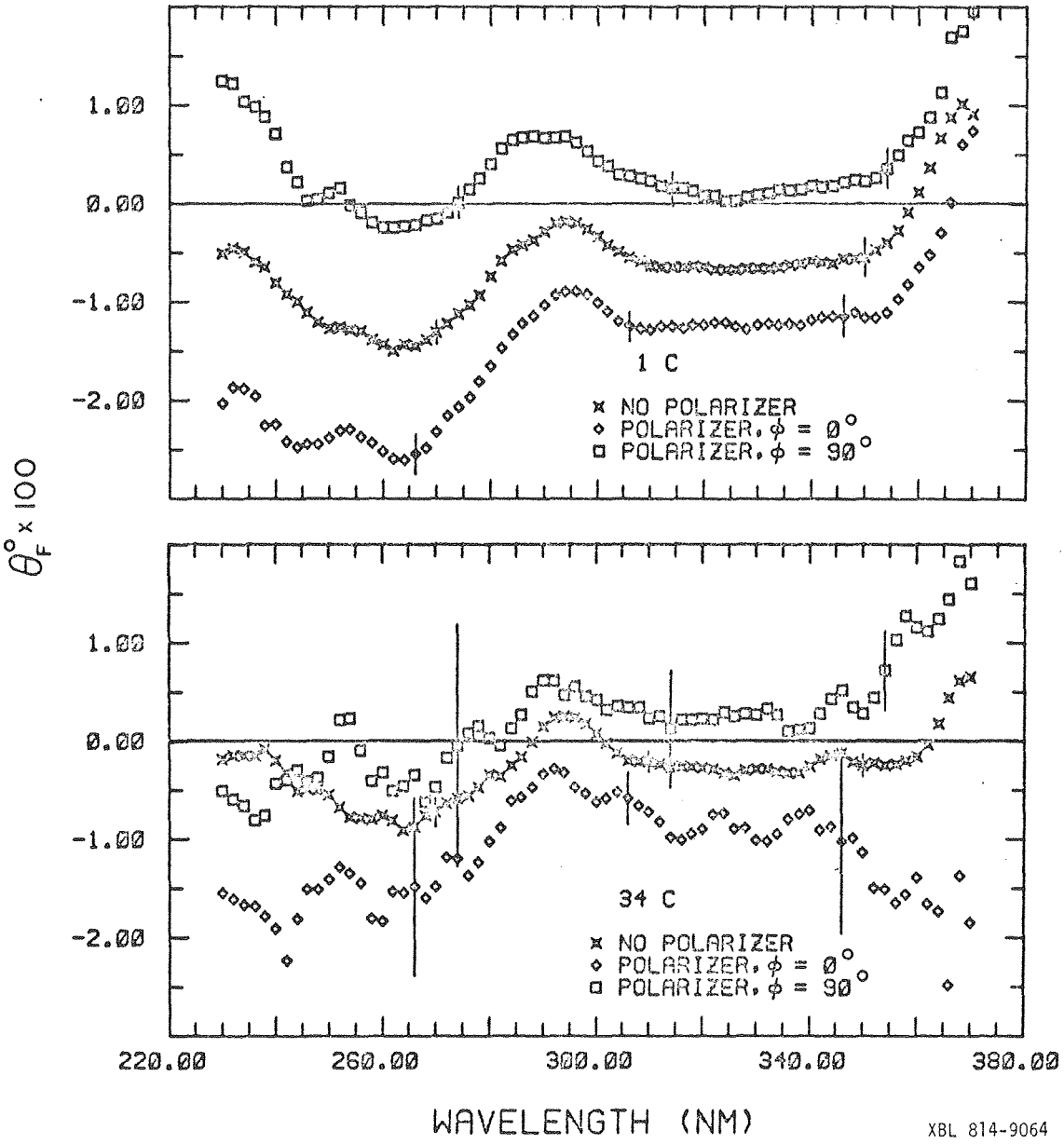
1.00
0.00
-1.00
-2.00
1 C
NO POLARIZER
POLARIZER, φ = 0°
POLARIZER, φ = 90°
$\theta_F^\circ \times 100$
1.00
0.00
-1.00
-2.00
34 C
NO POLARIZER
POLARIZER, φ = 0°
POLARIZER, φ = 90°
220.00
260.00
300.00
340.00
380.00
WAVELENGTH (NM)

XBL 814-9064

The average Kuhn anisotropy of $dCA_5G:dCT_5G:EI$ calculated via equation (1) (Table V) is presented in Figure 4.6. The two spectra are similarly shaped, only the magnitudes of the bands have changed. We have not made the instrumental corrections necessary for reducing the instrumental artifacts of the FDCD spectrometer which are exacerbated in photoselecting systems (Lobenstine & Turner, 1979, 1980). Thus, the results at 1^0C contain some error of unknown magnitude, but we believe the main effect is to shift the relative position of the zero line for this spectrum.

Relying on similarities between the FDCD spectra for analogous deoxyribo- and ribo- dimer complexes with ethidium ion, the FDCD spectrum for $dCA_5G:dCT_5G:EI$ at 1^0C can be compared with the spectra for each of the binding sites in Figure 4.7. Here the FDCD spectra for CpA:UpG:EI, ApA:UpU:EI, and ApG:CpU:EI represent ethidium ion binding in the dC-dA:dT-dG, dA-dA:dT-dT, and dA-dG:dC-dT sites of the heptamer, respectively. There is no close agreement between the spectrum of the heptamer and one of the "site" spectra, even for the presumably preferred dC-dA:dT-dG site, although the general patterns for all are similar. A search for the reasons behind this lack of agreement poses more questions than it answers.

On an obvious level, whether the spectra for the ribo- dimers resemble those of their deoxyribo- analogues is open to further study. Only two cases to date have been studied, CpG vs. dCpG and UpA vs. dTpA, and any similarities between the latter two were restricted to some parts of the spectrum. One way to escape this problem altogether is to take FDCD spectra with the ribo- minihelix $rCA_5G:rCU_5G$, plus ethidium ion.

Figure 4.6. Kuhn anisotropy of a 1:1:1 complex of dCA_5G:dCT_5G:EI at 1^0C (top) and 34^0C (bottom). Vertical lines represent estimated errors.

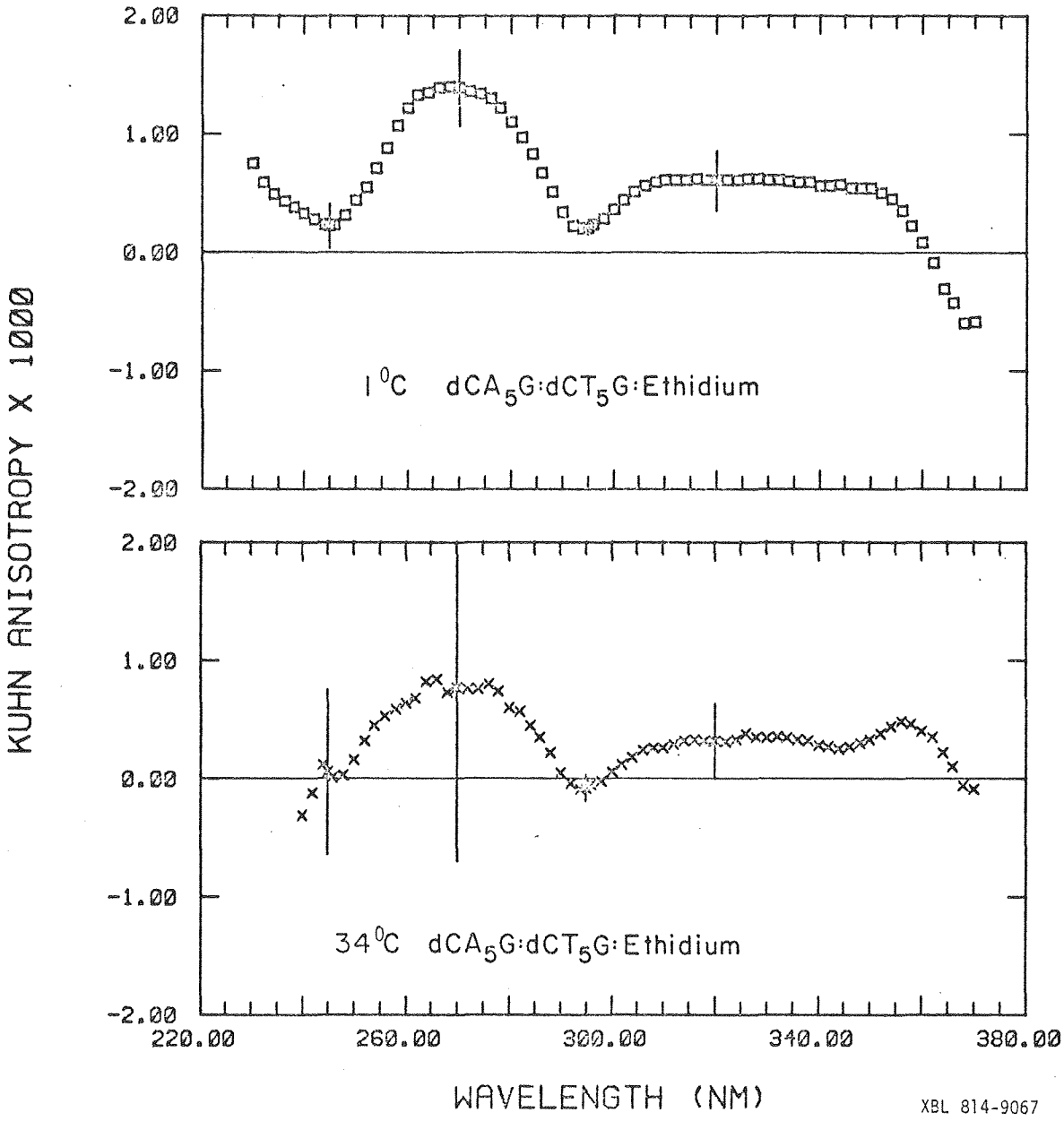
2.00
1.00
0.00
-1.00
-2.00
1 °C dCA5G:dCT5G:Ethidium
2.00
1.00
0.00
-1.00
-2.00
34 °C dCA5G:dCT5G:Ethidium
220.00
260.00
300.00
340.00
380.00
KUHN ANISOTROPY X 1000
WAVELENGTH (NM)

XBL 814-9067

Figure 4.7. Kuhn anisotropy of 1:1:1 complex of dCA_5G:dCT_5G: EI compared with those of dimer:dye complexes representing the binding sites in the heptamer minihelix. Vertical lines represent estimated errors.

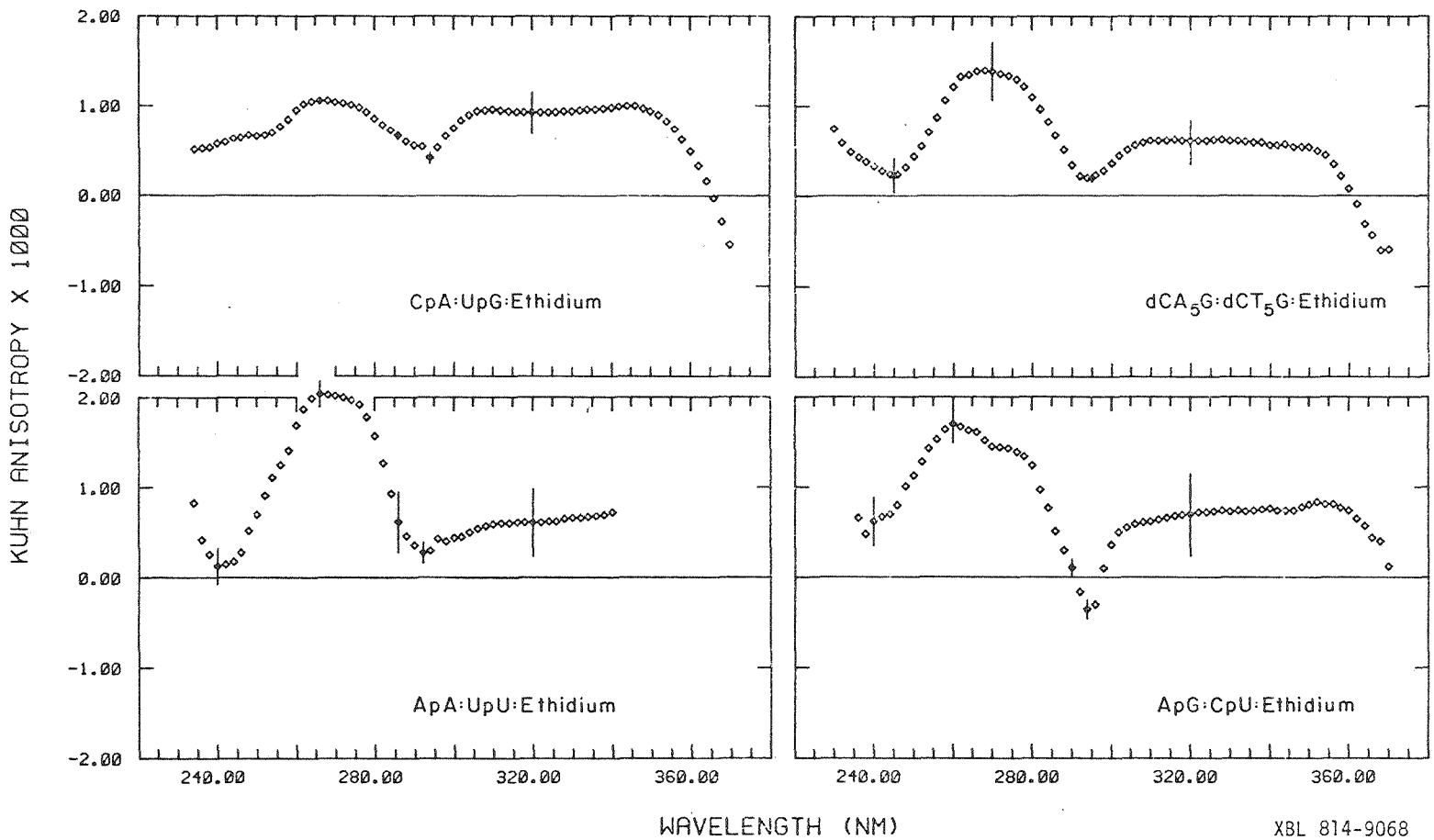
KUHN ANISOTROPY X 1000
2.00
1.00
0.00
-1.00
-2.00
CpA:UpG:Ethidium
dCA5G:dCT5G:Ethidium
ApA:UpU:Ethidium
ApG:CpU:Ethidium
240.00
280.00
320.00
360.00
WAVELENGTH (NM)
XBL 814-9068

Another questionable assumption is the maintenance of relative preferences for ethidium ion binding to the different types of sites. The relative preferences for binding from dimer studies are 50:1.6:1 for the dC-dA:dT-dG, dA-dG:dC-dT, and dA-dA:dT-dT sites, respectively (ignoring the deoxyribo- vs. ribo- question). Tinoco and co-workers (1981) found that the best fits to melting curves of ethidium ion in dCA_5G:dCT_5G or rCA_5G:rCU_5G were obtained by assuming the dye bound preferentially in the Py(3'-5')Pu site relative to any of the Pu(3'-5')Pu sites. This site's binding constant was only 10 times larger than those for the other sites, a preference less than that seen in the dimers. In any case, there is some dye bound in sites other than the dC-dA:dT-dG site. Thus, the FDCD signal is partly from each of the three types of sites. For more than one fluorescent species, the Kuhn anisotropy, g_F, is given by

$$g_F = \sum_i \phi_i C_i \Delta\varepsilon_i / \sum_i \phi_i C_i \varepsilon_i \qquad (4)$$

where $\Delta\varepsilon_i$ is the molar CD of species i, ε_i is the molar extinction coefficient of species i, C_i is the molar concentration of species i, and ϕ_i is the quantum yield of species i (Tinoco & Turner, 1976). Even with the assumption of equivalent quantum yields for each site, this expression is not simply a concentration-weighted average of individual site anisotropies. Resolution of contributions from individual sites is an onerous task requiring more experimental evidence than is presently available.

It is apparent from this attempt to measure preferential dye binding in oligomers by FDCD that the sequence must be carefully chosen.

There must be a strong preference for ethidium ion binding to one of the sites and/or the number of different site types must be minimized. A further factor which may complicate the picture in the current case, or any other, is possible contributions to the CD spectrum from bases further away from the dye than those in the binding site. Dye binding to sequences such as $A_n + U_n$ where n = 2 to ~10 would be useful in examining the effects of bases beyond the nearest neighbors and/or other bound dye molecules on the FDCD spectrum of the complex.

Chapter V

COUNTERION EFFECTS ON DNA:ETHIDIUM ION COMPLEXES

1. Introduction

The DNA molecule, a polyanion, is sensitive to cation concentration. In general, double-stranded nucleic acids are stabilized by higher counterion concentrations (see Bloomfield et al., 1974, for review), and large conformational changes in DNA with salt/solvent conditions have been observed, as in the B form to A form transition (Ivanov et al., 1973; Ivanov et al., 1974) and the B form to C form transition (Ivanov et al., 1974). Application of polyelectrolyte theory to DNA properties in different salt concentrations has been done; one of the more successful theories is that of Manning (1978, review).

The ethidium iom, a cation, is sensitive to the salt concentration when binding to DNA (LePecq & Paoletti, 1967; Aktipis & Kindelis, 1973; Houssier et al., 1974). Furthermore, in addition to the normal intercalation binding with DNA, there is a weaker, outside binding associated with ethidium-DNA electrostatic interactions (Waring, 1965). Such binding becomes predominant at high dye-to-phosphate ratios.

The induced circular dichroism (CD) of ethidium ion (EI) bound to DNA as a function of added salt has been studied previously. Aktipis and Kindelis (1973) observed no change with ionic strength in the $\Delta\varepsilon^{307}_{bound}$ vs. r curve (Figure 1.5). In this study they increased the NaCl concentration from 0 to 5 M in a basal buffer of 0.04 M tris-HCl, pH 7.9 for the DNA/dye solutions. Houssier and co-workers

(1974), working in 0.1 M and 1 mM NaCl buffers, found coincident $\Delta\varepsilon^{308}_{bound}$ vs. r curves for the induced CD of ethidium ion; however, their binding curve was at slightly higher values of $\Delta\varepsilon_{bound}$ relative to that of Aktipis and Kindelis (1973). More recently, Pardi (1980) compared the magnitude of the induced CD at 307 nm for *E. coli* DNA/ethidium ion complexes at the same binding ratio, but in different salt solutions. He found that $\Delta\varepsilon_{bound}$ was larger for the same complex in 0.6 mM Na^+ than in 50 to 500 mM Na^+, suggesting that there may actually be an ionic strength dependence for the bound dye's induced CD. In a CNDO/S study of the optical properties of ethidium ion, LeBret and Chalvet (1977) found that the shift of the dye's visible absorption band upon intercalation in DNA was almost entirely due to interaction of the dye with the phosphates of the DNA backbone. These last two works suggest that electrostatic interactions between charged groups and the bound dye may be very important in determining its optical properties.

We have run a series of experiments designed to further investigate the ionic strength dependence of the ethidium ion's induced CD when bound in DNA. We use the approach of Pardi (1980), who first dialyzed DNA samples against doubly distilled water to remove excess counterions from the DNA. This enables us to achieve lower effective Na^+ concentrations when the DNA is finally diluted in the buffer. Our results qualitatively support his: at lower counterion concentrations, $\Delta\varepsilon$ per bound dye increases relative to measurements made in higher counterion concentrations, all other things being equal. Applying Manning's theory (1978) to the DNA/EI complexes, we calculate the effective counterion concentrations in the "bound" and "free" states and

discuss a possible correlation between these electrostatic properties and the induced CD of the dye.

2. Experimental

A) Materials

Calf thymus DNA was purchased from Worthington Biochemical. A stock solution was prepared with ~200 mg of the DNA in ~200 ml of buffer (100 mM NaCl, 1 mM tris, 1 mM EDTA, pH 7.5). This solution was kept in the cold. Ethidium bromide was prepared as in Chapter II. All dye stock solutions were in doubly distilled water; their concentrations were between 0.4 and 2.5 mM.

Buffer solutions of NaCl/tris (hydroxymethyl) aminomethane were all mixed with doubly distilled water in prerinsed glassware. A high salt solution of 100 mM NaCl, 1.0 mM tris was prepared in a volumetric flask by dilution of an aliquot of 0.10 mM tris-HCl buffer, pH 7.6 (Sigma) and a weighed amount of NaCl (Sigma). The pH of the solution was 7.6 as measured with a glass electrode (Sigma) attached to a pH meter (Radiometer). A second buffer (1.0 mM NaCl, 10 μM tris) was prepared in the same fashion; the low salt solution of 0.1 mM NaCl, 1.0 μM tris was made by dilution of this stock with doubly distilled water. The pH of this solution was ~6.5.

B) Methods

i) Dialyses

Calf thymus DNA was dialyzed to remove excess counterions following the approach of Record (1975). Preliminary phenol extractions on the DNA showed no contaminating protein was present; the A_{260}/A_{280} ratio for the DNA was 1.9. Aliquots (5-10 ml) of DNA stock solution were sheared by repeated passage through a 30-gauge Teflon needle, af-

ter which they were tied in dialysis tubing (VWR Scientific) cleaned by the method in Brewer et al. (1974).

All dialysis solution volumes were ~40x the original volume of DNA in each bag. Each sample was dialyzed in the cold for 24 hours against the original buffer (100 mM NaCl, 1 mM tris, 1 mM EDTA, pH 7.5), followed by another run vs. the same buffer without the EDTA. Next, four successive 24 hour dialyses vs. doubly distilled water were run to remove excess sodium ions. Samples were removed from the tubes and stored in the cold in sealed flasks.

Possible DNA denaturation during the dialysis was tested with optical melts on the Gilford 250. Samples were first degassed by bubbling with helium. In Figure 5.1 the melting curves for dialyzed and undialyzed samples at 1:5 dilution in the high salt solution are displayed; the dialyzed sample possesses a higher pre-melt baseline because of dilution of the DNA stock during dialysis. The melting temperature for each sample is around 83^0C. The expected melting temperature in 200 mM Na^+ is 86^0C (Marmur & Doty, 1962), based upon the 42% G+C content of calf thymus DNA (Chan et al., 1979); since the salt content in our experiments is only 80 mM Na^+, the actual melting temperature is slightly lower than the prediction, as expected. The breadth of the transition, defined as the inverse of the transition slope (Record, 1975), was 11^0C for each.

To more accurately compare any differences between the two samples, the hypochromicity, h, defined as $100(1 - A_{260}^{25^0C}/A_{260}^{90^0C})$, was calculated for each sample. For the undialyzed case, h_{260} = 20%, while for the dialyzed case, h_{260} = 16%. These values are both less than the commonly reported values for double-stranded nucleic acids

Figure 5.1. Melts of calf thymus DNA stocks before (□) and after (X) dialysis to remove excess Na^+ ions. Aliquots of stocks were diluted to 5x their volume with 100 mM NaCl, 1.0 mM tris. Actual NaCl concentration is ~80 mM for the dialyzed sample, 100 mM for the undialyzed sample. Absorbances at 260 nm and 25^0C are 0.69 for the dialyzed sample and 0.94 for the undialyzed sample; cell length is 2 mm.

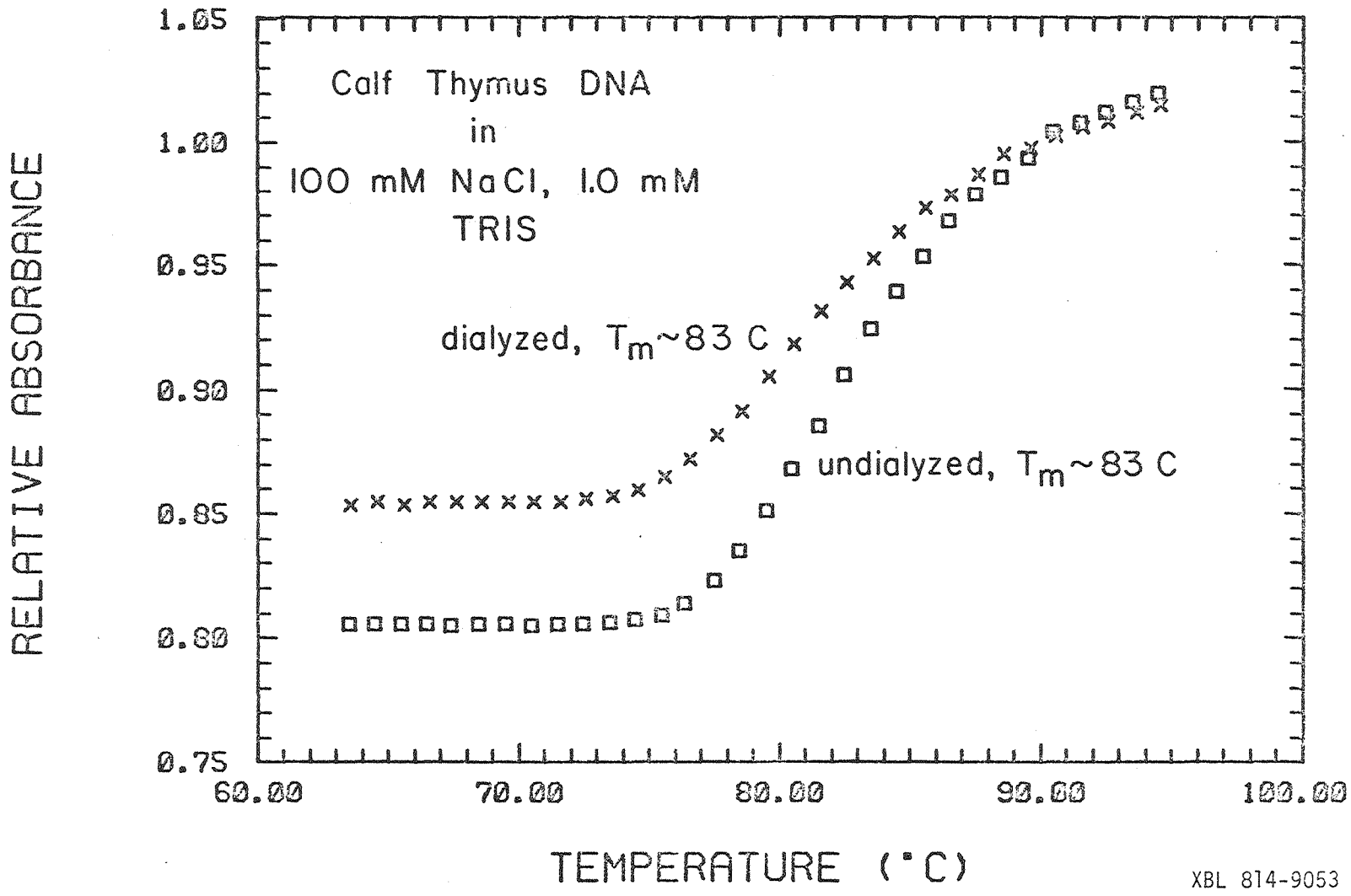
Calf Thymus DNA
in
100 mM NaCl, 1.0 mM
TRIS
dialyzed, T_m~83 C
undialyzed, T_m~83 C
RELATIVE ABSORBANCE
1.05
1.00
0.95
0.90
0.85
0.80
0.75
60.00
70.00
80.00
90.00
100.00
TEMPERATURE (°C)

XBL 814-9053

(Bloomfield et al., 1974), indicating some denaturation of the DNA sample might have occurred before the dialysis. The decrease in the hypochromicity after dialysis indicates further denaturation of the stock occurred. Nonetheless, the fact that there is a large population of double-stranded structures in the dialyzed stock, as witnessed by the melting curve, and that the dialysis procedure is reproducible allows us to prepare and use DNA samples by our method with confidence.

ii) Spectral Studies

The concentration of calf thymus DNA after dialysis was measured by diluting aliquots with 100 mM NaCl, 1 mM tris, pH 7.6 and taking the absorbance spectrum. For the DNA at 260 nm, an extinction coefficient per residue of 6600 L/mol-cm was used (Mahler et al., 1964). Concentrations of DNA in subsequent measurements were calculated from the dilution factor of the stock. DNA and dye mixtures were prepared with micropipets (Pipetman) and volumetric flasks. All volumes were checked by weighing the flask after each addition.

Scatchard analyses for the determination of ethidium ion binding constants with DNA were performed as in Waring (1965). Absorbance spectra in the visible region were taken in 1 cm quartz cells, digitized, and stored as in Chapter II. The temperature in the sample compartment was 25.0 ± 0.5^{0}C during the measurements. CD spectra of the DNA/EI solutions at either constant dye or constant DNA concentrations were run on the Cary 60 in 1 cm or 2 cm cells. The temperature was maintained at 25.0 ± 0.2^{0}C by thermoelectric cooling. Spectra were acquired, digitized, and stored as in Chapter II, also. The small contribution from the DNA to each spectrum was subtracted be-

fore the spectra were converted to the molar CD per bound dye basis.

iii) Theory

The theory of polyelectrolyte solutions and counterion condensation has been actively developed over the past fifteen years. We use the work of Manning (review, 1978) in our analyses.

A linear polyelectrolyte is characterized by a regular arrangement of charged groups along the length of the molecule. In DNA these groups are the phosphates and each possesses a formal -1 charge. The strong electrostatic repulsion forces between the groups are eased by condensation of a counterion on the macromolecule; incomplete binding of counterions in the equilibrium state strikes a balance between the maximization of entropy by counterion dissociation and minimization of charge-charge repulsion energy by binding. The condensed counterions migrate freely along the macromolecule and are in equilibrium with the uncondensed counterions; no site binding is invoked.

In Manning's treatment, the linear charge density of the polyelectrolyte, b, is the parameter governing the extent of counterion condensation through the dimensionless parameter ξ:

$$\xi = q^2/\varepsilon kTb \quad (= 7.1/b \text{ in water at } 25^0C) \qquad (1)$$

where q is the electronic charge, ε is the bulk dielectric constant of solvent, k is Boltzmann's constant, T is the Kelvin temperature, and b has the units of Å ngstroms/charge. Condensation of counterions will occur if $\xi > 1$, thus decreasing the linear charge density, and stop when $\xi = 1$. The effective charge per group is then $(N\xi)^{-1}$ where N is the absolute value of the counterion valence. Once the polyions are stabilized via the condensation, the interactions between them

and the remaining ions are amenable to the Debye-Hückel analysis. Manning's theory thus separates the counterions in a polyelectrolyte solution into two classes: 1) those which are condensed or "bound" to the polyion to ease the charge-charge repulsion and 2) those which are "free" in the remainder of the solution and interact with the partially charge-neutralized polyion according to the Debye-Hückel approximation.

For native DNA in the B form, the rise along the helix axis per base pair is 3.4 Å and there are two phosphate groups with -1 charges in this distance. Therefore, b is 1.7 Å and ξ is 4.2 (Manning, 1972). Condensation of Na^+ ions occurs in this case and the fractional charge per phosphate is reduced to $\xi^{-1} = 0.24$ by the "binding" of 0.76 Na^+ ions per phosphate.

One consequence of this theory is important for our purposes: if the density of charge on the polyelectrolyte is changed, the extent of counterion condensation will change. The ethidium ion carries a +1 charge and intercalates between base pairs of the DNA for $r < 0.25$ in the neighbor exclusion model. Thus, intercalation of the dye reduces the polyion charge density in two ways: by a formal neutralization of one of the -1 phosphate charges and by lengthening the helix 3.4 Å for each bound dye. With this simple model of dye binding, an expression for the average axial distance per charge as a function of the binding ratio r (up to the neighbor exclusion limit of $r = 0.25$) is

$$b = [1 + 3r/(1 - r)] \qquad (2)$$

where b is in Ångstroms. This relation is derived in Appendix D.

Several other quantities of interest are also derived by Manning. The number of counterions associated per fixed charge (in a 1:1 salt like NaCl) is

$$\theta_1 = 1 - \xi^{-1} \ . \tag{3}$$

The volume surrounding the polyelectrolyte within which the counterions are considered "bound" is

$$V_p = 41.1(\xi - 1)b^3 \tag{4}$$

where V_p is in cm^3/mole phosphate if b is in Ångstroms. The radius of a cylinder with volume V_p and length b aligned axially along the polyion length is

$$a = (V_p/\pi b L_{Avo})^{1/2} \tag{5}$$

where a is in Ångstroms and L_{Avo} is Avogadro's number. The local effective counterion concentration within V_p is

$$C_1^{loc} = 1000\ \theta_1/V_p \tag{6}$$

where C_1^{loc} is in moles/liter. These equations are all valid for native DNA and a total counterion concentration (1:1 salt) under 100 mM; we will apply them to DNA bound with intercalated dye.

3. Results

A) Stability of DNA

The stability of the dialyzed DNA in the Scatchard and CD experiments' conditions was tested via melts of representative solutions made with each of the two buffers. In Figure 5.2 the melts for 0.31 mM calf thymus DNA prepared by dilution of the dialyzed stock with

Figure 5.2. Melts for dialyzed calf thymus DNA (0.31 mM) prepared with solutions of 0.1 mM NaCl/1.0 μM tris (X) and 100 mM NaCl/1.0 mM tris (□). The T_m is 45 ± 1^{0}C in low salt (~0.45 mM Na^+) and 80 ± 1^{0}C in high salt (80 mM NaCl). Absorbances (2 mm cell) at 25^{0}C and 250 nm are 0.41 and 0.39 for the low and high salt solutions, respectively.

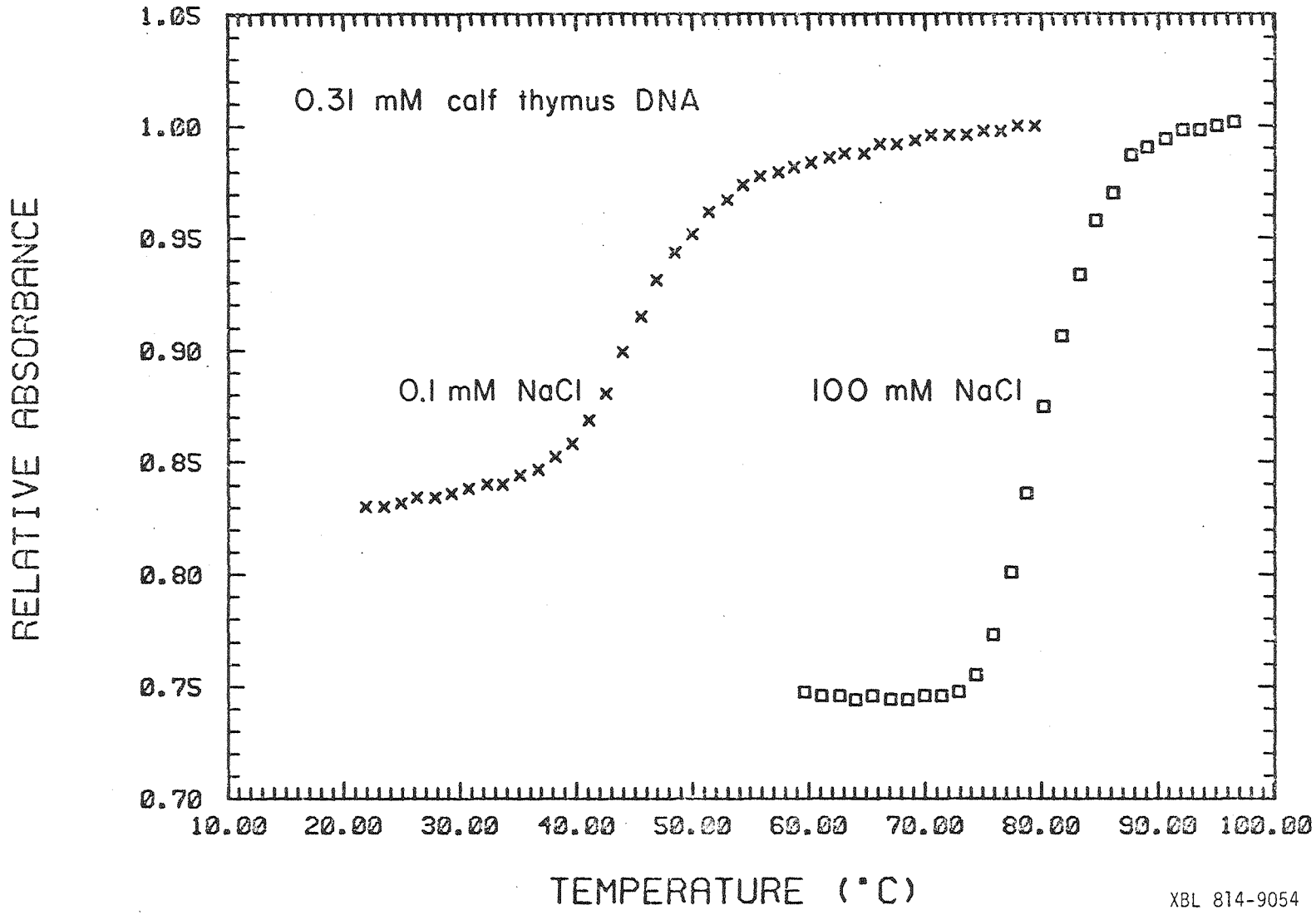
0.31 mM calf thymus DNA
0.1 mM NaCl
100 mM NaCl
RELATIVE ABSORBANCE
1.05
1.00
0.95
0.90
0.85
0.80
0.75
0.70
10.00
20.00
30.00
40.00
50.00
60.00
70.00
80.00
90.00
100.00
TEMPERATURE (°C)

XBL 814-9054

either 100 mM NaCl/1.0 mM tris and 0.1 mM NaCl/1.0 μM tris are presented. The T_m for the DNA in the high salt case is 80 ± 1^{0}C, while in the low salt case it is 45 ± 1^{0}C. At the temperature of the Scatchard and CD experiments, 25^{0}C, the DNA remains double-stranded according to these results.

A point requiring clarification in this chapter is the value of the total sodium ion concentration in the DNA/dye solutions. Dialysis of the DNA vs. doubly distilled water removed a large number of sodium ions from the solution, but the Donnan effect requires some to remain with the nucleic acid above the amount needed to maintain charge neutrality. For example, Record (1975), in the dialysis of T4 DNA vs. doubly distilled water, found that 2.5 Na^+ ions per phosphate remained in the solution after 18 hours. In a preliminary experiment, we analyzed for Na^+ with atomic absorption spectroscopy. Our results indicated that roughly 1.2 Na^+ ions were present per DNA phosphate. The important point is that the total Na^+ concentration in solution is *not* that of the buffer because of these counterions associated with the DNA and also becuase of dilution of the buffer (80% or more of the final solution volume is from the salt solution). With the constant DNA concentration (0.31 mM) employed in the low salt CD studies, the Na^+ concentration is at least 0.45 mM, depending upon the reliability of the Na^+ analyses. In the high salt solutions the Na^+ concentration is 80 mM or greater and the Na^+ contribution from DNA is minimal.

B) Binding of Ethidium Ion to DNA

Constant amounts of ethidium ion were titrated with DNA in the two salt solutions at 25^{0}C. Absorbance spectra at each salt level are

shown in Figures 5.3 and 5.4. The total dye concentration is near 0.03 mM and all is bound in ~0.5 mM DNA. The isosbestic points near 394 and 510 nm are indicative of two states for ethidium ion: free in solution and bound to the nucleic acid. For fully bound dye, the visible wavelength of maximum absorbance is 520 nm, a result which is in agreement with previous studies (Waring, 1965).

For ligands binding independently to equivalent sites on a macromolecule, the equilibrium between bound and free ligands is given by the Scatchard (1949) equation:

$$r/c_f = Kn - Kr \qquad (7)$$

where r is the ratio of bound ethidium ion per DNA phosphate, c_f is the free dye concentration in moles/liter, n is the total number of binding sites per DNA phosphate, and K is the binding constant. The concentration of free dye is calculated from the total concentration of dye and the quantity $A_{mix} - A_{dye}$, measured at 465 nm; this last quantity gives a measure of the amount of dye bound in a two-state analysis. The DNA concentration is calculated from the dilution factor as mentioned earlier.

The Scatchard plot for calf thymus DNA/EI mixtures prepared with the 100 mM NaCl/1.0 mM tris buffer is shown in Figure 5.5. Again, because the salt solution is diluted in mixing with DNA/dye, the Na^+ concentration is less than 100 mM; the median value for the counterion concentration is 86 mM Na^+.

A least squares fit to the data yields an equilibrium constant of 9.7 (± 0.7) x 10^5 M^{-1} and 0.20 ± 0.02 binding sites/phosphate. This result is in fair agreement with LePecq and Paoletti (1967), who ob-

Figure 5.3. Titration of 0.032 mM ethidium ion (□) with dialyzed calf thymus DNA. DNA concentration as phosphate:

(◇) 0.015 mM

(X) 0.030 mM

(▽) 0.045 mM

(+) 0.076 mM

(O) 0.50 mM

Solutions were prepared with 0.1 mM NaCl, 1.0 μM tris; the actual Na^+ concentration depends upon DNA concentration.

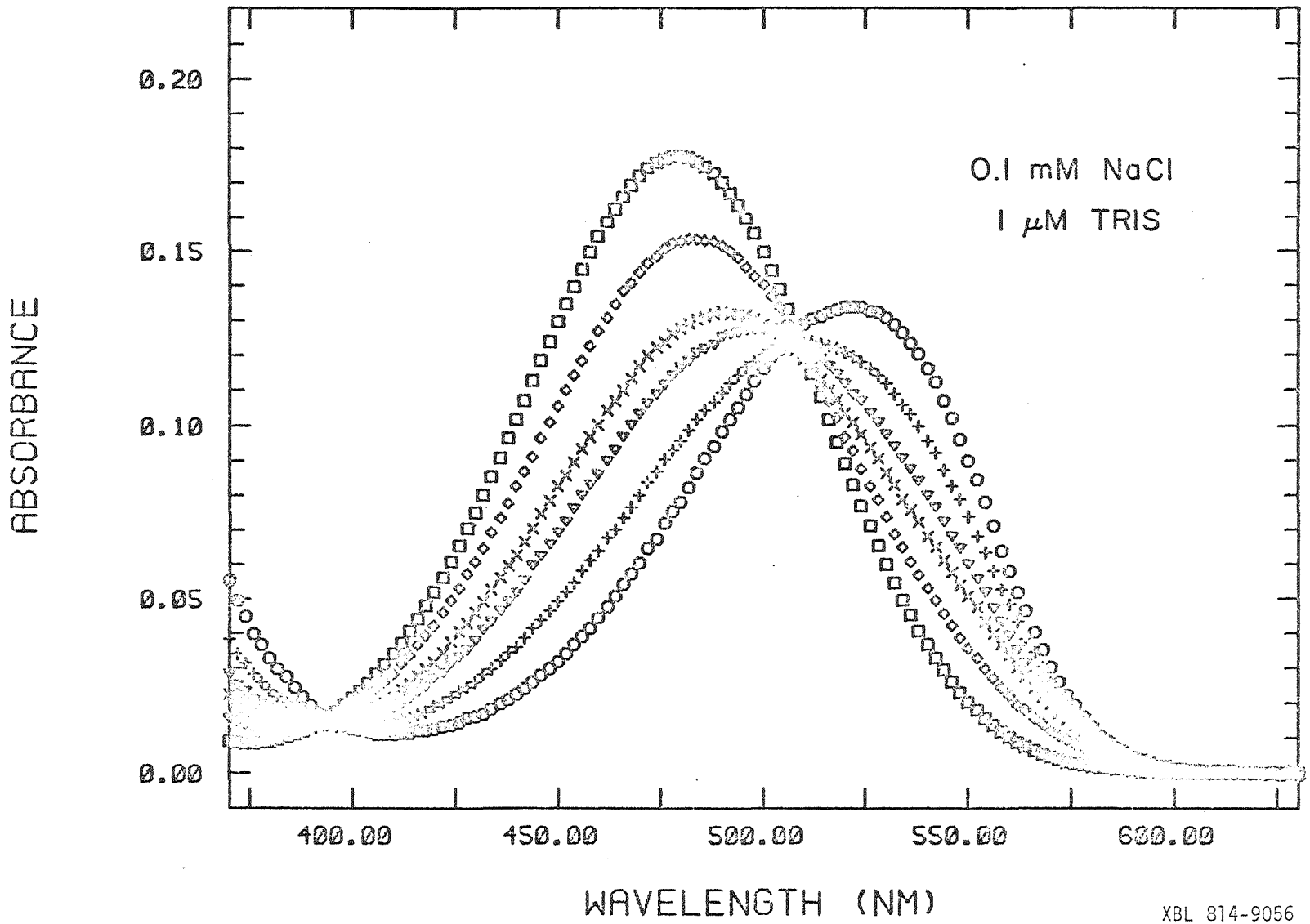
0.20
0.15
0.10
0.05
0.00
ABSORBANCE
400.00
450.00
500.00
550.00
600.00
WAVELENGTH (NM)
0.1 mM NaCl
1 μM TRIS

XBL 814-9056

Figure 5.4. Titration of 0.033 mM ethidium ion (□) with dialyzed calf thymus DNA. DNA concentration as phosphate:

(◇) 0.054 mM

(X) 0.11 mM

(▽) 0.14 mM

(+) 0.19 mM

(0) 0.53 mM

Solutions were prepared with 100 mM NaCl, 1.0 mM tris; the actual Na^+ concentration depends upon DNA concentration.

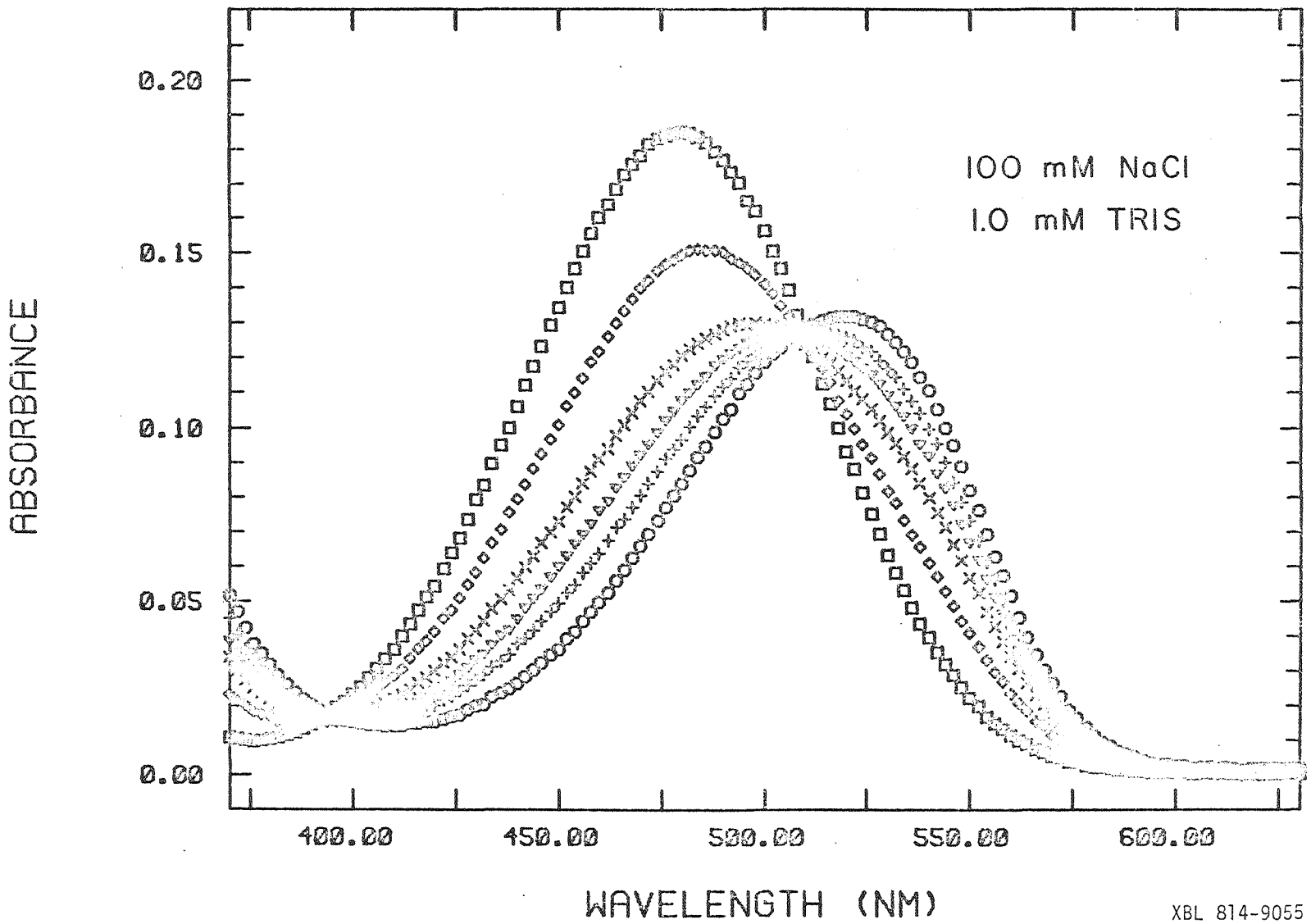
100 mM NaCl
1.0 mM TRIS
ABSORBANCE
0.20
0.15
0.10
0.05
0.00
400.00
450.00
500.00
550.00
600.00
WAVELENGTH (NM)

XBL 814-9055

Figure 5.5. Scatchard plot for ethidium ion binding in dialyzed calf thymus DNA at 25^0C. Buffer used is 100 mM NaCl/1.0 mM tris; the median Na^+ concentration is ~86 mM for points fitted by least squares routine. Vertical lines represent estimated errors. Least squares fit to all points except for those above r = 0.19 is represented by sloping line. For this fit, $K = 9.7\ (\pm 0.7) \times 10^5\ M^{-1}$ and $n = 0.20 \pm 0.02$.

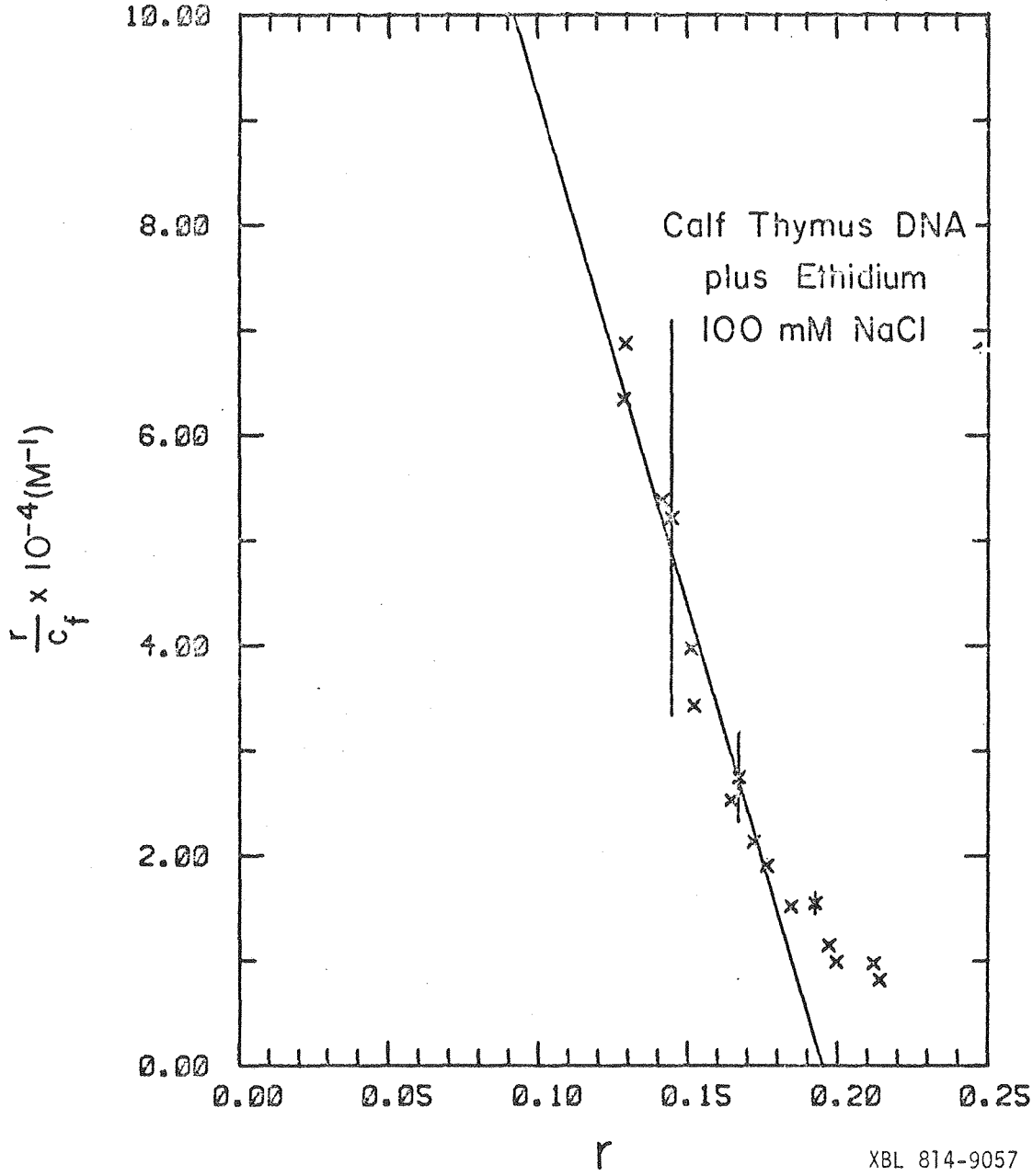
10.00
8.00
6.00
4.00
2.00
0.00
0.00
0.05
0.10
0.15
0.20
0.25
r
$\frac{r}{c_f} \times 10^{-4} (M^{-1})$
Calf Thymus DNA
plus Ethidium
100 mM NaCl

XBL 814-9057

tained a dye binding constant with calf thymus DNA of 6.6×10^5 M^{-1} at 23^0C in 90 mM Na^+.

In the mixture prepared with the low salt solution (0.1 mM NaCl, 1.0 μM tris), all solutions with total dye/DNA phosphate < 0.25 display coincident absorbance spectra that are characteristic of fully bound ethidium ion. The equilibrium constant in this case is too large to be measured by this method. Previous workers (LePecq & Paoletti, 1967; Aktipis & Kindelis, 1973; Houssier et al., 1974) found that the equilibrium constant for ethidium ion binding to DNA increased as the counterion concentration decreased. For our purposes, it is sufficient to say that all dye is bound to the nucleic acid at dye/phosphate ratios below 0.25 in our low salt solutions. For the CD solutions with a constant DNA concentration and variable dye concentrations in the low salt mixtures, the measured absorbance spectra all resemble that of fully bound ethidium ion.

C) Induced CD of DNA/Ethidium Ion Complexes

The induced CD spectra of ethidium ion bound to calf thymus DNA in the two different salt solutions are shown in Figure 5.6. Two features are apparent upon inspection and comparison of the spectra. The first is the relative constancy of $\Delta\varepsilon_{bound}$ at 375 nm, especially in the high salt mixtures. Comparison of spectra at the same binding ratio in the two salt solutions turns up the second feature: $\Delta\varepsilon_{bound}$ is greater in the lower salt concentration at either 307 or 330 nm relative to the high salt case.

The increase in $\Delta\varepsilon^{307}_{bound}$ with r, the binding ratio, is shown in Figure 5.7. The curve assembled from the previous studies of Dalgleish et al. (1971) and Aktipis and co-workers (1973, 1974), which

Figure 5.6. Induced CD spectra of DNA/EI complexes at different binding ratios and salt concentrations. Na^+ concentrations are ~86 mM (median value, top) and ~0.45 mM (bottom).

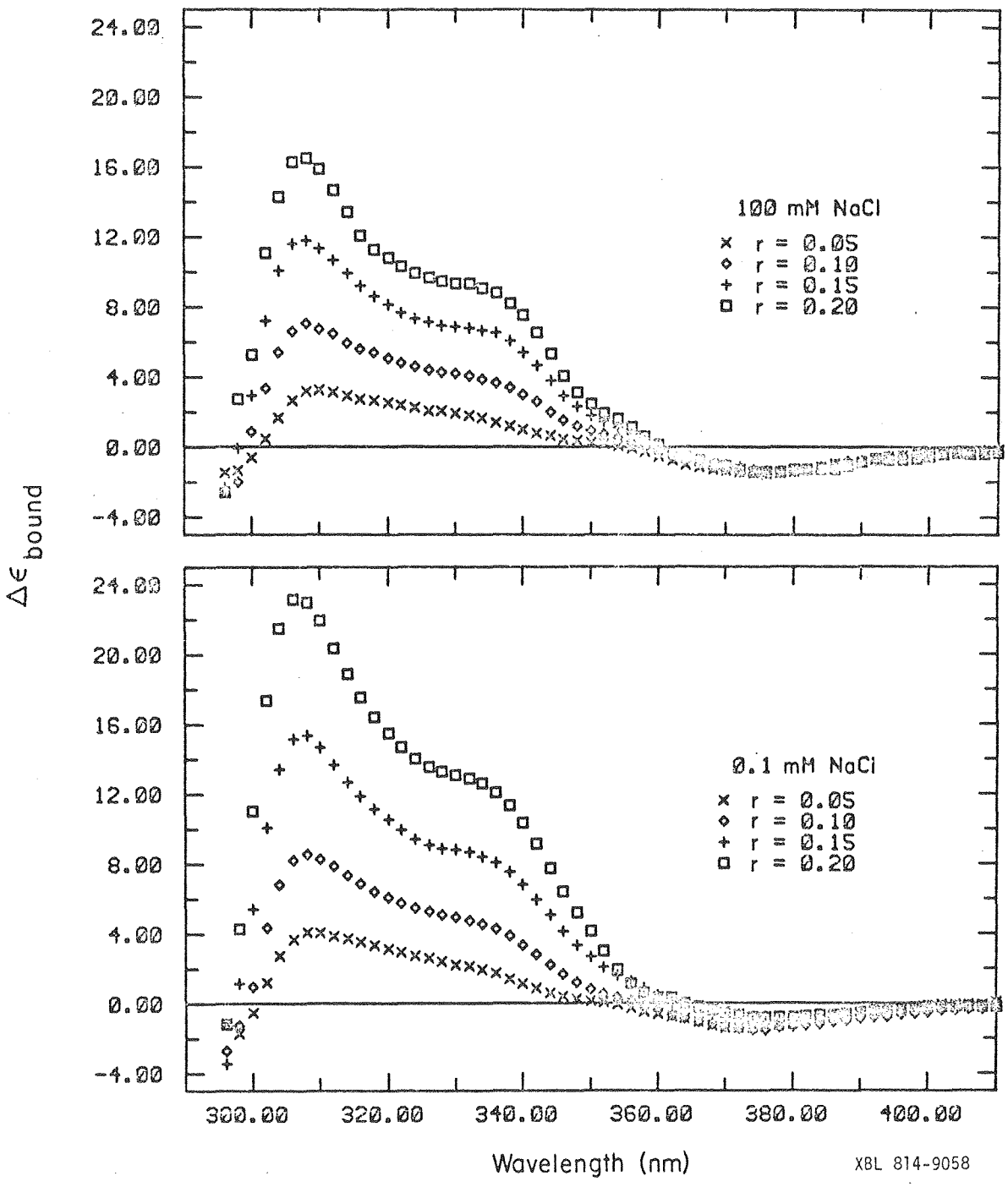
24.00
20.00
16.00
12.00
8.00
4.00
0.00
-4.00
100 mM NaCl
× r = 0.05
◇ r = 0.10
+ r = 0.15
□ r = 0.20
0.1 mM NaCl
× r = 0.05
◇ r = 0.10
+ r = 0.15
□ r = 0.20
Δε bound
300.00
320.00
340.00
360.00
380.00
400.00
Wavelength (nm)
XBL 814-9058

Figure 5.7. Variation of the magnitude of the induced CD per bound dye at 307 nm with the extent of ethidium ion binding and counterion concentration. Spectra run in solutions prepared with 0.1 mM NaCl/1.0 μM tris (X) have actual Na^+ concentration of ~0.45 mM. Spectra run in solutions prepared with 100 mM NaCl / 1.0 mM tris (◯) have median Na^+ concentration of ~86 mM. Vertical lines represent estimated errors; solid line represents a synthesis of data from previous studies of Dalgleish et al. (1971) and Aktipis and co-workers (1973, 1974).

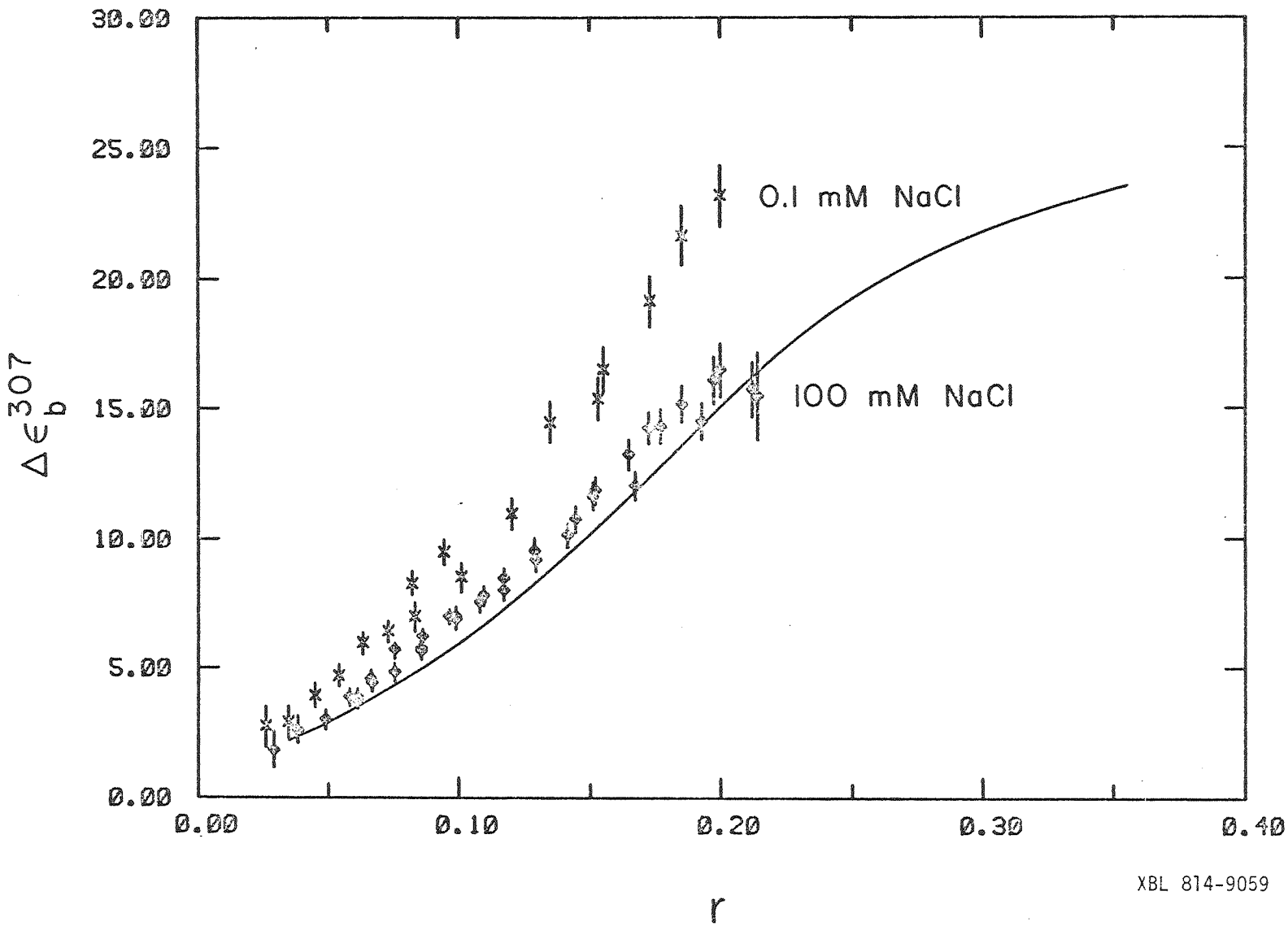
30.00
25.00
20.00
15.00
10.00
5.00
0.00
0.00
0.10
0.20
0.30
0.40
$\Delta\epsilon_b^{307}$
r
0.1 mM NaCl
100 mM NaCl

XBL 814-9059

were all at counterion concentrations of 40 mM or greater is also shown. Our data in the high salt case agree with previous results, although we generally obtain slightly higher values of $\Delta\varepsilon_{bound}$ (~1 L/mol-cm) throughout the range of our mixes; Houssier et al. (1974) obtained slightly higher $\Delta\varepsilon_{bound}^{308}$ values also. Our low salt curve is in direct conflict with these previous studies: we find a change in the ionic strength of the mixture affects the magnitude of $\Delta\varepsilon_{bound}^{307}$. In the low salt solution, the induced CD at 307 nm is larger than in high salt, all things being equal. Furthermore, the difference between the two cases grows as the extent of binding increases.

We believe past failures to observe an effect on $\Delta\varepsilon_{bound}^{307}$ from different salt concentrations is attributable to the conditions used to vary r: constant dye and variable DNA concentrations. Variable DNA concentrations necessarily alter the effective counterion concentration; at lower salt concentrations these alterations can be sizable, often increasing the effective counterion concentration manyfold, as in this study. When we measured the induced CD of ethidium ion in the DNA/dye mixtures from the Scatchard analyses at low salt, the $\Delta\varepsilon_{bound}^{307}$ vs. r curve (data not shown) closely resembled that of the high salt solution. This was especially true at lower r values where the amount of added DNA (and hence, added Na^+) was larger. Only when we kept the DNA concentration constant could we be sure of maintaining a fixed Na^+ concentration throughout the range of r values. The fact that the dye is completely bound to the DNA under our experimental conditions allowed us to take this approach. At higher salt concentrations, 10 mM or greater, the variable DNA concentration in solutions from Scatchard analyses is less of a problem: the

Na^+ contribution from the DNA aliquot is a smaller fraction of the total counterion concentration.

D) Counterion Changes with Dye Binding

The ability to alter the magnitude of $\Delta\varepsilon^{307}_{bound}$ in DNA/ethidium ion complexes by simply lowering the counterion concentration is an intriguing observation. This phenomenon suggests that charged groups, either the counterions or the phosphate groups, or both in concert, may be responsible in part for these variations, and quite possibly, the increase in $\Delta\varepsilon^{307}_{bound}$ with increasing r. We employ polyelectrolyte theory to examine this question. We begin our analysis from the viewpoint that electrostatic interactions between the ionic groups and the dye are solely responsible for variations in the CD spectrum with binding ratio. We will discuss other effects later.

The average axial distance per charge calculated via equation (2), and the effective charge/phosphate, ξ^{-1}, from equation (1), as a function of the extent of ethidium ion binding in DNA are presented in Figure 5.8. The combined effects of helix lengthening and charge neutralization result in a doubling of the effective phosphate charge in fully loaded DNA (r = 0.25) compared with unaltered DNA (r = 0.00). The values of b and ξ^{-1}, together with other quantities of interest, are presented at discrete values of r in Table VI.

According to these calculations, the interaction of ethidium ion causes a decrease in the condensed charge/phosphate ratio and an expansion of the volume within which the counterions are considered "bound". The net result of these two effects is a steep drop in the effective local concentration of the counterion, C_1^{loc}, as the extent of binding increases. The counterions are divided into two classes

Figure 5.8. Calculated distance per phosphate (b) and fractional charge per phosphate (ξ^{-1}) vs. binding ratio for ethidium ion intercalation in DNA. Equations (1) and (2) were used to create curves.

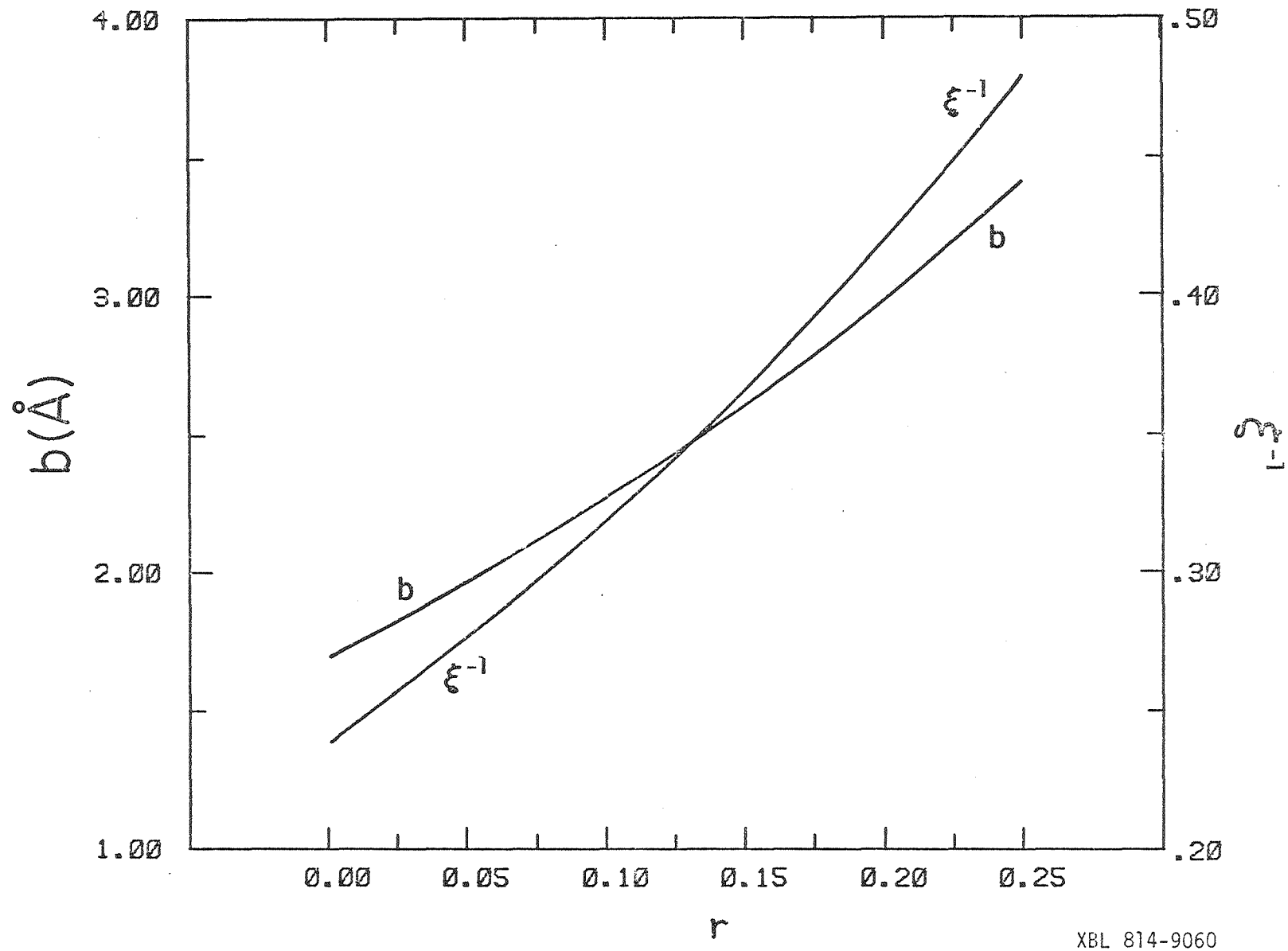
4.00
3.00
2.00
1.00
b(Å)
.50
.40
.30
.20
ξ^{-1}
0.00
0.05
0.10
0.15
0.20
0.25
r
b
ξ^{-1}
b
ξ^{-1}

XBL 814-9060

TABLE VI

CONDENSED ION PARAMETERS FOR DNA/ETHIDIUM ION COMPLEXES

Bound dye/phosphate (r)	0.00	0.05	0.10	0.15	0.20	0.25
Axial distance/phosphate (b)	1.70 Å	1.97 Å	2.27 Å	2.60 Å	2.98 Å	3.40 Å
Charge/phosphate (ξ^{-1})	0.239	0.277	0.319	0.366	0.419	0.479
Counterions/phosphate (θ_1)	0.761	0.723	0.681	0.634	0.581	0.521
Bound ion volume/mole phosphate (V_p)	643 cm^3	820 cm^3	1026 cm^3	1251 cm^3	1508 cm^3	1757 cm^3
Bound ion radius (a)	14.1 Å	14.8 Å	15.4 Å	15.9 Å	16.3 Å	16.5 Å
Local counterion concentration (C_1^{loc})	1.18 M	0.88 M	0.66 M	0.51 M	0.38 M	0.30 M

in Manning's approach to polyelectrolyte properties: 1) those condensed on the macromolecule and 2) those remaining free in solution. In the current case, consideration of our results using these two classes is very helpful. The locally condensed counterions (and the phosphate groups) should exert a large influence upon the electronic properties of the bound dye molecule: they are physically closer to the binding sites and their concentration is much larger than those free in solution (and even the *total* counterion concentrations for our experiments). The atmosphere of uncondensed counterions, which extends outward from the outer radius of the condensed ion volume (a), should exert smaller effects upon dye electronic properties, because of both its greater distance from the binding sites and also its lower effective concentration.

One of the main tenets of Manning's theory is the strict requirement for counterion condensation to relieve the charge-charge repulsions in the helix backbone of DNA; condensation will occur even to the point of virtual depletion of the counterion in the Debye-Hückel atmosphere (Manning, 1977). For the Na^+ concentrations employed in our study, ~0.45 mM and ~86 mM, this requirement applies and its consequence is simple: in both solutions the local concentrations of condensed counterions are those calculated in Table VI. Thus there is no difference between the two salt solutions at the level of the strongest electrostatic effect from the counterions on the dye, despite the vastly different total counterion concentrations.

A possible correlation between the local counterion concentration and the magnitude of $\Delta\varepsilon^{307}_{bound}$ exists: the local counterion concentration decreases as both the extent of binding rises and, by extension

to the experimental results, $\Delta\varepsilon^{307}_{bound}$ rises. The locally bound counterions, together with the phosphates, constitute the source of a perturbing field on the bound dye. This field may be responsible for the variations in $\Delta\varepsilon_{bound}$ with r between 300 and 350 nm since the local counterion concentration varies with r. To restate and generalize the correlation: higher counterion concentrations cause lower magnitudes in the induced CD between 300 and 350 nm of ethidium ion bound in DNA.

To qualitatively examine the possible effects of the Debye-Hückel atmosphere on the induced CD, we estimated the total Na^+ concentration in the low (~0.45 mM) salt and high (~86 mM) salt solutions. Using the binding data for DNA/EI complexes in Table VI, we calculate the amount of Na^+ ions removed from solution during condensation by multiplying the counterion/phosphate ratio, θ_1, by the total DNA concentration (0.31 mM). Subtraction of this quantity from the total Na^+ concentration provides an estimate of the concentration of ions in the Debye-Hückel atmosphere that interact with the partially neutralized polyions. These values are presented at each r value in Table VII.

The immediately obvious effect is the absence of any significant change at high salt in the Debye-Hückel atmosphere Na^+ concentration from the bulk Na^+ concentration in solution. This is due to the low concentration of DNA relative to the salt concentration. Conversely, the removal of Na^+ ions by condensation in low salt causes significant (30% to 50%) reductions in the concentration of free Na^+. We said earlier that any field due to these free counterions will be a weaker perturbant of the bound dyes' optical properties than the con-

TABLE VII

DISTRIBUTION OF COUNTERIONS IN DNA/ETHIDIUM ION MIXTURES

Bound/phosphate (r)	0.00	0.05	0.10	0.15	0.20	0.25
Counterions/phosphate (θ_1)	0.761	0.723	0.681	0.634	0.581	0.521
Condensed counterions[a]	0.24 mM	0.22 mM	0.21 mM	0.20 mM	0.18 mM	0.16 mM
Free counterions, low salt[b]	0.21 mM	0.23 mM	0.24 mM	0.25 mM	0.27 mM	0.29 mM
Free counterions, high salt[c]	86 mM	86 mM	86 mM	86 mM	86 mM	86 mM
Local counterion concentration (C_1^{loc})	1.18 M	0.88 M	0.66 M	0.51 M	0.38 M	0.30 M

[a]DNA concentration (0.31 mM) x θ_1

[b]Total counterion concentration = ~0.45 mM Na^+.

[c]Total counterion concentration = ~86 mM Na^+.

densed ions because of both their greater distance and lower concentration. Comparison of the effective concentrations for the local and free counterions shows a tremendous difference between the two domains of up to four orders of magnitude.

The Debye-Hückel atmosphere and its potential field may be responsible for the difference between the $\Delta\varepsilon^{307}_{bound}$ vs. r curves in the different salt solutions (Figure 5.7). In this case, the low salt curve, for which the free counterion concentration is lower than in the high salt solution, has consistently higher values for $\Delta\varepsilon^{307}_{bound}$ at equal values for r. This free counterion field seemingly affects the dye CD just like the local counterion field: lower counterion concentrations cause larger magnitudes in the induced CD between 300 and 350 nm, all other things being equal. However, because these effects are weaker for the counterions in this atmosphere, the local counterion field remains the predominant perturbant. Thus, the shape of the $\Delta\varepsilon^{307}_{bound}$ vs. r curve remains generally the same in each case; the effect of the weaker field is to displace the curve in low salt to higher $\Delta\varepsilon_{bound}$ values.

4. Discussion

From the viewpoint of electrostatic effects, we have only considered interactions between the dye transitions and the potential fields of the counterions, both condensed and free. Possible significant correlations between the magnitude of the induced CD in the near UV and the strength of these fields (as measured by the ion concentrations) are evident in our results. The fields attributed to these counterions are but a part of the total electrostatic picture and the ions are only well-characterized along a radial direction

from the helix axis; they are not bound in any specific fixed site (Manning, 1978) relative to the intercalated dye.

We have ignored the geometrically "fixed" charge groups in the nucleic acid/dye complex. These groups are the phosphates, each with a -1 charge (the nucleic acid plus condensed ions constitute the species of interest for the polyelectrolyte theory, but the formal charges on each ionic group have not been removed), and other intercalated ethidium ions, each with a +1 charge. Each phosphate (two in all) connecting the nucleosides comprising the two nearest neighbor base pairs of the binding site and probably each phosphate (four more) in the immediately adjacent sites excluded from binding are geometrically invariant relative to the dye, no matter what the binding ratio, and so contribute to the CD as part of the asymmetry of the site. Phosphates farther away than two base pairs, and other dye molecules, constitute a possible binding ratio-dependent electrostatic contribution to the total induced CD of the ethidium ion because the relative position of these groups to a bound dye will depend upon how far they are from the dye and the extent of binding. This contribution to the total electrostatic potential field, together with that of the counterions, represents an attractive mechanism for the binding ratio dependence of the near UV induced CD in DNA/EI complexes. This theory was proposed by Lee and co-workers (1973), who recognized the possible role of other dye molecules intercalating near previously bound dye. We have taken it a step further and introduced the counterions' contributions to the perturbing field.

The geometry of DNA in aqueous solution (Bram & Beeman, 1971;

Bram, 1971) is very similar to the B form geometry obtained in fiber diffraction studies (Arnott & Hukins, 1972). The solution geometry of the DNA was also independent of ionic strength between the values of 50 to 150 mM NaCl in wide-angle X-ray scattering experiments (Bram, 1971) and between the values of 1.3 to 200 mM NaCl in viscosity measurements (Rosenberg & Studier, 1969). These types of measurements are not as sensitive to small changes in the double helix geometry as the CD spectrum is. Recently, Johnson et al. (1981) reported a study in which magnitude changes in the CD band at 275 nm for nucleic acids were correlated with changes in the helix winding angle and the propeller angle (twist) between the two bases in a base pair.

We measured the CD of our dialyzed DNA in the two salt solutions used in the induced CD study (data not shown). There was a decrease of ~10% in the magnitude of the long wavelength CD band when measured at lower salt concentrations. Pardi (1980) saw a comparable effect in his study with *E. coli* DNA. These decreases are due to conformational changes in the DNA: most likely a slight decrease in the propeller angle and/or a slight increase in the winding angle (Johnson et al., 1981). These different geometries of the nucleic acid can affect the induced CD of the dye in other ways besides the effects due to different geometries for the charged groups relative to the dye. Any significant interactions between the bound dyes and bases farther from the base pairs of the binding site would also be affected. This is a second possiblity for the origin of the difference between the $\Delta\varepsilon^{307}_{bound}$ vs. r curves we measured earlier (Figure 5.7). The difficulty in trying to decide between the relative importance of different geometries vs. charge effects as the source of induced CD

variations lies in the interconnection of the two: a change in one necessitates a change in the other. CD calculations offer the best chance for resolving the question. We discuss this further in the next chapter.

Chapter VI

CONCLUSIONS

1. The Problem Revisited

We began this dissertation with the intention of settling two questions about the induced circular dichroism (CD) of ethidium ion in nucleic acids. First, what is the contribution of the inherent asymmetry of the intercalation site to the induced CD of the ethidium ion between 300 and 350 nm? Second, what possible mechanism(s) account for the increase in the molar CD per bound dye ($\Delta\varepsilon_{bound}$) at 307 nm as the extent of binding increases? The two hypotheses presented up to the time of this writing address the second question more than the first. One of them, the dye-dye exciton mechanism (Aktipis & Kindelis, 1973; Houssier et al., 1974), holds that the site asymmetry CD contribution is small and the greater likelihood of dye-dye interactions at higher binding ratios accounts for the increase in $\Delta\varepsilon_{bound}$. The second mechanism links increases in the induced CD of the dye with the changes intercalation produces in the potential field or environment of the bound dye(s) (Lee et al., 1973). In the course of this study we have obtained new evidence bearing upon each of these hypotheses. We will review these discoveries and their implications, after which we will propose a model which may be the answer to the questions above. Finally, we propose some experiments which will test our model or provide some useful information.

2. New Evidence Bearing on the Problem

One of the first clues that the dye-dye exciton mechanism might not be responsible for the changes in the induced CD between 300 and

350 nm of bound ethidium ion was the large magnitudes of the induced CD for 2:1 dimer:dye complexes. These magnitudes per bound dye at 307 nm were of comparable size to the spectrum from fully loaded DNA (Pardi, 1980). For example, $\Delta\varepsilon^{307}_{bound}$ for CpG:CpG:EI is 22 L/mol-cm, while in calf thymus DNA at r = 0.25, $\Delta\varepsilon^{307}_{bound}$ is ~19 L/mol-cm (see Figure 1.5). Since only one dye molecule is present in the complex with the dimers, and it is intercalated between the base pairs of the mini-helix, the large magnitude of its induced CD is not attributable to dye-dye interactions.

We measured the induced CD of ethidium ion intercalated in several more sequences of complementary dimers. The results all reflect one fact: the induced CD per bound dye is quite large between 300 and 350 nm. These complexes represented the simplest unit of the bound drug in complexes with the nucleic acids, and as such, their CD spectra are attributable to only one thing: the asymmetry of the binding site. This result directly contradicts one of the basic assumptions of the dye-dye exciton mechanism, namely, that the induced CD due to the asymmetry of the site is low.

Another piece of evidence cited in favor of the dye-dye exciton mechanism was the occurence of a negative lobe in the CD spectrum centered near 295 nm at high ionic strengths (Aktipis & Kindelis, 1973; Balcerski & Pysh, 1976). This band, of roughly equal size with the positive lobe centered near 307 nm, is masked at lower ionic strengths by the larger, positive lobe of the nucleic acid's CD near 270 nm, according to these authors. A conservative CD spectrum such as this is characteristic of an exciton interaction between identical chromophores (Tinoco, 1963).

In our studies of the 2:1 dimer:dye complexes via fluorescence detected circular dichroism, we obtained the CD spectrum of these complexes well below 300 nm, where the large excesses of dimers present in the mixtures usually mask the complexes' CD spectra. We found either true negative lobes or relative minima in the CD spectra near 295 nm for most of the 2:1 complexes studied. In all cases, a positive CD lobe occurs above 300 nm. Since only one dye is present in each complex, dye-dye excitons are not responsible for this pattern of bands. This suggests that such bands in the CD spectra of DNA/EI complexes need not solely be attributed to dye-dye excitons either. Another exciton mechanism involving transitions on both the DNA bases and the dye was presented by Houssier et al. (1974). Such interactions might be operating here, although the magnitude of the bands would not change with the binding ratio. This type of spectral contribution would be grouped with others from the asymmetry of the site.

In our experiments on the binding behavior and circular dichroism of ethidium ion in calf thymus DNA mixtures of different salt concentrations, we found that the concentration of the counterions affected the magnitude of $\Delta\varepsilon^{307}_{bound}$ for solutions at the same binding ratio, r. The fact that an environmental effect, such as the counterion concentration, can produce changes in the CD spectrum is reminiscent of the mechanism of Lee et al. (1973), which connects changes in the bound dye's optical properties with changes in the perturbing potential field at the binding site as other sites fill. Using electrostatic theories of DNA's polyelectrolyte behavior (Manning, 1978), we examined possible sources of the change in the field: the atmosphere of counterions, both condensed and free, which associate with the nucleic acid. Other con-

ceivable sources of change in the field are the relative positions of other charged groups with the dye: the phosphates of the helix backbone and other intercalated dye molecules, and the relative orientations of base pairs beyond the binding site with the dye.

3. The Model

We have discovered some facts which suggest that the variation of $\Delta\varepsilon^{307}_{bound}$ with the binding ratio, r, is not the result of an increased chance of dye-dye exciton interactions at higher binding ratios. Before proposing a model based upon the alternate mechanism, we realize we have by no means uncovered an overwhelming amount of evidence to prove or disprove either mechanism. Instead, we believe the facts are more consistent with an explanation based upon a mechanism incorporating the perturbing potential field as the source of the spectral behavior.

The main points of the model are as follows: 1) the spectral properties (CD) of the 2:1 dimer:dye complexes best represent those of the nucleic acids at high binding ratios; 2) the potential field arising from charged groups contributes a component to the induced CD which reduces the magnitude of $\Delta\varepsilon^{307}_{bound}$; 3) at the lowest binding levels, this last component is dominant, so $\Delta\varepsilon^{307}_{bound}$ is reduced to its lowest levels; and 4) $\Delta\varepsilon^{307}_{bound}$ increases as r increases because the combined geometric and electrostatic changes associated with the intercalation of dye diminish the contribution of the perturbing field, and the CD contribution from the asymmetry of the site (i.e., the dimer:dye spectrum) gains ascendancy in the sum of all effects.

In selecting the CD spectrum of fully bound DNA/EI complex as the analogue of the 2:1 dimer:dye complexes' spectra, we recognize that

$\Delta\varepsilon_{bound}^{\lambda\ max}$ varies with the particular sequence of bases present in the complex (Table III). The arrangement of bases and dye in the binding site may be freer to assume energetically favorable conformations in the dimer:dye complexes than in the longer sequences, where the adjacent bases and the backbone may restrict the number of possible conformations. Alternatively, the other perturbants of the dye's electronic properties (electrostatic fields, etc.) may serve to make the values for $\Delta\varepsilon_{bound}^{307}$ in each site more uniform in the polymer. We feel compelled to use the dimer/dye complexes as models for the fully loaded DNA because they display large magnitudes for $\Delta\varepsilon_{bound}$, because the spectra for the DNA/dye complexes maintain shapes similar to the dimer/dye spectra throughout the range of binding ratios, and because the magnitude of $\Delta\varepsilon_{bound}^{305}$ for ethidium ion bound in both dC-dG sites of pdC-dG-dC-dG minihelices is virtually identical with $\Delta\varepsilon_{bound}^{305}$ for the dCpG:dCpG:EI complex (Chapter II).

Once we select the asymmetry of the binding site as the basis for the large magnitudes in $\Delta\varepsilon_{bound}^{307}$ at the high binding ratios, the question of variations in the CD with the binding ratio can be approached from a new point of view. Rather than ask why $\Delta\varepsilon_{bound}^{307}$ starts off at low values and increases with r, we now want to know why it decreases as more dye molecules return to solution (r is decreasing). If we make use of the perturbing field mechanism, we can answer this: the strength of the perturbation varies with the binding ratio. Whether the electrostatic field, the relative geometry of more distant bases and the bound dyes, or other sources constitute the sole source of the field, or all contribute to it is difficult to say just at this time. We have shown that significant changes with dye binding occur in the

condensed counterion concentrations, an electrostatic effect, but whether this plays any role in altering the bound dyes' induced CD requires further study. Whatever the source of the perturbing field, its contribution to the total CD of the dye at 307 nm is negatively signed and so subtracts from the (assumed virtually constant) CD contribution from the site asymmetry.

4. Further Experiments

We have arrived at a model for the behavior of the induced CD between 300 and 350 nm of ethidium ion bound in DNA. The evidence supporting this model is certainly scanty at this point, but with the following experiments, support and refinement (and possibly overthrow) of the model may be forthcoming.

One of the weak links in the model is our reliance upon data from dimer/dye studies and DNA/dye studies only: the two are linked in the model even though there is very little evidence that anything true at one extreme holds at the other. Further studies of ethidium ion binding with complementary oligomers will aid in determining the validity of the correspondence. In particular, the question of whether a dimer/dye complex spectrum (CD) adequately represents longer sequences can be answered with CD measurements at different dye:helix ratios with complementary sequences like $rA_n + rU_n$, where all potential intercalation sites have the same sequence, or $r(C\text{-}A)_n + r(U\text{-}G)_n$, where two types of intercalation site exist, but one is presumably preferred over the other because it is Py(3'-5')Pu instead of Pu(3'-5')Py. Both types of sequences could be studied as polymers, also, and the deoxyribo- analogues could be compared with the ribo- sequences.

The effect of environment and/or perturbing field on the induced

CD of ethidium ion in DNA could be tested further by measuring the CD spectrum of the dye in the presence of competing intercalating species, such as proflavine and methylene blue (Lee et al., 1973), which are also cations, or 4-nitroquinoline-1-oxide (4-NQO) (Winkle, 1979), which is uncharged. In each case the charge density of the DNA would change as both the ethidium ion and the competing species bound. If the binding ratio of ethidium ion to the DNA, r_{EI}, and the binding ratio of the competing species, r_{comp}, could be obtained in some manner, then, by comparison of the magnitude of the ethidium ion's induced CD at 307 nm in this system with that of the ethidium ion alone with DNA at the same r_{EI} value, one could determine the validity of the environment/perturbing field model. The model predicts that $\Delta\varepsilon^{307}_{bound}$ in the ethidium ion/competitor/DNA mixture would be larger than $\Delta\varepsilon^{307}_{bound}$ in the ethidium ion/DNA mixture because the *total* of occupied sites is greater in the former. The two cationic dyes would work well because their induced CD bands are at wavelengths greater than 400 nm; 4-NQO would work well because it apparently does not acquire an induced CD spectrum when intercalated in nucleic acids (Winkle, 1979).

Finally, computer calculations of the CD spectrum for ethidium ion bound in different dimer sequences or in a polymer would be useful, at least for predicting changes in the spectrum as the nearby bases changed. The coordinates for ethidium ion bound in 5-iodoUpA and 5-iodoCpG from the X-ray studies (Tsai et al., 1977; Jain et al., 1977) would be a good starting point for the dimer/dye calculations. Sobell and co-workers (1977) have also published coordinates for ethidium ion bound in a DNA sequence by juxtaposing the dimer coordinates (representing the binding site) with the B form coordinates (representing

the remainder of the molecule). Beginning with the dimer complex and adding succeeding base pairs to each end of the structure, one could obtain a clearer picture of the role of the base pairs outside the binding site on the induced CD of the bound dye with calculations on each new structure. Similarly, one could investigate the effect of the electrostatic fields of the phosphates and the counterions on the spectrum using the larger structure. The methods of calculation employed by Johnson et al. (1981) seem particularly useful for this problem.

BIBLIOGRAPHY

Aktipis, S., & Kindelis, A. (1973) *Biochemistry 12*, 1213-1221.

Aktipis, S., & Martz, W. W. (1970) *Biochem. Biophys. Res. Commun. 39*, 307-313.

Aktipis, S., & Martz, W. W. (1974) *Biochemistry 13*, 112-118.

Aktipis, S., Martz, W. W., & Kindelis, A. (1975) *Biochemistry 14*, 326-331.

Allen, F. S., Gray, D. M., Roberts, G. P., & Tinoco, I., Jr. (1972) *Biopolymers 11*, 853-879.

Armstrong, R. W., Kurucsev, T., & Strauss, U. P. (1970) *J. Amer. Chem. Soc. 92*, 3174-3181.

Arnott, S., & Hukins, D. W. L. (1972) *Biochem. Biophys. Res. Commun. 47*, 1504-1509.

Balcerski, J. S., & Pysh, E. S. (1976) *Nuc. Acids Res. 3*, 2401-2409.

Benesi, H. A., & Hildebrand, J. H. (1949) *J. Amer. Chem. Soc. 71*, 2703-2707.

Bevington, P. R. (1969) *Data Reduction and Error Analysis for the Physical Sciences*, McGraw-Hill, New York.

Bloomfield, V. A., Crothers, D. M., & Tinoco, I., Jr. (1974) *Physical Chemistry of Nucleic Acids*, Harper & Row, New York.

Borer, P. N. (1972) Ph.D. dissertation, University of California, Berkeley.

Bram, S. (1971) *J. Mol. Biol. 58*, 277-288.

Bram, S., & Beeman, W. W. (1971) *J. Mol. Biol. 55*, 311-324.

Bresloff, J. L., & Crothers, D. M. (1975) *J. Mol. Biol. 95*, 103-123.

Brewer, J. M., Pesce, A. J., & Ashworth, R. B. (1974) *Experimental Techniques in Biochemistry*, Prentice-Hall, Englewood Cliffs,

New Jersey.

Cassim, J. Y., & Yang, J. T. (1969) *Biochemistry 8*, 1947-1951.

Chan, A., Kilkuskie, R., & Hanlon, S. (1979) *Biochemistry 18*, 84-91.

Dalgleish, D. G., Fujita, H., & Peacocke, A. R. (1969) *Biopolymers 8*, 633-645.

Dalgleish, D. G., Peacocke, A. R., Fey, G., & Harvey, C. (1971) *Biopolymers 10*, 1853-1863.

Davanloo, P., & Crothers, D. M. (1976) *Biochemistry 15*, 5299-5305.

Dorman, B. P., Hearst, J. E., & Maestre, M. F. (1973) *Methods Enzymol. 27*, 767-796.

Douthart, R. J., Burnett, J. P., Beasley, F. W., & Frank, B. H. (1973) *Biochemistry 12*, 214-220.

Genest, D., Wahl, Ph., & Auchet, J. C. (1974) *Biophys. Chem. 1*, 266-278.

Houssier, C., Hardy, B., & Fredericq, E. (1974) *Biopolymers 13*, 1141-1160.

Hudson, B., & Jacobs, R. (1975) *Biopolymers 14*, 1309-1312.

Ivanov, V. I., Minchenkova, L. E., Schyolkina, A. K., & Poletayev, A. I. (1973) *Biopolymers 12*, 89-110.

Ivanov, V. I., Minchenkova, L. E., Minyat, E. E., Frank-Kamenetskii, M. D., & Schyolkina, A. K. (1974) *J. Mol. Biol. 87*, 817-833.

Jackson, K., & Mason, S. F. (1971) *Trans. Faraday Soc. 67*, 966-989.

Jain, S. C., Tsai, C.-C., & Sobell, H. M. (1977) *J. Mol. Biol. 114*, 317-331.

Johnson, B. B., Dahl, K. S., Tinoco, I., Jr., Ivanov, V. I., & Zhurkin, V. B. (1981) *Biochemistry 20*, 73-78.

Kastrup, R. V., Young, M. A., & Krugh, T. R. (1978) *Biochemistry 17*,

4855-4865.

Khorana, H. G. (1968) *Pure Appl. Chem. 17*, 349-381.

Kindelis, A., & Aktipis, S. (1978) *Biopolymers 17*, 1469-1484.

Kornberg, A. (1980) *DNA Replication*, W. H. Freeman, San Francisco.

Krugh, T. R., Laing, J. W., & Young, M. A. (1976) *Biochemistry 15*, 1224-1228.

Krugh, T. R., & Reinhardt, C. G. (1975) *J. Mol. Biol. 97*, 133-162.

Krugh, T. R., Wittlin, F. N., & Cramer, S. P. (1975) *Biopolymers 14*, 197-210.

LeBret, M., & Chalvet, O. (1977) *J. Mol. Struct. 37*, 299-319.

LeBret, M., LePecq, J.-B., Barbet, J., & Roques, B. P. (1977) *Nuc. Acids Res. 4*, 1361-1379.

Lee, C. H., Chang, C.-T., & Wetmur, J. G. (1973) *Biopolymers 12*, 1099-1122.

Lee, C.-H., & Tinoco, I., Jr. (1978) *Nature (London) 274*, 609-610.

LePecq, J.-B., & Paoletti, C. (1967) *J. Mol. Biol. 27*, 87-106.

Lerman, L. S. (1961) *J. Mol. Biol. 3*, 18-30.

Lobenstine, E. W., & Turner, D. H. (1979) *J. Amer. Chem. Soc. 101*, 2205-2207.

Lobenstine, E. W., & Turner, D. H. (1980) *J. Amer. Chem. Soc. 102*, 7786-7787.

Mahler, H. R., Kline, B., & Mehrotra, B. D. (1964) *J. Mol. Biol. 9*, 801-811.

Manning, G. S. (1972) *Biopolymers 11*, 937-949.

Manning, G. S. (1977) *Biophys. Chem. 7*, 95-102.

Manning, G. S. (1978) *Q. Rev. Biophys. 11*, 179-246.

Marmur, J., & Doty, P. (1962) *J. Mol. Biol. 5*, 109-118.

McCann, J., Choi, E., Yamasaki, E., & Ames, B. N. (1975) *Proc. Nat. Acad. Sci. USA 72*, 5135-5139.

Nelson, J. W., Martin, F. H., & Tinoco, I., Jr. (1981) *Biopolymers*, in press.

Ornstein, R. L., & Rein, R. (1979a) *Biopolymers 18*, 1277-1291.

Ornstein, R. L., & Rein, R. (1979b) *Biopolymers 18*, 2821-2847.

Paoletti, J., & LePecq, J.-B. (1971) *J. Mol. Biol. 59*, 43-62.

Pardi, A. (1980) Ph.D. dissertation, University of California, Berkeley.

Patel, D. J., & Canuel, L. L. (1976) *Proc. Nat. Acad. Sci. USA 73*, 3343-3347.

Record, M. T., Jr. (1975) *Biopolymers 14*, 2137-2158.

Record, M. T., Jr., Woodbury, C. P., & Lohman, T. M. (1976) *Biopolymers 15*, 893-915.

Reinhardt, C. G., & Krugh, T. R. (1978) *Biochemistry 17*, 4845-4854.

Rosenberg, A. H., & Studier, F. W. (1969) *Biopolymers 7*, 765-774.

Savitsky, A., & Golay, M. J. E. (1964) *Anal. Chem. 36*, 1627-1639.

Scatchard, G. (1949) *Ann. N.Y. Acad. Sci. 51*, 660-672.

Sobell, H. M., Tsai, C.-C., Jain, S. C., & Gilbert, S. G. (1977) *J. Mol. Biol. 114*, 333-365.

Streisinger, G., Okada, Y., Emrich, J., Newton, J., Tsugita, A., Terzaghi, E., & Inouye, M. (1966) *Cold Spring Harbor Symp. Quant. Biol. 31*, 77-84.

Sutherland, J. C., & Sutherland, B. M. (1970) *Biopolymers 9*, 639-653.

Tinoco, I., Jr. (1963) *Radiation Res. 20*, 133-139.

Tinoco, I., Jr., Ehrenberg, B., & Steinberg, I. Z. (1977) *J. Chem. Phys. 66*, 916-920.

Tinoco, I., Jr., Martin, F. H., Nelson, J. W., & Pardi, A. (1981) *Die Makromolekulare Chemie*, in press.

Tinoco, I., Jr., & Turner, D. H. (1976) *J. Amer. Chem. Soc. 98*, 6453-6456.

Tomlinson, B. L. (1968) Ph.D. dissertation, University of California, Berkeley.

Tsai, C.-C., Jain, S. C., & Sobell, H. M. (1977) *J. Mol. Biol. 114*, 301-315.

Turner, D. H. (1978) *Methods Enzymol. 49*, 199-214.

Turner, D. H., Tinoco, I., Jr., & Maestre, M. F. (1974) *J. Amer. Chem. Soc. 96*, 4340-4342.

Waring, M. J. (1965) *J. Mol. Biol. 13*, 269-282.

Waring, M. J. (1970) *J. Mol. Biol. 54*, 247-279.

Warshaw, M. M. (1966) Ph.D. dissertation, University of California, Berkeley.

Watson, J. D. (1976) *The Molecular Biology of the Gene*, W. A. Benjamin, New York.

Watson, J. D., & Crick, F. H. C. (1953a) *Nature (London) 171*, 737-738.

Watson, J. D., & Crick, F. H. C. (1953b) *Nature (London) 171*, 964-967.

Williams, R. E., & Seligy, V. L. (1974) *Can. J. Biochem. 52*, 281-287.

Winkle. S. A. (1979) Ph.D. dissertation, University of California, Berkeley.

Young, M. A., & Krugh, T. R. (1975) *Biochemistry 14*, 4841-4847.

Appendix A

COMPUTER PROGRAMS FOR ERROR ANALYSIS AND DATA FITTING IN BENESI-HILDEBRAND PLOTS AND $\Delta\varepsilon_{bound}$

1. Benesi-Hildebrand Plots

A) Description

The programs BHFIT1, BHFIT2, and BHFIT3 fit dimer/dye titration data to 1:1, 2:1, or 1:1:1 binding stoichiometries, calculate the errors associated with the binding constant and $\varepsilon_b - \varepsilon_f$, and prepare plots of the data using the general graphics package in OS/8. The programs are writen in FORTRAN, compiled with .R FORT under the /I and /O options, and saved as core image files with .SAVE SYS BHFITN, where N = 1, 2, or 3. All listings are available on paper tape.

The data consists of absorbance differences between the dye alone and the mixture of dimer and dye at some wavelength (DABS), the initial dinucleoside phosphate concentrations ([NUC1] and [NUC2]), and the estimated errors (standard deviations) in each, if desired. These values correspond to $A - \varepsilon C^0_{EI}$, $C^0_{NpN_a}$, and $C^0_{NpN_b}$ in equation (4) of Chapter II, respectively. The first fitting does not weight the data in any fashion; the second fits the data by weighting each point according to its associated error.

B) Listing

i) BHFIT1

```
C     THIS PROGRAM FITS DIFFERENCE IN ABSORBANCE VERSUS ADDED
C     NUCLEOTIDE CONCENTRATION DATA IN A BENESI-HILDEBRAND PLOT.

         COMMON FNRET,FNDATA,N,NSIZE,NTHETA,NSYM,NCOR,
     2           NTIT,TITLE,NXTIT,XTITLE,NYTIT,YTITLE,NEW,
     3           XMIN,XMAX,XINCH,YMIN,YMAX,YINCH,
     4           XST,XTIC,XINC,YST,YTIC,YINC,LTIC,
     5           NSILAB,NORXL,NORYL,NSITIT,NORXT,NORYT,
     6           XFACT,XSIGN,NXMAX,YFACT,YSIGN,NYMAX,
     7           DABS,YER,CN1,ER1,CN2,ER2,X,SGX,Y,SGY,ALF1,
     8           A,SGA,B,SGB,NPTS,NFTST,CDYE,IDYE,K,RK,ERNRM,IER
         DIMENSION TITLE(7),XTITLE(7),YTITLE(7)
         DIMENSION DABS(15),CN1(15),CN2(15),SGX(15),SGY(15)
         DIMENSION ALF1(15),X(15),Y(15),NPTS(5),CDYE(5)
         DIMENSION ER1(15),ER2(15),YER(15)
500      FORMAT('1:1(=1), 2:1(=2), OR 1:1:1(=3) COMPLEX? 'I1)
510      FORMAT(/)
520      FORMAT('HOW MANY DIFFERENT [DYE]? 'I1)
530      FORMAT('ENTER ERRORS? (1=YES,2=NO) 'I1)
540      FORMAT('# POINTS= ',I2)
550      FORMAT('[DYE]= ',E13.5)
560      FORMAT(/'                                ERROR   ERROR   ERROR')
565      FORMAT(' [NUC1]  [NUC2]  DABS    [NUC1]  [NUC2]   DABS'/)
600      FORMAT('E13.5)
610      FORMAT('          'E13.5)
620      FORMAT('                    'E13.5)
630      FORMAT('                              'E13.5)
640      FORMAT('                                        'E13.5)
650      FORMAT('                                                'E13.5)
700      FORMAT('[DYE'I1']= 'E11.3'  # POINTS= 'I2)
710      FORMAT('[NUC1]= 'E11.3'  [NUC2]= 'E11.3'  DELTA= 'E11.3/
     $          'ERNUC1= 'E11.3'  ERNUC2= 'E11.3'  ERY= 'E11.3/)

C     ZERO ERROR ARRAYS.

         FNRET='BHFIT1'
         FNDATA='BHDATA'
1        DO 2 I=1,15
           ER1(I)=0
           ER2(I)=0
           CN2(I)=0
           YER(I)=0
2        CONTINUE

C     ESTABLISH MODE.

10       RK=1.
         READ(1,500)K
         IF(K-1)10,15,11
11       IF(K-2)10,13,12
12       IF(K-3)10,15,10
13       RK=2.
```

```
C     ENTER DATA. DABS IS ABSORBANCE DIFFERENCE NORMALIZED TO 1 CM
C     PATH, CNUC IS ADDED NUCLEOTIDE CONCENTRATION, CNER IS ERROR
C     IN ADDED NUCLEOTIDE CONCENTRATION, AND YER IS ERROR IN Y VALUE
C     AS DERIVED FROM THE ERROR IN DELTA ABSORBANCE.

15       WRITE(1,510)
         READ(1,520)IDYE
         LIMLO=0
         LIMHI=0
         READ(1,530)IER
         DO 29 I=1,IDYE
           WRITE(1,510)
           READ(1,540)NPTS(I)
           READ(1,550)CDYE(I)
           LIMLO=LIMHI+1
           LIMHI=LIMHI+NPTS(I)
           WRITE(1,560)
           WRITE(1,565)
           DO 28 M=LIMLO,LIMHI
             READ(1,600)CN1(M)
             IF(K-3)21,20,21
20           READ(1,610)CN2(M)
21           READ(1,620)DABS(M)
             IF(IER-1)28,24,28
24           READ(1,630)ER1(M)
             IF(K-3)26,25,26
25           READ(1,640)ER2(M)
26           READ(1,650)YER(M)
28         CONTINUE
           NPTST=LIMHI
29       CONTINUE

C     LIST ENTERED DATA.

         WRITE(1,510)
         DO 30 I=1,IDYE
           WRITE(1,700)I,CDYE(I),NPTS(I)
30       CONTINUE
         WRITE(1,510)
         DO 35 M=1,NPTST
           WRITE(1,710)CN1(M),CN2(M),DABS(M),ER1(M),ER2(M),YER(M)
           ALF1(M)=0
35       CONTINUE

C     AT THIS POINT, THE PROGRAM CONTINUES ON THE FILE 'BHFIT2.SY'.

         CALL CHAIN('BHFIT2')
         END
```

ii) BHFIT2

```
C     THIS PROGRAM FITS DIFFERENCE IN ABSORBANCE VERSUS ADDED
C     NUCLEOTIDE CONCENTRATION DATA IN A BENESI-HILDEBRAND PLOT.

         COMMON FNPET,FNDATA,N,NSIZE,NTHETA,NSYM,NCOR,
     2           NTIT,TITLE,NXTIT,XTITLE,NYTIT,YTITLE,NEW,
     3           XMIN,XMAX,XINCH,YMIN,YMAX,YINCH,
     4           XST,XTIC,XINC,YST,YTIC,YINC,LTIC,
     5           NSILAB,NORXL,NORYL,NSITIT,NORXT,NORYT,
     6           XFACT,XSIGN,NXMAX,YFACT,YSIGN,NYMAX,
     7           DABS,YER,CN1,ER1,CN2,ER2,X,SGX,Y,SGY,ALF1,
     8           A,SGA,B,SGB,NPTS,NPTST,CDYE,IDYE,K,RK,ERNRM,IER
         DIMENSION TITLE(7),XTITLE(7),YTITLE(7)
         DIMENSION DABS(15),CN1(15),CN2(15),SGX(15),SGY(15)
         DIMENSION ALF1(15),X(15),Y(15),NPTS(5),CDYE(5)
         DIMENSION ER1(15),ER2(15),YER(15)
500      FORMAT(/'*****************************************************'/)
510      FORMAT(/'FIT W/O ERRORS'/)
520      FORMAT('J= 'I2'  X(J)= 'E11.3'  Y(J)= 'E11.3'  ALPHA(J)= 'F7.4)
530      FORMAT(/'ALPHA('I2') DID NOT CONVERGE IN 100 STEPS')
540      FORMAT('TYPE -CR- TO FIT W/ ERRORS; -1-, -CR- TO SKIP 'I1)
550      FORMAT(/'FIT W/ ERRORS'/)
560      FORMAT(/)


C     FIRST RUN DOES NOT WEIGH FOR ERRORS;
C     SECOND RUN BEGINS WITH FIRST RUN VALUES, BUT WEIGHS FOR ERRORS.
C     A IS Y INTERCEPT, B IS SLOPE.
C     IFLAG IS RUN NUMBER FLAG: 0=1ST, 1=2ND.

         A=1.
         B=1.
         SGA=1.
         SGB=1.
         IFLAG=0
         WRITE(1,500)
         WRITE(1,510)
40       EQUKO=0
```

```
C     CALCULATE X AND Y GRAPH VALUES AND THEIR ASSOCIATED ERRORS.
C     Y ERROR = ENTERED Y ERROR + PROPAGATED X ERROR.
C     SGX AND SGY ARE VARIENCES; SGA AND SGB ARE STANDARD DEVIATIONS.
C     ERNRM IS THE LOWEST Y ERROR FOR NORMALIZING ALL ERRORS IN WEIGHING.
C     VALN IS AMOUNT OF FREE DIMER.

42       ERNRM=0
         LIMLO=0
         LIMHI=0
         DO 55 I=1,IDYE
           LIMLO=LIMHI+1
           LIMHI=LIMHI+NPTS(I)
           DO 50 M=LIMLO,LIMHI
             CALL FREE (VALNEW,FRE1,FRE2,M,I)
             X(M)=1./VALNEW
             Y(M)=CDYE(I)/DABS(M)
             CN1ER=(RK+ER1(M)/FRE1)**2.
             CN2ER=(ER2(M)/FRE2)**2.
             SGX(M)=X(M)*X(M)*(CN1ER+CN2ER)
             SGY(M)=YER(M)*YER(M)
     $           +B*B*SGX(M)+X(M)*X(M)*SGB*SGB+SGA*SGA
             WRITE(1,520)M,X(M),Y(M),ALF1(M)

C     ASSIGN FIRST ERROR AS NORMALIZING VALUE TO START WITH;
C     THEREAFTER, SUBSTITUTE NEW ERROR VALUE IF SMALLER.
C     THIS SIMPLY KEEPS NUMBERS FROM OVERFLOWING IN FLTSQ.

             IF(M-1) 47,48,47
47           IF(ERNRM-SGY(M)) 50,50,48
48           ERNRM=SGY(M)
50         CONTINUE
55       CONTINUE

C     FIT LINE.

         CALL FLTSQ (IFLAG)
```

```
C     CALCULATE FRACTION OF DYE BOUND IN COMPLEX TO WITHIN .001 ALPHA.

         EQK=A/B
         KK=0
         LIMLO=0
         LIMHI=0
         DO 66 M=1,IDYE
           LIMLO=LIMHI+1
           LIMHI=LIMHI+NPTS(M)
           DO 64 J=LIMLO,LIMHI
             DO 62 I=1,100
               CALL FREE (VALNEW,FRE1,FRE2,J,M)
               ALPH=EQK*VALNEW
               ALPH=ALPH/(1.+ALPH)
               DIFF=ABS(ALPH-ALF1(J))
               ALF1(J)=ALPH
               IF(DIFF-.001*ALF1(J)) 64,62,62
62           CONTINUE
             WRITE(1,530)J
             KK=1000
64         CONTINUE
66       CONTINUE

C     IF CONVERGANCE OF ALPHA DID NOT OCCUR, ABORT RUN.

         IF(KK-1000) 68,82,68

C     CALCULATE EQUILIBRIUM CONSTANT TO WITHIN .01 K.

68       DIFF=ABS(EQK-EQUKO)
         EQUKO=EQK

C     IF CONVERGANCE OF K DID NOT OCCUR, RECALCULATE WITH NEW VALUES.

         IF(DIFF-.01*EQK) 70,42,42
70       IF(IFLAG) 80,72,80

C     CHECK TO SEE IF CALCULATION WITH WEIGHING ERRORS IS POSSIBLE.

72       IF(IER-1) 80,74,80
74       WRITE(1,500)
         READ(1,540)I
         IF(I) 80,76,80
76       WRITE(1,550)
         IFLAG=1
         GO TO 40
80       WRITE(1,560)

C     AT THIS POINT, THE PROGRAM CONTINUES ON THE FILE 'BHFIT3.SV'.

         CALL CHAIN('BHFIT3')

C     RETURN TO START IF ALPHA DID NOT CONVERGE.

82       CALL CHAIN(FNRET)
         END
```

a) Subroutine FREE

```
C     THIS PROGRAM FITS DIFFERENCE IN ABSORBANCE VERSUS ADDED
C     NUCLEOTIDE CONCENTRATION DATA IN A BENESI-HILDEBRAND PLOT.

      SUBROUTINE FREE (VALNEW,FRE1,FRE2,M,I)
      COMMON FNRET,FNDATA,N,NSIZE,NTHETA,NSYM,NCOR,
     2         NTIT,TITLE,NXTIT,XTITLE,NYTIT,YTITLE,NEW,
     3         XMIN,XMAX,XINCH,YMIN,YMAX,YINCH,
     4         XST,XTIC,XINC,YST,YTIC,YINC,LTIC,
     5         NSILRB,NORXL,NORYL,NSITIT,NORXT,NORYT,
     6         XFACT,XSIGN,NXMAX,YFACT,YSIGN,NYMAX,
     7         DABS,YER,CN1,ER1,CN2,ER2,X,SGX,Y,SGY,ALF1,
     8         A,SGA,B,SGB,NPTS,NPTST,CDYE,IDYE,K,RK,ERNRM,IER
      DIMENSION TITLE(7),XTITLE(7),YTITLE(7)
      DIMENSION DABS(15),CN1(15),CN2(15),SGX(15),SGY(15)
      DIMENSION ALF1(15),X(15),Y(15),NPTS(5),CDYE(5)
      DIMENSION ER1(15),ER2(15),YER(15)

C     CALCULATE THE AMOUNT OF DIMER FREE AT EQUILIBRIUM

      FRE1=CN1(M)-RK*ALF1(M)*CDYE(I)
      FRE2=CN2(M)-RK*ALF1(M)*CDYE(I)
      IF(K-2)10,20,30
10    VALNEW=FRE1
      FRE2=1.
      GOTO 40
20    VALNEW=FRE1*FRE1
      FRE2=1.
      GOTO 40
30    VALNEW=FRE1*FRE2
40    RETURN
      END
```

b) Subroutine FLTSQ

```
C     THIS PROGRAM FITS DIFFERENCE IN ABSORBANCE VERSUS ADDED
C     NUCLEOTIDE CONCENTRATION DATA IN A BENESI-HILDEBRAND PLOT.

         SUBROUTINE FLTSQ (IFLAG)
         COMMON FNRET,FNDATA,N,NSIZE,NTHETA,NSYM,NCOR,
     2           NTIT,TITLE,NXTIT,XTITLE,NYTIT,YTITLE,NEW,
     3           XMIN,XMAX,XINCH,YMIN,YMAX,YINCH,
     4           XST,XTIC,XINC,YST,YTIC,YINC,LTIC,
     5           NSILAS,NORXL,NORYL,NSITIT,NORXT,NORYT,
     6           XFACT,XSIGN,NXMAX,YFACT,YSIGN,NYMAX,
     7           DABS,YER,CN1,ER1,CN2,ER2,X,SGX,Y,SGY,ALF1,
     8           A,SGA,B,SGB,NPTS,NPTST,CDYE,IDYE,K,RK,ERNRM,IER
         DIMENSION TITLE(7),XTITLE(7),YTITLE(7)
         DIMENSION DABS(15),CN1(15),CN2(15),SGX(15),SGY(15)
         DIMENSION ALF1(15),X(15),Y(15),NPTS(5),CDYE(5)
         DIMENSION ER1(15),ER2(15),YER(15)

C     CALCULATE THE LEAST SQUARES FIT TO A LINE FOR A DATA SET.
C     MODIFIED FROM THE PROGRAM 'LINFIT' IN 'DATA REDUCTION
C     AND ERROR ANALYSIS FOR THE PHYSICAL SCIENCES', BY
C     P. R. BEVINGTON, MCGRAW-HILL, 1969, PP.104-5.

500      FORMAT('Y INTERCEPT= 'E12.5'  SLOPE= 'E12.5)
510      FORMAT('SIGMA B= 'E12.5'  SIGMA M= 'E12.5)
520      FORMAT('R= 'F8.5)
530      FORMAT('K= 'E10.3/)
         SUM=0
         SUMX=0
         SUMY=0
         SUMX2=0
         SUMY2=0
         SUMXY=0
         DO 50 L=1,NPTST

C     IF NO ERRORS ENTERED, WEIGHT = 1. (ONLY WILL RUN ONCE).

           XI=X(L)
           YI=Y(L)
           WEIGHT=ERNRM/SGY(L)
           IF(IFLAG) 49,48,49

C     IF NOT WEIGHING FOR ERRORS, WEIGHT = 1..

48         WEIGHT=1.
49         SUM=SUM+WEIGHT
           SUMX=SUMX+WEIGHT*XI
           SUMY=SUMY+WEIGHT*YI
           SUMX2=SUMX2+WEIGHT*XI*XI
           SUMY2=SUMY2+WEIGHT*YI*YI
           SUMXY=SUMXY+WEIGHT*XI*YI
50       CONTINUE
         DELTA=SUM*SUMX2-SUMX*SUMX
         A=(SUMX2*SUMY-SUMX*SUMXY)/DELTA
         B=(SUMXY*SUM-SUMX*SUMY)/DELTA
         C=NPTST-2
         VARNCE=(SUMY2+A*A*SUM+B*B*SUMX2-2.*(A*SUMY+B*SUMXY-A*B*SUMX))/C

C     IF WEIGHING FOR ERRORS, VARNCE=SMALLEST Y ERROR.

         IF(IFLAG) 51,52,51
51       VARNCE=ERNRM
52       SGA=SQRT(VARNCE*SUMX2/DELTA)
         SGB=SQRT(VARNCE*SUM/DELTA)
         R=(SUM*SUMXY-SUMX*SUMY)/SQRT(DELTA*(SUM*SUMY2-SUMY*SUMY))
         WRITE(1,500)A,B
         WRITE(1,510)SGA,SGB
         WRITE(1,520)R
         EQK=A/B
         WRITE(1,530)EQK
         RETURN
         END
```

iii) BHFIT3

```
C     THIS PROGRAM FITS DIFFERENCE IN ABSORBANCE VERSUS ADDED
C     NUCLEOTIDE CONCENTRATION DATA IN A BENESI-HILDEBRAND PLOT.

         COMMON FNRET,FNDATA,N,NSIZE,NTHETA,NSYM,NCOR,
     2           NTIT,TITLE,NXTIT,XTITLE,NYTIT,YTITLE,NEW,
     3           XMIN,XMAX,XINCH,YMIN,YMAX,YINCH,
     4           XST,XTIC,XINC,YST,YTIC,YINC,LTIC,
     5           NSILAB,NORXL,NORYL,NSITIT,NORXT,NORYT,
     6           XFACT,XSIGN,NXMAX,YFACT,YSIGN,NYMAX,
     7           DABS,YER,CN1,ER1,CN2,ER2,X,SGX,Y,SGY,ALF1,
     8           A,SGA,B,SGB,NPTS,NPTST,CDYE,IDYE,K,RK,ERNRM,IER
         DIMENSION TITLE(7),XTITLE(7),YTITLE(7)
         DIMENSION DABS(15),CN1(15),CN2(15),SGX(15),SGY(15)
         DIMENSION ALF1(15),X(15),Y(15),NPTS(5),CDYE(5)
         DIMENSION ER1(15),ER2(15),YER(15)
         DIMENSION XX(15),YY(15)

C     PRINT OUT FINAL VALUES FOR K, DELTA EPSILON, X, Y, [COMPLEX],
C     AND ERRORS IN EACH (NOT [COMPLEX]).
C     PROCEED TO PLOTTING ROUTINE, IF DESIRED.

208      FORMAT('J= 'I2' X(J)= 'E13.5' Y(J)= 'E11.3' ALPHA(J)= 'F7.4)
209      FORMAT(/'FINAL K= 'E12.4'  FINAL DELTA EPSILON= 'E12.4)
210      FORMAT('SIGMA K= 'E12.4'  SIGMA DELTA EPSILON= 'E12.4/)
211      FORMAT('J= 'I2' DX(J)= 'E12.4' DY(J)= 'E10.2' [COMPLEX]= 'E12.4)
250      FORMAT(/)
260      FORMAT('PLOT DATA? (0=NO,1=YES) 'I1)
600      FORMAT('NORMALIZER TO MAKE X AXIS INTEGRAL = 'E12.4)
610      FORMAT('NORMALIZER TO MAKE Y AXIS INTEGRAL = 'E12.4)
620      FORMAT('I= 'I2'  NORMALIZED X(I)= 'F8.3'  NORMALIZED Y(I)= 'F8.3)
700      FORMAT('NEW GRAPH? (0=NO,1=YES) 'I1)
710      FORMAT('NEW PARAMETERS? 'I1)
720      FORMAT('XMIN=0, XST=XMIN')
730      FORMAT('XMAX= 'E12.4)
735      FORMAT('XINCH= 'E12.4)
740      FORMAT('XTIC=XINC= 'E12.4)
750      FORMAT('YMAX=0, YST=YMIN')
760      FORMAT('YMIN= 'E12.4)
765      FORMAT('YINCH= 'E12.4)
770      FORMAT('YTIC=YINC= 'E12.4)
780      FORMAT('SYMBOL # 'I1)
785      FORMAT('SYMBOL SIZE 'I1)
790      FORMAT('CALCOMP(0) OR TEKTRONIX(1) 'I1)
800      FORMAT('ALL OK? 'I1)
810      FORMAT(2A6)
```

```
      DO 2 J=1,NPTST
        WRITE(1,208)J,X(J),Y(J),ALF1(J)
2     CONTINUE
      DELEP=1./A
      EQK=A/B
      AE2=SGA*SGA/(A*A)
      BE2=SGB*SGB/(B*B)
      ERK=ABS(EQK*SQRT(AE2+BE2))
      ERD=ABS(DELEP*SQRT(AE2))
      WRITE(1,209)EQK,DELEP
      WRITE(1,210)ERK,ERD
      LIMLO=0
      LIMHI=0
      DO 4 I=1,IDYE
        LIMLO=LIMHI+1
        LIMHI=LIMHI+NPTS(I)
        DO 3 J=LIMLO,LIMHI
          ERX=SQRT(SGX(J))
          ERY=SQRT(SGY(J))
          CNNUC=ALF1(J)*CDYE(I)
          WRITE(1,211)J,ERX,ERY,CNNUC
3       CONTINUE
4     CONTINUE
      WRITE(1,250)
      READ(1,260)I
      IF(I)8,6,8
6     CALL CHAIN(FNRET)

C   SET VARIABLES THAT ARE UNCHANGED

8     NTHETA=0
      NCOR=100
      NTIT=0
      NXTIT=0
      NYTIT=0
      LTIC=8
      NSILAB=2
      NSITIT=2
      NORXL=0
      NORYL=0
      NORXT=0
      NORYT=1
```

```
C     ENTER "NORMALIZING" POWERS OF TEN

10       WRITE(1,250)
         READ(1,600)XNRM
         READ(1,610)YNRM
         DO 20 I=1,NPTST
           XX(I)=X(I)/XNRM
           YY(I)=Y(I)/YNRM
           WRITE(1,620)I,XX(I),YY(I)
20       CONTINUE
         READ(1,800)INP
         IF(INP)22,10,22

C     PREPARE FOR PLOTTING

22       WRITE(1,250)
         READ(1,700)NEW
         READ(1,710)INP
         IF(INP)25,30,25
25       XMIN=0
         WRITE(1,720)
         READ(1,730)XMAX
         READ(1,735)XINCH
         XST=XMIN
         READ(1,740)XTIC
         XINC=XTIC
         YMAX=0
         WRITE(1,750)
         READ(1,760)YMIN
         READ(1,765)YINCH
         YST=YMIN
         READ(1,770)YTIC
         YINC=YTIC
30       READ(1,780)NSYM
         READ(1,785)NSIZE
         READ(1,790)INP
         IF(INP)35,40,35
35       NCOR=150
40       READ(1,800)INP
         IF(INP)50,22,50
50       CALL OOPEN('DSK',FNDATA)
         DO 55 I=1,NPTST
           WRITE(4,810)XX(I),YY(I)
55       CONTINUE
         N=NPTST
         CALL OCLOSE

C     AT THIS POINT, THE PROGRAM TRANSFERS CONTROL TO THE GENERAL
C     PLOTTING SYSTEM, RETURNING AFTER PLOTTING TO 'BHFIT1.FT'.

         CALL CHAIN('GENPLT')
         END
```

C) Sample Run

```
.R BHFIT1

1:1(=1), 2:1(=2), OR 1:1:1(=3) COMPLEX? 2

HOW MANY DIFFERENT [DYE]? 1
ENTER ERRORS? (1=YES,2=NO) 1

# POINTS= 6
[DYE]= .043E-03

                                ERROR    ERROR    ERROR
 [NUC1]  [NUC2]  DABS           [NUC1]   [NUC2]    DABS

1.5E-03
                 -.032
                                .05E-03
                                                   .22E-03
2.0E-03
                 -.040
                                .06E-03
                                                   .14E-03
2.0E-03
                 -.040
                                .06E-03
                                                   .14E-03
2.9E-03
                 -.063
                                .08E-03
                                                   .63E-04
3.9E-03
                 -.080
                                .09E-03
                                                   .42E-04
7.0E-03
                 -.113
                                .16E-03
                                                   .24E-04

[DYE1]=   0.430E-04  # POINTS=  6

[NUC1]=   0.150E-02  [NUC2]=   0.000E-00  DELTA=  -0.320E-01
ERNUC1=   0.500E-04  ERNUC2=   0.000E-00  ERY=   0.220E-03

[NUC1]=   0.200E-02  [NUC2]=   0.000E-00  DELTA=  -0.400E-01
ERNUC1=   0.600E-04  ERNUC2=   0.000E-00  ERY=   0.140E-03

[NUC1]=   0.200E-02  [NUC2]=   0.000E-00  DELTA=  -0.400E-01
ERNUC1=   0.600E-04  ERNUC2=   0.000E-00  ERY=   0.140E-03

[NUC1]=   0.290E-02  [NUC2]=   0.000E-00  DELTA=  -0.630E-01
ERNUC1=   0.800E-04  ERNUC2=   0.000E-00  ERY=   0.630E-04

[NUC1]=   0.390E-02  [NUC2]=   0.000E-00  DELTA=  -0.800E-01
ERNUC1=   0.900E-04  ERNUC2=   0.000E-00  ERY=   0.420E-04

[NUC1]=   0.780E-02  [NUC2]=   0.000E-00  DELTA=  -0.113E-00
ERNUC1=   0.160E-03  ERNUC2=   0.000E-00  ERY=   0.240E-04
```

```
*************************************************

FIT W/O ERRORS

J=  1  X(J)=   0.444E+06  Y(J)=  -0.134E-02  ALPHA(J)=  0.0000
J=  2  X(J)=   0.250E+06  Y(J)=  -0.107E-02  ALPHA(J)=  0.0000
J=  3  X(J)=   0.250E+06  Y(J)=  -0.107E-02  ALPHA(J)=  0.0000
J=  4  X(J)=   0.119E+06  Y(J)=  -0.683E-03  ALPHA(J)=  0.0000
J=  5  X(J)=   0.657E+05  Y(J)=  -0.538E-03  ALPHA(J)=  0.0000
J=  6  X(J)=   0.164E+05  Y(J)=  -0.381E-03  ALPHA(J)=  0.0000
Y INTERCEPT= -0.40529E-03  SLOPE= -0.23243E-08
SIGMA B=  0.58050E-04  SIGMA M=  0.24341E-09
R= -0.97876
K=  0.174E+06

J=  1  X(J)=   0.459E+06  Y(J)=  -0.134E-02  ALPHA(J)=  0.2754
J=  2  X(J)=   0.259E+06  Y(J)=  -0.107E-02  ALPHA(J)=  0.4025
J=  3  X(J)=   0.259E+06  Y(J)=  -0.107E-02  ALPHA(J)=  0.4025
J=  4  X(J)=   0.123E+06  Y(J)=  -0.683E-03  ALPHA(J)=  0.5861
J=  5  X(J)=   0.679E+05  Y(J)=  -0.538E-03  ALPHA(J)=  0.7198
J=  6  X(J)=   0.168E+05  Y(J)=  -0.381E-03  ALPHA(J)=  0.9123
Y INTERCEPT= -0.40473E-03  SLOPE= -0.22509E-08
SIGMA B=  0.57385E-04  SIGMA M=  0.23279E-09
R= -0.97927
K=  0.180E+06

J=  1  X(J)=   0.459E+06  Y(J)=  -0.134E-02  ALPHA(J)=  0.2814
J=  2  X(J)=   0.259E+06  Y(J)=  -0.107E-02  ALPHA(J)=  0.4097
J=  3  X(J)=   0.259E+06  Y(J)=  -0.107E-02  ALPHA(J)=  0.4097
J=  4  X(J)=   0.123E+06  Y(J)=  -0.683E-03  ALPHA(J)=  0.5934
J=  5  X(J)=   0.679E+05  Y(J)=  -0.538E-03  ALPHA(J)=  0.7259
J=  6  X(J)=   0.168E+05  Y(J)=  -0.381E-03  ALPHA(J)=  0.9147
Y INTERCEPT= -0.40479E-03  SLOPE= -0.22492E-08
SIGMA B=  0.57389E-04  SIGMA M=  0.23265E-09
R= -0.97927
K=  0.180E+06
```

```
TYPE -CR- TO FIT W/ ERRORS; -1-, -CR- TO SKIP

FIT W/ ERRORS

J=  1  X(J)=   0.459E+06  Y(J)=  -0.134E-02  ALPHA(J)=  0.2816
J=  2  X(J)=   0.259E+06  Y(J)=  -0.107E-02  ALPHA(J)=  0.4099
J=  3  X(J)=   0.259E+06  Y(J)=  -0.107E-02  ALPHA(J)=  0.4099
J=  4  X(J)=   0.123E+06  Y(J)=  -0.683E-03  ALPHA(J)=  0.5936
J=  5  X(J)=   0.679E+05  Y(J)=  -0.538E-03  ALPHA(J)=  0.7261
J=  6  X(J)=   0.168E+05  Y(J)=  -0.381E-03  ALPHA(J)=  0.9147
Y INTERCEPT= -0.35462E-03  SLOPE= -0.25632E-08
SIGMA B=  0.53863E-04  SIGMA M=  0.42031E-09
R= -0.98871
K=  0.138E+06

J=  1  X(J)=   0.457E+06  Y(J)=  -0.134E-02  ALPHA(J)=  0.2326
J=  2  X(J)=   0.258E+06  Y(J)=  -0.107E-02  ALPHA(J)=  0.3493
J=  3  X(J)=   0.258E+06  Y(J)=  -0.107E-02  ALPHA(J)=  0.3493
J=  4  X(J)=   0.123E+06  Y(J)=  -0.683E-03  ALPHA(J)=  0.5299
J=  5  X(J)=   0.677E+05  Y(J)=  -0.538E-03  ALPHA(J)=  0.6713
J=  6  X(J)=   0.168E+05  Y(J)=  -0.381E-03  ALPHA(J)=  0.8919
Y INTERCEPT= -0.35044E-03  SLOPE= -0.26095E-08
SIGMA B=  0.53588E-04  SIGMA M=  0.46608E-09
R= -0.98974
K=  0.134E+06

J=  1  X(J)=   0.456E+06  Y(J)=  -0.134E-02  ALPHA(J)=  0.2274
J=  2  X(J)=   0.258E+06  Y(J)=  -0.107E-02  ALPHA(J)=  0.3427
J=  3  X(J)=   0.258E+06  Y(J)=  -0.107E-02  ALPHA(J)=  0.3427
J=  4  X(J)=   0.123E+06  Y(J)=  -0.683E-03  ALPHA(J)=  0.5226
J=  5  X(J)=   0.677E+05  Y(J)=  -0.538E-03  ALPHA(J)=  0.6648
J=  6  X(J)=   0.168E+05  Y(J)=  -0.381E-03  ALPHA(J)=  0.8890
Y INTERCEPT= -0.34966E-03  SLOPE= -0.26175E-08
SIGMA B=  0.53951E-04  SIGMA M=  0.48039E-09
R= -0.98994
K=  0.134E+06
```

```
J=  1 X(J)=    0.45626E+06 Y(J)=   -0.134E-02 ALPHA(J)=   0.2265
J=  2 X(J)=    0.25754E+06 Y(J)=   -0.107E-02 ALPHA(J)=   0.3416
J=  3 X(J)=    0.25754E+06 Y(J)=   -0.107E-02 ALPHA(J)=   0.3416
J=  4 X(J)=    0.12268E+06 Y(J)=   -0.683E-03 ALPHA(J)=   0.5213
J=  5 X(J)=    0.67717E+05 Y(J)=   -0.538E-03 ALPHA(J)=   0.6636
J=  6 X(J)=    0.16764E+05 Y(J)=   -0.381E-03 ALPHA(J)=   0.8885

FINAL K=    0.1336E+06  FINAL DELTA EPSILON=   -0.2860E+04
SIGMA K=    0.3203E+05  SIGMA DELTA EPSILON=    0.4413E+03

J=  1 DX(J)=    0.3082E+05 DY(J)=    0.32E-03 [COMPLEX]=    0.9739E-05
J=  2 DX(J)=    0.1568E+05 DY(J)=    0.20E-03 [COMPLEX]=    0.1469E-04
J=  3 DX(J)=    0.1568E+05 DY(J)=    0.20E-03 [COMPLEX]=    0.1469E-04
J=  4 DX(J)=    0.6875E+04 DY(J)=    0.10E-03 [COMPLEX]=    0.2242E-04
J=  5 DX(J)=    0.3172E+04 DY(J)=    0.76E-04 [COMPLEX]=    0.2854E-04
J=  6 DX(J)=    0.6945E+03 DY(J)=    0.59E-04 [COMPLEX]=    0.3821E-04


PLOT DATA? (0=NO,1=YES) 1


NORMALIZER TO MAKE X AXIS INTEGRAL = 1.E+05
NORMALIZER TO MAKE Y AXIS INTEGRAL = 1.E-04
I=  1  NORMALIZED X(I)=     4.563  NORMALIZED Y(I)=  -13.437
I=  2  NORMALIZED X(I)=     2.575  NORMALIZED Y(I)=  -10.750
I=  3  NORMALIZED X(I)=     2.575  NORMALIZED Y(I)=  -10.750
I=  4  NORMALIZED X(I)=     1.227  NORMALIZED Y(I)=   -6.825
I=  5  NORMALIZED X(I)=     0.677  NORMALIZED Y(I)=   -5.375
I=  6  NORMALIZED X(I)=     0.168  NORMALIZED Y(I)=   -3.805
ALL OK? 1


NEW GRAPH? (0=NO,1=YES) 1
NEW PARAMETERS? 1
XMIN=0, XST=XMIN
XMAX= 5.
XINCH= 8.
XTIC=XINC= 1.
YMAX=0, YST=YMIN
YMIN= -16.
YINCH= 6.
YTIC=YINC= 4.
SYMBOL # 1
SYMBOL SIZE 2
CALCOMP(0) OR TEKTRONIX(1)
ALL OK? 1

 PLOT IS BOUND FOR CALCOMP

 PLOT EVERY NTH POINT, N = 1
 RE-PLOT DATA?

1:1(=1), 2:1(=2), OR 1:1:1(=3) COMPLEX?
```

2. Equilibrium Concentrations/$\Delta\varepsilon_{bound}$

A) Description

The program EQ calculates the equilibrium concentration of dimer(s) and dye for 1:1, 2:1, or 1:1:1 stoichiometries and also calculates $\Delta\varepsilon^{\lambda}_{bound}$ and its associated error. The program is written in FORTRAN, compiled with .R FORT, and saved as a core image file with .SAVE SYS EQ. All listings are available on paper tape.

The data consists of the complex's equilibrium constant, the initial concentrations of dimer(s) and dye, and their errors for the calculation of the equilibrium concentrations. To calculate $\Delta\varepsilon_{bound}$, enter the measured induced CD (θ^0 x 100) and its error. Equations (2) and (6) of Chapter II are used in the calculations.

B) Listing

i) EQ

```
      COMMON WAVE,TH100,ERTH,NWAVE,CN1,CN2,C0,PLEX,
     2          B,K,RK,ALPHA,ERPLX,EC1,EC2,CSUM,SUM
      DIMENSION WAVE(6),TH100(6),ERTH(6)
700   FORMAT(///'THIS PROGRAM CALCULATES EQUILIBRIUM CONCENTRATIONS,')
710   FORMAT('CD DELTA EPSILONS, AND ERRORS FOR EACH.  TO CALCULATE')
720   FORMAT('EQUILIBRIUM VALUES ALONE, ENTER 0 FOR EACH ERROR AND')
730   FORMAT('NUMBER OF WAVELENGTHS.'/)
740   FORMAT(/)
750   FORMAT('1:1(=1), 2:1(=2), OR 1:1:1(=3) COMPLEX? 'I1)
800   FORMAT('EQUILIBRIUM CONSTANT (E10.4) = 'E10.4)
810   FORMAT('ERROR K (E11.5) = 'E11.5)
820   FORMAT('INITIAL [DYE] (E10.4) = 'E10.4)
830   FORMAT('ERROR [DYE] (E11.5) = 'E11.5)
840   FORMAT('INITIAL [DIMER 1] (E10.4) = 'E10.4)
850   FORMAT('INITIAL [DIMER 2] (E10.4) = 'E10.4)
860   FORMAT('ERROR [DIMER 1] (E11.5) = 'E11.5)
870   FORMAT('ERROR [DIMER 2] (E11.5) = 'E11.5)
875   FORMAT('PATH LENGTH (CM) = 'F7.4)
880   FORMAT('NUMBER OF DIFFERENT WAVELENGTHS (I1) = 'I1)
885   FORMAT('WAVELENGTH (F5.1) = 'F5.1)
890   FORMAT('THETA X 100 (E11.4) = 'E11.4)
895   FORMAT('ERROR IN THETA X 100 (E12.5) = 'E12.5)
900   FORMAT(/'NO CONVERGENCE OF ALPHA AFTER 50 STEPS'/)
910   FORMAT(///'K = 'E10.4)
920   FORMAT('[COMPLEX]:'19X' FINAL = 'E11.5' ERROR = 'E11.5)
930   FORMAT('[DYE]:   INITIAL = 'E10.4' FINAL = 'E11.5
     $          ' ERROR = 'E11.5)
940   FORMAT('[DIMER'I1']: INITIAL = 'E10.4' FINAL = 'E11.5
     $          ' ERROR = 'E11.5)
950   FORMAT(/'ALL ERRORS USED')
960   FORMAT(/'THETA ERRORS ZEROED')
970   FORMAT(/'DIMER, DYE, THETA ERRORS ZEROED')
999   FORMAT('NEW [DYE] OR SYSTEM? (0=NO, NZ=YES) 'I1)
C
      WRITE(1,700)
      WRITE(1,710)
      WRITE(1,720)
      WRITE(1,730)
10    CN2=0
      EC2=0
      RK=1.
      READ(1,750)K
      IF(K-1)10,15,11
11    IF(K-2)10,13,12
12    IF(K-3)10,15,10
13    RK=2.
```

```
C
C   ENTER CONCENTRATION DATA
C
15      READ(1,800)CAY
        READ(1,810)ERCAY
        READ(1,820)C0
        READ(1,830)ERC
17      READ(1,840)CN1
        IF(K-3)25,20,25
20      READ(1,850)CN2
25      READ(1,860)EC1
        IF(K-3)35,30,25
30      READ(1,870)EC2
C
C   ENTER CD DATA
C
35      READ(1,875)B
        READ(1,880)NWAVE
        DO 40 I=1,NWAVE
          WRITE(1,740)
          READ(1,885)WAVE(I)
          READ(1,890)TH100(I)
          READ(1,895)ERTH(I)
40      CONTINUE
C
C   CALCULATE EQUILIBRIUM CONCENTRATIONS
C
        ALPHA=0
        CSUM=(ERCAY/CAY)**2. +(ERC/C0)**2.
        DO 50 I=1,50
          CALL FREE (FRE1,FRE2,VALNEW)
          ALF=CAY*VALNEW
          ALFA=ALF/(1. +ALF)
          DIFF=ABS(ALFA-ALPHA)
          ALPHA=ALFA
          PLEX=C0*ALPHA
          C=C0-PLEX
          CALL FREE (FRE1,FRE2,VALNEW)
          IF(DIFF-.001*ALPHA)60,60,50
50      CONTINUE
        WRITE(1,900)
        GO TO 99
C
C   PRINT EQUILIBRIUM CONCENTRATIONS
C
60      ERPLX=SQRT(PLEX*PLEX*SUM)
        WRITE(1,910) CAY
        WRITE(1,920) PLEX,ERPLX
        WRITE(1,930) C0,C,ERC
        WRITE(1,940)1,CN1,FRE1,EC1
        IF(K-2)70,65,70
65      WRITE(1,940)2,CN2,FRE2,EC2
70      IF(NWAVE)99,99,75
```

```
C
C   CALCULATE DELTA EPSILON, IF DESIRED
C
75      WRITE(1,950)
        CALL THETA
        DO 80 I=1,NWAVE
          ERTH(I)=0
80      CONTINUE
        WRITE(1,960)
        CALL THETA
        ERPLX=ABS(PLEX*ERCAY/CAY)
        WRITE(1,970)
        CALL THETA
99      WRITE(1,740)
        READ(1,999)I
        WRITE(1,740)
        IF(I) 10,17,10
        END
```

ii) Subroutine THETA

```
      SUBROUTINE THETA
      COMMON WAVE,TH100,ERTH,NWAVE,CN1,CN2,C0,PLEX,
     2          B,K,RK,ALPHA,ERPLX,EC1,EC2,CSUM,SUM
      DIMENSION WAVE(6),TH100(6),ERTH(6)
710   FORMAT(/F5.1' NM: THETA X 100 = 'E11.4' ERROR = 'E12.5)
720   FORMAT(F5.1' NM: DELTA EPSILON = 'E10.3' ERROR = 'E11.4)
C
      DO 10 I=1,NWAVE
        DELEP=TH100(I)/(2298.*PLEX*B)
        SUM=(ERTH(I)/ABS(TH100(I)))**2.+(ERPLX/PLEX)**2.
        ERDEL=SQRT(DELEP*DELEP*SUM)
        WRITE(1,710) WAVE(I),TH100(I),ERTH(I)
        WRITE(1,720) WAVE(I),DELEP,ERDEL
10    CONTINUE
      RETURN
      END
```

iii) Subroutine FREE

```
      SUBROUTINE FREE (FRE1,FRE2,VALNEW)
      COMMON WAVE,TH100,ERTH,NWAVE,CN1,CN2,C0,PLEX,
     2          B,K,RK,ALPHA,ERPLX,EC1,EC2,CSUM,SUM
      DIMENSION WAVE(6),TH100(6),ERTH(6)
C
      FRE1=CN1-RK*ALPHA*C0
      FRE2=CN2-RK*ALPHA*C0
      IF(K-2)52,54,56
52    VALNEW=FRE1
      SUM=CSUM+(RK*EC1/CN1)**2.
      FRE2=1.
      RETURN
54    VALNEW=FRE1*FRE1
      SUM=CSUM+(RK*EC1/CN1)**2.
      FRE2=1.
      RETURN
56    VALNEW=FRE1*FRE2
      SUM=CSUM+(RK*EC1/CN1)**2.+(RK*EC2/CN2)**2.
      RETURN
      END
```

C) Sample Run

```
.R EQ


THIS PROGRAM CALCULATES EQUILIBRIUM CONCENTRATIONS,
CD DELTA EPSILONS, AND ERRORS FOR EACH.   TO CALCULATE
EQUILIBRIUM VALUES ALONE, ENTER 0 FOR EACH ERROR AND
NUMBER OF WAVELENGTHS.

1:1(=1), 2:1(=2), OR 1:1:1(=3) COMPLEX? 2
EQUILIBRIUM CONSTANT (E10.4) = 1.3E+05
ERROR K (E11.5) = .3E+05
INITIAL [DYE] (E10.4) = .043E-03
ERROR [DYE] (E11.5) = .002E-03
INITIAL [DIMER 1] (E10.4) = 2.9E-03
ERROR [DIMER 1] (E11.5) = .03E-03
PATH LENGTH (CM) = 1.
NUMBER OF DIFFERENT WAVELENGTHS (I1) = 1


WAVELENGTH (F5.1) = 305.
THETA X 100 (E11.4) = .712
ERROR IN THETA X 100 (E12.5) = .034


K = 0.1300E+06
[COMPLEX].                          FINAL = 0.22128E-04 ERROR = 0.52293E-05
[DYE]:    INITIAL = 0.4300E-04 FINAL = 0.20972E-04 ERROR = 0.20000E-05
[DIMER1]: INITIAL = 0.2900E-02 FINAL = 0.28557E-02 ERROR = 0.30000E-04

ALL ERRORS USED

305.0 NM: THETA X 100 =  0.7120E-00 ERROR =  0.34000E-01
305.0 NM: DELTA EPSILON =  0.976E+01 ERROR =  0.2352E+01

THETA ERRORS ZEROED

305.0 NM: THETA X 100 =  0.7120E-00 ERROR =  0.00000E-00
305.0 NM: DELTA EPSILON =  0.976E+01 ERROR =  0.2306E+01

DIMER, DYE, THETA ERRORS ZEROED

305.0 NM: THETA X 100 =  0.7120E-00 ERROR =  0.00000E-00
305.0 NM: DELTA EPSILON =  0.976E+01 ERROR =  0.2251E+01

NEW [DYE] OR SYSTEM? (0=NO, NZ=YES) 1


1:1(=1), 2:1(=2), OR 1:1:1(=3) COMPLEX?
```

Appendix B

SUPER SPECTRUM DATA SYSTEM

The Super Spectrum system of programs is a lineal descendant of the system described by Tomlinson (1968) and is used to acquire and process data from the Cary 60 and Cary 118 spectrometers with a PDP 8/E computer (Digital) and a RK-8E disk drive. The updates and corrections to the program have been extensive; the main differences are modification of the pen averaging routine to use the exact "stable averaging" algorithm (Savitsky & Golay, 1964), the addition of plotting routines, and the creation of an overlay to transmit data to the Lawrence Berkeley Lab computer system.

Complete operating instructions and listings of the programs are on the enclosed microfiche. All programs are stored on punched card decks and on GSS tape 10515 at LBL. A handbook describing operation of the system and assembly of the programs has been prepared from the OPERATE program - this is available in the lab.

Appendix C

COMPUTER PROGRAMS AT LBL

1. Introduction

The programs PREPARE, SMOOTHS, and PROCESS translate, average, smooth, and perform other manipulations with spectra from Super Spectrum. The programs are designed to run in succession: the output from one is the input to the next. These programs are descended from the programs described in Borer (1972). More information on the ID requirements and formats of the spectra for proper operation in this system is listed in the OPERATE program of Super Spectrum (Appendix B).

2. Program PREPARE

A) Operation

i) Input

The hexadecimal spectra files on PSS created by the transmission overlay from Super Spectrum.

ii) Output

The file OUTPUT contains a summary of the data translation. Misread lines are listed here. This is usually placed in the HOLDOUT queue for immediate viewing.

The file TAPE10 contains intermediate listings and plots of the data. This is usually deleted, but may be DISPOSEd to microfiche, if necessary.

The file TAPE30 contains the translated spectra in a form acceptable for SMOOTHS. This file is carried over to the next program when the two programs are run in tandem (below).

iii) Errors

Stray or missing bits in the PSS file will always prevent SMOOTHS from starting after translation of all files is completed (if possible). The line in error will be listed as read with an error message on the file OUTPUT. The original listing of hexadecimal lines will contain the correct information for comparison. The entire data file may not be read if there is an error in the parameter line (1st line) of a new spectrum; correction of this error is necessary before the rest of the file will be read.

B) Listing

i) Program PREPARE

ii) Subroutine UNLOAD

iii) Function U NLOAD

iv) Subroutine REDO

v) Subroutine PRNPLT

vi) Subroutine PLSCAL

```
      PROGRAM PREPARE (INPUT,OUTPUT,TAPE13,TAPE5=INPUT,TAPE10,TAPE30)
C****
C**** ****THIS VERSION OF -PREPARE- IS COMPATABLE WITH THE LATEST
C**** ****UPDATE OF -SUPER SPECTRUM- ONLY (1980).  NO PREVIOUS LIST-
C**** ****ON THIS GSS TAPE IS SO STRUCTURED.
C****
C**** THIS PROGRAM READS DATA OUT OF PSS AND TRANSLATES IT FROM HEXA-
C**** DECIMAL MODE.  DATA WAS READ IN THROUGH HILL OVERLAY (NUMBER 2) OF
C**** SUPER SPECTRUM AND STORED AS HEXADECIMAL CHARACTERS, THREE CHARAC-
C**** TERS/WORD. 25 WORDS/LINE, PLUS CHECKSUM.  TAPE5 FILE CONTAINS THE
C**** DATA OUT OF PSS.  TAPE10 FILE WILL CONTAIN PRELIMINARY TRANSMIS-
C**** SION OF THE DATA, AND WILL BE FURTHER USED IN THE PROGRAM SMOOTH.
C**** TAPE30 FILE IS THE TRANSLATED DATA AND WILL ALSO GO TO THE PROGRAM
C**** SMOOTH.  TAPE30 CAN ALSO BE STORED ON TAPE.  ANY ERRORS IN TRANS-
C**** MISSION HALT WRITING ON TAPE10 AND TAPE30 AND DELETE THEM.  TAPE13
C**** CONTAINS THE FILE CONTROL AND IS REWRITTEN IF TRANSMISSION ERRORS
C**** OCCUR TO HALT THE PROGRAM SEQUENCE.  A TRANSMISSION SUMMARY IS
C**** PRINTED ON THE FILE OUTPUT, ALONG WITH ANY ERROR MESSAGES.
C****
      COMMON/CD/CD(300)
      COMMON/WAVE/WAVE(300)
      COMMON/IDATA/IDATA(300)
      COMMON/ISUM/ISUM(40)
      REAL CD,WAVE
      INTEGER IDATA,ISUM
      DIMENSION PARAM(6)
      INTEGER IEXP(3),IMAN(3),IHEAD(8),IPUNPR(3)
 700  FORMAT(*1*,*COMPUTE SHIFTS? *,A3,5X,* PUNCH AV DATA? *,A3,5X,
     $* SMOOTH DATA? *,A3)
 701  FORMAT(3A3)
 702  FORMAT(*0*,4X,*ID*,6X,*VSTART*,4X,*VEND*,5X,*VINCR*,8X,*OD*,10X,
     $*E*,9X,*SCALE*,3X,*NPTS*,/,64X,*(X 0.001)*,/)
 718  FORMAT(*-*,I3,* SPECTRA READ FROM FILE*)
 740  FORMAT(26R3)
 741  FORMAT(*-*,I4,A2,A2,//,1X,*START= *,F7.2,* NM, END= *,F7.2,
     $* NM, INCREMENTING BY *,F7.2,* NM*,/,1X,*ODFACT= *,F10.3,
     $*, EPSLON= *,F10.3,*, SCALE(X 0.001)= *,F10.6,/,1X,I3,
     $* DATA POINTS*,///,(1H ,24(O4,1X),O4))
 742  FORMAT(*1*,I4,A2,A2,2X,3(F7.2,2X),2(F10.3,2X),F10.6,2X,I3,//)
 743  FORMAT(3(13X,F6.0,3X,F13.4))
 744  FORMAT(I4,A2,A2,3(F7.2),2(F10.3),F10.6,I3)
 745  FORMAT(I4)
 746  FORMAT(*1*)
 747  FORMAT(*0*,*UNPACKING OF DATA HALTED, UNABLE TO SET NUMPTS*)
 748  FORMAT(* *,I4,A2,A2,2X,3(F7.2,2X),2(F10.3,2X),F10.6,2X,I3)
 749  FORMAT(A8,A2)
 750  FORMAT(*-*,*ONE OR MORE TRANSMISSION ERRORS HAVE OCCURRED AND MUST
     $ BE CORRECTED BEFORE COMPLETE WORKUP OF DATA IS POSSIBLE*)
      REWIND 10
      REWIND 30
      READ(5,701) IPUNPR
      PRINT 700, IPUNPR
      WRITE(30,701) IPUNPR
      PRINT 702
      NSPECT=0
```

```
      ITRER=0
40    INTRNS=0
C**** TRANSLATE SPECTRUM CONTROLS
      READ(5,740) (IDATA(I),I=1,25),ISUM(1)
      IF(EOF(5).NE.0) GO TO 49
      WRITE(10,746)
      CALL UNLOAD (1,1,INTRNS)
      DO 410 I=1,4
        IHEAD(I)=(IDATA(I).AND.178)
410   CONTINUE
      ID1=IHEAD(1)*1000+IHEAD(2)*100+IHEAD(3)*10+IHEAD(4)
      DO 411 I=5,8
        INT=IDCODE(IDATA(I))
        IHEAD(I)=INT
411   CONTINUE
      ID2P=IHEAD(5)*100B+IHEAD(6)
      ID3P=IHEAD(7)*100B+IHEAD(8)
      DECODE(10,749,ID2P) IGAR,ID2
      DECODE(10,749,ID3P) IGAR,ID3
      PARAM(1)=(FLOAT(IDATA(9)*100000B+IDATA(10)))/10.
      PARAM(2)=FLOAT(IDATA(11))
      PARAM(3)=(FLOAT(1+((.NOT.IDATA(12)).AND.7777B)))/10.
      NPTS=1+((.NOT.IDATA(13)).AND.7777B)
      DO 43 I=1,3
        J=3*(4+I)
        IEXP(I)=IDATA(J-I)
        IMAN(I)=IDATA(J)*100000B+IDATA(J+1)
        IF((IEXP(I).AND.40000B).EQ.0) GO TO 42
        IEXP(I)=-(1+((.NOT.IEXP(I)).AND.77778))
42      PARAM(I+3)=FLOAT(IMAN(I))*(2.**(IEXP(I)-23))
43    CONTINUE
      IF(NSPECT.EQ.0.AND.INTRNS.NE.0) GO TO 48
      IF(NSPECT.EQ.0.AND.INTRNS.EQ.0) NUMPTS=NPTS
      IF(NSPECT.NE.0.AND.INTRNS.NE.0.AND.NUMPTS.NE.NPTS) GO TO 48
      IF(NSPECT.NE.0.AND.INTRNS.EQ.0.AND.NUMPTS.NE.NPTS) NUMPTS=NPTS
C**** TRANSLATE SPECTRUM POINTS
      READ(5,740) ((IDATA(J+I-1),I=1,25),ISUM(J/25+2),J=1,NUMPTS,25)
      LNCNT=((NUMPTS+24)/25)+1
      CALL UNLOAD (2,LNCNT,INTRNS)
      NSPECT=NSPECT+1
      IF(INTRNS.NE.0) GO TO 430
      PRINT 748,ID1,ID2,ID3,(PARAM(I),I=1,6),NPTS
430   ITRER=ITRER+INTRNS
      IF(ITRER.NE.0) GO TO 40
C**** TAPE10 WILL GO TO MICROFICHE WITH TRANSMISSION DATA, RAW DATA
C**** TABLES, AND PLOTS
      WRITE(10,741) ID1,ID2,ID3,PARAM,NPTS,(IDATA(I),I=1,NUMPTS)
      DO 44 I=1,NPTS
        WAVE(I)=PARAM(1)-FLOAT(I-1)*PARAM(3)
        IF((IDATA(I).AND.40000B).EQ.0) GO TO 431
        IDATA(I)=IDATA(I)+777777777777777700008
431     CD(I)=PARAM(6)*IDATA(I)
44    CONTINUE
      WRITE(10,742) ID1,ID2,ID3,PARAM,NPTS
      II=NPTS/3+1
```

```
      DO 45 I=1,II
        J=I+II
        K=J+II
        WRITE(10,743) WAVE(I),CD(I),WAVE(J),CD(J),WAVE(K),CD(K)
 45   CONTINUE
      WRITE(10,742) ID1,ID2,ID3,PARAM,NPTS
      IDEV=10
      XMAX=PARAM(1)
      XINC=(PARAM(1)-PARAM(2))/100.
      TWICE=XINC/0.5
      M=TWICE
      IF(M.NE.TWICE) XINC=0.5*(M+1)
      ISY=1
      CALL PRNPLT (WAVE(1),CD(1),XMAX,XINC,YMAX,YINC,0,ISY,NPTS,IDEV)
C**** TAPE30 WILL GO TO SMOOTHING PROGRAM AND TO STORAGE ON TAPE
      WRITE(30,744) ID1,ID2,ID3,PARAM,NPTS
      WRITE(30,745) (IDATA(I),I=1,NPTS)
      GO TO 40
 48   PRINT 747
      CALL REDO
 49   PRINT 718,NSPECT
      WRITE(10,700) IPUNPR
      WRITE(10,718) NSPECT
      ENDFILE 30
      IF(ITRER.EQ.0) CALL EXIT
      PRINT 750
      CALL REDO
      END
```

```
      SUBROUTINE UNLOAD (LOLIM,LNCNT,INTRNS)
C**** CONVERTS LINES OF HEXADECIMAL DATA (26 WORDS/LINE, 78 CHARACTERS)
C**** TO BINARY FORM
C**** LAST WORD (3 CHARACTERS) IN EACH LINE IS CHECKSUM
      COMMON/IDATA/NDATA(300)
      COMMON/ISUM/NSUM(40)
      INTEGER NDATA,NSUM
      INTEGER N(3),NHEAD(8),LDATA(25)
 751  FORMAT(* *,8X,*CONTROL LINE OF SPECTRUM *,8R1,
     $*, OCTAL ERROR IN NTOT= *,O4)
 752  FORMAT(* *,8X,*DATA LINE NUMBER *,I2,* OF SPECTRUM *,8R1,
     $*, OCTAL ERROR IN NTOT= *,O4)
 753  FORMAT(*+*,8X,*ERROR IN DATA TRANSMISSION*,/,9X,
     $*ERROR IN DATA TRANSMISSION*)
 754  FORMAT(* *,8X,25(R3,1X),1X,R3)
      INDEX=0
      DO 57 I=LOLIM,LNCNT
        NTOT=0
        DO 51 J=1,25
          INDEX=INDEX+1
C**** SAVE LINE FOR POSSIBLE ERROR PRINTING
          LDATA(J)=NDATA(INDEX)
          N(1)=(NDATA(INDEX).AND.77B)
          N(2)=(NDATA(INDEX).AND.7700B)/100B
          N(3)=(NDATA(INDEX).AND.770000B)/10000B
C**** DISPLAY MODE HEXADECIMAL TO BINARY CONVERSION
C**** DISPLAY MODE REPRESENTS 0-9=33-44B, A-F=01-06B
          DO 50 K=1,3
            IF((N(K).AND.70B).EQ.0) N(K)=N(K)+44B
            N(K)=N(K)-33B
 50       CONTINUE
          NTOT=NTOT+N(1)+N(2)+N(3)
          NDATA(INDEX)=N(1)+16*N(2)+256*N(3)
 51     CONTINUE
C**** CHECK LINE TRANSMISSION
        N(1)=(NSUM(I).AND.77B)
        N(2)=(NSUM(I).AND.7700B)/100B
        N(3)=(NSUM(I).AND.770000B)/10000B
        DO 52 J=1,3
          IF((N(J).AND.70B).EQ.0) N(J)=N(J)+44B
          N(J)=N(J)-33B
 52     CONTINUE
        NTOT=NTOT-N(1)-16*N(2)-256*N(3)
        IF(LOLIM.NE.1) GO TO 54
C**** SAVE ID FOR POSSIBLE ERROR PRINTING
        DO 53 J=1,8
          NHEAD(J)=IDCODE(NDATA(J))
 53     CONTINUE
 54     IF(NTOT.EQ.0) GO TO 57
C**** NOTE ERRORS THAT OCCURRED IN TRANSMISSION
        INTRNS=INTRNS+1
        IF(LOLIM.NE.1) GO TO 55
        PRINT 753
        PRINT 751,NHEAD,NTOT
        PRINT 754,(LDATA(L),L=1,25),NSUM(I)
        GO TO 57
 55     PRINT 753
        PRINT 752,I-1,NHEAD,NTOT
        PRINT 754,(LDATA(L),L=1,25),NSUM(I)
 57   CONTINUE
      RETURN
      END
```

```
      FUNCTION IDCODE(ITTY)
C**** CHARACTER IN 8-BIT ASCII CODE TO 6-BIT DISPLAY CODE CONVERSION
      DIMENSION ISPEC(27)
      DATA (ISPEC(J),J=1,27)/53B,55B,52B,57B,50B,51B,44B,75B,40B,54B,
     $56B,34B,33B,35B,72B,4*40B,36B,2*40B,76B,3*40B,73B/
      ITTY=ITTY.AND.0077B
      IF(ITTY.GE.33B) GO TO 60
      IDCODE=ITTY
      RETURN
60    IF(ITTY.LT.60B.OR.ITTY.GT.71B) GO TO 61
      IDCODE=ITTY-25B
      RETURN
61    DO 62 I=1,27
         IF(ITTY.EQ.ISPEC(I)) GO TO 63
62    CONTINUE
      RETURN
63    IDCODE=I+44B
      RETURN
      END
```

```
      SUBROUTINE REDO
C**** REWRITE THE CONTROL FILE TO END RUN
800   FORMAT(*DELETE,TAPE10,TAPE30.*)
802   FORMAT(*DISPOSE,OUTPUT=PR,HO,T=(TRANSMISSION/ERRORS).*)
803   FORMAT(*END.*)
      REWIND 13
      WRITE(13,800)
      WRITE(13,802)
      WRITE(13,803)
      REWIND 13
      CALL EXIT
      END
```

```
      SUBROUTINE PRNPLT (X,Y,XMAX,XINCR,YMAX,YINCR,ISX,ISY,NPTS)
C**** PRINTER PLOT ROUTINE    M.S.ITZKOWITZ    MAY 1967
C**** PLOTS THE DATA GIVEN BY X(I) AND Y(I), WHERE I=1,NPTS,
C**** ON A 51 X 101 GRID
C**** IF ISX OR ISY ARE NONZERO, THE CORRESPONDING MAXIMUM
C**** AND INCREMENTAL STEP ARE COMPUTED
C**** IF XINCR OR YINCR ARE ZERO, THE PROGRAM RETURNS WITH AN ERROR NOTE
C**** NO INPUT ARRAYS ARE DESTROYED
C**** IF SCALING IS DONE, THE CORRESPONDING NEW VALUES OF THE MAXIMUM
C**** AND STEP SIZE ARE RETURNED
      DIMENSION X(NPTS),Y(NPTS),IGRID(105),XAXIS(11)
      INTEGER BLANK,DOT,PLUS,STAR
      DATA BLANK/1H /
      DATA DOT/1H./
      DATA PLUS/1H+/
      DATA STAR/1H*/
900   FORMAT(18X,11(*++*,9X))
901   FORMAT(15X,103(*.*))
902   FORMAT(14X,105A1)
903   FORMAT(1X,E11.4,1X,*++*,105A1,***)
904   FORMAT(7X,11(E10.3))
905   FORMAT(*0*,4X,*NUMBER OF POINTS= *,I4,*     Y INCREMENT= *,E11.4,
     $*     Y MAXIMUM= *,E11.4,*     Y MINIMUM= *,E11.4)
906   FORMAT(* *,/////,*SCALING ERROR IN PRNPLT*)
      ISCLER=0
      IF(ISX.NE.0) CALL PLSCAL (X,XMAX,XINCR,NPTS,100,XDMAX,XDMIN,
     $ISCLER)
      IF(ISY.NE.0) CALL PLSCAL (Y,YMAX,YINCR,NPTS,50,YDMAX,YDMIN,
     $ISCLER)
      IF(ISCLER.NE.0) RETURN
      IF(XINCR.EQ.0.OR.YINCR.EQ.0) GO TO 78
      XAXMIN=0.01*XINCR
      YAXMIN=0.01*YINCR
      IZERO=YMAX/YINCR+1.5
      JZERO 103.5-XMAX/XINCR
      IF(JZERO.GT.103.OR.JZERO.LT.4) JZERO=2
      PRINT 900
      PRINT 901
      DO 76 I=1,51
        IF(I.NE.IZERO) GO TO 71
        DO 70 J=1,105
          IGRID(J)=PLUS
70      CONTINUE
        GO TO 73
71      DO 72 J=1,105
          IGRID(J)=BLANK
72      CONTINUE
73      IGRID(JZERO)=PLUS
        IGRID(104)=DOT
        IGRID(2)=DOT
        DO 74 K=1,NPTS
          ITEST=(YMAX-Y(K))/YINCR+1.5
          IF(ITEST.NE.I) GO TO 74
          J=103.5-(XMAX-X(K))/XINCR
          IF(J.GT.103) J=105
          IF(J.LT.3) J=1
          IGRID(J)=STAR
74      CONTINUE
        IF(MOD(I,10).EQ.1) GO TO 75
        PRINT 902,IGRID
        GO TO 76
75      YAXIS=YMAX-(I-1)*YINCR
        IF(ABS(YAXIS).LT.YAXMIN) YAXIS=0
        PRINT 903,YAXIS,IGRID
76    CONTINUE
      PRINT 901
      PRINT 900
        DO 77 M=1,11
          XAXIS(M)=XMAX-XINCR*(FLOAT(11-M))*10.0
          IF(ABS(XAXIS(M)).LT.XAXMIN) XAXIS(M)=0
77      CONTINUE
        PRINT 904,XAXIS
        PRINT 905,NPTS,YINCR,YDMAX,YDMIN
        RETURN
78      PRINT 906
        RETURN
        END
```

```
      SUBROUTINE PLSCAL (V,VMAX,VINCR,NPTS,NDIVIS,DMAX,DMIN,ISCLER)
C**** SCALING ROUTINE FOR PRNPLT    M.S.ITZKOWITZ    MAY 1967
C**** FULL SCALE OF PLOT IS ADJUSTED AND THE MAXIMUM POINT IS ADJUSTED
C**** TO BE AN INTEGRAL MULTIPLE OF 5.0*VINCR
      DIMENSION RLIM(11),V(NPTS)
      DATA (RLIM(I),I=1,11)/1.25,1.60,2.00,2.50,3.20,4.00,5.00,6.40,
     $8.00,10.00,12.50/
907   FORMAT(* *,/////,*PLSCAL CALLED TO SCALE ARRAY WITH ZERO RANGE*)
      VMIN=V(1)
      VMAX=V(1)
      DO 80 I=1,NPTS
        IF(V(I).LT.VMIN) VMIN=V(I)
        IF(V(I).GT.VMAX) VMAX=V(I)
80    CONTINUE
      QRANGE VMAX-VMIN
      IF(QRANGE.LE.0) GO TO 91
      QRANGE=(ALOG(QRANGE))/ALOG(10.0)
      IF(QRANGE.LE.0) GO TO 82
      IRANGE=QRANGE
      GO TO 83
82    IRANGE=-QRANGE
      IRANGE=-IRANGE-1
83    QRANGE=QRANGE-FLOAT(IRANGE)
      RANGE=10.0**QRANGE
C**** RANGE IS BETWEEN 1.0 AND 10.0
      DO 84 I=1,9
        IF(RANGE.GE.RLIM(I)) GO TO 84
        RANGE=RLIM(I)
        ILIM=I
        GO TO 85
84    CONTINUE
      RANGE=10.0
      ILIM=10
85    TRANGE=RANGE*(10.0**IRANGE)
      VINCR=TRANGE/FLOAT(NDIVIS)
      IF(VMAX.LE.0) GO TO 87
      IMAX=VMAX/(5.0*VINCR)
      XMAX=5.0*VINCR*FLOAT(IMAX+1)
      GO TO 88
87    IMAX=-VMAX/(5.0*VINCR)
      XMAX=5.0*VINCR*FLOAT(-IMAX+1)
88    IF(VMIN.GT.(XMAX-TRANGE)) GO TO 90
      IF(ILIM.GE.11) ILIM=1
      ILIM=ILIM+1
      RANGE=RLIM(ILIM)
      IF((RANGE-10.0).LT.0) GO TO 85
      RANGE=RANGE/10.0
      IRANGE=IRANGE+1
      GO TO 85
90    DMAX=VMAX
      DMIN=VMIN
      VMAX=XMAX
      RETURN
91    PRINT 907
      ISCLER=1
      RETURN
      END
```

3. Program SMOOTHS

A) Operation

i) Input

The translated spectra on the TAPE30 file from PREPARE.

ii) Output

The file TAPE10 contains intermediate listings and plots of the data. This is usually deleted, but may be DISPOSEd to microfiche if necessary.

The file OUTPUT (= TAPE7) contains listings and plots of all averaged spectra and difference spectra created with the ID codes ST, SU, US, SM, and MS.

The file PUNCH contains the averaged and smoothed spectra in a form acceptable for PROCESS. This file is punched and the deck serves as input in the next program (see note, below).

iii) Errors

The order of spectra in the file is important. Spectra with AV codes will be averaged with the next in line whether they are in the right order or not. Spectra with ID codes SU, US, SM, and MS require a second spectrum previously prepared by either one of these commands or the ST code. If this spectrum is not present, an error message is left and the next series of spectra are run.

B) Listing

i) Program SMOOTHS

ii) Subroutine LETSEE

iii) Subroutine SHIFTS

iv) Subroutine WRAPUP

v) Subroutine PRNPLT and Subroutine PLSCAL (see PREPARE)

```
      PROGRAM SMOOTHS (INPUT,OUTPUT,PUNCH,TAPE30=INPUT,TAPE7=OUTPUT,
     $TAPE10)
****
**** ****THIS IS THE LATEST VERSION OF THE PROGRAM -SMOOTHS- AND
**** ****IS FULLY COMPATABLE WITH ANY VERSION OF -SUPER SPECTRUM-.
****
**** THIS PROGRAM READS THE TRANSLATED SPECTRA FROM THE PROGRAM PREPARE
**** LOCATED ON THE FILE TAPE30, SMOOTHES IT WITH A 13-POINT CUBIC,
**** AVERAGES IT, AND CALCULATES DIFFERENCE SPECTRA.  A PUNCHED DECK OF
**** THE RESULTS IS PRODUCED FOR FURTHER WORKING UP OF THE DATA IN
**** OTHER PROGRAMS.  THE TAPE10 FILE IS CARRIED OVER FROM PREPARE AND
**** WILL CONTAIN THE LISTS AND PLOTS OF AV TYPE DATA.  TAPE10 SHOULD
**** BE DISPOSED TO MICROFICHE, AND THE TAPE7 FILE SHOULD BE DISPOSED
**** TO THE PRINTER.
****
**** IPUNPR(N) MEANINGS---
**** (1)=YES, COMPUTE BASELINE SHIFTS; =NO , DISREGARD SH COMMANDS
**** (2)=YES, PUNCH DATA TO BE AVERAGED; =NO , PUNCH RESULTS ONLY
**** (3)=YES, SMOOTH THE DATA; =NO , NO SMOOTHING
****
**** CONTRL(N) MEANINGS---
**** (1) IS MAXIMUM WAVELENGTH IN NM, (2) IS MINIMUM WAVELENGTH IN NM,
**** (3) IS NM PER POINT, (4) IS OD FACTOR, (5) IS E FACTOR, AND (6) IS
**** SCALE (X0.001)
****
**** USE OF AV, ST, SY, MS, SU, AND US COMMANDS---
**** IPUNPR(I) SETTINGS--- 1=YES, 2=NO, 3=YES.
**** CONSIDER THE FOLLOWING SEQUENCE OF SPECTRA---
**** 1001AVNN,1002STNN,1003AVNN,1004SM02, WHERE NN IS ANY TWO LETTERS.
**** IN THIS SEQUENCE, 1001 WILL BE SMOOTHED, LISTED, AND PLOTTED.
**** 1002 WILL ALSO BE SMOOTHED, LISTED, AND PLOTTED; 1001 AND
**** 1002 THEN WILL BE AVERAGED TOGETHER, LISTED, PLOTTED,
**** PUNCHED, AND THE RESULT STORED AS 1002.  1003 AND 1004 WILL BOTH
**** INDIVIDUALLY BE SMOOTHED, ETC.; 1003 AND 1004 THEN WILL BE
**** AVERAGED TOGETHER, ETC., AND THE RESULT STORED AS 1004.  FINALLY,
**** THE DIFFERENCE SPECTRUM (1004-1002)XE/OD WILL BE CALCULATED,
**** LISTED, PLOTTED, PUNCHED, AND STORED AS 1005RSLT.
**** REPLACING SM BY MS WILL CALCULATE, ETC., 1005=(1002-1004)XE/OD
**** REPLACING SM BY SU WILL CALCULATE, ETC., 1005=1004-1002
**** REPLACING SM BY US WILL CALCULATE, ETC., 1005=1002-1004
****
**** DO IT AGAIN COMMANDS---
**** ASSUME LAST OPERATION WAS 1004SM02.
**** D REPEATS PREVIOUS OPERATION.  1004D302 WILL CALCULATE, ETC.,
**** 1007=1004+03=(1004-1002)XE/OD.
**** 1004B302 CALCULATES, ETC., 1007=(1004-1002)XE/OD (SM)
**** 1004C302 CALCULATES, ETC., 1007=(1002-1004)XE/OD (MS)
**** 1004E302 CALCULATES, ETC., 1007=1004-1002        (SU)
**** 1004F302 CALCULATES, ETC., 1007=1002-1004        (US)
****
**** BASELINE SHIFT CORRECTIONS---
**** 1006X250 WILL CORRECT SPECTRUM 1006 FOR A POSSIBLE PARALLEL BASE-
**** LINE SHIFT AT 250 NM AND BELOW BEFORE SMOOTHING AND STORE RESULT
**** IN 1006.  IN FURTHER WORKUP (SMOOTHING, AVERAGING, ETC.) THIS IS
**** TREATED AS AN AV COMMAND.
```

```
C**** 1001AVSH WILL CHECK FOR THE FIRST OCCURRANCE OF THE LARGEST BASE-
C**** LINE SHIFT IN THE FIRST 30 POINTS OF THE 1001 SPECTRUM RAW DATA
C**** AND CORRECT FOR IT THROUGHOUT THE SPECTRUM FROM THAT POINT ON. A
C**** STSH COMBINATION IS ALSO LEGAL.
C****
C**** CONFIDENCE LIMITS AND OTHER STUFF
C**** IF 3 OR MORE SPECTRA ARE AVERAGED TOGETHER, THE 95 PERCENT
C**** CONFIDENCE LIMIT IS RETURNED IN THE LISTING.
C**** UP TO 10 SPECTRA MAY BE AVERAGED TOGETHER AND FIFTY MAY BE STORED
C**** INTERNALLY.  EACH SPECTRUM MAY HAVE UP TO 300 DATA POINTS.
C****
      COMMON/CD/CD(300)
      COMMON/CONSCN/CONTRL(6),SVCTRL(6),NPTS,NPTSSV
      COMMON/PRCONF/PRCONF(300)
      COMMON/R/R(300)
      COMMON/WAVE/WAVE(300)
      COMMON/IDATA/IDATA(300)
      COMMON/ICN/ID2,ID3,ID4,ID5,ID6,ID7,ID8
      COMMON/IPUN/IPUNPR(3)
      REAL CD,CONTRL,PRCONF,R,SVCTRL,WAVE
      INTEGER IDATA,IPUNPR
      DIMENSION T(13),TL(10)
      DIMENSION DIFFER(300),SIGMA(300)
      DIMENSION A(50,300),AVSPCT(10,300),CONFID(50,300)
      INTEGER ID(10),SPCT(50),TOTNUM
      INTEGER AV,MS,SH,SM,ST,SU,US
      INTEGER AVFLG
      DATA AV/2HAV/
      DATA MS/2HMS/
      DATA SH/2HSH/
      DATA SM/2HSM/
      DATA ST/2HST/
      DATA SU/2HSU/
      DATA US/2HUS/
      DATA (TL(I),I=2,10)/12.706,4.303,3.182,2.776,2.571,2.447,2.365,
     $2.306,2.262/
701   FORMAT(3A3)
702   FORMAT(I4,A2,A2,3(F7.2),2(F10.3),F10.6,I3)
703   FORMAT(A1)
704   FORMAT(I4)
705   FORMAT(*1*,I4,* SMOOTH*)
706   FORMAT(*0*,3X,*ID*,6X,*VSTART*,4X,*VEND*,5X,*VINCR*,8X,*OD*,10X,
     $*E*,10X,*SCALE*)
707   FORMAT(* *,I4,A2,A2,2X,3(F7.2,2X),3(F10.3,2X))
708   FORMAT(* *,I4,A2,A2,* CONTAINS SHIFT CORRECTION= *,E10.4)
709   FORMAT(I4,* SMOOTH*)
720   FORMAT(*1*,I4,* IS AVERAGE OF *,10(I4,2X)).
721   FORMAT(I4,* IS AVERAGE OF *,11(I4,1X))
725   FORMAT(I2)
726   FORMAT(A1,11)
731   FORMAT(*1*,I4,* IS EQUAL TO (*,I4,* - *,I4,*)X(E= *,F8.4,
     $*)/(OD= *,F8.4,*)*)
732   FORMAT(I4,* IS EQUAL TO (*,I4,* - *,I4,*)X(E= *,F8.4,*)/(OD= *,
     $F8.4,*)*)
733   FORMAT(*1*,I4,* IS EQUAL TO (*,I4,* - *,I4,*)*)
```

```
734   FORMAT(I4,* IS EQUAL TO (*,I4,* - *,I4,*)*)
742   FORMAT(*1*,////////,*SPECTRUM *,I4,* IS NOT IN LIST*)
C**** INITIALIZE PARAMETERS
C**** NOSPEC=NUMBER OF SPECTRA TO BE AVERAGED BY AV AND SIMILAR CONTROLS
C**** TOTNUM=NUMBER OF RESULTING SPECTRA FROM AVERAGING AND OTHER WORKUP
      TOTNUM=1
      DO 10 I=1,50
        SPCT(I)=0
        DO 10 J=1,300
          CONFID(I,J)=-100.
10    CONTINUE
      REWIND 30
      READ(30,701) IPUNPR
1     NOSPEC=1
      DO 12 I=1,300
        R(I)=0
        DIFFER(I)=0
        SIGMA(I)=0
        PRCONF(I)=-100.
12    CONTINUE
2     ID6=0
      ID8=0
      CRCN=0
      READ(30,702) ID1,ID2,ID3,CONTRL,NPTS
      IF(EOF(30).NE.0) CALL WRAPUP
      DECODE(1,703,ID2) ID5
      IF(ID5.EQ.1HB.OR.ID5.EQ.1HC.OR.ID5.EQ.1HD) GO TO 400
      IF(ID5.EQ.1HE.OR.ID5.EQ.1HF) GO TO 400
      DO 13 I=1,6
        SVCTRL(I)=CONTRL(I)
13    CONTINUE
      NPTSSV=NPTS
      DO 14 I=1,NPTS
        READ(30,704) IDATA(I)
        R(I)=CONTRL(6)*IDATA(I)
14    CONTINUE
      SCALE=CONTRL(6)*1000.0
      IF(ID5.EQ.1HX) CALL SHIFTS (CRCN)
      IF(ID2.EQ.SH.OR.ID3.EQ.SH) ID8=1
      IF(IPUNPR(1).EQ.3HNO .OR.ID3.EQ.2HNB) ID8=0
      IF(ID8.EQ.1) CALL SHIFTS (CRCN)
      NSMTH=1
      IF(IPUNPR(2).EQ.3HNO ) GO TO 18
C**** 13 POINT SMOOTHING ROUTINE
C**** R=UNSMOOTHED DATA, CD=SMOOTHED DATA, T=TEMPORARY STORAGE
      N=NPTS-12
      DO 15 I=2,13
        J=I-1
        T(I)=R(J)
15    CONTINUE
      DO 17 I=1,N
        J=I+12
        DO 16 K=1,12
          KK=K+1
          T(K)=T(KK)
```

```
16        CONTINUE
          T(13)=R(J)
          SUM=25.*T(7)+24.*(T(6)+T(8))+21.*(T(5)+T(9))+16.*(T(4)+T(10))
     $    +9.*(T(3)+T(11))-11.*(T(1)+T(13))
          L=I+6
        CO(L)=SUM/143.
17      CONTINUE
        NSMTH=NPTS-6
18      DO 19 I=1,6
          CO(I)=R(I)
19      CONTINUE
        DO 20 I=NSMTH,300
          CO(I)=R(I)
20      CONTINUE
        IF(ID2.EQ.ST.OR.ID2.EQ.AV) GO TO 21
        IF(ID2.EQ.MS.OR.ID2.EQ.SM) GO TO 21
        IF(ID2.EQ.US.OR.ID2.EQ.SU) GO TO 21
C**** ALL OTHER ID2 COMBINATIONS ARE INVALID
        GO TO 1
C**** SAVE DATA FOR AVERAGING
21      ID(NOSPEC)=ID1
        DO 22 I=1,NPTS
          AVSPCT(NOSPEC,I)=CO(I)
          SIGMA(I)=SIGMA(I)+CO(I)
22      CONTINUE
        IF(ID2.NE.AV) NOSPEC=NOSPEC-1
        NOSPEC=NOSPEC+1
        IF(NOSPEC.EQ.11) GO TO 99
C**** PUT INDIVIDUAL COMPONENTS ON MICROFICHE FILE
        IDEV=10
        WRITE(IDEV,705) ID1
        WRITE(IDEV,706)
        WRITE(IDEV,707) ID1,ID2,ID3,(CONTRL(I),I=1,5),SCALE
        IF(CRCN.NE.0) WRITE(IDEV,708) ID1,ID2,ID3,CRCN
        IF(IPUNPR(2).EQ.3HYES) PUNCH 709,ID1
C**** AVFLG FLAGS AV TYPE DATA FOR PROPER DISPOSAL (TO MICROFICHE)
        AVFLG=1
        CALL LETSEE (ID1,AVFLG)
        IF(ID2.EQ.AV) GO TO 2
C**** COMPUTE AVERAGED SPECTRUM
99      DO 100 I=1,NPTS
          CO(I)=SIGMA(I)/FLOAT(NOSPEC)
100     CONTINUE
        IF(NOSPEC.LT.3) GO TO 103
C**** COMPUTE 95 PERCENT CONFIDENCE LIMITS
        DO 101 J=1,NOSPEC
          DO 101 I=1,NPTS
            DIFFER(I)=(CO(I)-AVSPCT(J,I))**2+DIFFER(I)
101     CONTINUE
        DO 102 I=1,NPTS
          DIFFER(I)=SQRT(DIFFER(I)/(FLOAT(NOSPEC)-1.0))
          PRCONF(I)=TL(NOSPEC)*DIFFER(I)/SQRT(FLOAT(NOSPEC))
102     CONTINUE
103     SPC1(TOTNUM)=ID1
        DO 104 I=1,NPTS
```

```
          A(IOTNUM,I)=CD(I)
          CONFID(IOTNUM,I)=PRCONF(I)
 104    CONTINUE
        IOTNUM=IOTNUM+1
        WRITE(7,720) ID1,(ID(I),I=1,NOSPEC)
        WRITE(7,706)
        WRITE(7,707) ID1,ID2,ID3,(CONTRL(I),I=1,5),SCALE
        IF((IPUNPR(2).EQ.3HYES).AND.(NOSPEC.EQ.1)) PUNCH 721,ID1,
       $(ID(I),I=1,NOSPEC)
C**** AVFLG FLAGS ST TYPE DATA FOR PROPER DISPOSAL (TO PUNCH OR NOT)
        AVFLG=0
        IF(NOSPEC.EQ.1) AVFLG=2
        CALL LETSEE (ID1,AVFLG)
        IF(ID2.EQ.ST) GO TO 1
C**** SM,SU,US,MS HANDLER
 300    DECODE(2,725,ID3) ID4
        ID7=ID2
        ISECID=(100*(ID1/100))+ID4
        ID1P50=ID1+50
        IF(ISECID.GE.ID1P50) ISECID=ISECID-100
        DO 303 NUM=1,IOTNUM
          IF(SPCT(NUM).EQ.ISECID) GO TO 304
 303    CONTINUE
        WRITE(7,742) ISECID
        GO TO 1
 304    IF(PRCONF(5).GE.0.AND.CONFID(NUM,5).GE.0) 305,307
 305    DO 306 I=1,NPTS
          PRCONF(I)=SQRT(PRCONF(I)**2+CONFID(NUM,I)**2)
 306    CONTINUE
 307    CON=1.0
        IF(ID2.EQ.MS.OR.ID2.EQ.US) CON=-1.0
        DO 308 I=1,NPTS
          CD(I)=(CD(I)-A(NUM,I))*CON
 308    CONTINUE
        IF(ID2.EQ.SU.OR.ID2.EQ.US) GO TO 311
        FAC=CONTRL(4)/CONTRL(5)
        IF(PRCONF(5).GE.0.AND.CONFID(NUM,5).GE.0) FAC=1.0
        DO 310 I=1,NPTS
          CD(I)=(CD(I)*CONTRL(5)/CONTRL(4)
          PRCONF(I)=PRCONF(I)*CONTRL(5)/CONTRL(4)*FAC
 310    CONTINUE
 311    IDOLD=ID1
        ID1=ID1+1+ID6
        IF(ID2.EQ.SU.OR.ID2.EQ.US) GO TO 314
        IF(ID2.EQ.MS) GO TO 313
        IF(ID2.NE.SM) GO TO 1
        WRITE(7,731) ID1,IDOLD,ISECID,CONTRL(5),CONTRL(4)
        PUNCH 732,ID1,IDOLD,ISECID,CONTRL(5),CONTRL(4)
        GO TO 316
 313    WRITE(7,731) ID1,ISECID,IDOLD,CONTRL(5),CONTRL(4)
        PUNCH 732,ID1,ISECID,IDOLD,CONTRL(5),CONTRL(4)
        GO TO 316
 314    IF(ID2.EQ.US) GO TO 315
        WRITE(7,733) ID1,IDOLD,ISECID
        PUNCH 734,ID1,IDOLD,ISECID
```

```
      GO TO 316
315   WRITE(7,723) ID1,ISECID,IDOLD
      PUNCH 734,ID1,ISECID,IDOLD
316   WRITE(7,706)
      ID2=2HRS
      ID3=2HLT
      WRITE(7,707) ID1,ID2,ID3,(CONTRL(I),I=1,5),SCALE
      SPCT(TOTNUM)=ID1
      DO 317 I=1,NPTS
        A(TOTNUM,I)=CD(I)
        CONFID(TOTNUM,I)=PRCONF(I)
317   CONTINUE
      TOTNUM=TOTNUM+1
C**** AVFLG FLAGS RESULTANT DATA FOR PROPER DISPOSAL (TO PRINTER)
      AVFLG=0
      CALL LETSEE (ID1,AVFLG)
      GO TO 1
C*********************************************************************
C**** DO IT AGAIN OPTION
400   DECODE(2,726,ID2) ID5,ID6
      IF(CONTRL(1).EQ.SVCTRL(I)) GO TO 403
      DO 402 I=1,6
        CONTRL(I)=SVCTRL(I)
402   CONTINUE
      NPTS=NPTSSV
403   ID2=ID7
      IF(ID5.EQ.1HB) ID2=SM
      IF(ID5.EQ.1HC) ID2=MS
      IF(ID5.EQ.1HE) ID2=SU
      IF(ID5.EQ.1HF) ID2=US
      DO 404 I=1,NPTS
        READ(30,704) KILLPT
404   CONTINUE
      ID6=ID6-1
      DO 405 NUM=1,TOTNUM
        IF(SPCT(NUM).EQ.ID1) GO TO 406
405   CONTINUE
      WRITE(7,742) ID1
      GO TO 1
406   DO 407 I=1,NPTS
        CD(I)=A(NUM,I)
        PRCONF(I)=CONFID(NUM,I)
407   CONTINUE
      GO TO 300
      END
```

```
      SUBROUTINE LETSEE (ID1,AVFLG)
C**** PRINT/PLOT/IPUNCH DATA
      COMMON/CD/CD(300)
      COMMON/CONSCN/CONTRL(6),SVCTRL(6),NPTS,NPTSSV
      COMMON/PRCONF/PRCONF(300)
      COMMON/WAVE/WAVE(300)
      COMMON/ID1/ID2,ID3,ID4,ID5,ID6,ID7,ID8
      COMMON/IPUN/IPUNPR(3)
      REAL CD,CONTRL,PRCONF,SVCTRL,WAVE
      INTEGER AVFLG,IPUNPR
708   FORMAT(*0*,3(15X,*LAMBDA*,5X,*READING*,2X),/)
709   FORMAT(3(15X,F6.1,3X,F11.4))
710   FORMAT(*0*,15X,3(*LAMBDA*,5X,*READING*,5X,*INTERVAL*,3X),/)
711   FORMAT(15X,3(F6.1,3X,F11.4,3X,F8.6,3X))
712   FORMAT(*1*,I4,* SMOOTH*)
713   FORMAT(I4,A2,A2,2X,4(F8.3,2X),E13.6,2X,E13.6,1X,I1)
714   FORMAT(10F8.4)
715   FORMAT(10F8.3)
716   FORMAT(*END OF *,I4,* SMOOTHS DECK*)
      IF(AVFLG.EQ.2) IDEV=7
      IF(AVFLG.EQ.1) IDEV=10
      IF(AVFLG.EQ.0) IDEV=7
      DO 70 I=1,NPTS
        WAVE(I)=CONTRL(1)-FLOAT(I-1)*CONTRL(3)
70    CONTINUE
      II=NPTS/2+1
      IF(PRCONF(5).GE.0) GO TO 72
      WRITE(IDEV,708)
      DO 71 I=1,II
        J=I+II
        K=J+II
        WRITE(IDEV,709) WAVE(I),CD(I),WAVE(J),CD(J),WAVE(K),CD(K)
71    CONTINUE
      GO TO 74
72    WRITE(IDEV,710)
      DO 73 I=1,II
        J=I+II
        K=J+II
        WRITE(IDEV,711) WAVE(I),CD(I),PRCONF(I),WAVE(J),CD(J),PRCONF(J),
     $  WAVE(K),CD(K),PRCONF(K)
73    CONTINUE
74    WRITE(IDEV,712) ID1
      XMAX=CONTRL(1)
      XINC=(CONTRL(1)-CONTRL(2))/100.0
      TWICE=XINC/0.5
      M=TWICE
      IF(M.NE.TWICE) XINC=0.5*(M+1)
      ISY=1
      CALL PRNPLT (WAVE(1),CD(1),XMAX,XINC,YMAX,YINC,0,ISY,NPTS,IDEV)
      IF(IPUNPR(2).EQ.3HNO .AND.AVFLG.EQ.1) RETURN
      IF(IPUNPR(2).EQ.3HNO .AND.AVFLG.EQ.2) RETURN
      DO 75 I=1,NPTS
        IF(CD(I).LT.-99.0.OR.CD(I).GT.999.0) IFORMT=1
75    CONTINUE
      IF(IFORMT.NE.1) IFORMT=0
      CONTRO=CONTRL(3)*10.0
      SCALE=CONTRL(6)*1000.0
      PUNCH 713,ID1,ID2,ID3,(CONTRL(I),I=1,2),CONTRO,SCALE,(CONTRL(J),
     $J=4,5),IFORMT
      IF(IFORMT.EQ.1) GO TO 76
      PUNCH 714,(CD(I),I=1,NPTS)
      GO TO 77
76    PUNCH 715,(CD(I),I=1,NPTS)
77    PUNCH 716,ID1
      RETURN
      END
```

```
      SUBROUTINE SHIFTS (CRCN)
C**** BASELINE SHIFT CALCULATIONS AND CORRECTIONS
      COMMON/CD/CD(300)
      COMMON/CONSCN/CONTRL(6),SVCTRL(6),NPTS,NPTSSV
      COMMON/R/R(300)
      COMMON/ICN/ID2,ID3,ID4,ID5,ID6,ID7,ID8
      REAL CD,CONTRL,R,SVCTRL
750   FORMAT(I2)
751   FORMAT(A1,I1)
      IF(ID8.EQ.1) GO TO 205
C**** X(WAVELENGTH) HANDLER
      DECODE(2,750,ID3) ID4
      DECODE(2,751,ID2) ID5,ID6
      SWAVE=100*ID6+ID4
      I=1+(CONTRL(1)-SWAVE)/CONTRL(3)
      DIFF=R(I-1)-R(I)+R(I-1)-R(I-2)
      DO 200 J=I,NPTS
        R(J)=R(J)+DIFF
200   CONTINUE
      ID2=2HAV
      ID6=0
      CRCN=DIFF
      RETURN
C**** SH HANDLER
205   CRCN=0
      NPNT=3
      DO 206 I=3,30
        DIFF=R(I-1)-R(I)+R(I-1)-R(I-2)
        IF(ABS(DIFF).LE.ABS(CRCN)) GO TO 206
        CRCN=DIFF
        NPNT=I
206   CONTINUE
      IF(CRCN.EQ.0) RETURN
      DO 207 J=NPNT,NPTS
        R(J)=R(J)+CRCN
207   CONTINUE
      IF(ID2.EQ.2HSH) ID2=2HAV
      RETURN
      END
```

```
      SUBROUTINE WRAPUP
C**** CLOSE UP SHOP
      ENDFILE 10
      REWIND 10
      ENDFILE 7
      REWIND 7
      CALL EXIT
      END
```

4. Program PROCESS

A) Operation

i) Input

The punched deck from SMOOTHS (see note, below).

ii) Output

The file OUTPUT contains listings and plots of all spectra resulting from the manipulations governed by the variable OPTION.

The file TAPE17 contains resultant files for which NEWID was blank or zero. It may be recovered with DISPOSE, but is usually deleted.

The file TAPE7 contains resultant files for which NEWID was non-zero, It is usually saved, either by DISPOSE to the punch or by storage on GSS or PSS.

iii) Errors

The order of spectra is not important, but a spectrum required in a manipulation must either be read in as input or created prior to the request for all necessary spectra. If the spectrum is not present, an error message is left and the next control card is read.

NOTE: NON-FATAL ERROR

In all options but LOOK, MULT, DIFF, PSCD, and EMCD, the quantity CONTRL(5)/CONTRL(6) (i.e. OD/E from Super Spectrum) is first multiplied with the data points in each spectrum before the remainder of the algebra is performed. It is vital that all required spectra are put on the right basis (e.g. equal path lengths for the FDCD, CD, and absorbance spectra in the FDCD option) prior to starting a maneuver.

Example:

Spectrum Type	Path length	OD or CONTRL(5)	E or CONTRL(6)
FDCD	2 mm	1 → 1	500 → 100
CD	3 mm	3 → 1	1000 → 100
absorbance	1 cm	1 → 1	100 → 100

where the number to the left of the arrow represents the value of the constant up through the punching of the data deck by SMOOTHS and the number to the right of the arrow represents the value of the constant as changed to normalize the spectra to one path length before running in PROCESS.

B) Listing

i) Program PROCESS

ii) Subroutine WRAPUP

iii) Subroutine SEARCH

iv) Subroutine DOMATH

v) Subroutine TITLES

vi) Subroutine SEEIT

vii) Subroutine PRNPLT and Subroutine PLSCAL (see PREPARE)

```
      PROGRAM PROCESS (INPUT,OUTPUT,TAPE7,TAPE17)
C
C     THIS PROGRAM PERFORMS AN ALGEBRAIC ADDITION OF UP TO FIVE SPECTRA.
C     INPUT OF DATA AND COMMANDS IS THROUGH PUNCHED CARDS.  OUTPUT OF
C     RESULTS IS EITHER THROUGH PUNCHED CARDS OR TO PSS OR TAPE, BOTH
C     OF WHICH ARE PERFORMED VIA A DISPOSE OF TAPE7.
C
C     THE PUNCHED DECK FROM SMOOTH PROGRAM IS READ IN FIRST, FOLLOWED
C     BY A CARD WITH STOP IN FOUR LEFT COLUMNS.
C
C     ALGEBRAIC MANIPULATION CONTROL DECK
C
C       GENERAL DECK ORDER IS LABEL CARD, CONTROL CARD, LABEL CARD,
C       CONTROL CARD, ETC..., HOWEVER, IF A DELTA EPSILON CALCULATION
C       IS PERFORMED WITH FDCD, PSCD, OR EMCD, A CARD WITH THE PATH
C       LENGTH (B) AND THE CONCENTRATION (CONC) MUST FOLLOW THE CONTROL
C       CARD (FORMAT IS F8.4, E14.6).
C       LABEL CARD HAS LABEL(SPACE) IN FIRST 6 COLUMNS, FOLLOWED BY ANY
C       PARTICULAR ALPHANUMERIC STRING TO BE PRINTED AT THE TOP OF EACH
C       LISTING AND PLOT.
C       CONTROL CARD FORMAT IS 6(F8.4,I4),A4,I4.
C       C(1) IS IN FIRST F8.4. C(2) IS IN SECOND F8.4.
C       SPECT(N) IS IN NTH I4 (UP TO 6).
C       A4 IS OPTION AND I4 IS NEWID (IF DESIRED).
C     OPTIONS
C       (N) IS SPECT(N)TH SPECTRUM.
C       LOOK - WRITES AND PLOTS SPECTRUM ONLY.
C       MULT - MULTIPLIES SPECT(1) BY C(1) OR DIVIDES SPECT(1) BY C(2)
C       OR MULTIPLIES SPECT(1) BY (C(1)/C(2)), DEPENDING UPON WHICH
C       NUMBER(S) ARE NONZERO.
C       DIFF - CALCULATES SPECT(1) + (C(1)/C(2))*SPECT(2).
C       FLEX - CALCULATES AN EXCITATION PROFILE CORRECTED FOR PRE-SLIT
C       ABSORPTION FROM EXCITATION PROFILE(1), ABS(2), PATHLENGTH TO
C       SLIT IN CM(C(1)), AND PATHLENGTH OF ABS SPECTRUM IN CM(C(2)).
C       QUAN - CALCULATES A QUANTITY PROPORTIONAL TO THE QUANTUM YIELD
C       FROM THE QUANTITIES USED IN FLEX, PLUS THE SLIT WIDTH IN
C       CM(C(3)).  SEE FREDERICQ AND HOUSSIER, BIOPOLYMERS 11, 2281-
C       2298 (1972) FOR EQUATIONS.
C       NORM - NORMALIZES SPECT(1) TO SPECT(2) AT A WAVELENGTH C(1) IN
C       NM.
C       RATO - COMPUTES SPECT(1)/SPECT(2) RATIO.
C       FDCD - CALCULATES FLUOROPHORE ANISOTROPY FROM (1)FDCD, (2)CD,
C       AND (3)ABS.  FLUOROPHORE DELTA EPSILON IS CALCULATED WITH (4)ABS
C       FLUOROPHORE, IN ADDITION TO OTHERS.  A COMPONENT ANALYSIS IS
C       PROVIDED FOR ANISOTROPY CALCULATIONS ONLY, AND PRODUCES A LIST
C       OF THAT PORTION OF THE ANISOTROPY DERIVED FROM THE FDCD SIGNAL
C       AND THAT PORTION DUE TO THE CD SIGNAL.
C       PSCD - CALCULATES AVERAGE FLUOROPHORE ANISOTROPY FROM FDCD
C       ANISOTROPIES (1)WITHOUT POLARIZER, (2)WITH POLARIZATION PLANE
C       VERTICAL, AND (3)WITH POLARIZATION PLANE HORIZONTAL.  AVERAGE
C       FLUOROPHORE DELTA EPSILON IS CALCULATED WITH (4)ABS FLUOROPHORE
C       IN ADDITION TO THE OTHERS.
C       EMCD - CALCULATES FLUOROPHORE ANISOTROPY IN 33 DIRECTION FROM
C       FDCD ANISOTROPIES IN THE SAME ORDER AS IN PSCD.  FLUOROPHORE
C       DELTA EPSILON IN 33 DIRECTION IS CALCULATED FROM ABSORPTION AND
```

```
C         FDCD MEASUREMENTS IN THE SAME ORDER AS IN PSCD, ALSO.
C         NRCD - CALCULATES TOTAL ANISOTROPY FROM (2)CD AND (3)ABS.
C         SCCD - CALCULATES SCATTERER DELTA EPSILON FROM (1)FDCD AND
C         (3)ABS.
C       NEWID
C         IF NEWID IS BLANK OR 0000 OR LESS THAN -1000, THE RESULTING
C         SPECTRUM IS NOT STORED INTERNALLY.  IF NEWID IS BETWEEN -1 AND
C         -999, THE ID IS **TEMPORARY** AND IS NOT LOGGED IN THE LAB
C         RECORD SO IT MAY BE USED AGAIN (BUT NOT IN THE SAME RUN THROUGH
C         PROCESS).  IN ALL CASES NOT COVERED UNDER THE FIRST SENTENCE,
C         THE SPECTRUM IS STORED INTERNALLY.  UP TO 100 SPECTRA MAY BE
C         STORED IN ONE RUN (300 POINTS EACH).
C
C       A LABEL CARD THAT IS BLANK OR ONE THAT HAS STOP   IN THE FIRST
C       SIX COLUMNS WILL HALT THE PROGRAM.
C
        COMMON/A/A(100,300)
        COMMON/CD/CD(300),FPRT(300),CPRT(300)
        COMMON/CONTRL/CONTRL(100,6)
        COMMON/CSPINL/C(5),SPECT(5),INDEX(5),LBL(13)
        COMMON/ID/ID(100)
        COMMON/PARAM/NPTS,NUM,NEWID,OPTION,TOTNUM,WVEMAX,WVEMIN
        REAL A,CD,CONTRL,C,WVEMAX,WVEMIN
        INTEGER ID,INDEX,LBL,SPECT,TOTNUM
        INTEGER IHEAD(12)
600     FORMAT(*1*,*THE FOLLOWING SPECTRA WERE READ INTO MEMORY*,//,
       $4X,*ID*,6X,*VSTART*,4X,*VEND*,5X,*VINCR*,
       $7X,*SCALE*,8X,*CD*,10X,*E*,/)
601     FORMAT(* *,I4,A2,A2,2X,3(F7.2,2X),3(F10.3,2X))
602     FORMAT(*0*,I4,* SPECTRA READ INTO MEMORY*)
604     FORMAT(*1*,12A6)
700     FORMAT(12A6)
701     FORMAT(I4,A2,A2,2X,4(F8.3,2X),E13.6,2X,E13.6,1X,I1)
702     FORMAT(10F8.4)
703     FORMAT(10F8.3)
704     FORMAT(10F8.2)
705     FORMAT(1HX,23X)
706     FORMAT(5(E10.4,I4),2X,A4,I4)
C
C       READ SPECTRA INTO MEMORY
C       TOTNUM IS THE TOTAL NUMBER OF SPECTRA READ IN
C
        REWIND 7
```

```
      PRINT 600
      DO 5 M=1,100
        READ 700,IHEAD
        IF(IHEAD(1).EQ.6HSTOP  ) GO TO 6
        READ 701,ID(M),ID2,ID3,(CONTRL(M,ML),ML=1,6),IFORMT
        NPTS=(CONTRL(M,1)-CONTRL(M,2))/(CONTRL(M,3)/10.)
        IF(ID(M).EQ.ID(M-1)) ID(M-1)=0
        PRINT 601,ID(M),ID2,ID3,(CONTRL(M,ML),ML=1,6)
        IF=IFORMT-1
        IF(IF) 1,2,3
1       READ 702,(A(M,I),I=1,NPTS)
        GO TO 4
2       READ 703,(A(M,I),I=1,NPTS)
        GO TO 4
3       READ 704,(A(M,I),I=1,NPTS)
4       READ 705
5     CONTINUE
6     TOTNUM=M-1
      PRINT 602,TOTNUM
7     DO 8 ICLR=1,300
        CD(ICLR)=0
        FPRT(ICLR)=0
        CPRT(ICLR)=0
8     CONTINUE
      WVEMIN=0.0
      WVEMAX=1000.0
      READ 700,LBL
      IF(LBL(1).EQ.6HSTOP  .OR.LBL(1).NE.6HLABEL ) CALL WRAPUP
      PRINT 604,(LBL(NN),NN=2,13)
      READ 706,((C(KI),SPECT(KI)),KI=1,5),OPTION,NEWID
      NOTIN=0
      CALL SEARCH (NOTIN)
      IF(NOTIN.NE.0) GO TO 7
      CALL DOMATH
      CALL SEEIT
      GO TO 7
      END
```

```
      SUBROUTINE WRAPUP
C     CLOSE FILE AND EXIT
      ENDFILE 7
      REWIND 7
      ENDFILE 17
      REWIND 17
      CALL EXIT
      END


      SUBROUTINE SEARCH (NOTIN)
      COMMON/CONTRL/CONTRL(100,6)
      COMMON/CSPINL/C(5),SPECT(5),INDEX(5),LBL(13)
      COMMON/ID/ID(100)
      COMMON/PARAM/NPTS,NUM,NEWID,OPTION,TOTNUM,WVEMAX,WVEMIN
      REAL CONTRL,C,WVEMAX,WVEMIN
      INTEGER ID,INDEX,LBL,SPECT,TOTNUM
603   FORMAT(* *,/////,* SPECTRUM *,I4,* IS NOT IN MEMORY*)
      DO 100 I=1,5
        INDEX(I)=1
100   CONTINUE
      ILO=1
      IHI=2
      IF(OPTION.EQ.4HLCOR) IHI=1
      IF(OPTION.EQ.4HNRCD) ILO=2
      IF(OPTION.EQ.4HMULT) IHI=1
      IF(OPTION.EQ.4HNRCD.OR.OPTION.EQ.4HSCCD) IHI=3
      IF(OPTION.EQ.4HFDCD.OR.OPTION.EQ.4HPSCD.OR.OPTION.EQ.4HEMCD) IHI=4
      DO 104 I=ILO,IHI
        IF(I.EQ.2.AND.OPTION.EQ.4HSCCD) GO TO 104
        IF(I.EQ.4.AND.SPECT(I).EQ.0000) GO TO 105
        IF(SPECT(I).EQ.0000.OR.SPECT(I).LT.-999) GO TO 102
        DO 101 N=1,TOTNUM
          IF(SPECT(I).EQ.ID(N)) GO TO 103
101     CONTINUE
102     PRINT 603,SPECT(I)
        NOTIN=1
        RETURN
103     INDEX(I)=N
104   CONTINUE
105   NUM=INDEX(ILO)
      NPTS=(CONTRL(NUM,1)-CONTRL(NUM,2))/(CONTRL(NUM,3)/10.)
      IF(WVEMAX.GT.CONTRL(NUM,1)) WVEMAX=CONTRL(NUM,1)
      IF(WVEMIN.LT.CONTRL(NUM,2)) WVEMIN=CONTRL(NUM,2)
      RETURN
      END
```

```
      SUBROUTINE DOMATH
      COMMON/A/A(100,300)
      COMMON/CD/CD(300),FPRT(300),CPRT(300)
      COMMON/CONTRL/CONTRL(10),6)
      COMMON/CSPINL/C(5),SPECT(5),INDEX(5),LBL(13)
      COMMON/ID/ID(100)
      COMMON/PARAM/NPTS,NUM,NEWID,OPTION,TOTNUM,WVEMAX,WVEMIN
      REAL A,CD,CONTRL,C,WVEMAX,WVEMIN
      INTEGER ID,INDEX,LBL,SPECT,TOTNUM
707   FORMAT(F8.4,E14.6)
C
C     ASSIGN INDICES AND SELECT PROPER OPTION
C
      J=INDEX(1)
      K=INDEX(2)
      L=INDEX(3)
      M=INDEX(4)
      IF(OPTION.EQ.4HLOOK) GO TO 15
      IF(OPTION.EQ.4HMULT) GO TO 20
      IF(OPTION.EQ.4HDIFF) GO TO 25
      IF(OPTION.EQ.4HFLEX) GO TO 30
      IF(OPTION.EQ.4HQUAN) GO TO 30
      IF(OPTION.EQ.4HNORM) GO TO 33
      IF(OPTION.EQ.4HRATO) GO TO 35
      IF(OPTION.EQ.4HFOCD) GO TO 40
      IF(OPTION.EQ.4HPSCD) GO TO 40
      IF(OPTION.EQ.4HEMCD) GO TO 40
      IF(OPTION.EQ.4HNRCD) GO TO 55
      IF(OPTION.EQ.4HSCCD) GO TO 60
      RETURN
C
C      WRITE OUT AND PLOT SPECTRUM
C
15    DO 17 I=1,NPTS
        CD(I)=A(J,I)
17    CONTINUE
C
C     MULTIPLY/DIVIDE SPECTRUM BY CONSTANT(S)
C
20    IF(C(1).EQ.0) C(1)=1.0
      IF(C(2).EQ.0) C(2)=1.0
      DO 22 I=1,NPTS
        CD(I)=(C(1)/C(2))*A(J,I)
22    CONTINUE
      GO TO 64
C
C     ADD/SUBTRACT TWO SPECTRA
C
25    IF(C(1).EQ.0) C(1)=1.0
      IF(C(2).EQ.0) C(2)=1.0
      DO 26 I=1,NPTS
        CD(I)=A(J,I)+(C(1)/C(2))*A(K,I)
26    CONTINUE
      GO TO 64
C
```

```
C       COMPUTE FLUORESCENCE EXCITATION PROFILES OR QUANTUM YIELDS
C
30      IF(C(2).EQ.0) C(2)=1.0
        DO 31 I=1,NPTS
          JJ=CONTRL(J,1)-WVEMAX+I
          KK=CONTRL(K,1)-WVEMAX+I
          AK=A(K,KK)*CONTRL(K,5)/CONTRL(K,6)
          ABSCM=AK/C(2)
          FCORR=10.0**(ABSCM*C(1))
          EXP=-ABSCM*C(3)
          SLIT=(1.0-10.0**EXP)
          IF(OPTION.EQ.4HFLEX) SLIT=1.0
          CO(I)=A(J,JJ)*(CONTRL(J,5)/CONTRL(J,6))*(FCORR/SLIT)
31      CONTINUE
        GO TO 64
C
C       NORMALIZE SPECT(1) TO SPECT(2) AT WAVELENGTH C(1)
C
33      NWAVE=((CONTRL(J,1)-C(1))/(CONTRL(J,3)/10.))+1
        IF(A(J,NWAVE).EQ.0) RETURN
        DNORM=(A(K,NWAVE)*CONTRL(K,5)/CONTRL(K,6))/(A(J,NWAVE)*CONTRL(J,5)
       $/CONTRL(J,6))
        DO 34 I=1,NPTS
          JJ=CONTRL(J,1)-WVEMAX+I
          CO(I)=DNORM*A(J,JJ)*(CONTRL(J,5)/CONTRL(J,6))
34      CONTINUE
        GO TO 64
C
C       COMPUTE RATIO OF TWO SPECTRA
C
35      DO 36 I=1,NPTS
          JJ=CONTRL(J,1)-WVEMAX+I
          KK=CONTRL(K,1)-WVEMAX+I
          AJ=A(J,JJ)*CONTRL(J,5)/CONTRL(J,6)
          AK=A(K,KK)*CONTRL(K,5)/CONTRL(K,6)
          IF(AK.EQ.0) AK=0.001
          CO(I)=AJ/AK
36      CONTINUE
        GO TO 64
C
C       GET DATA FOR FDCD, PSCD, AND EMCD
C
40      DO 50 I=1,NPTS
          JJ=CONTRL(J,1)-WVEMAX+I
          KK=CONTRL(K,1)-WVEMAX+I
          LL=CONTRL(L,1)-WVEMAX+I
          S1=A(J,JJ)
          S2=A(K,KK)
          S3=A(L,LL)
          IF(OPTION.EQ.4HPSCD) GO TO 48
          IF(OPTION.EQ.4HEMCD) GO TO 49
          IF(OPTION.NE.4HFDCD) RETURN
C
C       COMPUTE FLUORPHORE ANISOTROPY
C
```

```
      IF(A(L,LL).LT.0.00001) GO TO 46
      AK=A(K,KK)*CONTRL(K,5)/CONTRL(K,6)
      AL=A(L,LL)*CONTRL(L,5)/CONTRL(L,6)
      DELADA=AK/(2.0*32.98*AL)
      EXPA=10.0**(-AL)
      DELAEA=2.303*AK*EXPA/(2.0*32.98*(1.0-EXPA))
      GO TO 47
46    DELADA=0.0
      DELAEA=0.0
47    AJ=A(J,JJ)*CONTRL(J,5)/CONTRL(J,6)
      CDC=DELADA-(AJ/28.65)-DELAEA
      CD(I)=2000.0*CDC
      FPRT(I)=-2000.0*AJ/28.65
      CPRT(I)=2000.0*(DELADA-DELAEA)
      GO TO 50
C
C     COMPUTE AVERAGE FLUOROPHORE ANISOTROPY
C
48    CD(I)=(2.0*S2*S1-S3*S1-S2*S3)/(S2-2.0*S3+S1)
      GO TO 50
C
C     COMPUTE FLUOROPHORE ANISOTROPY IN 33 DIRECTION
C
49    CD(I)=(3.0*S2*S3-2.0*S1*S3-S1*S2)/(S2-2.0*S3+S1)
50    CONTINUE
C
C     COMPUTE DELTA EPSILON FOR FDCD, PSCD, AND EMCD
C
      IF(SPECT(4).EQ.0000) GO TO 64
      READ 707,B,CONC
      DO 51 I=1,NPTS
        MM=CONTRL(M,1)-WVEMAX+I
        AM=A(M,MM)*CONTRL(M,5)/CONTRL(M,6)
        CD(I)=CD(I)*AM/(1000.0*B*CONC)
51    CONTINUE
      GO TO 64
C
C     COMPUTE TOTAL ANISOTROPY
C
55    J=INDEX(2)
      DO 58 I=1,NPTS
        KK=CONTRL(K,1)-WVEMAX+I
        LL=CONTRL(L,1)-WVEMAX+I
        IF(A(L,LL).GE.0.00001) GO TO 57
        CD(I)=0
        GO TO 58
57      AK=A(K,KK)*CONTRL(K,5)/CONTRL(K,6)
        AL=A(L,LL)*CONTRL(L,5)/CONTRL(L,6)
        CDC=AK/(32.98*AL)
        CD(I)=1000.0*CDC
58    CONTINUE
      GO TO 64
C
C     COMPUTE DELTA EPSILON OF SCATTERER
C
60    DO 63 I=1,NPTS
        JJ=CONTRL(J,1)-WVEMAX+I
        LL=CONTRL(L,1)-WVEMAX+I
        IF(A(L,LL).GE.0.00001) GO TO 62
        CD(I)=0
        GO TO 63
62      AJ=A(J,JJ)*CONTRL(J,5)/CONTRL(J,6)
        AL=A(L,LL)*CONTRL(L,5)/CONTRL(L,6)
        EXPAB=10.0**AL
        CDC=AL*(EXPAB-1.0)*AJ/(14.325*((EXPAB-1.0)-2.303*AL))
        CD(I)=CDC
63    CONTINUE
64    CALL TITLES (J,K,L,M)
      RETURN
      END
```

```
      SUBROUTINE TITLES (J,K,L,M)
      COMMON/A/A(100,300)
      COMMON/CD/CD(300),FPRT(300),CPRT(300)
      COMMON/CONTRL/CONTRL(100,6)
      COMMON/CSPINL/C(5),SPECT(5),INDEX(5),LBL(13)
      COMMON/ID/ID(100)
      COMMON/PARAM/NPTS,NUM,NEWID,OPTION,TOTNUM,WVEMAX,WVEMIN
      REAL A,CD,CONTRL,C,WVEMAX,WVEMIN
      INTEGER ID,INDEX,LBL,SPECT,TOTNUM
625   FORMAT(* *,I4,* IS *,I4,* X (*,E10.4,*/*,E10.4,*)*)
630   FORMAT(* *,I4,* IS *,I4,* + ( *,E10.4,* / *,E10.4,* ) X *,I4)
650   FORMAT(* *,I4,* IS FLUOROPHORE ANISOTROPY(X1000) FROM FDCD= *,I4,
     $*, CD= *,I4,*, AND ABS= *,I4)
651   FORMAT(* *,I4,* IS AVERAGE FLUOROPHORE ANISOTROPY(X1000) FROM ANIS
     $OTROPY= *,I4,*, PHI=0 ANISOTROPY= *,I4,*, AND PHI=90 ANISOTROPY= *
     $,I4)
652   FORMAT(* *,I4,* IS FLUOROPHORE ANISOTROPY ALONG 33 DIRECTION(X1000
     $) FROM ANISOTROPY= *,I4,*, PHI=0 ANISOTROPY= *,I4,*, AND PHI=90 AN
     $ISOTROPY= *,I4)
653   FORMAT(* *I4,* IS FLUOROPHORE DELTA EPSILON FROM FDCD= *,I4,
     $*, CD= *,I4,*, ABS= *,I4,*, AND ABSF= *,I4)
654   FORMAT(* *,I4,* IS AVERAGE FLUOROPHORE DELTA EPSILON FROM ANISOTRO
     $PY  *,I4,*, PHI=0 ANISOTROPY= *,I4,*, PHI=90 ANISOTROPY= *,I4,
     $*, AND ABSF= *,I4)
655   FORMAT(* *,I4,* IS FLUOROPHORE DELTA EPSILON IN 33 DIRECTION FROM
     $ANISOTROPY= *,I4,*, PHI=0 ANISOTROPY= *,I4,*, PHI=90 ANISOTROPY= *
     $,I4,*,*,/,* AND ABSF= *,I4)
656   FORMAT(* *,I4,* IS TOTAL ANISOTROPY (X1000) FROM CD= *,I4,
     $* AND ABS= *,I4)
657   FORMAT(* *,I4,* IS SCATTERER DELTA EPSILON FROM FDCD= *,I4,
     $* AND ABS= *,I4)
660   FORMAT(* *,I4,* IS CORRECTED FLUORESCENCE EXCITATION PROFILE OF *,
     $I4,* USING *,I4,*, PRE-SLIT PATH *,F8.4,* CM*)
661   FORMAT(* *,I4,* IS PROPORTIONAL TO QUANTUM YIELD OF *,I4,* USING *
     $,I4,*, PRE-SLIT PATH *,F8.4,* CM, SLIT WIDTH *,F8.4,* CM*)
662   FORMAT(* *,I4,* IS *,I4,* NORMALIZED TO *,I4,* AT *,F8.4,* NM*)
663   FORMAT(* *,I4,* IS *,I4,* / *,I4)
664   FORMAT(* *,I4,* LISTING*)
680   FORMAT(*+*,*THIS*)
681   FORMAT(* *,I4,* IS A TEMPORARY, REUSABLE FILE NUMBER*)
825   FORMAT(I4,* IS *,I4,* X (*,E10.4,*/*,E10.4,*)*)
830   FORMAT(I4,* IS *,I4,* + ( *,E10.4,* / *,E10.4,* ) X *,I4)
850   FORMAT(I4,* IS FL ANISO (X1000) FROM FDCD= *,I4,*, CD= *,I4,
     $*, AND ABS= *,I4)
851   FORMAT(I4,* IS AVG FL ANISO (X1000) FROM FA= *,I4,*, PHI0= *,I4,
     $*, AND PHI90= *,I4)
852   FORMAT(I4,* IS FL ANISO 33 (X1000) FROM FA= *,I4,*, PHI0= *,I4,
     $*, AND PHI90= *,I4)
853   FORMAT(I4,* IS FL DEL EPS FROM FDCD= *,I4,*, CD= *,I4,
     $*, ABS= *,I4,*, AND ABSF= *,I4)
854   FORMAT(I4,* IS AVG FL DEL EPS FROM FA= *,I4,*, PHI0= *,I4,
     $*, PHI90= *,I4,*, AND ABSF= *,I4)
855   FORMAT(I4,* IS FL DEL EPS 33 FROM FA= *,I4,*, PHI0= *,I4,
     $*, PHI90= *,I4,*, AND ABSF= *,I4)
856   FORMAT(I4,* IS TOTAL ANISOTROPY(X1000) FROM CD= *,I4,* AND ABS= *,
```

```
      $I4)
857   FORMAT(I4,* IS SCATTERER DELTA EPSILON FROM FOCD= *,I4,
      $* AND ABS= *,I4)
860   FORMAT(I4,* IS CORR FL EX PROFILE OF *,I4,* USING *,I4,*, PRE-SLIT
      $ PATH *,F8.4,* CM*)
861   FORMAT(I4,* IS QUANTUM YIELD OF *,I4,* USING *,I4,*, P-S CM *,
      $F8.4,*, SLIT CM*,F8.4)
862   FORMAT(I4,* IS *,I4,* NORMALIZED TO *,I4,* AT *,F8.4,* NM*)
863   FORMAT(I4,* IS *,I4,* / *,I4)
864   FORMAT(I4,* LISTING*)
C
C     STORE RESULTS IF DESIRED
C
      IDEV=7
      IF(NEWID.GT.0000) GO TO 300
      IF(NEWID.LT.-999.OR.NEWID.EQ.0000) GO TO 299
      PRINT 681,NEWID
      GO TO 300
299   NEWID=0
      IF(OPTION.EQ.4HLOOK) GO TO 303
      PRINT 680
      GO TO 303
300   TOTNUM=TOTNUM+1
      ID(TOTNUM)=NEWID
      CONTRL(TOTNUM,1)=WVEMAX
      CONTRL(TOTNUM,2)=WVEMIN
      DO 301 I=3,6
        CONTRL(TOTNUM,I)=CONTRL(NUM,I)
301   CONTINUE
      NPTS=(CONTRL(TOTNUM,1)-CONTRL(TOTNUM,2))/(CONTRL(TOTNUM,3)/10.)
      DO 302 I=1,NPTS
        A(TOTNUM,I)=CD(I)
302   CONTINUE
      NUM=TOTNUM
C
C     PRINT, PUNCH TITLES
C     TAPE17 IS THE ''DEAD LETTER FILE'' FOR UNIDENTIFIED SPECTRA
C
303   IF(NEWID.EQ.0) IDEV=17
      IF(OPTION.EQ.4HMULT) GO TO 400
      IF(OPTION.EQ.4HDIFF) GO TO 401
      IF(OPTION.EQ.4HNRCD) GO TO 403
      IF(OPTION.EQ.4HSCCD) GO TO 404
      IF(OPTION.EQ.4HFCCD.AND.SPECT(4).NE.0000) GO TO 405
      IF(OPTION.EQ.4HPSCD.AND.SPECT(4).NE.0000) GO TO 406
      IF(OPTION.EQ.4HEYCD.AND.SPECT(4).NE.0000) GO TO 407
      IF(OPTION.EQ.4HPSCD) GO TO 408
      IF(OPTION.EQ.4HCNCD) GO TO 409
      IF(OPTION.EQ.4HCOCD) GO TO 410
      IF(OPTION.EQ.4HFLEX) GO TO 411
      IF(OPTION.EQ.4HQUAN) GO TO 412
      IF(OPTION.EQ.4HNORM) GO TO 413
      IF(OPTION.EQ.4HSATC) GO TO 414
      IF(OPTION.EQ.4HLOOK) GO TO 415
      RETURN
```

```
400   WRITE(IDEV,825) NEWID,SPECT(1),C(1),C(2)
      PRINT 625,NEWID,SPECT(1),C(1),C(2)
      RETURN
401   WRITE(IDEV,830) NEWID,SPECT(1),C(1),C(2),SPECT(2)
      PRINT 630,NEWID,SPECT(1),C(1),C(2),SPECT(2)
      RETURN
402   WRITE(IDEV,856) NEWID,ID(K),ID(L)
      PRINT 656,NEWID,ID(K),ID(L)
      RETURN
404   WRITE(IDEV,857) NEWID,ID(J),ID(L)
      PRINT 657,NEWID,ID(J),ID(L)
      RETURN
405   WRITE(IDEV,852) NEWID,ID(J),ID(K),ID(L),ID(M)
      PRINT 653,NEWID,ID(J),ID(K),ID(L),ID(M)
      RETURN
406   WRITE(IDEV,854) NEWID,ID(J),ID(K),ID(L),ID(M)
      PRINT 654,NEWID,ID(J),ID(K),ID(L),ID(M)
      RETURN
407   WRITE(IDEV,855) NEWID,ID(J),ID(K),ID(L),ID(M)
      PRINT 655,NEWID,ID(J),ID(K),ID(L),ID(M)
      RETURN
408   WRITE(IDEV,851) NEWID,ID(J),ID(K),ID(L)
      PRINT 651,NEWID,ID(J),ID(K),ID(L)
      RETURN
409   WRITE(IDEV,852) NEWID,ID(J),ID(K),ID(L)
      PRINT 652,NEWID,ID(J),ID(K),ID(L)
      RETURN
410   WRITE(IDEV,850) NEWID,ID(J),ID(K),ID(L)
      PRINT 650,NEWID,ID(J),ID(K),ID(L)
      RETURN
411   WRITE(IDEV,860) NEWID,ID(J),ID(K),C(1)
      PRINT 660,NEWID,ID(J),ID(K),C(1)
      RETURN
412   WRITE(IDEV,861) NEWID,ID(J),ID(K),C(1),C(3)
      PRINT 661,NEWID,ID(J),ID(K),C(1),C(3)
      RETURN
413   WRITE(IDEV,862) NEWID,ID(J),ID(K),C(1)
      PRINT 662,NEWID,ID(J),ID(K),C(1)
      RETURN
414   WRITE(IDEV,863) NEWID,ID(J),ID(K)
      PRINT 663,NEWID,ID(J),ID(K)
      RETURN
415   WRITE(IDEV,864) ID(J)
      PRINT 664,ID(J)
      RETURN
      END
```

```
      SUBROUTINE SEEIT
      COMMON/CD/CD(300),FPRT(300),CPRT(300)
      COMMON/CONTRL/CONTRL(100,6)
      COMMON/CSPINL/C(5),SPECT(5),INDEX(5),LBL(13)
      COMMON/PARAM/NPTS,NUM,NEWID,OPTION,TOTNUM,WVEMAX,WVEMIN
      REAL CD,CONTRL,C,WVEMAX,WVEMIN
      INTEGER ID,INDEX,LBL,SPECT,TOTNUM
      REAL WAVE(300)
672   FORMAT(* *,*ANISOTROPY COMPONENT ANALYSIS OF *,I4)
673   FORMAT(*0*,15X,3(*LAMBDA*,3X,*FOCD PART*,4X,*CD PART*,6X),/)
674   FORMAT(16X,3(F6.1,2X,F9.5,3X,F9.5,5X))
675   FORMAT(*0*,3(15X,*LAMBDA*,5X,*READING*,2X),/)
676   FORMAT(1X,3(15X,F6.1,2X,F12.5))
677   FORMAT(* *,*SPECTRUM *,I4)
678   FORMAT(*1*,12A6)
875   FORMAT(I4,6X,4(F8.3,2X),E13.6,2X,E13.6,1X,I1)
876   FORMAT(10F8.4)
877   FORMAT(10F8.3)
878   FORMAT(10F8.2)
879   FORMAT(*END OF *,I4,* PROCESS DECK*)
C
C     PUNCH, PRINT, AND PLOT RESULTS
C
      IDEV=7
      IF(NEWID.EQ.0) IDEV=17
      DO 80 I=1,NPTS
        IF(CD(I).LT.-999.9.OR.CD(I).GT.9999.9) IFORMT=2
80    CONTINUE
      DO 81 I=1,NPTS
        IF(CD(I).LT.-99.9.OR.CD(I).GT.999.9) IFORMT=1
81    CONTINUE
      IF(IFORMT.NE.1.AND.IFORMT.NE.2) IFORMT=0
      WRITE(IDEV,875) NEWID,(CONTRL(NUM,I),I=1,6),IFORMT
      IF=IFORMT+1
      IF(IF) 82,83,84
82    WRITE(IDEV,876) (CD(I),I=1,NPTS)
      GO TO 85
83    WRITE(IDEV,877) (CD(I),I=1,NPTS)
      GO TO 85
84    WRITE(IDEV,878) (CD(I),I=1,NPTS)
85    WRITE(IDEV,879) NEWID
      PRINT 675
```

```
      DO 86 N=1,NPTS
        WAVE(N)=CONTRL(NUM,1)-FLOAT(N-1)*(CONTRL(NUM,3)/10.)
86    CONTINUE
      II=NPTS/3+1
      DO 87 I=1,II
        J=I+II
        K=J+II
        PRINT 676,WAVE(I),CD(I),WAVE(J),CD(J),WAVE(K),CD(K)
87    CONTINUE
      IF(OPTION.NE.4HFOCD.OR.SPECT(4).NE.0000) GO TO 89
      PRINT 678,(LBL(NN),NN=2,13)
      PRINT 672,NEWID
      PRINT 673
      II=NPTS/3+1
      DO 88 I=1,II
        J=I+II
        K=J+II
        PRINT 674,WAVE(I),FPRT(I),CPRT(I),WAVE(J),FPRT(J),CPRT(J),
     $  WAVE(K),FPRT(K),CPRT(K)
88    CONTINUE
89    PRINT 678,(LBL(NN),NN=2,13)
      PRINT 677,NEWID
      XMAX=CONTRL(NUM,1)
      XINC=(CONTRL(NUM,1)-CONTRL(NUM,2))/100.0
      TWICE=XINC/0.5
      M=TWICE
      IF(M.NE.TWICE) XINC=0.5*(M+1)
      ISY=1
      CALL PRNPLT (WAVE(1),CD(1),XMAX,XINC,YMAX,YINC,0,ISY,NPTS)
      RETURN
      END
```

5. Control Deck for Running PREPARE and SMOOTHS in Tandem

```
RUNCD,7,200,100000.448402
*NOSTAGE
FETCHPS,CDLIB,LGO,PREPARE
LIBCOPY,CDLI3,TAPE5/BR,DATA.
LINK,X,PP=[TAPE5,OUTPUT,CONTROL].
DELETE,TAPE5,LGO.
COPY,OUTPUT/RB,ORXR,TAPE6/BR.
DISPOSE,TAPE6=PR,HO,DT=I.
STOTAPE,TAPE30=/NELSONJW/KSD/DATA/PREPARE/DATASET,10515.
FETCHPS,CDLIB,LGO,SMOOTHS.
LINK,X,PP=[TAPE30,OUTPUT,PUNCH].
DELETE,TAPE10,TAPE30,LGO.
DISPOSE,OUTPUT=PR,DT=I.
END.
```

6. Conversion of a Spectrum

A) The spectrum as printed by the -G- option of Super Spectrum.

```
RUN ID 0000STKD
OD =  0.100000E+01
E =  0.100000E+01

LAMBDA (A) RAW DATA
  4000       .0000
  3900       .1999
  3800       .3999
  3700       .5999
  3600       .7999
  3500       .9999
  3400      1.1999
  3300      1.3999
  3200      1.5999
  3100       .0999
  3000       .0999
  2900      1.5999
  2800      1.3999
  2700      1.1999
  2600       .9999
  2500       .7999
  2400       .5999
  2300       .3999
  2200       .1999
  2100       .0000
```

B) The spectrum as represented internally in the PDP/8E by Super Spectrum during transmission.

All numbers are octal.

Locations give data field in first digit, address in remaining digits, e.g. 12002 is location 2002 of data field 1.

Location	Contents.... Data Points							
14000	0000	0310	0620	1130	1440	1750	2260	2570
14010	3100	0144	0144	3100	2570	2260	1750	1440
14020	1130	0620	0310	0000	0000	0000	0000	0000

Location	Contents.... Spectrum Parameters							
15740	0000	0000	0260	0260	0260	0260	0323	0324
15750	0313	0304	0000	7640	0310	7634	7754	0001
15760	2000	0000	0001	2000	0000	7767	2030	4467
15770	0000	0000	0000	0000	0000	0000	0000	0000

The spectrum ID	(ASCII 8-bit characters)	is at	15742+
The starting wavelength	(in Å, double precision)	is at	15752+
The ending wavelength	(in nm, single precision)	is at	15754
The increment between points	(in Å, single precision)	is at	15755
The number of points	(negated, single precision)	is at	15756
The constant OD	(floating point)	is at	15757+
The constant E	(floating point)	is at	15762+
The scale (x 0.001)	(floating point)	is at	15765+
The data points	(each x 1000, single precision)	are at	14000+

C) The spectrum as typed at the keyboard during transmission and stored in PSS.

This is the input to PREPARE.

The parameter line is first, followed by data line(s).

```
0B00B00B00B00D30D40CB0C4000FA00C8F9CFEC00140000000014000000
    FF7418937000000000013D

0000C81902583203E84B0578640064064640578 4B03E832025819 00C8
    00000000000000000000104
```

There are 25 12-bit numbers represented per line with a checksum at the end. A line is filled in with zeroes if there are fewer than 25 numbers to send.

Hexadecimal to Binary Conversion

0 = 0000	4 = 0100	8 = 1000	C = 1100
1 = 0001	5 = 0101	9 = 1001	D = 1101
2 = 0010	6 = 0110	A = 1010	E = 1110
3 = 0011	7 = 0111	B = 1011	F = 1111

Sample Conversion for ID Characters K and D

K =	0 3 1 3	in 8-bit ASCII
	000 011 001 011	in binary
	0000 1100 1011	in binary
	0 C B	in hexadecimal
D =	0 3 0 4	in 8-bit ASCII
	000 011 000 100	in binary
	0000 1100 0100	in binary
	0 C 4	in hexadecimal

These are found in the first line above, starting with the 19th character.

D) The spectrum as written on TAPE30 by PREPARE after conversion.

This is the input to SMOOTHS.

```
0000STKD 400.00 200.00  10.00     1.000     1.000  0.001000 20

   0 200 400 600 800100012001400160 0 100 1001600140012001000 800 600
 400 200   0
```

E) The spectrum as punched by SMOOTHS.

Punch raw data option is on, smoothing is off.

```
0000STKD   400.000   200.000   100.000     1.000 0.100000E+01
 0.100000E+01 0

   .0000   .2000   .4000   .6000   .8000  1.0000  1.2000  1.4000
  1.6000   .1000

   .1000  1.6000  1.4000  1.2000  1.0000   .8000   .6000   .4000
   .2000   .0000

END OF 0000 SMOOTHS DECK
```

Appendix D

DNA/ETHIDIUM ION COMPLEX CHARGE DENSITY

1/ Ethidium ion is 3.4 Å thick and carries a +1 charge. B form DNA in the absence of dye binding is 3.4 Å long per base pair. Each base pair contains two phosphate groups, each with a -1 charge.

2/ Assume nearest neighbor exclusion model. Then, for a DNA helix 2n base pairs long there are 4n phosphate groups but only n binding sites. Each binding site is composed of 2 nucleotide units per strand.

3/ Binding site states are:

Empty 2 base pairs = 6.8 Å long

4 phosphates = -4 net charge

Occupied 2 base pairs + dye = 10.2 Å long

4 phosphates + dye = -3 net charge

4/ Use r, the extent of binding, to follow titration.

r = ethidium ion bound/DNA (as phosphate)

$= k/4n$, where k = number of bound dyes (1)

$r_{max} = 0.25$ in neighbor exclusion limit

5/ b = distance/charge =

$$[6.8(n - k) + 10.2(k)]/[4(n - k) + 3(k)] \quad (2)$$

Combine (1) and (2) to eliminate k,

then $b = 1.7[1 + 3r/(1 - r)]$

The $1/(1 - r)$ dependence was previously found for DNA titration by acids by Record et al. (1976).